The Role of the MLK Family in Cancer and Resistance to Targeted Therapies

A thesis submitted to the University of Manchester for the degree of Doctor of Philosophy in the Faculty of Medical and Human Sciences

2015

Zoe Catherine Edwards
Faculty of Medical and Human Sciences
School of Medicine

Contents

Word count: 56,456

List of figures

List of tables

Abbreviations

4EBP1 = eIF4E-binding protein 1

ABL = Abelson tyrosine protein kinase 1

ACC = acetyl-CoA carboxylase

ACTB = gene encoding β-actin

ADP = adenosine diphosphate

AKT = PKB, protein kinase B (first identified as a viral oncogene in thymic lymphomas of the Akr mouse strain)

AMP = adenosine monophosphate

AMPK = AMP-activated protein kinase

ANOVA = analysis of variance

AP-1 = activator protein 1

ARF = alternate reading frame of the *CDKN2A* locus

ATF = activating transcription factor

ATM = ataxia telangiectasia mutated serine/threonine kinase

ATP = adenosine triphosphate

ATR = ataxia telangiectasia and RAD3-related serine/threonine kinase

B2M = gene encoding β2-microglobulin

BAD = BCL2-associated death promoter

BAX = BCL2-associated X protein

BBC3 = BCL2-binding component 3

BCL2 = B-cell lymphoma 2

BCL2A1 = BCL2-related protein A1

BIM = BCL2-like 11

BrdU = bromodeoxyuridine (5-bromo-2'-deoxyuridine)

BSA = bovine serum albumin

BTG2 = B-cell translocation gene 2

CCLE = Cancer Cell Line Encyclopaedia

CCND1 = gene that encodes cyclin D1 protein

CDC42 = cell division cycle 42

CDK = cyclin-dependent kinase

CDKN1A = CDK inhibitor 1A ($p21^{Cip1}$)

CDKN1B = CDK inhibitor 1A ($p27^{Kip1}$)

CDKN2A = CDK inhibitor 2A

cFOS = FBJ (Finkel-Biskis-Jinkins) murine osteosarcoma viral oncogene homologue

CHIP = C terminus of HSC70-interacting protein

CHK1/2 = checkpoint kinase 1/2

cJUN = derived from ASV17 provirus, named after ju-nana (the number 17 in Japanese)

CNA = copy number alteration

COT = cancer Osaka thyroid

CREB = cAMP response element binding protein

CRIB = CDC42/RAC-interactive binding

CRUK-MI = Cancer Research UK Manchester Institute

CSC = cancer stem cell

C_T = cycle threshold

CXCL12 = chemokine (C-X-C motif) ligand 12

DCUN1D1 = DCN1(defective in cullin neddylation 1)-like protein 1

DLK = dual leucine zipper-bearing kinase

DMEM = Dulbecco's modified Eagle medium

DMSO = dimethyl sulphoxide

DNA = deoxyribonucleic acid

Dox = doxycycline

ECL = enhanced chemiluminescence

ECM = extracellular matrix

EDTA = ethylenediaminetetraacetic acid

EGF = epidermal growth factor

EGFR = epidermal growth factor receptor

EHS = Engelbreth-Holm-Swarm

EIF4 = eukaryotic translation initiation factor 4

ELK1 = ETS-like gene 1

EMA = European Medicines Agency

EPHA2 = ephrin receptor A2

ERBB3 = ERBB2 receptor tyrosine kinase 3

ERK = extracellular signal-regulated kinase

ETS = v-ets avian erythroblastosis virus E26 oncogene homologue

ETV4 = ETS variant 4

EV = empty vector

FACS = fluorescence-activated cell sorting

FBS = foetal bovine serum

FDA = United States Food and Drug Administration

FGF = fibroblast growth factor

FGFR = fibroblast growth factor receptor

FOXE1 = forkhead box E1

FOXO = forkhead box class O

GAB1 = GRB2-associated binding protein 1

GAP = GTPase-activating protein

GAPDH = glyceraldehyde 3-phosphate dehydrogenase

GCK = glucokinase (hexokinase 4)

GDP = guanosine diphosphatase

GEF = guanine nucleotide exchange factor

GISTIC = Genomic Identification of Significant Targets in Cancer algorithm

GOF = gain-of-function

GRB2 = growth factor receptor-bound protein 2

GSK3 = glycogen synthase kinase 3

GTP = guanosine triphosphate

GTPase = guanosine triphosphatase

HDAC = histone deacetylase

HGF = hepatocyte growth factor

HNSCC = head and neck squamous cell carcinoma

HPV = human papilloma virus

HSF1 = heat shock transcription factor 1

HSP = heat shock protein

hTERT = human telomerase reverse transcriptase, the catalytic subunit of telomerase

IDMEM = Iscove's modified DMEM

IGFR = insulin-like growth factor receptor

IκB = inhibitor of NFκB

IKK = IκB kinase

IL = interleukin

INK4A = inhibitor of CDK4A

IRS1 = insulin receptor substrate 1

JIP = JNK-interacting protein

JNK = cJUN N-terminal kinase

K-sfm = keratinocyte serum-free medium

KA = kinase-active

KD = kinase-dead

LB = Luria Bertani

LKB1 = liver kinase B1

LOF = loss-of-function

LSCC = lung squamous cell carcinoma

LYN = LCK/YES-related novel protein tyrosine kinase

LZK = leucine zipper-bearing kinase

MAP3K = mitogen-activated protein kinase kinase kinase

MAP2K = mitogen-activated protein kinase kinase

MAPK = mitogen-activated protein kinase

MBCF = Molecular Biology Core Facility

MCS = multiple cloning site

MDM2 = mouse double minute 2 homologue

MDR = multi-drug resistance gene

MEF = mouse embryonic fibroblast

MEK = MAPK/ERK kinase

MET = HGFR, hepatocyte growth factor receptor

MKK3/4/6/7 = MAPK kinase 3/4/6/7

MLK = mixed lineage kinase

MLL1/2 = mixed lineage leukaemia 1/2

MMP = matrix metalloprotease

MOI = multiplicity of infection

MOZ = monocytic leukemia zinc finger protein

MPP = 1-methyl-4-phenylpyridinium

MPTP = 1-methyl-4-phenyl-1,2,3,6-tetrahydropyridine

mRNA = messenger RNA

mTOR = mammalian target of rapamycin

mTORC = mTOR complex

MTT = 3-[4,5-dimethylthiazol-2-yl]-2,5-diphenyl tetrazolium bromide

MYC = v-myc avian myelocytomatosis viral oncogene homologue

NEAA = non-essential amino acids

NF-Y = nuclear transcription factor Y

NFκB = nuclear factor κ-light-chain-enhancer of activated B cells

NGF = neuronal growth factor

NIK = NFκB-inducing kinase

NOXA = PMAIP1, phorbol-12-myristate-13-acetate-induced protein 1

ORF = open reading frame

P-loop = phosphate-binding loop

PAK1 = p21-activated kinase 1

PARP = poly ADP-ribose polymerase

PBS = phosphate buffered saline

PCR = polymerase chain reaction

PDGFR = platelet-derived growth factor receptor

PDK1 = PIP_3-dependent kinase 1

PH = pleckstrin homology domain

PI3K = phosphatidylinositol 3-kinase

PIK3C2G = gene encoding PI3K catalytic subunit class II gamma

PIK3CA = gene encoding PI3K catalytic subunit alpha

PIN1 = peptidylprolyl cis/trans isomerase, NIMA-interacting 1

PIP_2 = phosphatidylinositol-4,5-bisphosphate

PIP_3 = phosphatidylinositol-3,4,5-trisphosphate

PKC = protein kinase C

PRAS40 = proline-rich AKT substrate of 40 kDa

PRDX3 = peroxiredoxin 3

PTB = phosphotyrosine-binding domain

PTEN = phosphatase and tensin homologue

PUMA = p53-upregulated modulator of apoptosis

PVDF = polyvinylidene fluoride

qRT-PCR = real-time quantitative reverse transcription PCR

RAB35 = RAS-related protein RAB35

RAC = RAS-related C3 botulinum toxin substrate

RAF = proteins named after rapidly accelerated fibrosarcoma (three forms known as ARAF, BRAF and CRAF)

RAPTOR = regulatory-associated protein of mTOR

RAS = proteins named after rat sarcoma (three proteins known as HRAS, KRAS, NRAS)

Rb = retinoblastoma protein

RBD = RAS binding domain

RHEB = RAS homologue enriched in brain

RHO = RAS-homologous

RICTOR = rapamycin-insensitive companion of mTOR

RNA = ribonucleic acid

ROS = reactive oxygen species

RPMI = Roswell Park Memorial Institute medium

RT = room temperature

RT-PCR = reverse transcription PCR

RTK = receptor tyrosine kinase

S6 = ribosomal protein S6

S6K = S6 kinase

SAM = sterile-α-motif

SCC = squamous cell carcinoma

SDM = site-directed mutagenesis

SDS-PAGE = sodium dodecyl sulphate-polyacrylamide gel electrophoresis

SH2/3 = SRC homology 2/3

shRNA = short hairpin RNA

siRNA = small interfering RNA

SKIL = SKI-like proto-oncogene

SLPR = Slipper

SOS = son of sevenless

SOX = SRY (sex determining region Y)-box

SRC = SRC proto-oncogene, non-receptor tyrosine kinase, abbreviation of sarcoma

STAT = signal transducer and activator of transcription

SV40 = simian virus 40

TAE = tris-acetate-EDTA

TCGA = The Cancer Genome Atlas

Tet = tetracycline

TGF = transforming growth factor

TGFBR2 = transforming growth factor beta receptor 2

TLOC1 = SEC62 homologue, pre-protein translocation factor

TNF = tumour necrosis factor

TOP1 = topoisomerase 1

TP53 = tumour protein p53 gene

TP63 = tumour protein p63 gene

TR = tetracycline repressor

TSC1/2 = tuberous sclerosis 1/2

UADT = upper aerodigestive tract

ULK1 = UNC51-like autophagy activating kinase 1

Unt = untreated

V/V = volume/volume

W/V = weight/volume

WCL = whole cell lysate

WT = wild-type

ZAK = zipper sterile-α-motif kinase

Abstract

The University of Manchester

Zoe Edwards

A thesis submitted for the degree of Doctor of Philosophy

The Role of the MLK Family in Cancer and Resistance to Targeted Therapies

2015

The mixed lineage kinases (MLKs) are a family of MAP3Ks that consists of three subfamilies: the MLK subfamily, comprising MLK1–4; the dual leucine zipper-bearing kinases (DLKs), composed of DLK and leucine zipper-bearing kinase (LZK); and the zipper sterile-α-motif kinases (ZAKα and ZAKβ). Alterations in MLK proteins have been found in various cancers, including MLK1 mutations in melanoma, and copy number gain of LZK in squamous cell carcinoma (SCC). However, the role of these kinases in cancer has not been well defined. This project has focused on evaluating the functional consequences of MLK mutation and overexpression in cancer.

The first part of this thesis concerns the role of MLK1–4 in vemurafenib resistance in melanoma. MLKs phosphorylate MKK4/7 and MKK3/6 to activate the JNK and p38 pathways, respectively. We found that MLK1–4 can also directly phosphorylate MEK to activate the ERK pathway, enabling them to mediate resistance to the BRAF inhibitor vemurafenib in melanoma. Overexpression of MLK1–4 reactivated ERK, improved survival, and rescued cells from apoptosis induced by RAF inhibitor treatment. Increased expression of MLK1–4 was identified in patients who developed resistance to vemurafenib, and expression of MLK1 could mediate resistance in a xenograft model. Additionally, activating mutations were found in MLK1 in melanoma patients and could potentially confer *de novo* resistance to BRAF inhibitors.

In the second part of this thesis, the role of LZK in SCC is explored. LZK resides on chromosome 3q, which is subject to copy number gain in ~80% of head and neck squamous cell carcinomas (HNSCC), as well as other squamous cancers. HNSCC accounts for ~600,000 cases and 300,000 deaths per year worldwide. Analysis of HNSCC cell lines with copy number gain of 3q revealed that LZK mRNA and protein levels were increased compared with control cell lines. Knockdown of LZK by siRNA reduced cell viability and survival in two HNSCC cell lines, but not control cells. Knockdown by inducible shRNA reduced survival, proliferation, and colony forming ability of HNSCC lines with 3q gain, but not control lines without copy number gain of the gene. Further work needs to be completed to determine the exact mechanism of this effect, but initial data indicated that regulation of AKT or of gain-of-function p53 by LZK maintains cancer cell proliferation. This study needs to be extended to a wider range of cell lines, but these results suggest that copy number gain of LZK can play a pro-proliferative role in HNSCC.

Declaration

No portion of the work referred to in the thesis has been submitted in support of an application for another degree or qualification of this or any other university or other institute of learning.

Copyright statement

1. The author of this thesis (including any appendices and/or schedules to this thesis) owns certain copyright or related rights in it (the "Copyright") and s/he has given The University of Manchester certain rights to use such Copyright, including for administrative purposes.
2. Copies of this thesis, either in full or in extracts and whether in hard or electronic copy, may be made **only** in accordance with the Copyright, Designs and Patents Act 1988 (as amended) and regulations issued under it or, where appropriate, in accordance with licensing agreements which the University has from time to time. This page must form part of any such copies made.
3. The ownership of certain Copyright, patents, designs, trade marks and other intellectual property (the "Intellectual Property") and any reproductions of copyright works in the thesis, for example graphs and tables ("Reproductions"), which may be described in this thesis, may not be owned by the author and may be owned by third parties. Such Intellectual Property and Reproductions cannot and must not be made available for use without the prior written permission of the owner(s) of the relevant Intellectual Property and/or Reproductions.
4. Further information on the conditions under which disclosure, publication and commercialisation of this thesis, the Copyright and any Intellectual Property and/or Reproductions described in it may take place is available in the University IP Policy (see http://documents.manchester.ac.uk/DocuInfo.aspx?DocID=487), in any relevant Thesis restriction declarations deposited in the University Library, The University Library's regulations (see http://www.manchester.ac.uk/library/aboutus/regulations) and in The University's policy on Presentation of Theses

Acknowledgments

I am very grateful for the support I have received over my time at CRUK-MI. First, I want to thank my supervisor, Dr John Brognard, for his invaluable guidance and encouragement throughout my PhD. I also want to thank my co-supervisor, Dr Donald Ogilvie, and my advisor, Dr Angeliki Malliri, for their advice over the course of my doctoral training, and Dr Ogilvie in particular for his helpful comments on my thesis manuscript.

I want to thank past and present members of the Signalling Networks in Cancer group for their moral support and technical assistance during my PhD. Special mention goes to Dr Anna Marusiak, Dr Eleanor Trotter and Dr Pedro Torres; it has been a pleasure to work with them on these projects. I also want to thank Dr Shameem Fawdar and Dr Natalie Stephenson for training me in various techniques.

I also want to express my gratitude to our collaborators, including Dr Maria Girotti, Dr Willy Hugo, Phil Chapman, and Dr Henry Wood, for their expertise in conducting some of the experiments contained within this thesis.

Finally, my thanks go to Cancer Research UK for funding this work.

1 Introduction: The MLK family

1.1 MAPK signalling

Mitogen-activated protein kinase (MAPK) signalling pathways are conserved throughout evolution and involved in a diverse array of cell signalling events. They consist of a sequence of kinases, which are each activated by phosphorylation and thus enabled to act downstream. On activation by upstream signals, for example a growth factor binding its receptor, MAPK kinase kinases (MAP3Ks) phosphorylate MAPK kinases (MAP2Ks) on serine and threonine residues. This induces conformational changes leading to the activation of MAP2Ks, which then phosphorylate MAPK proteins on threonine and tyrosine residues. Activated MAPKs translocate to the nucleus to mediate their effects via the phosphorylation of transcription factors, leading to transcription of target genes. In this way a signal is transmitted to promote the expression of a particular set of genes, enabling a cell to respond to a range of stimuli.

The mixed lineage kinase (MLK) family function as MAP3Ks. As yet, their cellular function in homeostasis and disease has not been clearly defined. This thesis focuses on: (1) determining whether MLK proteins have a role in mediating resistance to BRAF inhibitors in metastatic melanoma and (2) evaluating the functional consequences of LZK amplification in squamous cell carcinoma.

1.2 Structure and regulation of MLKs

1.2.1 MLK structure

The MLKs are a family of serine/threonine protein kinases with tyrosine kinase properties (Dorow *et al.*, 1993), although so far no tyrosine kinase activity has been attributed to MLK family proteins (Rana *et al.*, 2013). The family consists of three subfamilies: the MLK subfamily, comprising MLK1–4; the dual leucine zipper-bearing kinases (DLKs), composed of DLK and leucine zipper-bearing kinase (LZK); and the zipper sterile-α-motif kinases (ZAKα and ZAKβ). Figure 1A shows the domain structure of these proteins.

These subfamilies are characterised based on sequence homology and domain structure. MLK1–4 contain a SRC homology 3 (SH3) domain (Gallo and Johnson, 2002), a kinase

domain, two leucine zippers separated by a 13 amino acid spacer (Dorow *et al.*, 1993), and a CDC42/RAC-interactive binding (CRIB) motif. The DLKs contain a kinase domain and two leucine zippers separated by a 31 amino acid spacer. Both ZAK isoforms contain one leucine zipper, while ZAKα also has a sterile-α-motif (SAM) domain (Gallo and Johnson, 2002). The MLK carboxy terminus is rich in serine, threonine and proline residues and is presumed to be a regulatory region to distinguish between the MLKs in terms of function.

These structures alone indicate the potential complexity of signalling mediated by MLK family proteins. MLKs possess a variety of domains that mediate protein-protein interactions: SH3 domains enable binding to proline-rich sequences; leucine zippers allow binding to other leucine zipper domains and as such are often involved in dimerization; and the CRIB domain mediates binding to RAC (RAS-related C3 botulinum toxin substrate) and CDC42 (cell division cycle 42), upstream activators of the MLKs (Teramoto *et al.*, 1996). SAM domains allow binding to both proteins and RNA (Kim and Bowie, 2003), though the binding partners of the ZAK SAM domain are yet to be discovered.

Furthermore, the MLKs display different expression profiles, demonstrating another potential level of regulation. While MLK3 is widely expressed (Gallo *et al.*, 1994), northern blot analysis has demonstrated that other members appear to be restricted to certain tissues. This approach examines mRNA levels from heart, brain, placenta, lung, liver, skeletal muscle, kidney and pancreatic tissue. MLK2 was found to be highly expressed in brain and skeletal muscle (Dorow *et al.*, 1995); MLK4α and MLK4β were both detected in the pancreas, kidney, liver, lung and brain, while MLK4β, but not MLK4α, was detected in skeletal muscle (Kashuba *et al.*, 2011); DLK was predominantly expressed in the brain (Holzman *et al.*, 1994); LZK was most strongly detected in the pancreas, brain, placenta and liver (Sakuma *et al.*, 1997); and ZAK was most strongly expressed in heart, placenta, pancreas, liver and lung tissue (Liu *et al.*, 2000a). MLK3 is the best studied of the MLK subfamily, while of the DLK subfamily DLK itself has been most comprehensively investigated, thus much of the following review focuses on these two proteins.

MLK proteins are not conserved throughout evolution, but are restricted to higher eukaryotes. *Drosophila* (Stronach and Perrimon, 2002) and *Xenopus* (Poitras *et al.*, 2003) possess MLK homologues, while yeast do not have MLKs (Bisson *et al.*, 2008).

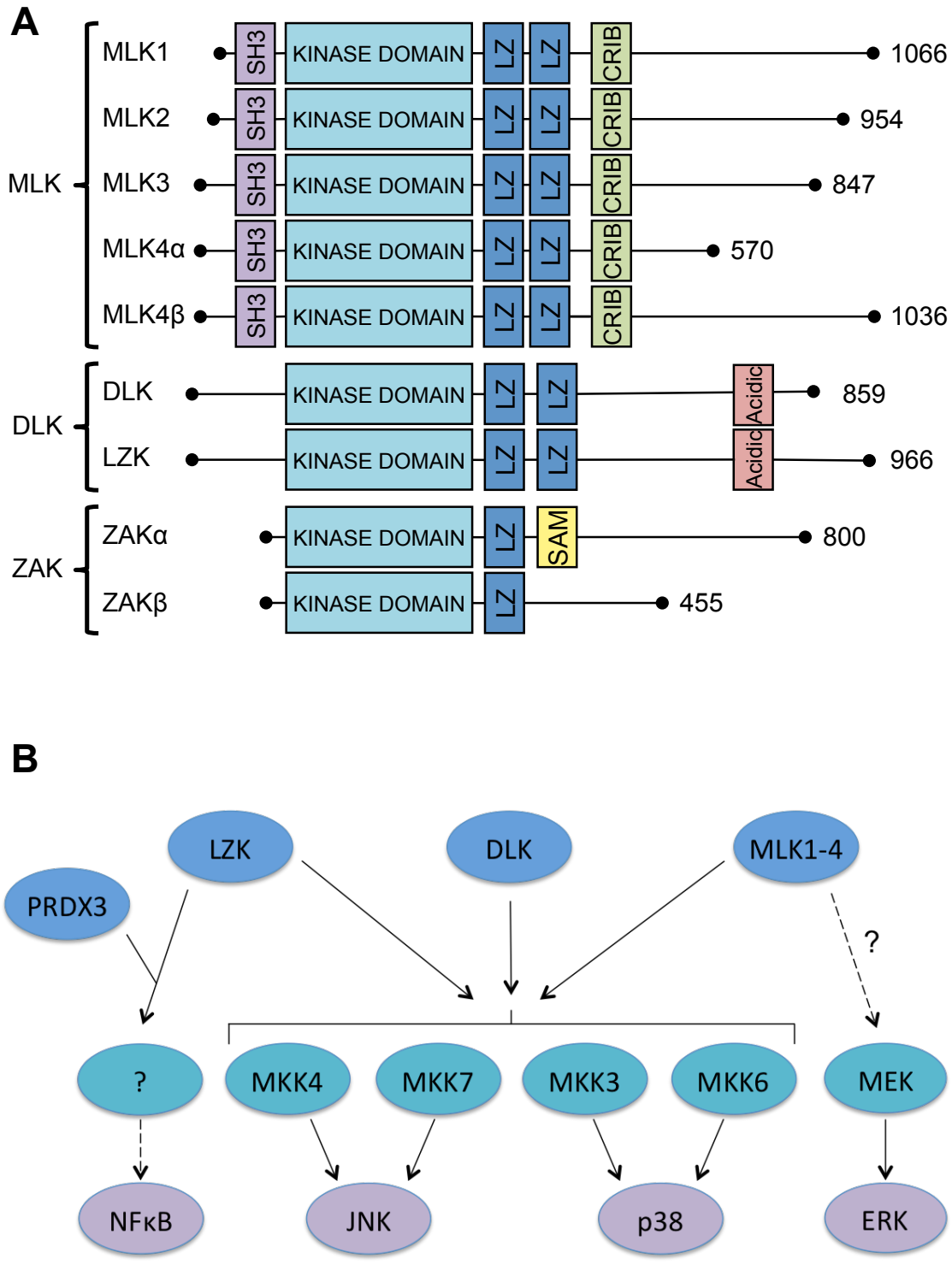

Figure 1: The mixed lineage kinase (MLK) family. A: Domain structure of MLK family proteins (adapted from Gallo & Johnson, 2002). All family members have a kinase domain and a leucine zipper (LZ) region. MLK subfamily proteins (MLK1–4) also possess SRC homology 3 (SH3) and CDC42/RAC-interactive binding (CRIB) domains. **B:** Signalling pathways activated by MLK family proteins. All MLK family members can activate JNK and p38 pathways. LZK can also activate the NFκB pathway, while MLK1–4 have a potential role in ERK activation. ZAK is not shown but may be able to activate all four pathways.

1.2.2 Regulation of MLKs

MLK proteins are activated by a sequence of events starting with relief of autoinhibition, followed by dimerisation and autophosphorylation. The MLK subfamily (MLK1–4) of proteins contain an SH3 domain, which for MLK3 has been demonstrated to be involved in autoinhibition; this domain binds a conserved proline to lock the protein in its closed form, preventing ATP binding. This is surprising, as MLK3 has a large proline-rich carboxy terminus, containing nine potential SH3 consensus sequences (PXXP). It is not clear why the SH3 domain instead binds a single proline, for which the binding affinity is expected to be lower. This could be an evolutionary strategy to enable the activation of MLK3 by other proteins containing SH3 binding motifs of higher affinity, which would be favoured over the autoinhibitory intramolecular interaction. Lower affinity interactions are possible in the case of intramolecular binding due to conformational effects; a higher effective concentration can be reached as the binding domains may be positioned close together in the folded protein (Zhang and Gallo, 2001).

For MLK1–4, activation is achieved by upstream proteins such as GTP-bound RAC or CDC42, which bind the CRIB domain (Teramoto *et al.*, 1996), relieving autoinhibition and allowing dimerisation and downstream activation (Bock *et al.*, 2000). The above model of autoinhibition has been demonstrated for MLK3, and it is possible that different mechanisms exist for MLK1, MLK2 and MLK4. However, the similarity in domain structure between these proteins, the conservation of the relevant proline residue, and the fact that the *Drosophila* MLK subfamily homologue Slipper (SLPR) also appears to be activated by this mechanism (Garlena *et al.*, 2010) suggest that this is likely to be common for MLK1–4.

All MLKs contain at least one leucine zipper, which enables them to bind similar sequences on other proteins. Leucine zippers contain repeats of leucine, isoleucine or valine, and can interact with similar motifs by forming coiled coils stabilised by hydrophobic interactions (Gallo and Johnson, 2002). As such, this region is involved in dimerisation of MLKs. For MLK3, DLK, LZK and ZAK, homodimerisation was shown to be required for JNK (cJUN N-terminal kinase) activation, as deletion of the leucine zipper region removed their ability to stimulate the pathway (Leung and Lassam, 1998; Nihalani *et al.*, 2000; Ikeda *et al.*, 2001b; Huang *et al.*, 2004). Homodimerisation is necessary for autophosphorylation of MLK3, DLK and ZAK on positive regulatory sites (Leung and

Lassam, 1998; Nihalani *et al.*, 2000; Huang *et al.*, 2004). Autophosphorylation on Thr277 in the activation loop of MLK3 is both required and sufficient to activate the protein for downstream signalling, while phosphorylation on Ser281 aids activation (Leung and Lassam, 2001). For MLK1, the key phosphorylation site is Thr312, with Thr304, Thr305 and Ser308 also contributing to activation (Durkin *et al.*, 2004).

The DLKs become activated by a distinct mechanism to the MLKs, as they do not possess CRIB or SH3 domains, indicating that they are not regulated by autoinhibition or by CDC42/RAC. It has been suggested that DLK is more readily able to dimerise than the MLK subfamily, and that these regulatory steps are not necessary (Handley *et al.*, 2007). Homodimerisation of DLK or LZK has been shown to be sufficient for their activation (Ikeda *et al.*, 2001b; Nihalani *et al.*, 2001). However, there must be some method of preventing erroneous activation of the DLKs. One potential mechanism is regulation of protein stability via a JNK-dependent feedback loop. Under normal conditions, DLK protein levels are strictly controlled via an ubiquitin-dependent degradation pathway. When neuronal cells are subjected to stress conditions, such as withdrawal of neuronal growth factor (NGF), DLK is stabilised via a JNK-dependent mechanism; JNK directly phosphorylates DLK on two residues distinct from its activation loop (T43 and S533), protecting it from degradation and creating a positive feedback loop for DLK signalling (Huntwork-Rodriguez *et al.*, 2013).

A further level of regulation occurs via scaffolding proteins such as the JNK-interacting proteins (JIPs). The JIP family consists of JIP1–4; all are able to bind JNK and MKK7 (MAPK kinase 7), but the affinities for the different JNK isoforms and MLK proteins vary (Yasuda *et al.*, 1999), illustrating a potential for specificity of signalling outcomes. Scaffolding proteins are believed to aid localisation and phosphorylation, promoting the appropriate response to a set of signals by recruiting the correct proteins and preventing inappropriate activation and cross-talk within the cell (Handley *et al.*, 2007). JIPs sequentially recruit signalling proteins to enable transmission of a signal to JNK. They hold MLKs in an inactive, monomeric form until a stimulus promotes dissociation of the complex, followed by dimerisation and autophosphorylation of the MLK. This allows association of JNK with JIP, and enables MLK proteins to activate the downstream pathway (Nihalani *et al.*, 2001).

The C terminal region of the MLK family is not well characterised, and does not have a

clear domain structure. This region is likely to be involved in dictating protein specificity between these kinases, as there is significant divergence in terms of sequence in the C terminus of MLKs (Gallo and Johnson, 2002). This could lead to a wide array of different protein-protein interactions that may help to determine the function and activity of each MLK member. For example, the C terminus of LZK (801–966) is required for the activation of MKK4 and JNK, but not MKK7 (Ikeda *et al.*, 2001b), suggesting that as yet uncharacterised domains in the C terminal region of LZK help to determine which kinase is activated downstream. Additionally, a large number of potential phosphorylation sites were detected within this region in MLK3 (Vacratsis *et al.*, 2002), which could provide a mechanism to regulate protein activity. Many of these sites in MLK3 are consensus motifs for proline-directed kinases, a class of proteins that includes MAPKs, CDKs (cyclin-dependent kinases) and GSK3 (glycogen synthase kinase 3) (Vacratsis *et al.*, 2002). There is evidence that MLKs are regulated by positive feedback downstream, as DLK, MLK2 and MLK3 can be regulated by JNK phosphorylation (Phelan *et al.*, 2001; Schachter *et al.*, 2006; Huntwork-Rodriguez *et al.*, 2013).

1.3 MLK signalling and function

1.3.1 Downstream signalling pathways

MLKs are MAP3Ks that are capable of activating various MAPK signalling pathways (Fig. 1B). Much of the research into signalling pathways activated by MLKs has involved ectopic expression of these kinases, which are constitutively active when overexpressed and do not require activation by agonists or coexpression of upstream activators. At present, details pertaining to endogenous regulation of downstream pathways by the MLKs have been limited, and research in this area has mostly focused on MLK3 (Rana *et al.*, 2013).

1.3.1.1 The JNK pathway

The archetypal downstream pathway is the JNK pathway; MLKs can phosphorylate MKK4 and MKK7 that in turn phosphorylate JNK (Rana *et al.*, 1996; Teramoto *et al.*, 1996; Tibbles *et al.*, 1996; Hirai *et al.*, 1997; Sakuma *et al.*, 1997; Liu *et al.*, 2000a; Nihalani *et al.*, 2000). Phosphorylated JNK then activates downstream members of the AP-1 (activator protein 1) complex such as cJUN and ATF2 (activating transcription

factor 2), stabilising and activating these transcription factors to promote an increase in their transcriptional activity. The JNK pathway regulates apoptosis, differentiation and migration, and is activated in stress situations, such as on exposure to inflammatory cytokines, DNA damage, osmotic stress and heat shock (Gallo and Johnson, 2002). Various upstream agonists can activate MLK signalling. For example, MLK3 mediates the cellular response to the pro-apoptotic signal ceramide and its upstream inducer TNFα (tumour necrosis factor alpha), specifically via stimulation of the JNK pathway (Sathyanarayana *et al.*, 2002). In support of this, mouse embryonic fibroblasts (MEFs) prepared from *Mlk2*$^{-/-}$/*Mlk3*$^{-/-}$ mice exhibited resistance to TNFα-induced cell death. Additionally, these mice displayed reduced expression of inflammatory cytokines in response to lipopolysaccharide stimulation (Kant *et al.*, 2011).

1.3.1.2 The p38 pathway

MLKs can also induce activation of the p38 pathway when overexpressed, via phosphorylation of MKK3/6 (Fan *et al.*, 1996; Tibbles *et al.*, 1996; Cuenda and Dorow, 1998). Like JNK, p38 is activated by stress and cytokines; its activation leads to growth arrest and apoptosis, and it also has a role in inflammation and activation of immune cells. MLK3 has been proposed to be involved in the apoptotic p38 response to TGFβ1 (transforming growth factor beta 1), likely via MKK6 activation (Kim *et al.*, 2004). The scaffolding protein JIP2 can associate with p38 to mediate activation of this pathway downstream of MLKs (Buchsbaum *et al.*, 2002).

1.3.1.3 The ERK pathway

In addition, MLK3 has been shown to phosphorylate MEK1 (MAPK/ERK kinase) in a kinase-dependent manner; this led to an activation of ERK (extracellular signal-regulated kinase; for details concerning this pathway see section 3.2.1.1) downstream that could be blocked with a MEK inhibitor (Hartkamp *et al.*, 1999). In fact, RNAi studies have shown that MLK3 is required for the activation of JNK, p38 and ERK MAPK cascades by a variety of mitogens, including growth factors and TNF (Chadee and Kyriakis, 2004). The involvement of MLK3 in the activation of the ERK cascade was proposed to be via formation of a complex with BRAF and CRAF (Chadee *et al.*, 2006), which was required for the activating phosphorylation of BRAF at Thr598 and Ser601. MLK3 did not directly

phosphorylate BRAF (Chadee and Kyriakis, 2004), and MLK3 knockdown effects could be rescued by expression of a kinase-dead form of the protein; these data suggested a scaffolding role for MLK3, independent of its kinase activity (Chadee *et al.*, 2006). However, a study utilising mouse models to investigate this phenomenon found that MLK3 knockout mice had no defects in any of these signalling modules, which led the authors to conclude that this protein is not required for ERK signalling (Brancho *et al.*, 2005). It is possible that there is a degree of functional redundancy between the MLK proteins, and that one of the other MLKs takes on the role of MLK3 in the mouse model. Previous studies have demonstrated precedence for the ability of MLK proteins to perform the same roles (Kim *et al.*, 2004; Kant *et al.*, 2011). In the RNAi studies, it may be that other MLKs are not expressed in the cell lines used, or that there was insufficient time allowed for the other MLKs to compensate for the loss of MLK3.

More recently, the purified kinase domain of MLK4 has been shown to directly phosphorylate MEK1 in an *in vitro* kinase assay (Martini *et al.*, 2013). In addition, overexpression of ZAK activated ERK in a lung cancer cell line; however, expression of a kinase-dead form was not tested so it is not known whether this effect is kinase-dependent (Yang *et al.*, 2010b). The DLKs have not been reported to activate the ERK pathway; overexpression of LZK did not activate the ERK pathway (Ikeda *et al.*, 2001a) and overexpression of DLK did not activate ERK2 (Fan *et al.*, 1996).

1.3.1.4 The NFκB pathway

Overexpression of ZAK promotes NFκB (nuclear factor κ-light-chain-enhancer of activated B cells) activity, although the mechanism and physiological relevance of this has not been determined (Liu *et al.*, 2000a). LZK also appears to have a role in the activation of NFκB, due to an interaction with peroxiredoxin 3 (PRDX3). LZK overexpression weakly activated NFκB in cells, while coexpression with PRDX3 significantly activated the pathway. LZK associated with and activated IKKβ (IκB kinase β) in a kinase-dependent fashion; however, LZK could not directly phosphorylate IKKβ and the downstream substrate that connects LZK to IKKβ is not yet known. Activation of NFκB protects cells from apoptosis by inducing expression of BCL2 (B-cell lymphoma 2) proteins and inhibitors of JNK signalling, thus it was suggested that PRDX3 may promote activation of NFκB by LZK as a way to avoid JNK-mediated apoptosis (Masaki *et al.*, 2003). The ability to associate with JIP1 or PRDX3 suggests that these regulatory proteins

may be important in determining the outcome of LZK activation in response to different stimuli.

1.3.2 Functions of MLK family proteins

The role of the MLKs in cellular function has not yet been fully defined, but they have been proposed to be involved in the regulation of a variety of cellular events, including developmental and chemotactic migration (Stronach and Perrimon, 2002; Poitras *et al.*, 2003; Brancho *et al.*, 2005; Swenson-Fields *et al.*, 2008), as well as promotion of G2/M transition during mitosis (Swenson *et al.*, 2003; Cronan *et al.*, 2012; Rangasamy *et al.*, 2012). MLKs also have a role in the apoptotic pathway in certain situations, such as in response to the cytokines TNFα (Sathyanarayana *et al.*, 2002; Kant *et al.*, 2011) and TGFβ (Kim *et al.*, 2004). Much of the research implicating MLKs in the apoptotic pathway has focused on neuronal disease (discussed below, section 1.4.1).

The *Drosophila* MLK1–4 homologue SLPR is involved in dorsal closure in the fly embryo (Stronach and Perrimon, 2002); MLK2 is required for pronephric tubule formation during embryonic development in *Xenopus* (Poitras *et al.*, 2003); and *Mlk3*$^{-/-}$ mice show thinning of the dorsal epidermis (Brancho *et al.*, 2005). It was therefore suggested that MLK proteins play a role in migration, and indeed MLK3 is important in directed migration, as siRNA depletion of the protein reduced the chemotactic response to serum (Swenson-Fields *et al.*, 2008). Thus MLK proteins appear to have a role in embryonic development, and may have a wider role in mediating cellular migration.

MLK3 has also been proposed to have a role in mitosis, localising to the centrosomes and inducing disruption of microtubules during G2/M transition, helping to promote entry into M phase (Swenson *et al.*, 2003). An inhibitor of the MLK family, CEP11004, inhibited proliferation of transformed cell lines by preventing spindle formation, stopping entry into M phase and causing mitotic arrest. This inhibition was partially reversed by ectopic expression of MLK3 (Cha *et al.*, 2006). The experimental use of inhibitors such as CEP11004 should be analysed with caution; these drugs are staurosporine analogues and so may have off-target effects (Davis *et al.*, 2011). For example, the related CEP1347 compound can inhibit PAK1 (p21-activated kinase 1) as well as the MLKs (Nheu *et al.*, 2002). However, a recent study using breast cancer cell lines found that knockdown of MLK3 caused mitotic infidelity, with an increase in multi- and micro-nucleated cells

(Cronan *et al.*, 2012). In addition, MLK3 can phosphorylate the prolyl isomerase PIN1, which in turn promotes G2/M transition via cyclin D1 stabilisation (Rangasamy *et al.*, 2012); these results suggest that MLK3 may indeed play a role in mitosis.

DLK has emerged as a key regulator of neuronal development (reviewed in Tedeschi and Bradke, 2013). The role of DLK is complex; it can promote degenerative and regenerative processes both in development and in disease situations (see section 1.4.1). Importantly, knockout *Dlk*$^{-/-}$ mice died at the perinatal stage due to defects in axon growth and neural migration, particularly in the pyramidal neurons of the neocortex (Hirai *et al.*, 2006). Ghosh *et al.* found that DLK also has a role in regulating programmed cell death of excess peripheral neurons during development, using an *in vitro* NGF withdrawal model that simulates nutrient competition during development. During later stages of foetal development, *Dlk*$^{-/-}$ mice had increased numbers of dorsal root ganglion and spinal root neurons (Ghosh *et al.*, 2011), which were not examined in detail in the previous study of *Dlk*$^{-/-}$ mice (Hirai *et al.*, 2006). DLK mediates its role in programmed cell death through an interaction with JIP3, which leads to a specific activation of the apoptotic JNK pathway. JNK is highly activated in neuronal cells and is required to regulate homeostasis and growth. This suggests that scaffolding proteins have a crucial role in distinguishing between homeostatic and apoptotic JNK signalling (Ghosh *et al.*, 2011).

DLK also has a critical role in detecting and determining the response to axonal damage. DLK acts as a sensor of neuronal injury, and induces expression of genes involved in both axon regeneration and apoptosis. This is illustrated by the response to optic nerve crush injury in DLK knockout mice; after deletion of DLK, axons showed improved survival after injury, but regrowth was abrogated, demonstrating that DLK has an important role in coordinating both apoptotic and regenerative responses after axon damage (Watkins *et al.*, 2013). The specific outcome of DLK signalling may be dependent on a variety of factors, such as the level of damage involved, and alternative cellular stimuli and interacting proteins. The complex role of DLK suggests that it is an important regulator of neuronal growth both in development and pathogenic processes and must be finely tuned to promote the appropriate growth response for different situations (Tedeschi and Bradke, 2013). LZK, the sister protein of DLK, may also have a role in neuronal growth, as knockdown of LZK in murine primary embryonic cortical neurons increased length of neurons (Dickson *et al.*, 2010). However, so far this has only be examined *in vitro* and no LZK knockout rodent models have yet been reported.

Elucidating the physiological roles of the MLK subfamily is complicated by the number of members; *Mlk1*$^{-/-}$/*Mlk2*$^{-/-}$ mice showed no clear phenotypic defects (Bisson *et al.*, 2008), while *Mlk3*$^{-/-}$ mice were broadly normal with only a slight thinning of the dorsal epidermis (Brancho *et al.*, 2005). There is likely a degree of functional redundancy between the MLK proteins that could account for this.

1.4 MLKs and disease

1.4.1 MLKs and neurodegenerative disease

MKK4, MKK7 and JNK are implicated in stress-induced apoptosis in neurons (Tournier, 2013). As such, a role for MLKs upstream of MKK4/7–JNK in neurodegenerative disease such as Alzheimer's and Parkinson's has been postulated. Early experiments utilising overexpression assays showed that MLK1, MLK2, MLK3 or DLK induced apoptosis in a neuronal cell line via the MKK4/7–JNK–cJUN pathway, and this could be blocked by treatment with the pan-MLK inhibitor CEP1347 (Xu *et al.*, 2001). Additionally, withdrawal of growth factors from neuronal cell lines led to apoptosis via a pathway that appeared to involve activation of MLK3, and CEP11004 treatment prevented this apoptosis. The proposed mechanism was that NGF withdrawal ablates activation of the PI3K/AKT survival pathway, which would normally suppress the activation of GSK3β. When this suppression is removed, GSK3β is able to phosphorylate two residues in the carboxy terminus of MLK3 (S789 and S793), leading to JNK-mediated apoptosis (Mishra *et al.*, 2007). JNK promotes apoptosis via phosphorylation of 14-3-3 proteins causing the release of pro-apoptotic factors such as BAX (BCL2-associated X protein) and FOXO (forkhead box class O) (Wagner and Nebreda, 2009).

MLK2 may have a role in Huntington's disease, which is caused by a mutant form of the huntingtin protein. Huntingtin contains a polyglutamine repeat region, the expansion of which is responsible for the onset of disease associated with increased neuronal apoptosis. The normal form of huntingtin interacts with MLK2 via its SH3 domain, whereas the polyglutamine-expanded version does not bind MLK2. This frees MLK2 to activate JNK, leading to apoptosis and potentially neurodegeneration (Liu *et al.*, 2000b).

Recently a key role for DLK in various models of brain injury and neurodegenerative disease has been elucidated, in accordance with its role in coordinating response to neuronal damage (see section 1.3.2). Deletion of DLK reduced death of retinal ganglion cells in a murine model of glaucoma. Supporting a role for this kinase, overexpression of DLK promoted death of retinal ganglia, while overexpression of a kinase-dead form of the protein enhanced cell survival, suggesting that it can act in a dominant-negative manner (Welsbie *et al.*, 2013). Mice with inducible knockout of DLK were resistant to neuronal degeneration due to kainic acid-induced excitotoxicity, a process thought to be involved in neuronal injury after brain trauma as well as neurodegenerative diseases including Alzheimer's (Pozniak *et al.*, 2013). In these models DLK acts via the downstream JNK pathway to mediate its pro-apoptotic effects (Pozniak *et al.*, 2013; Welsbie *et al.*, 2013) DLK-specific inhibitors have now been developed that show promise for the treatment of neurodegenerative disease; in a murine model of the disease, inhibition of DLK reduced activation of cJUN in response to MPTP (1-methyl-4-phenyl-1,2,3,6-tetrahydropyridine), a precursor of MPP (1-methyl-4-phenylpyridinium), which causes Parkinson's disease (Patel *et al.*, 2015). These data are consistent with the role of DLK in neuronal development, and indicate that DLK is a key regulator of neuronal apoptosis and regeneration that can be de-regulated in neuronal disease.

The apparent role of MLK2 and MLK3 in the pathogenic apoptosis of neurodegenerative disease led to the development of drugs to inhibit these proteins. However, while the inhibitor CEP1347 showed promising results in both *in vitro* and *in vivo* pre-clinical models, this drug was ineffective in a clinical trial for Parkinson's disease (Parkinson Study Group PRECEPT Investigators, 2007). DLK is a more convincing mediator of neurodegenerative disease, due to its role in response to neuronal injury in mouse models. CEP1347 is less specific for DLK compared to the other MLK proteins, providing only 60% inhibition of its activity *in vitro* at 500nM, versus 98% inhibition of MLK3. This compound also inhibits unrelated targets such as GCK (glucokinase) and NIK (NFκB-inducing kinase) to a greater extent than DLK (Maroney *et al.*, 2001); thus it is possible that DLK is not inhibited sufficiently to effect significant changes in downstream JNK activation, or that off-target effects negate any potential benefit. Alternatively, mouse models of disease may not accurately represent human neurodegenerative disease (Waldmeier *et al.*, 2006), and the MLKs might not be the main or the only contributors to neuronal cell death in human disease. Further testing, and eventual clinical trials, of the

newly developed DLK-specific inhibitor (Patel *et al.*, 2015) will elucidate whether this kinase is a key target in neurodegenerative disease.

1.4.2 MLKs and cancer

Mutations in MLK family proteins are observed in various cancers, for example MLK3 in gastric cancer (Velho *et al.*, 2010; Corso *et al.*, 2011), MLK1 in melanoma (Stark *et al.*, 2012), MLK4 in colon cancer (Martini *et al.*, 2013), and LZK in breast cancer (Stephens *et al.*, 2012; CCLE, 2015). However, their roles in cancer have not been well defined, and can seem contradictory, illustrating further that the role of this family is complex and dependent on various factors, such as cell-type and environment. As discussed previously, MLKs are involved in the apoptotic pathway via JNK or p38. However, JNK is also proposed to have a role in cellular transformation to a tumorigenic phenotype, and as such MLKs have been investigated for their role in cancer.

JNK can have complex and opposing roles in cancer (reviewed in Wagner and Nebreda, 2009; Tournier, 2013; Bubici and Papa, 2014). Signalling through the JNK pathway is lost by mutation in some cancers, for example JNK3 in brain tumours, which is likely a mechanism to avoid JNK-mediated apoptosis (Wagner and Nebreda, 2009). In addition, genetic deletion of JNK1 or JNK2 can promote tumour growth in murine models of breast cancer and prostate cancer (Tournier, 2013). However, in some animal models JNK has an oncogenic role, based upon its ability to activate members of the AP-1 complex. The downstream targets of AP-1 include regulators of cell cycle control and survival, as well as inflammatory mediators such as cytokines and proteases, which can promote invasive properties. Mouse models implicate JNK1 in the promotion of liver and gastric cancers, and JNKs are upregulated in human prostate cancer (Wagner and Nebreda, 2009). Elucidating the mechanisms at play is complicated by the existence of three JNK isoforms; at present it is not clear how far the targets of JNK1–3 differ from each other (Bubici and Papa, 2014). It has been proposed that JNK1 can be oncogenic, whereas JNK2 acts as a tumour suppressor; however, the opposite has been found in skin cancer (Finegan and Tournier, 2010), suggesting that tissue specificities are critical to the outcome of signalling. The duration of signalling is also crucial; transient JNK activation promotes survival, whereas prolonged activation mediates TNFα-dependent apoptosis (Wagner and Nebreda, 2009; Zhao *et al.*, 2012). This implies that the JNK cascade acts, in part, as a check on tumorigenic proliferation, but that cancer cells may be able to hijack or disrupt

the pathway to promote survival and invasion.

Analogous to JNK, the role of MKK4, the kinase downstream of MLK proteins in the JNK pathway, has been scrutinised. MKK4 is mutated at a low rate in some cancers, most commonly breast and pancreatic, and the majority of mutations are loss-of-function (LOF) (Kan *et al.*, 2010; Ahn *et al.*, 2011), implying a tumour suppressive role. On the other hand, one study utilising a skin-specific MKK4-deficient mouse model suggested an oncogenic role for this protein via the pro-survival targets of JNK, such as downregulation of p53 or increased epidermal growth factor receptor (EGFR) expression (Finegan and Tournier, 2010).

While the JNK pathway clearly has varying roles depending upon the specific cellular situation, the fact that most MKK4 mutations in cancer have been found to be LOF suggested that the same might be true for MLK mutations. Thylur *et al.* have proposed an anti-cancer role for MLK3, whereby it inhibits β-catenin signalling, leading to a reduction in the expression of survivin and MYC (v-myc avian myelocytomatosis viral oncogene homologue), and consequently promoting apoptosis (Thylur *et al.*, 2011). In contrast, overexpression of MLK3 in NIH3T3 cells initiated transformation in a kinase-dependent manner, indicating that MLK3 is involved in a signalling cascade that can promote tumourigenesis. This could be blocked or reversed by MEK inhibition, suggesting that MLK3 was signalling through the ERK pathway to mediate these effects (Hartkamp *et al.*, 1999).

MLK3 is important in the maturation to a malignant phenotype in breast cancer; specifically it is required for proliferation, migration and metastasis of breast cancer cells (Chen *et al.*, 2010; Chen and Gallo, 2012; Cronan *et al.*, 2012). MLK3 was found to be highly expressed in breast cancer cell lines, and knockdown or inhibition of the protein significantly impaired migration in 3D culture. Correspondingly, induction of MLK3 in poorly invasive breast cancer cells or normal breast epithelial cells promoted migration and proliferation (Chen *et al.*, 2010), while knockdown of MLK3 reduced migration and invasion of breast cancer cells towards chemokine ligand 12 (CXCL12) (Chen and Gallo, 2012). MLK3 signalling was shown to be responsible for activation of paxillin and subsequent dissociation of focal adhesions via negative regulation of RHO (RAS homologous protein), allowing increased migration of breast cancer cells (Chen and Gallo, 2012). These effects could be blocked with a JNK inhibitor (Chen *et al.*, 2010; Chen and

Gallo, 2012), but not with MEK or p38 inhibitors (Chen and Gallo, 2012), implying that MLK3 signals through the typical JNK pathway to promote migration. Knockdown of MLK3 in breast cancer cells has also been shown to reduce proliferation and promote apoptosis (Cronan *et al.*, 2012). In xenograft mouse models using metastatic breast cell lines, knockdown of MLK3 significantly reduced metastasis in two separate studies (Chen and Gallo, 2012; Cronan *et al.*, 2012) and decreased growth of the primary tumour in one of these studies (Cronan *et al.*, 2012). The evidence indicates that MLK3 acts in a pro-migratory manner in breast cancer, and may also have an anti-apoptotic role. The fact that MLK3 acts through the JNK pathway contradicts the proposed tumour suppressive role of JNK in breast cancer (reviewed in Bubici and Papa, 2014). The phenotypically distinct subtypes of breast cancer could potentially explain this apparent conflict; the majority of the cell lines used in these MLK3 studies were invasive carcinoma lines characterised as claudin-low (Prat *et al.*, 2010; Prat *et al.*, 2013). It may be that the pro-migratory role of JNK is co-opted in invasive breast cancer settings.

Similarly in gastric cancer MLK3 has been shown to be involved in the migratory response to gastrin stimulation. This also occurs via JNK pathway activation and involves expression of the matrix metalloprotease MMP7 that breaks down the extracellular matrix (ECM) to enable cancer cell invasion (Mishra *et al.*, 2010). In addition, MLK3 mutants found in gastric cancer had a greater transforming potential than the wild-type protein, and cells expressing these mutants formed invasive tumours in a xenograft mouse model (Velho *et al.*, 2010).

Recent studies have pointed to a role for MLK3 in ovarian cancer and melanoma (Zhan *et al.*, 2012; Zhang *et al.*, 2014). MLK3 was highly expressed in three ovarian cancer cell lines compared to immortalised normal controls and this corresponded with increased levels of phospho-MLK3. Knockdown of MLK3 reduced invasion, which was associated with reductions in activation of ERK and JNK as well as expression of MMPs (Zhan *et al.*, 2012). In melanoma, MLK3 was found to be upregulated in metastatic tumours as compared to primary melanomas, and in melanoma cell lines as compared to a normal control. Knockdown of MLK3 in cell lines reduced viability and invasion, and this was associated with a reduction in activated MKK7 and cJUN. In this case, overexpression of MLK3 appeared to be mediated by downregulation of a microRNA, miR-125b, that targets MLK3 (Zhang *et al.*, 2014). Overall, the role for MLK3 in breast cancer invasion is convincing, and recent evidence suggests it may have a pro-metastatic role in other cancer

types including gastric, ovarian and melanoma.

MLK4 mutation has been identified in 7% of colorectal cancer (Martini *et al.*, 2013; Marusiak *et al.*, manuscript accepted at Cancer Research); these mutations were proposed to be gain-of-function (GOF) and to promote tumourigenesis via activation of the ERK pathway (Martini *et al.*, 2013). However, work in our laboratory has shown that these mutations are LOF mutants that lose activity towards both the JNK and ERK pathways as compared to the wild-type kinase. Restoration of wild-type MLK4 into cells that harbour LOF mutants reduces proliferation *in vitro* and growth *in vivo*, and increases signalling through the MKK7–JNK–cJUN–p21/p15 pathway (Marusiak *et al.*, manuscript accepted at Cancer Research). Martini *et al.* based their assessment of these mutations on kinase assays comparing activity to that of the wild-type kinase; however, in this study the wild-type kinase construct showed the same level of activity as the kinase-dead, suggesting that there was an error in this construct and explaining why these mutants appeared to be GOF (Martini *et al.*, 2013). Recent data from my colleagues indicate that MLK4 colorectal cancer mutants are dominant-negative towards the wild-type kinase (Marusiak *et al.*, manuscript accepted at Cancer Research), which could account for the fact that expression of these mutants promoted tumour growth in xenograft models (Martini *et al.*, 2013). This new evidence suggests that MLK4 plays a tumour suppressive role in colorectal cancer.

1.5 Conclusions

The MAPK signalling cascade is not linear, but comprises a complex network of interacting proteins. The MLK family have a range of potential roles and protein interactions, and the dominant outcome of MLK signalling is likely dependent on a variety of factors, including cell type, cellular environment and disease phenotype. MLKs act as MAP3Ks and evidence suggests they regulate a diverse range of processes including migration, apoptosis and mitosis. Overexpression of MLK3, the best studied of the MLK family, can cause activation of all three MAPK pathways – ERK, JNK and p38 (Hartkamp *et al.*, 1999; Kim *et al.*, 2004). Its role in activating the JNK pathway is well established; however, its effect on the ERK pathway is not well defined and conflicting results have been seen. It seems likely that the main role for MLK3 is in activation of the JNK pathway, but that this MAP3K is able to signal through the other MAPKs in response to certain stimuli (Rana *et al.*, 2013). It is important to note that response to a particular

agonist is intricately fine-tuned through complex networks of protein interactions, and that intensity and duration of a signal also have important impacts on the cellular outcome. In this way, a cell is able to respond specifically to a range of stimuli. Together with the varying effects of MLK signalling in different tissue types, this can help to explain the divergent role for MLKs in both apoptotic and growth-promoting pathways.

2 Materials and Methods

2.1 Buffers and solutions

- **4x reduced SDS sample buffer**: 25% 1M Tris HCl (v/v, Invitrogen), 8% SDS (v/v, Gibco), 40% glycerol (v/v, Invitrogen), 0.008% bromophenol blue (w/v, Bio-Rad), 20% β-mercaptoethanol (v/v, Bio-Rad) in ddH_2O, adjusted to pH 6.8
- **PBS (phosphate buffered saline):** 8gm/l sodium chloride, 0.2g/l potassium chloride, 1.15g/l disodium hydrogen phosphate and 0.2g/l potassium dihydrogen phosphate, pH 7.3 (made by Cancer Research UK Manchester Institute (CRUK-MI) Lab Services)
- **PBST**: 0.05% Tween20 (Fisher) in PBS
- **Kinase buffer:** 10x kinase buffer (Cell Signaling, comprises 25mM Tris-HCl (pH 7.5), 5mM β-glycerophosphate, 2mM dithiothreitol, 0.1mM Na_3VO_4, 10mM $MgCl_2$) in ddH_2O
- **LB (Luria-Bertani) Broth:** 10μg/l tryptone, 5g/l yeast extract, 10g/l NaCl. Becton Dickson 244610, reconstituted and autoclaved by CRUK-MI Lab Services
- **LB Agar:** As LB Broth but with 1.5% Bacto Agar (Becton Dickinson 214030) added prior to autoclaving (CRUK-MI Lab Services)
- **Lysis buffer**: 10x cell lysis buffer (Cell Signaling, composed of 20mM Tris-HCl (pH 7.5), 150mM NaCl, 1mM Na_2EDTA, 1mM EGTA, 1% Triton, 2.5mM sodium pyrophosphate, 1mM β-glycerophosphate, 1mM Na3VO4, 1μg/ml leupeptin) in ddH_2O supplemented with protease inhibitor tablet (Roche)
- **Running buffer:** 10x TGS (Bio-Rad, 25mM Tris, 192mM glycine, 0.1% SDS) in ddH_2O
- **Transfer buffer:** 10x TG (Bio-Rad, 25mM Tris, 192mM glycine) in ddH_2O with 20% methanol (Fisher)
- **Tris-acetate-EDTA (TAE) buffer:** 50x TAE buffer from Fisher Scientific. Includes 40mM Tris, 20mM acetic acid, 1mM EDTA, pH 8.4. Diluted to make a 1x solution with water.

2.2 Molecular cloning and mutagenesis

2.2.1 DNA constructs

MLK1 in pCMV6-Entry vector was purchased from OriGene and transformed into XL1-Blue *E. coli* cells (Stratagene). DNA was purified using a Qiagen Miniprep Kit, according to manufacturer's protocol. Primers designed to add *att*B sites to the MLK1 gene were used in a polymerase chain reaction (PCR) with Platinum Pfx polymerase (Invitrogen) to amplify the gene. The product was run on a 0.8% agarose gel with Nancy-520 (Sigma Aldrich), the band cut out and extracted using a gel extraction kit (Qiagen, according to manufacturer's instructions). The gene was cloned into the pDONR221 vector by BP clonase reaction (Invitrogen, as per section 2.2.2) and from here the Gateway technology system (Invitrogen) was used for cloning into destination vectors.

HA-tagged (pCDNA3HA, gift from Prof Alexandra Newton) and FLAG-tagged (pReceiver-M12, GeneCopoeia) destination vectors were converted into Gateway destination vectors by Dr Eleanor Trotter. This was achieved by ligating the *ccd*B gene and the chloramphenicol resistance gene, flanked with *att*R sites, into the multiple cloning site (MCS) of the vector. MLK1 was cloned into these vectors from pDONR221 using the LR clonase reaction (Invitrogen, as per section 2.2.2).

MLK2 and MLK3 were obtained in the form of an ORFExpress Gateway Plus shuttle clone (GeneCopoeia) and cloned into destination vectors by Dr Eleanor Trotter using the LR clonase reaction. MLK4 was purchased in the pReceiver-M12 FLAG vector (EX-T3732-M12, GeneCopoeia).

For LZK and SOX2 (sex determining region Y-box 2), Dr Eleanor Trotter prepared cDNA from RNA extracted from HEK293T cells. LZK and SOX2 were amplified up with primers including *att*B flanking regions and the BP clonase reaction used to insert LZK into pDONR221. From here the Gateway system was used for cloning into destination vectors, as described above.

A pcDNA3.1(+) vector (Invitrogen) was used as an empty vector control where required. All primers were obtained from Eurofins MWG and are listed in Appendix I. Primers were made up to 100μM with water, according to provided datasheet, then diluted 1:10 to make a 10μM working stock.

2.2.2 Recombination reactions

BP clonase reaction (Invitrogen) was used to clone constructs into the pDONR221 vector. Reaction mix was as follows: 100ng *att*B-flanked MLK1 PCR product, 150ng pDONR221, made up to 5µl with water. 2µl BP clonase reaction mix was vortexed and added to reaction mix. Tubes were incubated in a heat block set at 25°C for ≥1h before addition of 1µl 2µg/µl proteinase K. Tubes were incubated at 37°C for 10min.

LR clonase reaction (Invitrogen) was used to clone constructs from pDONR221 to destination vectors. Reaction mix was as follows: 75ng donor vector, 75ng destination vector, 1µl LR clonase reaction mix, made up to 5µl with water. Tubes were incubated in a heat block set at 25°C for ≥1h before addition of 1µl 2µg/µl proteinase K. Tubes were incubated at 37°C for 10min.

For both LR and BP, reaction mix was transformed into OmniMAX One Shot cells, as described in section 2.2.4.

2.2.3 Site-directed mutagenesis

Site-directed mutagenesis was conducted using an Agilent QuikChange II kit. All primers were designed using Agilent's QuikChange Primer Design Program and obtained from Eurofins MWG. Reaction mix contained the following: 2.5µl reaction buffer, 1µl 50ng/µl plasmid, 0.5µl forward primer, 0.5µl reverse primer, 0.5µl dNTPs, 5µl betaine, 15µl H2O, 0.5µl Pfu in PCR tubes. Samples were run on a Bio-Rad S1000 Thermal Cycler PCR machine through the following program:

- 1 cycle: 95°C, 30s
- 16 cycles:
    - 95°C, 30s
    - 55°C, 1min
    - 68°C 1min/kb of relevant plasmid length

After PCR, 1µl Dpn1 was added to reaction and tubes incubated at 37°C for 1–16h before transformation into XL1-Blue Supercompetent cells.

2.2.4 Bacterial transformation

XL1-Blue Supercompetent cells (Agilent) were used for bacterial transformations, except after clonase reactions (LR and BP), when One Shot OmniMAX cells (Invitrogen) were used.

Cells were thawed on ice and 50µl/tube aliquoted into chilled 15ml Falcon tubes. 5µl PCR reaction mix (only 1µl required if using miniprep DNA as concentration is higher) was added and tubes left on ice for 30min. Samples were heat shocked in a water bath at 42°C for 45s and then put on ice for 2min. 1ml pre-heated LB was added to each tube and shaken at 225rpm for 1h at 37°C. Tubes were then spun at 4000rpm for 2min, supernatant was poured off and cells resuspended in the remaining medium for plating on LB plate containing selection antibiotic. Plates were incubated overnight.

For One Shot OmniMAX cells, procedure was as described above except that 1µl reaction mix was added to each aliquot of bacteria, and heat shock step was conducted for 30s.

2.2.5 Production and verification of constructs

Single colonies of transformed *E.coli* were picked from selective plates and grown overnight in 5ml LB containing selection antibiotic (100µg/ml ampicillin for destination vectors or 10µg/ml kanamycin for entry vectors). 10µl of the culture obtained was spotted onto selective plates for growth overnight, and this was used for preparation of glycerol stocks once sequencing had confirmed that the construct was correct. DNA was prepared from the rest of the 5ml culture by Qiagen Miniprep Kit, according to manufacturer's protocol.

Once the constructs were verified, stored plates were used to grow larger culture volumes. Transformed *E.coli* was picked into 100ml LB containing the appropriate selection antibiotic and shaken overnight at 37°C. 1ml was taken from this for preparation of glycerol stocks containing 25% glycerol (Sigma Aldrich), which were stored at -80°C. The remainder was used for DNA purification using a Qiagen Maxiprep Kit, according to manufacturer's protocol.

Concentration and purity of constructs was determined using a NanoDrop ND-1000 spectrophotometer (Thermo Scientific). Sanger sequencing (conducted by CRUK-MI Molecular Biology Core Facility (MBCF) on an ABI3130xl 16 capillary system) was used to confirm that all constructs used had the correct sequence and were inserted into the correct vector. For sequencing, 1.5µl 10µM sequencing primer was added to 400ng DNA and made up to 12µl with water.

2.3 RNA analysis

2.3.1 RNA preparation

At the appropriate time after treatment, cells were lysed with 350µl RLT (lysis buffer) containing 1% v/v 2-mercaptoethanol (Bio-Rad). Lysate was passed through a needle several times to aid lysis. Removal of genomic DNA and preparation of RNA was then conducted using a Qiagen RNeasy kit according to manufacturer's protocol. RNA concentration and purity was measured with a ND-1000 spectrophotometer (NanoDrop Technologies).

2.3.2 Reverse transcription PCR (RT-PCR)

A Superscript III one-step RT-PCR system with platinum Taq DNA polymerase (Invitrogen) was used to set up reactions in PCR tubes as follows: 12.5µl reaction mix, 0.5µl forward primer, 0.5µl reverse primer, 1µl enzyme, and RNA (for quantities see relevant methods section), made up to a total of 25µl with RNase-free water.

Tubes were placed in a Bio-Rad S1000 Thermal Cycler PCR machine and run with the following programme:

- cDNA synthesis: 55°C, 30min
- Denaturation: 94°C, 2min
- Amplification (25–30 cycles, dependent on gene being analysed):
    - Denaturing: 94°C, 15s
    - Annealing: 55°C, 30s
    - Extension: 68°C, 1min
- Annealing: 68°C, 5min.

Samples were run on a 2% agarose (Sigma Aldrich) in 1x TAE buffer (Fisher) gel for 30min at 100V and visualised with Nancy-520 (Sigma Aldrich) gel stain under UV light, using a Bio-Rad ChemiDoc Imaging System.

2.4 Protein analysis

2.4.1 Collection of whole cell lysate and measurement of protein concentration

Cells were lysed on ice using cold lysis buffer. After ≥1h lysate was scraped or pipetted up and down, and added to a 1.5ml Eppendorf tube. Tubes were vortexed for 30s, and spun down at 14300rpm for 10min. Whole cell lysate was removed to a fresh Eppendorf tube.

Pierce Protein Assay was used to determine protein concentration of whole cell lysates. 10µl lysate was added to a 96-well plate along with a range of protein standards (Pierce). 150µl Reagent B was added to each well. The plate was shaken at room temperature (RT) for 1min then incubated for 5min before being read at 595nm on a Bio-Rad Plate Reader. A standard curve was constructed using results from the protein standards and the concentration of each sample was calculated from the formula of this curve. Lysates were normalised to the sample with the lowest concentration by addition of lysis buffer. 4x sample buffer was added before analysis by western blot as described in section 2.4.2.

2.4.2 Western blot analysis

Cell lysates or kinase assays were analysed by Western blotting as follows: after addition of 4x reduced SDS sample buffer, samples were incubated at 100°C for 5min. Proteins were separated in running buffer by sodium dodecyl sulphate-polyacrylamide gel electrophoresis (SDS-PAGE) (12% polyacrylamide gels, Bio-Rad), alongside a protein standards ladder (Bio-Rad) for estimation of molecular weights. Proteins were transferred in transfer buffer to a polyvinylidene fluoride (PVDF) membrane (Bio-Rad), which was dried before probing with primary antibody in 2% bovine serum albumin (BSA) (VWR) in PBST, for 1h at RT or 4°C overnight. Membranes were washed 3x in PBST (10min) before probing with secondary antibody in 2% BSA in PBST for 1h at RT, followed by 3x wash with PBST. All probes and washes took place on a shaker. Membranes were then incubated with Pierce enhanced chemiluminescence substrate (ECL) (Thermo Scientific), exposed to film (Amersham), and imaged using a developer. For densitometry, images

were scanned and ImageJ 1.45s (NIH) software used to compare the relative density of bands.

2.4.3 Phosphoarrays

Two different phosphoarrays were used: a phospho-kinase array and a MAPK array (both from R&D Systems). These contain antibodies that have been spotted in duplicate on nitrocellulose membranes. Samples were lysed using Lysis Buffer 6 that was supplied with the kits and protein concentration was measured as described in section 2.4.1. Protocols were as manufacturer's instructions. For a list of the antibodies on each array, see Appendix VI.

Briefly, the phospho-kinase array procedure was as follows: membranes were incubated for 1h with supplied blocking buffer. Diluted lysates containing equal protein concentration were then incubated with the membranes overnight at 4°C. Membranes were washed 3x for 10min with 1x Wash Buffer, then incubated with Detection Antibody Cocktail (in Array Buffer 2/3) for the relevant membrane on a shaker for 2h. Membranes were again washed 3x for 10min, and then incubated while shaking with Streptavidin-HRP in Array Buffer 2/3 for 30min at RT. Membranes were subjected to a final wash step 3x for 10min, then incubated with prepared Chemi Reagent Mix for 1min and exposed to film for 1–10min.

Procedure was similar for MAPK array, except that only one membrane is used per sample for this assay, so the Detection Antibody Cocktail was added to the lysates for overnight incubation instead of being a separate incubation step.

2.4.4 Antibodies

Antibody	Supplier	Product code	Dilution
pACC (S79)	NEB	3661	1:1000
ACC	NEB	3676	1:1000
pAKT (T308)	NEB	4056	1:1000
pAKT (S473)	NEB	9271	1:1000
AKT (pan)	NEB	2920	1:1000
pAMPKα (T172)	NEB	2535	1:1000
AMPKα	NEB	2603	1:1000
BRAF	Santa Cruz	sc-5284	1:1000
p-cJUN (S63)	NEB	2361	1:1000
pERK1/2 (T202/Y204)	NEB	9101	1:1000
ERK1/2	NEB	4695	1:1000
FLAG M2	Sigma Aldrich	F1804	1:10,000
GAPDH	NEB	2118	1:1000
pGSK3β (S9)	NEB	5558	1:1000
HA	Covance	BIOT-101L	1:1000
pIKBα (S32)	NEB	2859	1:1000
IKBα	Novus Biologicals	NB100-56507	1:1000
pJNK (T183/Y185)	NEB	4668	1:1000
LZK	Abcam	ab88482	1:1000
pMEK (S217/S221)	NEB	9121	1:1000
pMKK4 (S257/T261)	NEB	9156	1:1000
MKK4	NEB	9152	1:1000
pMKK7 (S271/T275)	NEB	4171	1:1000
MLK1	NEB	5029	1:1000
mouse	NEB	7076	1:10,000
p27	NEB	3686	1:500
p-p38 (T180/Y182)	Genway	GWB-2F3845	1:1000
p-p53 (S392)	NEB	9281	1:1000
p53 DO-1	Santa Cruz	sc-126	1:1000
PARP	NEB	9532	1:1000
pPRAS40 (T246)	NEB	13175	1:1000
PTEN	NEB	9552	1:1000
rabbit	NEB	7074	1:10,000
pRAPTOR (S792)	NEB	2083	1:1000
SOX2	Abcam	ab97959	1:1000
α-tubulin	Sigma Aldrich	T9026	1:10,000
pULK1 (S467)	NEB	4634	1:1000

2.5 Cell culture

2.5.1 Transfection

Transfections were conducted using the appropriate medium for each cell type, but without the inclusion of pen-strep.

2.5.1.1 Transfection with Attractene

Attractene (Qiagen) was used for transient overexpression of cDNA. Forward transfection was used, meaning the cells were transfected the day after seeding. DNA and Attractene were diluted in Opti-MEM (Invitrogen) and mixture was incubated for 15min before addition to cells. Quantities are specified in the relevant methods sections.

2.5.1.2 Transfection with DharmaFECT1

DharmaFECT1 (Dharmacon) was used for transfection of siRNA in 12-well plates. In one tube, DharmaFECT1 was diluted in 100µl Opti-MEM. In a separate tube, siRNA was diluted in 100µl Opti-MEM. Each was incubated for 5min before mixing, and then mixture was incubated for 20min before adding to cells. Quantities are specified in the relevant methods sections.

2.5.1.3 Transfection with Lipofectamine2000

Lipofectamine2000 (Invitrogen) was used for transient overexpression of cDNA by forward transfection. In one tube, 4µl Lipofectamine2000 was diluted in 100µl Opti-MEM. In a separate tube, 2.2µg cDNA was diluted in 100µl Opti-MEM. Each was incubated for 5min before mixing, then mix was incubated for 20min before dropwise addition to cells.

2.5.1.4 Transfection with Lipofectamine LTX

Lipofectamine LTX (Invitrogen) was used for transient overexpression of cDNA for hard-to-transfect cells by forward transfection. Transfection was conducted in 6-well plates. In one tube, 2.5µg DNA and 2.5µl PLUS Reagent were diluted in 125µl Opti-MEM. In a second tube, 10µl Lipofectamine LTX Reagent was diluted in 125µl Opti-MEM. Diluted DNA was added to diluted LTX Reagent and the tube incubated for 5min before dropwise addition to cells.

2.5.2 Assays

2.5.2.1 MTT viability assays

Viability assays were conducted using MTT (3-[4,5-dimethylthiazol-2-yl]-2,5-diphenyl tetrazolium bromide) (Sigma Aldrich In Vitro Toxicology Assay Kit). This assay measures the activity of mitochondrial dehydrogenases, which cleave the tetrazolium ring of MTT to form formazan crystals. Formazan crystals are then dissolved in MTT Solubilisation Solution (acidified isopropanol-based solution) and read on a spectrophotometer. For MTT assays, cells were plated in triplicate in 96-well plates. After the appropriate treatment and incubation time, medium was removed and replaced with fresh medium containing 10% MTT solution (Sigma Aldrich, one vial of MTT dissolved in 3ml Opti-MEM). Cells were incubated for 2.5h before removal of medium and resolubilisation in MTT Solubilisation Solution (Sigma Aldrich). Plates were shaken at RT for 5min and read at 595nm on a Bio-Rad iMark Microplate Reader.

2.5.2.2 Crystal violet staining

Crystal violet dye (N-hexamethylpararosaniline) stains nuclei and can be used to assess relative growth and survival after treatment (Gillies *et al.*, 1986). For crystal violet assays, medium was removed and plates washed on ice with cold PBS. Cells were then fixed in cold methanol for 10min on ice before staining with 0.5% crystal violet in 25% methanol. After 10min staining, plates were washed carefully with water several times, and left to dry overnight. 10% acetic acid was then added and the plates shaken for 20min at RT to

dissolve the crystal violet (Kueng *et al.*, 1989). 100µl was added to a 96-well plate and read at 595nm.

2.5.2.3 BrdU

BrdU (5-bromo-2'-deoxyuridine) staining was used to measure cellular proliferation using a Calbiochem kit. BrdU is incorporated in place of thymidine when cells replicate their DNA, and can be quantified via labelling with a specific antibody to BrdU. Cells were seeded in triplicate in 96-well plates. 'Blank' wells containing just medium with no cells were set up, as well as 'background' wells to which no BrdU solution was to be added. At the appropriate time after treatment, 20µl 1:2000 BrdU in fresh medium was added to each well (except background wells). After 24h with BrdU reagent, medium was removed and 200µl Fixative/Denaturing Solution added for 30min at RT. Fixative/Denaturing Solution was then removed and plates kept in the fridge for <1 week before analysis.

On the day of analysis, anti-BrdU antibody was diluted 1:100 in Antibody Dilution Buffer (1x PBS, 4% BSA, 1% Pen-Strep, 0.1% Gentamycin), and 100µl of this solution added to each well for 1h at RT. Wells were washed 3x with 1x Wash Buffer (made from dilution of 20x Wash Buffer: 20x concentrated solution of PBS and surfactant, with 2% chloroacetamide). Peroxidase Goat Anti-Mouse IgG HRP Conjugate was diluted according to the batch number (usually 1:2000) in Conjugate Diluent (1x PBS, 4% BSA, 1% Pen-Strep, 0.1% Gentamycin, 0.224% Amphotericin B) and 100µl added to each well for 30min at RT. Plates were washed 3x with 1x Wash Buffer and then the entire plate was flooded with ddH2O. Contents of well were removed by tapping on paper towels before addition of 100µl Substrate Solution (Tetra-methylbenzidine solution) and incubation in the dark for 15min at RT. 100µl Stop Solution (2.5N sulphuric acid) was then added to wells in the same order, and absorbance measured using a Bio-Rad iMark Microplate Reader at 450-595nm (within 30min of Stop Solution addition).

2.5.2.4 Cell cycle analysis

A propidium iodide-based assay was used for cell cycle analysis. Propidium iodide is a fluorescent molecule that intercalates into DNA and is used to measure DNA content. After appropriate treatment and incubation time, medium with floating cells was collected

to FACS (fluorescence-activated cell sorting) tubes and plates trypsinised with 1ml 1x trypsin per well. Trysinised cells were added to the FACS tubes with the medium that was previously collected, and the tubes spun for 3min at 2000rpm. Supernatant was discarded and 1ml pre-chilled ethanol added dropwise to each tube while vortexing. Cells were kept at -20°C until analysis.

Prior to staining, tubes were spun for 5min at 2000rpm, and the supernatant discarded. 1ml PBS was added, tubes spun again at 2000rpm for 5min, and the supernatant discarded. BD Cycletest Plus DNA Reagent Kit was used for sample staining. 250µl Solution A (trypsin buffer) was added to each tube and mixed gently by tapping by hand. Tubes were left for 10min at RT before addition of 200µl Solution B (trypsin inhibitor and RNAse buffer) and mixed by tapping. Tubes were again incubated for 10min at RT before addition of 200µl cold Solution C (propidium iodide solution). Tubes were incubated for 10min in the dark in the fridge. Samples were kept in the dark at 2–8°C until analysis within 3h on a BD 3-colour FACSCalibur. Results were analysed using FlowJo.

3 Part One: MLKs mediate resistance to RAF inhibitors

3.1 Abstract

Metastatic melanoma is a form of skin cancer that displays a particularly aggressive and malignant phenotype. Over 50% of melanoma cases involve mutation of the BRAF protein, and of these more than 90% carry the amino acid substitution V600E. This is an activating mutation that results in constitutive activation of the MEK/ERK pathway, promoting survival and proliferation. BRAF inhibitors such as vemurafenib initially give good results, with a high rate of objective response and improved survival rates; however, resistance develops after approximately six months.

Our data have demonstrated a novel mechanism of resistance to BRAF inhibition, mediated by the mixed lineage kinase (MLK) family of proteins. MLKs are MAP3Ks, which are known to activate the JNK pathway. My results showed that MLK1 could also directly phosphorylate MEK in an *in vitro* kinase assay. Consistent with these results, overexpression of MLK1 in various cell lines resulted in increased MEK phosphorylation, which was dependent upon a functional MLK1 kinase domain, leading to activation of the ERK pathway. Expression of MLK1 in melanoma cell lines harbouring $BRAF^{V600E}$ reactivated the ERK pathway and promoted cell survival despite treatment with BRAF inhibitors. Other members of the laboratory have shown that this was also the case for MLK2–4. Overexpression of MLK1 promoted resistance to RAF inhibitors in mouse models, while MLK2 contributed to acquired resistance in a cell line model. Furthermore, MLKs were found to be upregulated in nine of 21 melanoma patients with acquired drug resistance. Lastly, a majority of MLK1 mutations identified in patients were found to be gain-of-function mutations. In conclusion these results have demonstrated a potential new mechanism of resistance to BRAF inhibition in melanoma, via the reactivation of the ERK pathway by MLK1–4.

These data have been published as follows:

Marusiak, A. A., **Edwards, Z. C.**, Hugo, W., Trotter, E. W., Girotti, M. R., Stephenson, N. L., Kong, X., Gartside, M. G., Fawdar, S., Hudson, A., Breitwieser, W., Hayward, N. K., Marais, R., Lo, R. S. & Brognard, J. (2014) Mixed lineage kinases activate MEK independently of RAF to mediate resistance to RAF inhibitors. *Nature Communications,* 5**,** 3901.

3.2 Introduction: Melanoma and BRAF inhibitor resistance

3.2.1 The ERK pathway in melanoma

3.2.1.1 The ERK cascade

The ERK cascade is a MAPK pathway that leads to the transcription of genes that promote cell division, survival and growth; therefore mutations in this pathway are frequently implicated in tumourigenesis (Davies *et al.*, 2002). This pathway is stimulated by cytokines or growth factors, which bind to receptor tyrosine kinases (RTKs) on the cell surface, initiating receptor dimerisation. This allows autophosphorylation on cytoplasmic domain tyrosine residues, generating binding sites for adaptor proteins with SH2 (SRC homology 2) or PTB (phosphotyrosine-binding) motifs, such as GRB2 (growth factor receptor-bound protein 2). GRB2 is thus recruited to the membrane along with its binding partner SOS (son of sevenless), a guanine nucleotide exchange factor (GEF) that activates the GTP-binding protein RAS. GTP-bound RAS recruits and binds to RAF proteins at the plasma membrane through the RAS binding domain, promoting dimerisation and activation of RAF (reviewed in McKay and Morrison, 2007). Activated RAF isoforms go on to phosphorylate MEK (a dual specificity Ser/Thr and Tyr kinase) on Ser218 and Ser222 in its activation loop (Yan and Templeton, 1994). Phospho-MEK (pMEK) phosphorylates ERK at Thr202 and Tyr204 within its activation loop, resulting in activation and translocation of ERK to the nucleus where it regulates transcription of target genes by phosphorylation of transcription factors including MYC, CREB (cAMP response element binding protein), cFOS (FBJ murine osteosarcoma viral oncogene homologue), ETS1 (E26 oncogene homologue 1) and ELK1 (ETS-like gene 1) (reviewed in Wortzel and Seger, 2011).

3.2.1.2 BRAF and melanoma

Metastatic melanoma is a form of skin cancer that displays a particularly aggressive and malignant phenotype. Over 50% of melanoma cases involve mutation of the BRAF protein, and of these more than 90% carry the amino acid substitution V600E, an activating mutation. Val600 resides close to the activation segment phosphorylation sites Thr598 and Ser601, and it is thought that the negatively-charged glutamate substitute acts in a phosphomimetic manner. This leads to constitutive activation; the mutant BRAF is over ten-fold more active than its WT counterpart *in vitro* (Davies *et al.*, 2002).

Consequent activation of the ERK pathway mediates proliferation (including cell cycle entry and progression), resistance to apoptosis, and invasion of melanoma cells. Inhibitors have been developed to target $BRAF^{V600E}$; these include PLX4032 (vemurafenib), which has been approved for use in the clinic by the United States Food and Drug Administration (FDA, 2012) and the European Medicines Agency (EMA, 2012). This drug initially provides clinical benefit, with a high rate of objective response (Flaherty *et al.*, 2010) and improved survival rates (Bollag *et al.*, 2010; Chapman *et al.*, 2011). However, resistance develops within 2–18 months, and relapse is inevitable (Flaherty *et al.*, 2010). As such there has been a major drive to find out what mechanisms of drug resistance occur in patients, and these are reviewed here.

3.2.2 Resistance to BRAF inhibitors

3.2.2.1 ERK pathway resistance mechanisms

Resistance mechanisms found so far have frequently involved changes in the RAS–RAF–MEK–ERK pathway, such as amplification of CRAF or of the BRAF mutant allele (Corcoran *et al.*, 2010), or activating mutations in one of the RAS isoforms. These all result in hyperactivation of the pathway. To date no 'gatekeeper' mutations in BRAF have been found in patient samples or cell lines. This is unusual, as mutations preventing drug binding within the target protein itself are a common mechanism of resistance to kinase inhibitors (Tuma, 2011). A mutation in BRAF at Thr529 was able to confer resistance when expressed in cell lines (Whittaker *et al.*, 2010), but this has not yet been observed in the clinic.

Alterations within the archetypal ERK signalling pathway that confer resistance involve activating mutation or amplification of one of its members. For example, expression of oncogenic RAS enables cells to proliferate in the presence of BRAF inhibitors (Johannessen *et al.*, 2010; Nazarian *et al.*, 2010) and NRAS mutations have been identified in post-treatment patient samples (Nazarian *et al.*, 2010). It is likely that RAS mutation acts by promoting CRAF activation, since activated RAS promotes dimerisation and transactivation of CRAF, enabling it to phosphorylate MEK. Furthermore, in the context of continued treatment with PLX4032, RAS mutations will hyperactivate the ERK pathway via the paradox effect, whereby inhibitor-bound RAF acts as a scaffold to promote activation of CRAF (Poulikakos *et al.*, 2010); this effect is discussed in section

3.2.3.

Elevated CRAF levels have also been shown to confer drug resistance (Montagut *et al.*, 2008; Johannessen *et al.*, 2010). It should be noted that 'selective' BRAF inhibitors such as PLX4032 in fact bind CRAF almost as efficiently as they bind mutant BRAF (Poulikakos *et al.*, 2010), but that an increase in CRAF levels can nonetheless mediate resistance by outnumbering inhibitor molecules, nullifying inhibition. Clinical trials have shown that over 80% inhibition of ERK phosphorylation is required to achieve tumour regression (Bollag *et al.*, 2010); this illustrates how upregulation of pathway members can be sufficient for resistance, by overwhelming the therapeutic drug level in cells.

Another mechanism of resistance involves a splice variant of $BRAF^{V600E}$, which was discovered in drug-resistant cell lines. $BRAF^{V600E}$ was aberrantly spliced leading to the exclusion of a sequence of exons that incorporate the RAS binding domain (RBD). Thus the protein can no longer bind RAS and is able to dimerise independently, leading to enhanced activation. Patient tumour samples were investigated and splice variants of $BRAF^{V600E}$ lacking the RBD were found in six of nineteen biopsies (Poulikakos *et al.*, 2011). Downstream of RAF, an activating point mutation in the drug-binding pocket of MEK1 was also able to confer resistance to both RAF and MEK inhibitors in cell lines. $MEK1^{F129L}$ possesses elevated kinase activity, possibly due to improved binding to CRAF, causing sustained pathway activation in the presence of inhibitors (Wang *et al.*, 2011). However, this has not yet been seen in patients.

A study by Johannessen *et al.* expressed a large library of kinase constructs in cells that are sensitive to PLX4720 (an analogue of PLX4032) to discover possible mediators of resistance. They found a protein (cancer Osaka thyroid (COT) kinase) outside of the typical RAS–RAF–MEK–ERK pathway that supports continued cell growth in the presence of inhibitor. COT is a MAP3K that can phosphorylate both MEK and ERK directly, allowing the cell to bypass the need for RAF proteins and enabling activation of the ERK pathway despite treatment with either RAF or MEK inhibitors. Inhibition of $BRAF^{V600E}$ by genetic methods or PLX4720 treatment led to an increase in COT protein levels in cells. Examination of a small number of patient samples showed that COT expression was moderately elevated in two of three tumour biopsies as compared to pre-treatment samples (Johannessen *et al.*, 2010). This supports the idea that increased COT may be a physiologically relevant mechanism of acquired resistance to BRAF inhibitors.

3.2.2.2 PI3K/AKT pathway resistance mechanisms

Some resistance mechanisms have been identified that do not rely on the ERK pathway. Instead they activate the PI3K/AKT pathway, which also promotes growth and survival and thus is often involved in tumourigenesis (Manning and Cantley, 2007; Brognard and Hunter, 2011). Activation of this pathway may allow for the continued growth of cancer cells despite inhibition of the ERK pathway (Gopal *et al.*, 2010). For example, AKT3 has a role in protecting cells from anoikis, a form of cell death caused by loss of proper interactions with the ECM. This is important in the development of a tumour to a malignant phenotype, as detachment from the ECM is required for invasion and eventual metastasis. Expression of active AKT3 partially protected cells from apoptosis induced by BRAF inhibition, and knockdown of AKT3 enhanced apoptosis of a PLX4720-resistant cell line on drug treatment (Shao and Aplin, 2010). However, these effects were not complete and this mechanism has yet to be proven clinically relevant.

Another study found that a panel of resistant cell lines had a variety of changes contributing to resistance, including elevated CRAF, RAS and pAKT. In this case, combination treatment with an AKT inhibitor reduced proliferation of the resistant cells (Su *et al.*, 2012a). Other mechanisms of resistance that are proposed to function via activation of AKT mostly involve elevated expression of receptor tyrosine kinases (RTKs), which is reviewed below.

3.2.2.3 Upregulation of RTKs

Other potential mechanisms include increased expression of RTKs, which can promote activation of both PI3K/AKT and ERK pathways. RTKs proposed to promote resistance to BRAF inhibitors include IGF1R (insulin-like growth factor 1 receptor) (Villanueva *et al.*, 2010), PDGFR(platelet-derived growth factor receptor)-α (Sabbatino *et al.*, 2014), PDGFRβ (Nazarian *et al.*, 2010) and EPHA2 (ephrin receptor A2) (Miao *et al.*, 2015).

Villanueva *et al.* generated drug-resistant cell lines in which IGF1R showed increased surface expression as compared to parental drug-sensitive cell lines. Analysis of pre-treatment and post-relapse samples from five patients revealed one sample in which IGF1R was higher post-relapse (Villanueva *et al.*, 2010). In a similar way, PDGFRβ overexpression has been proposed to confer resistance. This RTK also showed increased

expression in four out of 11 patient samples, as compared to the relevant pre-treatment biopsy (Nazarian *et al.*, 2010). However, in both these cases of RTK upregulation, inhibition of the receptor alone was not enough to cause cell death, simultaneous MEK inhibition was also required. In the Villanueva *et al.* study, CRAF was also elevated in resistant cell lines (Villanueva *et al.*, 2010). These studies suggest that ERK and PI3K/AKT can cooperate to promote proliferation, and that elevated IGF1R or PDGFRβ alone is insufficient to confer resistance. This highlights the critical role that the ERK cascade plays in melanoma, alongside the high frequency of activating mutations within this pathway (Davies *et al.*, 2002).

The EPHA2 RTK was also increased in PLX4032-resistant cell lines, and depletion or inhibition of this RTK partially restored sensitivity to the drug (Miao *et al.*, 2015). Inhibition of EPHA2 correlated with a reduction in phosphorylation of both ERK and AKT. Critically, increased expression of EPHA2 was detected in three of three patients who developed resistance to PLX4032, and one of three patients who developed resistance to a BRAF/MEK inhibitor combination. EPHA2 overexpression only confered partial resistance to PLX4032 (Miao *et al.*, 2015), and it is likely just one of the factors that contributes towards the resistant phenotype. Moreover, the importance of EPHA2 was not confined to the case of PLX4032 resistance, as inhibitors also caused apoptosis in cell lines and xenograft models that were sensitive to PLX4032 (Miao *et al.*, 2015). Furthermore, EPHA2 levels are elevated in both $BRAF^{V600E}$ and $BRAF^{WT}$ melanoma cell lines, and knockdown reduced viability of these lines (Udayakumar *et al.*, 2011). Thus it seems that EPHA2 may have a general role in melanomagenesis, and that further increased expression can reduce sensitivity to PLX4032. Combination treatment with BRAF and EPHA2 inhibitors is a promising treatment strategy that should be investigated further.

EGFR has also been shown to play a role in RAF inhibitor resistance. Increased levels of EGFR and phospho-EGFR were detected in resistant cell lines, including one derived from a xenograft model of drug resistance, as well as a resistant patient sample. Combination treatment with the EGFR inhibitor gefinitib and PLX4720 reduced growth of resistant cells both *in vitro* and *in vivo*. Exploration of downstream pathways indicated that increased EGFR correlated with an increase in activation of downstream SRC-family non-receptor tyrosine kinases including LYN, and treatment with the broad-specificity tyrosine kinase inhibitor dasatinib reduced growth of resistant cells *in vitro* and *in vivo*

(Girotti *et al.*, 2013). Expression of high levels of EGFR is the mechanism by which colorectal cancers avoid sensitivity to BRAF inhibitors (Corcoran *et al.*, 2012; Prahallad *et al.*, 2012), whereas expression of EGFR is relatively low in melanoma. Thus, an increase in EGFR levels is a feasible mechanism of resistance to RAF inhibition. Girotti *et al.* showed that a greater effect came from phospho-EGFR, and these increases were associated with elevated EGF (Girotti *et al.*, 2013).

Upregulation of several RTKs has been reported in BRAF inhibitor resistant cell lines and patient samples. In some cases, multiple RTKs were elevated in the same samples (Nazarian *et al.*, 2010; Sun *et al.*, 2014), and they could coordinate to activate the ERK and AKT pathways and reduce sensitivity of cells to BRAF inhibitors. For example, Sun *et al.* elucidated a mechanism of PLX4032 resistance in drug-resistant cell lines, in which knockdown of *SOX10* induced TGFBR2 (transforming growth factor beta receptor 2) expression, promoting a TGFβ signalling pathway that led to increased expression of a number of RTKs, including EGFR, PDGFRβ and ERBB3 (ERBB2 receptor tyrosine kinase 3). In this case, combination treatment of *SOX10*-knockdown cells with PLX4032 and the EGFR inhibitor gefitinib did not reduce proliferation. Instead combinatorial inhibition of the ERK and PI3K/AKT pathways was required to reduce cell survival (Sun *et al.*, 2014). The authors observed increased expression of EGFR in six of 16 patients that had progressed after treatment with BRAF or MEK inhibitors. Two of these patients showed reduced expression of *SOX10* suggesting that this could be a clinically relevant mechanism.

3.2.2.4 Innate resistance

Although PLX4032 has shown promising results compared to traditional chemotherapy, most of the patients only display a partial response, and complete responses are rare (Flaherty *et al.*, 2010; Chapman *et al.*, 2011). Two separate investigations have begun to elucidate a reason behind this limited response, which is proposed to be down to signals from the tumour microenvironment, specifically HGF (hepatocyte growth factor). Straussman *et al.* found that culturing melanoma cells in the presence of fibroblasts or fibroblast-conditioned medium abrogated response to PLX4720. Levels of HGF in culture conditions correlated with resistant phenotypes, and recombinant HGF enhanced proliferation despite PLX4720 treatment. Other RTK ligands, such as FGF1 (fibroblast growth factor 1) and EGF, could mediate some degree of rescue, but HGF was the only

one to restore ERK activation back to basal levels (Straussman *et al.*, 2012).

The findings of Wilson *et al.* confirm these results; they determined that HGF could induce complete or partial rescue of proliferation in ten of 18 melanoma cell lines (Wilson *et al.*, 2012). In both studies, HGF was the only factor tested that could activate both ERK and AKT (Straussman *et al.*, 2012; Wilson *et al.*, 2012), which can act cooperatively to promote growth. Dual inhibition of BRAF and MET, the RTK for which HGF is the ligand, prevented the resistance mediated by HGF (Wilson *et al.*, 2012) or stromal cell co-culture (Straussman *et al.*, 2012). Use of a xenograft mouse model showed that activation of MET with an agonistic antibody induced resistance to PLX4032 *in vivo* whereas inhibition of MET augmented the effects of BRAF inhibition (Wilson *et al.*, 2012).

Importantly, patients with high HGF expression prior to treatment displayed a significantly reduced response to PLX4032 (Straussman *et al.*, 2012; Wilson *et al.*, 2012) and a worse clinical outcome (Wilson *et al.*, 2012). These results indicate one of the reasons behind the variability seen in responses to BRAF inhibition, and provide a likely explanation for innate resistance to these drugs. It was also seen that after a short period of treatment five of ten patients had elevated expression of HGF (Straussman *et al.*, 2012). It was hypothesised that the heterogeneity of tumours could lead to subpopulations of cells with increased MET expression gaining a survival advantage, leading to expansion of this subset and thus resistance (Wilson *et al.*, 2012). In summary these results indicate that HGF-induced MET activation could be a commonly used mechanism to establish acquired resistance to BRAF inhibitors.

Other proposed mechanisms of intrinsic resistance involve altered regulation of BCL2 family members. For example, the anti-apoptotic gene *BCL2A1* (encoding BCL2-related protein A1) is amplified in ~30% of melanomas, and its expression in tumour samples is associated with reduced response to BRAF inhibition. Overexpression of BCL2A1 can protect cells from the apoptotic effects of PLX4720, while knockdown of the protein sensitised resistant cells to BRAF inhibition (Haq *et al.*, 2013). PTEN (phosphatase and tensin homologue) loss can also confer innate resistance in model systems. Cells with functional PTEN induced high levels of the pro-apoptotic BIM protein (BCL2-like 11) when treated with BRAF inhibitors. Conversely, cells that had lost PTEN showed increased AKT signalling, and less induction of BIM expression, although the clinical importance of this has not yet been demonstrated (Paraiso *et al.*, 2011).

3.2.3 Personalised medicine and the wild-type BRAF problem

There are several potential routes to BRAF inhibitor resistance, and more research needs to be conducted to determine the most effective treatment regimen in each case. For example, it has been shown that while BRAF inhibitors such as PLX4032 are effective at combating melanomas that harbour V600E mutations (Bollag *et al.*, 2010), these inhibitors actually promote growth and survival in tumours with wild-type (WT) BRAF and activating RAS mutations. This is associated with enhanced signalling through the ERK cascade (Flaherty *et al.*, 2010; Hatzivassiliou *et al.*, 2010; Heidorn *et al.*, 2010; Poulikakos *et al.*, 2010).

This initially seems paradoxical, as these inhibitors are ATP-competitive; they bind to the ATP binding site of RAF proteins, prohibiting binding of ATP itself. Since RAFs need to bind ATP in order to phosphorylate MEK downstream, the evidence that inhibitors promoted activation of the ERK pathway was confusing. Various groups have attempted to elucidate the mechanism behind this phenomenon and a general model has become clear. This model states that constitutively active RAS promotes dimerisation of RAF proteins, so that when inhibitor is added it binds one RAF protomer and causes transactivation of the other protein in the dimer (Fig. 2). This increases ERK signalling and thus promotes cell growth and survival. This phenomenon provided an explanation for the observation that 15–30% of patients treated with BRAF inhibitors develop skin carcinomas, 60% of which were found to harbour activating RAS mutations (Su *et al.*, 2012b). The exact mechanism of transactivation is not fully clear; it cannot occur via transphosphorylation due to the ATP-competitive nature of RAF inhibitors. Transactivation may involve allosteric effects due to conformational changes induced by inhibitor binding, or the loss of inhibitory transphosphorylation events (reviewed in Gibney *et al.*, 2013; Holderfield *et al.*, 2014).

Poulikakos *et al.* showed that treatment with low concentrations of a range of RAF inhibitors promoted ERK signalling in cells with WT BRAF, while at higher concentrations the inhibitors were capable of shutting down the pathway (Poulikakos *et al.*, 2010). In their study, knockout of BRAF had little effect whereas knocking out CRAF removed the ability of BRAF inhibitors to promote signalling. This tied in with the *in vitro* IC_{50} results for the inhibitor PLX4032, which showed that this compound inhibits CRAF better than WT BRAF, and nearly as well as it does $BRAF^{V600E}$ (Poulikakos *et al.*, 2010).

They also found that binding of inhibitor promoted the activating phosphorylation of CRAF. They therefore used a series of drug-sensitive and drug-resistant mutants of CRAF to demonstrate that inhibitors bind one protomer, causing transactivation of its partner protein. Mutants without the ability to dimerise did not show this transactivation, providing a convincing case for the above model (Poulikakos *et al.*, 2010). Furthermore, Hatzivassiliou *et al.* demonstrated that inhibitor treatment increased the growth rate of xenografts and proliferation of tumour cells in mice (Hatzivassiliou *et al.*, 2010), demonstrating the physiological relevance of these results.

Heidorn *et al.* agreed with the model of transactivation, although they stated that it is only selective BRAF inhibitors that have this effect (Heidorn *et al.*, 2010), whereas Poulikakos *et al.* found that this was true for a variety of RAF inhibitors. However, the Poulikakos *et al.* study showed that while pan-RAF inhibitors promoted the ERK pathway at low concentrations, they inhibited it at higher concentrations, presumably the point at which the majority of RAF proteins were inhibitor-bound (Poulikakos *et al.*, 2010). Heidorn *et al.* only used a high concentration of pan-RAF inhibitor (Heidorn *et al.*, 2010), explaining this apparent conflict and suggesting that all ATP-competitive RAF inhibitors would be capable of this effect. Supporting this hypothesis, ABL (Abelson tyrosine protein kinase) inhibitors that showed weak off-target binding to RAF proteins were also able to promote the paradox effect (Packer *et al.*, 2011).

Heidorn *et al.* also showed that a kinase-dead construct of BRAF promoted pathway activation in the same way as inhibitor treatment, suggesting that inactive BRAF acts as a scaffold to promote transactivation of CRAF. Importantly, when active KRAS and kinase-dead BRAF were induced in mouse melanocytes they cooperated to cause melanoma. The consequence of this is that other BRAF mutations found in cancer that were originally thought to be LOF actually act as GOF mutants in terms of activation of the ERK pathway (Heidorn *et al.*, 2010). These studies highlight the fact that selection of patients based on their tumour genotype is critical.

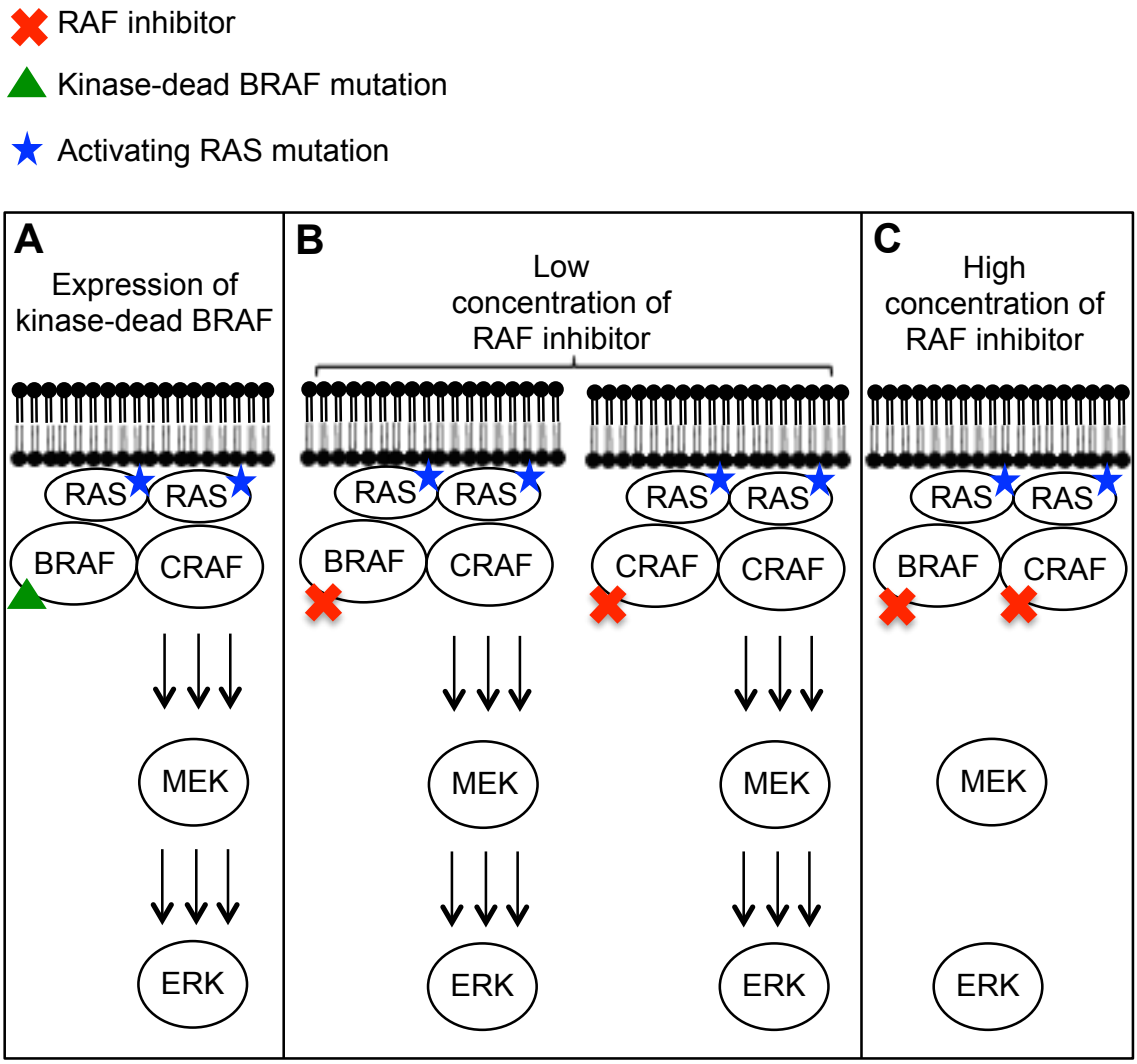

Figure 2: The paradox effect. Model to illustrate paradoxical activation of the MEK–ERK pathway in RAS mutant cells. Activating RAS mutations promote dimerisation of RAF proteins. **A:** Kinase-dead BRAF can drive CRAF activation in RAS mutant cells. **B:** At low concentrations, RAF inhibitors bind to one RAF protomer, leading to activation of the other promoter in the dimer and enabling enhanced activation of the MEK–ERK pathway. **C:** At high concentrations, RAF inhibitors can bind all RAF proteins, inhibiting MEK–ERK activation. Adapted from Gibney *et al.*, 2013.

Some of the identified RAF inhibitor resistance mechanisms, such as activation of RAS or elevated CRAF, induce activation of the ERK pathway via this paradox effect. In this case, continued treatment with PLX4032 can actually promote tumour growth. Inhibitors have therefore been developed that do not promote the paradox effect: so-called 'paradox-breaker' compounds. Paradox-breaking RAF-selective inhibitors were effective in cells that had developed resistance via RAS mutations (Le *et al.*, 2013) or BRAF splice variants (Basile *et al.*, 2014). Other next generation inhibitors that do not cause the paradox effect have been designed to inhibit BRAF, CRAF and SRC-family tyrosine kinases. These were effective in melanoma cells and xenografts with RAS mutations as well as $BRAF^{V600E}$. This included those that developed drug resistance through RAS mutations and

upregulation of RTKs which signal through SRC-family kinases (Girotti *et al.*, 2015).

More recently, a modification of the paradox effect model has been proposed, whereby RAF protomers normally inhibit their dimerisation partner via phosphorylation of the phosphate-binding loop (P-loop). Binding of a RAF inhibitor to one protomer prevents it from phosphorylating its dimerisation partner, relieving inhibition and allowing signalling downstream. Cells with mutations to alanine at P-loop phosphorylation sites exhibited higher basal ERK activation and were not subject to the paradox effect upon treatment with RAF inhibitors (Holderfield *et al.*, 2013). This model could explain both instances of paradoxical activation, as both kinase-dead BRAF and inhibited RAF would be catalytically inactive and thus unable to phosphorylate the other protomer in the dimer. However, it is difficult to reconcile these data with the existence of paradox-breaker RAF inhibitors, which inhibit the catalytic activity of RAF proteins without inducing the paradox effect. A possible explanation could be that paradox-breaker compounds function by preventing dimerisation of RAF proteins, but the exact mechanism of action of these compounds has not yet been elucidated.

3.2.4 Emerging targeted therapies

Many resistance mechanisms result in reactivation of the ERK pathway despite BRAF inhibition. For this reason clinical trials have been conducted to evaluate effects of the combination of BRAF and MEK inhibitors. Combinations tested include dabrafenib with trametinib (Sosman *et al.*, 2012; Long *et al.*, 2014; Robert *et al.*, 2015) and vemurafenib with cobimetinib (Ribas *et al.*, 2014). BRAF/MEK combination therapy reduces skin toxicity, improves response rates and enhances progression-free survival compared to single-agent therapy; however, resistance still develops eventually (Sosman *et al.*, 2012; Long *et al.*, 2014; Ribas *et al.*, 2014; Robert *et al.*, 2015) and no current treatment exists to address this issue. Of note, combination therapy is more effective in patients who have not previously been treated with BRAF inhibitors; those who have become resistant to BRAF inhibition are not as likely to respond to combination therapy. Thus this combination is best suited as a first-line treatment, and has now been approved for clinical use in this setting (Menzies and Long, 2014; Ribas *et al.*, 2014).

The recent development of ERK inhibitors (Aronov *et al.*, 2009; Morris *et al.*, 2013; Ward *et al.*, 2015) could potentially address the issue of resistance to the BRAF/MEK inhibitor

combination. For example, SCH772984 was found to be effective against BRAF and BRAF/MEK inhibitor-resistant cell and xenograft models, as well as against inhibitor-sensitive cells (Morris *et al.*, 2013). Clinical trials are currently underway to test some of these ERK inhibitors, including BVD523 and GDC0994 (ClinicalTrials.gov, 2015).

3.2.5 Conclusions

Clearly, there are several potential routes to BRAF inhibitor resistance, and research needs to be focused on common mechanisms that occur in a clinical setting. In the majority of cases resistance is associated with ERK pathway reactivation by a variety of mechanisms, including NRAS mutation, alternative BRAF splicing, and elevated levels of CRAF or COT kinase. The fact that BRAF inhibitor resistance is associated with reactivation of the ERK pathway suggested that combinatorial treatment with BRAF and MEK inhibitors might be effective. While this treatment delays the onset of resistance, patients still progress eventually on the combination treatment. Novel ERK inhibitors hold promise, as they are effective in models of resistance to BRAF/MEK combination; these are currently undergoing clinical trials. Alternatively, since the ERK and PI3K/AKT pathways can cooperate in the maintenance of a highly proliferative and malignant phenotype, it may be that co-inhibition of these pathways could provide a more long-term clinical response. Further research is required to elucidate the best treatment regimen for each resistance mechanism that occurs in the clinic.

3.2.6 MLKs and inhibitor resistance

Data generated by Dr Anna Marusiak and Dr Eleanor Trotter in this laboratory have indicated that some members of the MLK family are capable of the direct phosphorylation of MEK. Kinase assays proved that MLK3 and MLK4 could phosphorylate MEK1 *in vitro*, and overexpression of MLK3 or MLK4 in cells led to an increase in the levels of pMEK and pERK. On the other hand, ZAK could not phosphorylate MEK or activate the ERK pathway. It is therefore hypothesised that one or more members of the MLK family might be capable of mediating resistance to BRAF inhibitors, by bypassing the requirement for RAF proteins for ERK pathway activation (Marusiak *et al.*, 2014).

This project has characterised some of the remaining members of the MLK family, MLK1

and LZK, initially focusing on whether these proteins can mediate resistance to BRAF inhibitors in melanoma. In addition, a recent study found 15% of 85 cell lines from untreated melanoma patients had mutations in MLK1 (Stark *et al.*, 2012). If these mutants were GOF these patients might be inherently resistant to BRAF inhibition, making up part of the number of melanoma patients (~20–40% (Flaherty *et al.*, 2010; Chapman *et al.*, 2011)) that do not respond to PLX4032 treatment. These mutations have been characterised by overexpression to assess their activity.

3.2.7 Project aims

- Aim 1: Determine whether MLK1 and LZK can activate the ERK pathway in cells and phosphorylate MEK *in vitro*.
- Aim 2: For MLKs that can activate MEK–ERK, generate $BRAF^{V600E}$-positive melanoma cell lines with inducible expression of MLKs to assess whether the kinases can reactivate the ERK pathway and improve viability despite treatment with selective BRAF inhibitors.
- Aim 3: Make MLK1 melanoma mutants by site-directed mutagenesis (SDM) and investigate their activity towards the ERK pathway, to elucidate whether these are GOF or LOF mutations.

3.3 Materials and Methods

For general procedures, including molecular cloning, western blot and assay procedures please see section 2.

3.3.1 Cell culture

293T, A375 and MDA-MB-435 cell lines were obtained from ATCC. H157 and A2058 were kind gifts from Dr Phillip Dennis and Dr Geoff Margison. 293T and H157 cells were maintained in DMEM D6546 (Sigma Aldrich) supplemented with 10% foetal bovine serum (FBS) (Lonza), 1% pen-strep (Gibco, equivalent to 100Units/ml penicillin and 100µg/ml streptomycin) and 2mM L-glutamine (Gibco). A375, A2058 and MDA-MB-435 cells were maintained in RPMI 1640 + GlutaMAX (Gibco) with 10% FBS and 1% pen-strep. Incubation was at 37°C and 5% CO2. On reaching confluency, or when required for experiments, medium was aspirated and plates washed with sterile PBS (Sigma Aldrich) before being trypsinised (0.5% trypsin-EDTA (Gibco) in PBS) for 5min at 37°C.

3.3.2 Inhibitors

PLX4032, AZD6244 and Sorafenib were bought from Selleck Chemicals, L779450 and SP600125 from Merck, and U0126 from Cell Signaling. SB218078 was obtained from Santa Cruz Biotechnology. Inhibitors were dissolved in dimethyl sulphoxide (DMSO) (Fisher) and stored at -20°C. PLX4032 was used at 1µM, AZD6244 at 5µM, Sorafenib at 10µM, L779450 at 5µM, SP600125 at 20µM, U0126 at 5µM and SB218078 at 2µM. DMSO was the vehicle control.

3.3.3 Transient overexpression

For western blot analysis or kinase assays cells were seeded into 6- or 12-well plates. After 24h they were transiently transfected. Attractene was used for 293T and H157 cells (0.8µg DNA, 3µl Attractene in 80µl Opti-MEM for 12-well plates; 1.2µg DNA, 4.5µl Attractene in 100µl Opti-MEM for 6-well plates); see section 2.5.1.1 for Attractene protocol. Lipofectamine2000 was used for A375 and A2058 cells, see section 2.5.1.3 for protocol. After 48h cells were lysed on ice using cold lysis buffer (section 2.4.1). Where

required, inhibitors or DMSO control were added to cells 1h prior to lysis. Lysates were used for western blot analysis (section 2.4.2) or kinase assays (section 3.3.4).

3.3.4 Immunopreciptation and kinase assays

For kinase assays, FLAG-tagged constructs were transfected into cells in 6-well plates (section 3.3.3). Lysates were incubated with anti-FLAG M2 affinity beads (Sigma Aldrich) for 2h. Beads were washed 3x with lysis buffer and 2x with kinase buffer, before incubation (30min at 30°C) with 200μM ATP (Cell Signaling) and 0.5μg inactive MEK1 purified from baculovirus-infected insect cells (Carna).

3.3.5 Generation of tetracycline-inducible cell lines

Stable cell lines were generated by Dr Anna Marusiak, using the ViraPower HiPerform T-Rex Gateway Expression System (Invitrogen). Briefly, the protocol was as follows: 293FT cells (maintained in DMEM with 10% FBS, 4mM L-Glutamine, 1mM sodium pyruvate (Gibco) and 0.1mM non-essential amino acids (NEAA) (Gibco)) were transfected with MLK1 pLenti/TO/V5-DEST vector (converted from MLK1 in pDONR221 vector by LR clonase reaction, as section 2.2.2) or pLenti3.3/TR vector (for tetracycline repressor (TR) expression), using Lipofectamine2000. Lentiviral stocks were collected four days later. A375, Colo679 and A2058 melanoma lines were transduced with TR lentiviral stock, followed by MLK1 lentiviral stock. Cells expressing both constructs were selected for over ten days using 10μg/ml blasticidin (Invitrogen) and 500μg/ml geneticin (Gibco). Clones were expanded over 2–3 weeks before testing for inducible expression.

3.3.6 Experiments using tetracycline-inducible cells

3.3.6.1 Tetracycline

Tetracycline was supplied with the ViraPower HiPerform T-Rex Gateway Expression System kit (Invitrogen) used to generate tetracycline-inducible cell lines. Solution supplied was at 10mg/ml, this was diluted 1:10 to make working stocks for experiments. Tetracycline was used at 1μg/ml for induction of gene expression.

3.3.6.2 Western blot assays

Cells were seeded at 40,000/well in 12-well plates and incubated overnight before addition of 1µg/ml tetracycline where required.

For inhibitor treatment assays, cells were lysed 48h after seeding. PLX4032, L779450, Soranfenib, U0126 and AZD6244 inhibitors were added 1h before lysis. For the PLX4032/SP600125 assay, inhibitors were added 18h before lysis to ensure shutdown of the JNK pathway.

For BRAF knockdown, transfection with DharmaFECT1 (5µl in 12-well plates, see section 2.5.1.2), using 100nM BRAF SMARTpool siRNA (Dharmacon, Thermo Scientific) or negative control siRNA (Ambion), was conducted at the same time as cell seeding. Cells were lysed 48h later.

For PARP (poly ADP-ribose polymerase) assays, PLX4032 was added 24h after tetracycline and cells lysed 48h later.

3.3.6.3 MTT viability assays

Cells were seeded in triplicate at 2000/well into 96-well plates and incubated overnight. The following day tetracycline was added at 1µg/ml where required. After 24 hours inhibitors or DMSO were added. After four days medium was removed and plates analysed by MTT assay (see section 2.5.2.1).

3.3.7 Generation of PLX4032-resistant cells

Drug-resistant cells were generated by chronic treatment of A375 or MDA-MB-435 with 1µM PLX4032. Cells were treated daily and colonies picked after approximately 1 month. Clones were expanded into 12-well plates and then 10cm dishes for testing. Resistant cell lines were maintained in 1µM PLX4032.

3.3.8 Experiments with resistant cells

3.3.8.1 Inhibitor treatment

Cells were seeded at 40,000/well in 12-well plates and incubated for 48h. Inhibitor treatment with 1μM PLX4032 and/or 2μM SB218078 was for 1h prior to lysis.

3.3.8.2 Transient knockdown

Transient knockdown in MDA-MB-435 cells was conducted using DharmaFECT1 (5μl in 12-well plates, 0.5μl in 96-well plates), as section 2.5.1.2. MLK2 siRNA were purchased from Invitrogen (GGCUUUGAGCAUAAGAUCA) and Santa Cruz (sc-39111) and used at 100nM. Non-targeting negative control siRNA was from Ambion.

3.3.8.3 RT-PCR

RNA extraction and RT-PCR protocols are described in section 2.3. 500ng RNA was added for MLK2 and GAPDH (glyceraldehyde 3-phosphate dehydrogenase). 30 cycles of amplification were used for both genes. Primers detailed in Appendix I.

3.3.9 Statistics

Error bars shown on graphs represent ±standard deviation. Two-tailed Student's t-test (with unequal standard deviation assumed) was used to assess significance of differences between groups for assays.

3.4 Results

3.4.1 Overexpression of MLK1 activates the ERK and JNK pathways in cells

In order to elucidate the pathways activated by MLK1, an HA-tagged construct of this protein was overexpressed in 293T cells, which were chosen because they can be efficiently transfected and exhibit low endogenous MAPK activity. MLK1 expression led to increased phosphorylation of the expected downstream targets MKK4, MKK7 and JNK, as compared to the empty vector (EV) control (Fig. 3A). This was not the case for a kinase-dead (KD) construct of MLK1, made by SDM of the metal-chelating aspartate of the DFG motif (D294A), indicating that this was a kinase-dependent effect. On the other hand, only minimal activation of the p38 pathway was apparent. Tubulin was used as a loading control and demonstrates equal loading, while the HA blot shows MLK1 expression.

Expression of MLK1 also led to increased levels of phospho-MEK (pMEK) and pERK, again in a kinase-dependent fashion, suggesting that MLK1 can also activate the ERK pathway in cells. The ability of MLK1 to activate ERK opens up the possibility that this protein may be a route to resistance to BRAF inhibitors.

In conjunction with the KD construct described above, a kinase-active (KA) mutant was also prepared for comparison with WT MLK1, containing the mutation P496A. By alignment with MLK3, this residue is responsible for the autoinhibitory interaction with the SH3 domain that keeps MLK3 in its inactive conformation (Zhang and Gallo, 2001). However, for MLK1 this mutant did not appear to be any more active than the WT construct.

Work conducted in our laboratory by Dr Anna Marusiak and Dr Eleanor Trotter has shown that MLK2, MLK3 and MLK4 are also able to activate the ERK pathway (Marusiak *et al.*, 2014). MLK1–4 are all part of the MLK subfamily of proteins. The activity of LZK, one of the DLK subfamily, was also investigated by transient transfection in 293T cells. LZK activated JNK (Fig. 3B), unlike a KD mutant (K195M) made by mutation of the invariant ATP-binding lysine in the VAIK motif to a methionine. The latter is similar to lysine in size and shape, but without its positive charge, preventing interaction with the negatively-charged phosphates of ATP. This demonstrated that LZK activates JNK in a kinase-dependent fashion. However, it did not affect levels of pERK as

compared to MLK3, which was used as a positive control for ERK activation. This has also been shown to be the case for ZAK (work by Dr Eleanor Trotter), suggesting that activation of ERK by MLK family proteins is specific to MLK1–4 (Marusiak *et al.*, 2014).

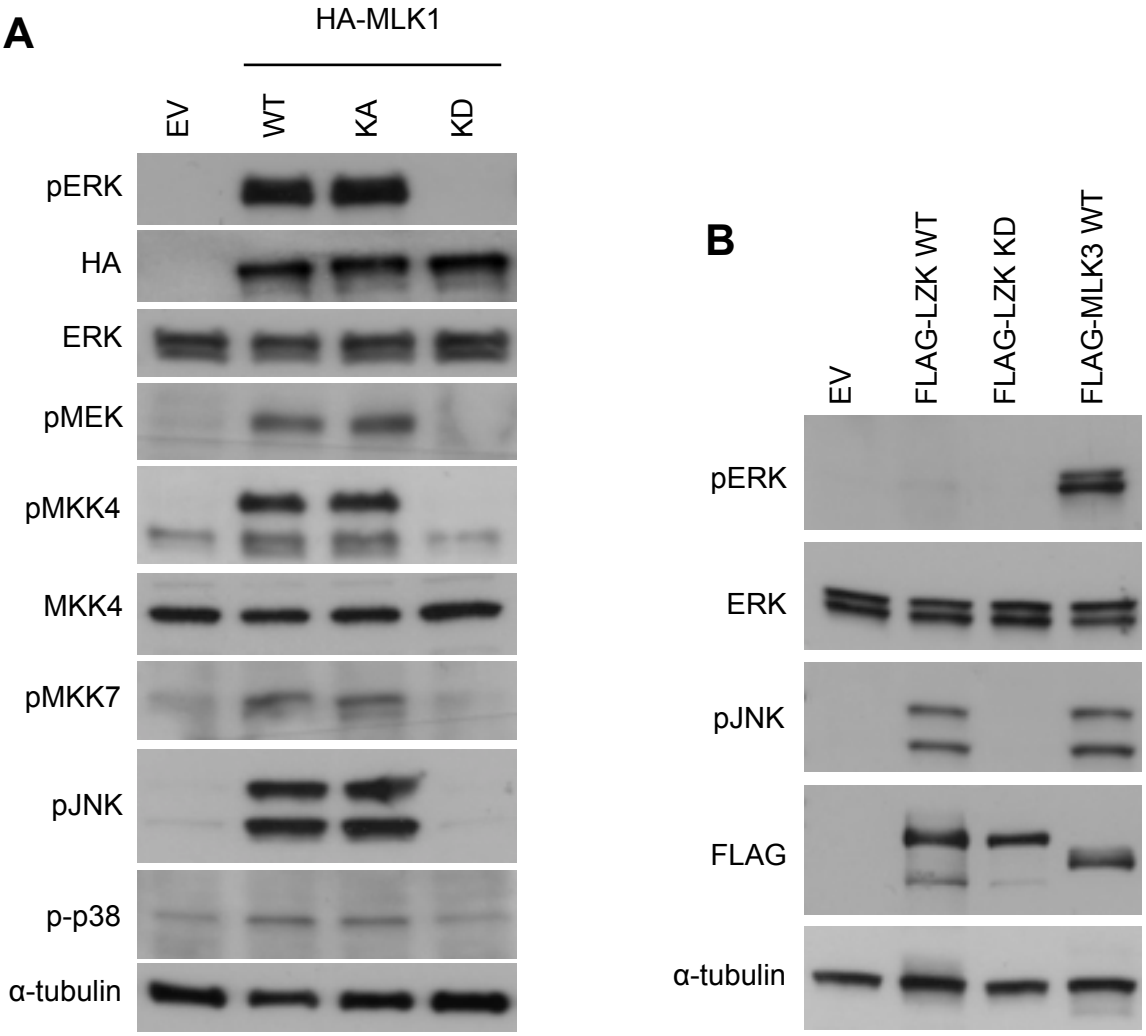

Figure 3: Activation of MAPK pathways by MLK family members. MLK constructs were overexpressed in 293T cells. Lysates were resolved by SDS-PAGE and analysed by western blot using antibodies for downstream MAPK components. α-tubulin was used to confirm equal loading. **A:** MLK1 WT (but not KD) activates the MKK4/MKK7–JNK and the MEK–ERK pathway. The HA blot demonstrates expression of MLK1. **B:** LZK activates the JNK pathway but not the ERK pathway, compared to MLK3 as a positive control.

3.4.2 MLK1 directly phosphorylates MEK

To determine the mechanism by which MLK1 activates the ERK pathway, a range of inhibitors were used to pinpoint the exact downstream targets. HA-MLK1 was overexpressed in 293T and H157 cells, and the cells treated with inhibitors for 1h before lysis. The pan-RAF inhibitor L779450 did not prevent the downstream phosphorylation of MEK or ERK upon increased expression of MLK1 (Fig. 4A – 293T cells; Fig. 4B – H157 cells), indicating that this occurred via a RAF-independent mechanism (experiment also conducted using sorafenib, another pan-RAF inhibitor – Fig. 4C). The MEK inhibitor U0126 (Fig. 4A–B; or AZD6244 – Fig. 4D) prevented the downstream phosphorylation of ERK, suggesting that MLK1 acts to phosphorylate MEK in cells, and does not act directly on ERK itself.

To confirm that MLK1 directly phosphorylates MEK, an *in vitro* kinase was performed in the presence of purified inactive MEK1. FLAG-MLK1 was overexpressed in 293T cells and immunoprecipitated using anti-FLAG beads for use in the assay. WT MLK1 directly phosphorylated MEK1, unlike the KD mutant (Fig. 4E). The 'no whole cell lysate' control proved that the inactive MEK1 had no autophosphorylation activity, while the EV control confirmed that phosphorylation of MEK1 was not due to proteins binding non-specifically to the anti-FLAG beads.

This assay was also conducted in the presence of either the pan-RAF inhibitor L779450 or the selective BRAF inhibitor PLX4032. Neither of these prevented the phosphorylation of MEK1 by MLK1, indicating that activation of the ERK pathway by MLK1 is a feasible method of resistance to BRAF inhibition. Inhibitors were either added to cells 1h before lysis (Fig. 4E) or added directly to the kinase assay, with identical results.

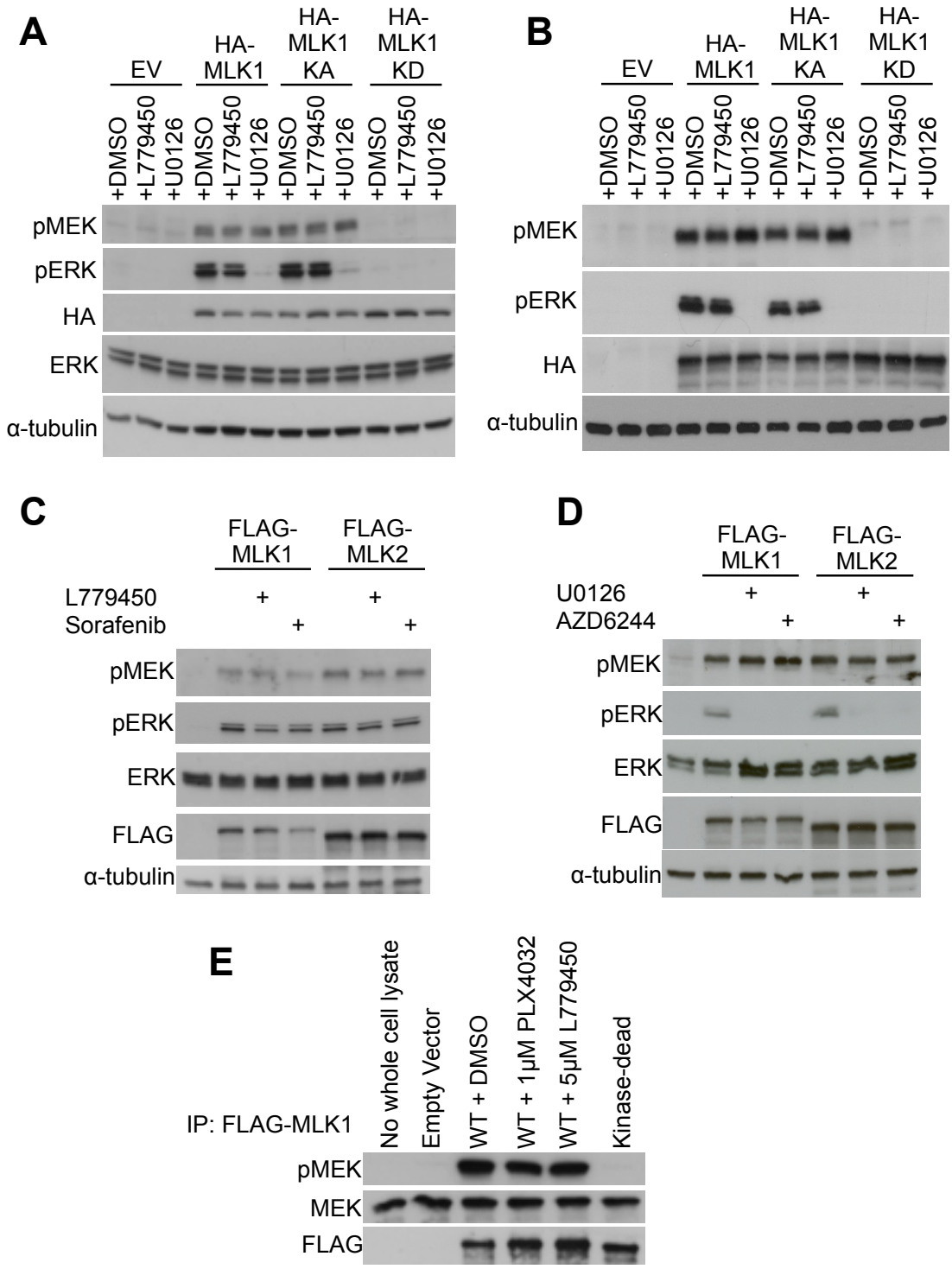

Figure 4: MLK1 acts at the level of MEK. A: After overexpression of HA-MLK1, 293T cells were treated with 5μM L779450 or 5μM U0126 for 1h before lysis. Pan-RAF inhibitor L779450 has no effect, whereas the MEK inhibitor U0126 prevents downstream activation of ERK, showing that MLK1 acts directly on MEK, and independently of RAF proteins. **B:** As (**A**) but with H157 cells. **C:** Overexpression of FLAG-tagged MLK1 or MLK2 in 293T cells, followed by treatment with 5μM L779450 or 10μM sorafenib for 1h. Pan-Raf inhibitors do not affect activation of ERK by MLK1 or MLK2. **D:** Overexpression of FLAG-tagged MLK1 or MLK2 followed by treatment with 5μM U0126 or 2μM AZD6244 for 1h. MEK inhibitors prevent activation of ERK by MLK1 or MLK2. **E:** MLK1 directly phosphorylates inactive MEK1 in an *in vitro* kinase assay. FLAG-tagged MLK1 WT or KD constructs were overexpressed in 293T cells, immunoprecipitated from lysates using anti-FLAG beads, and incubated with 200μM ATP and 0.5μg inactive MEK1. Treatment of cells with PLX4032 or L779450 before lysis does not prevent phosphorylation of MEK1 by MLK1.

3.4.3 MLKs mediate resistance to BRAF inhibitors in melanoma cell lines

3.4.3.1 Overexpression of MLK1 in melanoma cells reactivates the MEK/ERK pathway in the presence of PLX4032

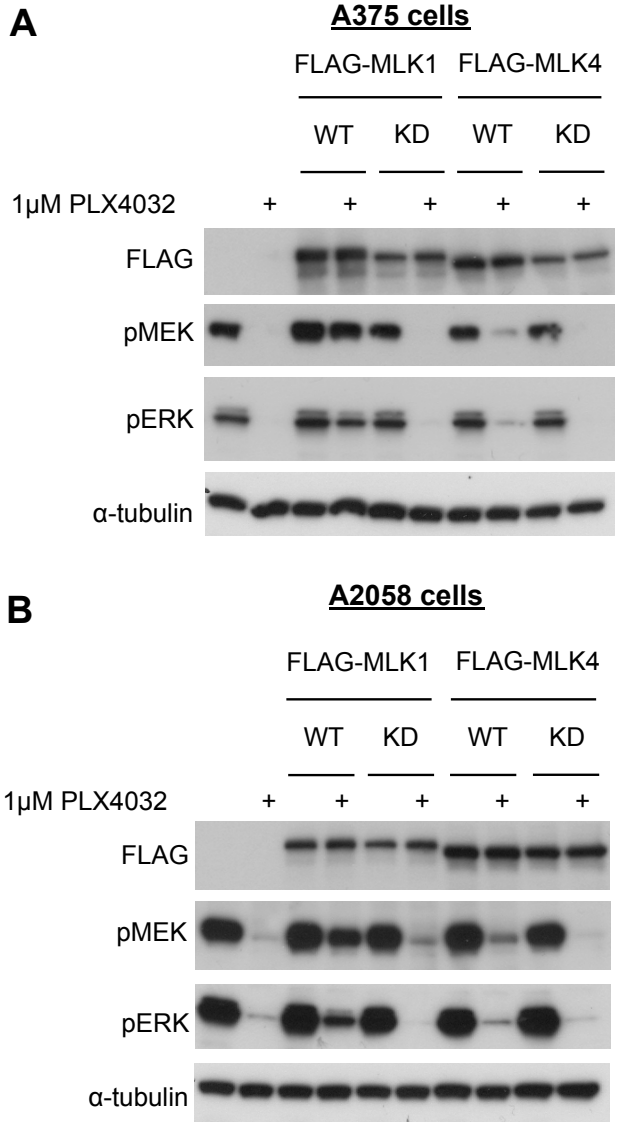

Figure 5: MLK1 rescues ERK activation after treatment with PLX4032. A: FLAG-MLK1 or -MLK4 WT or KD were transiently transfected into A375 melanoma cell lines. Treatment with vehicle control or PLX4032 was conducted 1h prior to lysis. PLX4032 abolishes pMEK/pERK, but expression of MLK1 or MLK4 rescues pathway activation. **B:** As (**A**) but using A2058 melanoma cells.

To test the hypothesis in a relevant expression system, FLAG-tagged MLK1 was transiently transfected into melanoma cell lines containing the $BRAF^{V600E}$ mutation (A375 and A2058 cells). Cells were treated with 1μM PLX4032 or DMSO vehicle control 1h before lysis. Basal activation of the ERK pathway was high in these cells, but phosphorylation of MEK and ERK was ablated by PLX4032 treatment. However, expression of MLK1 was able to reactivate the ERK pathway in the presence of RAF inhibitors (Fig. 5A – A375 cells, Fig. 5B – A2058 cells). This was also tested for MLK4,

which can also phosphorylate MEK and activate ERK. Expression of MLK4 did not enable the same level of reactivation of the pathway as compared with MLK1, suggesting that MLK1 may be more active towards the ERK pathway (Fig. 5). Consistent with previous results, expression of KD constructs (K151M for MLK4) could not activate the pathway.

3.4.3.2 Induction of MLK1 reactivates the ERK pathway, reduces apoptosis, and improves viability of melanoma cells despite BRAF inhibition

Stable cell lines with tetracycline-inducible expression of MLK1 were generated from A375 and A2058 melanoma cells. These were tested to ensure MLK1 could be induced, and to determine the effect of induction on MEK-ERK pathway activation. 1μg/ml tetracycline was added to cells 24h after seeding, and cells lysed 24h later. 1h before lysis cells were treated with 1μM PLX4032 or 5μM L779450. Induction of MLK1 expression upon tetracycline treatment was observed in both cell lines. Treatment with either inhibitor abrogated activation of the MEK–ERK pathway, but this effect was greatly diminished upon induction of MLK1 (Fig. 6A–B). To verify this finding, BRAF siRNA knockdown experiments were conducted in A375 cells. BRAF was efficiently knocked down, causing a reduction in pMEK; however, induction of MLK1 overcame this effect (Fig 6C).

MTT assays were then conducted to assess the effects of PLX4032 treatment and MLK1 induction in melanoma cells. Viability of cells was vastly reduced following PLX4032 treatment; however, MLK1 expression abrogated this effect and promoted near complete resistance (Fig. 6D). Reduced viability could be due to increased apoptosis of cells; this was assessed by PARP cleavage assay. Cleaved PARP was elevated when cells were treated with PLX4032, but on induction of MLK1 this effect was lost (Fig. 6E), indicating that MLK1 expression can mediate resistance to apoptosis caused by BRAF inhibition.

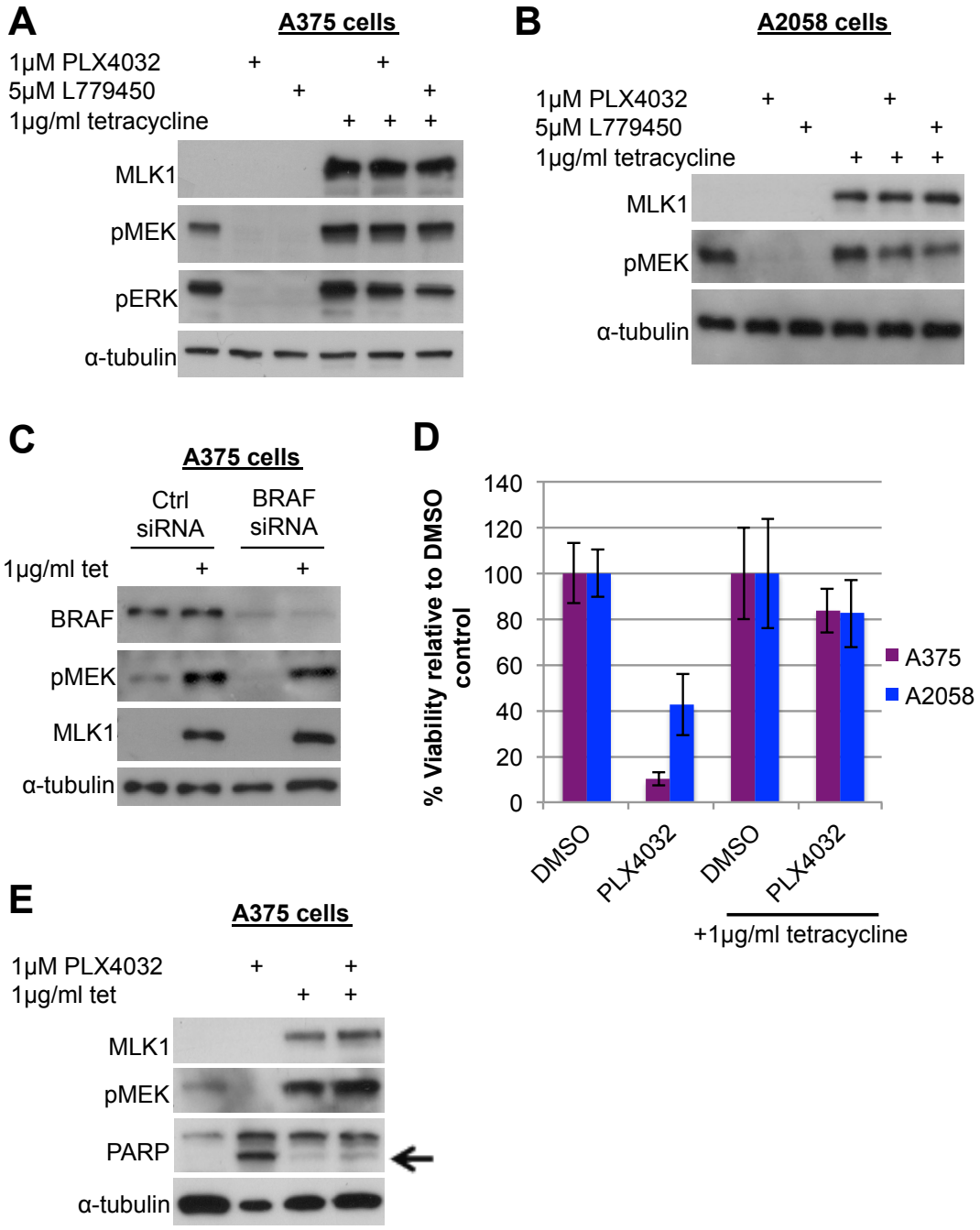

Figure 6: Induction of MLK1 reactivates ERK, reduces apoptosis, and improves viability of melanoma cells despite BRAF inhibition. A375 and A2058 cells with tetracycline-inducible MLK1 expression were generated. **A-B:** Induction of MLK1 rescues ERK pathway activation despite treatment with RAF inhibitors. Expression of MLK1 was induced by addition of 1μg/ml tetracycline 24h after cell seeding. 24h later cells were lysed and analysed by western blot. 1h prior to lysis cells were treated with 1μM PLX4032 or 5μM L779450. **A**=A375 cells, **B**=A2058 cells. **C:** MLK1 induction can rescue the ERK pathway after BRAF knockdown. Cells were transfected with BRAF or control siRNA, 1μg/ml tetracycline was added 24h later and cells lysed 48h after that. **D:** Induction of MLK1 improves viability of cells after treatment with PLX4032. Viability assessed by MTT assay after a four day incubation with inhibitors, and expressed relative to DMSO control cells. Graph shows average of three independent experiments, and error bars represent ±standard deviation. **E:** MLK1 induction can abrogate PARP cleavage induced by PLX4032. Cells were treated with PLX4032 for 48h prior to lysis. The arrow indicates cleaved PARP.

These data demonstrate that PLX4032 ablates activation of the ERK pathway, reduces viability, and promotes apoptosis in A375 and A2058 melanoma cells. However, tetracycline-induced expression of MLK1 in the presence of PLX4032 can rescue drug-induced cell death by reactivating the ERK pathway, improving overall viability. Dr Anna Marusiak conducted these experiments for MLK2–4, and obtained similar results showing that MLK2–4 can also promote resistance to PLX4032 in $BRAF^{V600E}$ melanoma cell lines (Marusiak *et al.*, 2014).

3.4.3.3 Activation of the JNK pathway is not responsible for rescue effects observed after MLK1 expression

Since MLK1 can also activate the JNK pathway, it is possible that the improvement in viability on MLK1 induction may be mediated via JNK. To test this hypothesis, an MTT assay was conducted in the presence of PLX4032 and a JNK inhibitor, SP600125. This inhibitor effectively shut down JNK activation that was increased due to tetracycline-induced MLK1 expression, preventing the downstream activation of cJUN (Fig. 7A). However, inhibition of JNK with SP600125 did not alter the viability of cells as compared to treatment with PLX4032 alone (Fig. 7B). Thus, the improvement of viability on MLK1 induction was not due to activation of the JNK pathway.

In agreement with previous results, high basal pMEK was abolished by treatment with PLX4032 (Fig. 7A, compare lane 2 with lane 1). Combination of SP600125 with PLX4032 did not further alter levels of pMEK (Fig. 7A, compare lane 3 with lane 2). When MLK1 expression was induced by tetracycline addition, activation of JNK and downstream cJUN was observed. As seen previously, MLK1 expression rescued MEK activation in the presence of PLX4032 (Fig. 7A, compare lane 5 with lane 2). Interestingly, SP600125 treatment led to a reduction in MLK1 expression; the reason for this is not known but it could be due to feedback regulation or off-target effects. This led to a decrease in pMEK levels as compared to the DMSO- and PLX4032-treated cells after MLK1 induction (Fig. 7A, compare lane 6 with lanes 4 and 5); however, pMEK levels were still sufficiently rescued to improve viability (Fig. 7B).

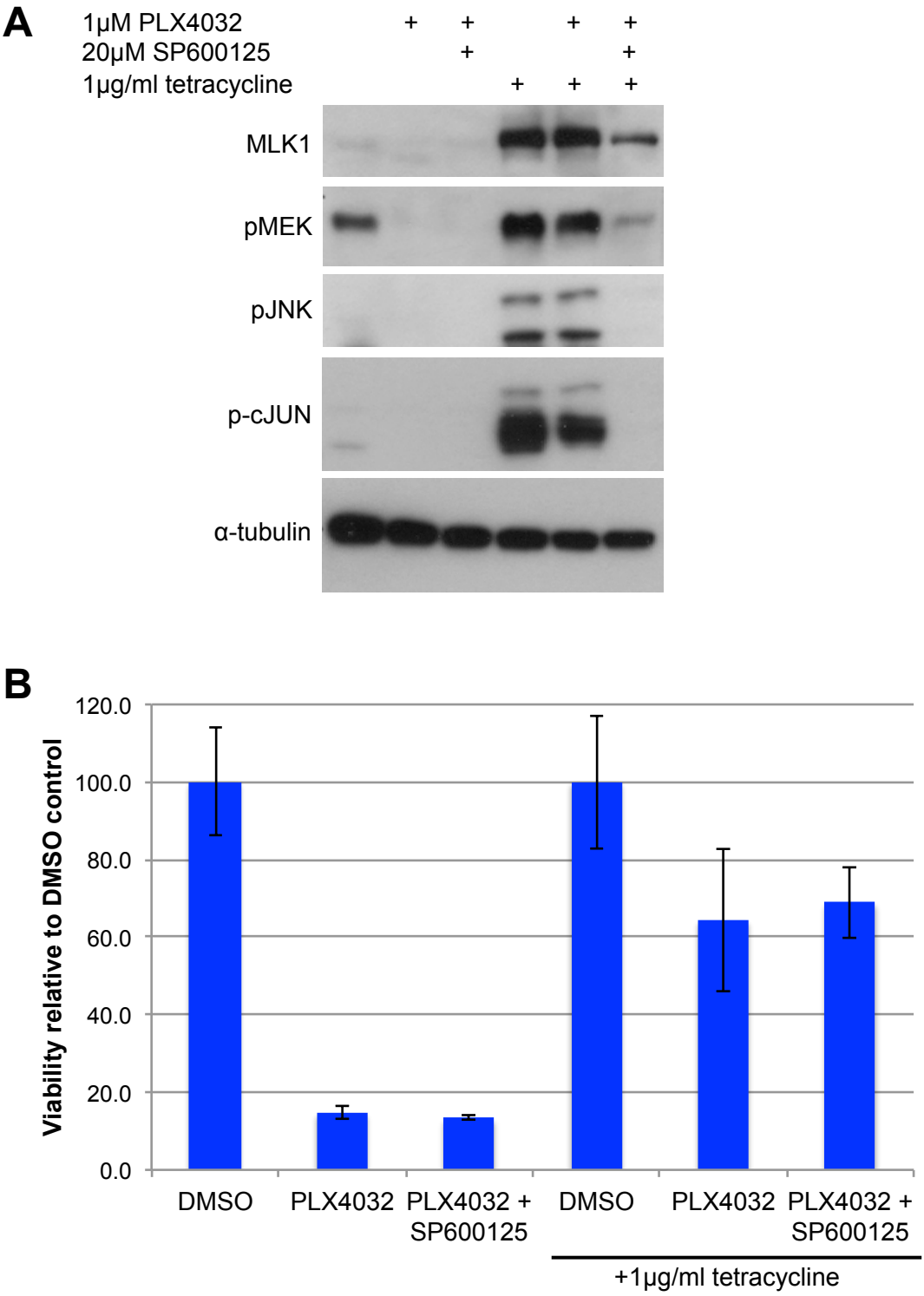

Figure 7: Rescue effect is JNK-independent. A375 cells with tetracycline-inducible MLK1 expression. **A:** The JNK inhibitor SP600125 effectively shuts down JNK signalling. 18h prior to lysis cells were treated with 1μM PLX4032 or 20μM SP600125. **B:** Induction of MLK1 improves viability of cells after treatment with PLX4032. Treatment with the JNK inhibitor SP600125 indicates that activation of the JNK pathway is not responsible for the rescue effects mediated by MLK1. Viability assessed by MTT assay after a four day incubation with inhibitors, and expressed relative to DMSO control cells. Graph displays average of 3 independent experiments and error bars represent ±standard deviation.

3.4.3.4 MLK2 promotes resistance to PLX4032 in MDA-MB-435 cell lines

Results shown so far have all involved overexpression of MLKs. Overexpression studies are a quick and useful tool to help determine the potential role of a protein in a particular aspect of cellular function. However, there are problems associated with this technique, mainly related to the large amount of protein expressed, which is unrepresentative of endogenous levels of an individual protein in a cell. This could lead to interactions being favoured that would not normally occur on a significant scale.

To determine whether MLKs could mediate resistance endogenously, resistant cell lines were generated from V600E-positive melanoma cell lines by chronic daily treatment with PLX4032. Resistant clones were selected from A375 and MDA-MB-435 melanoma lines and maintained in the presence of 1μM PLX4032. Depletion of MLK1–4 from resistant A375 clones had no effect on pERK, indicating that other resistance mechanisms occurred in this cell line (experiment performed by Dr Anna Marusiak, data shown in Marusiak *et al.*, 2014).

For the MDA-MB-435 parental line, PLX4032 treatment completely abolished pERK levels, whereas the resistant cells maintained high phosphorylated ERK despite drug treatment (Fig. 8A). Clones were initially screened for sensitivity to SB218078, a CHK1 (checkpoint kinase 1) inhibitor that was found to inhibit MLKs in a kinase inhibitor screen (Anastassiadis *et al.*, 2011). Kinase assays were conducted with immunoprecipitated FLAG-tagged MLK1 in the presence of inactive MEK1. Addition of 2μM SB218078 to the kinase assay inhibited phosphorylation of MEK1 by MLK1 (Fig. 8B).

SB218078 did not sensitise resistant A375 cells to PLX4032 (Marusiak *et al.*, 2014). However, when this compound was used on two MDA-MB-435 resistant clones (Res A and Res B) in combination with PLX4032, pERK levels were markedly reduced (Fig. 8A). siRNA knockdown was then used to investigate which, if any, of the MLKs might be involved. Knockdown of MLK1, 3 or 4 had no effect on pERK, but siRNA to MLK2 reduced ERK activation in both of the resistant cell lines (Fig. 8C). Knockdown of MLK2 also reduced viability of resistant cells as measured by MTT assay (Fig. 8D, work conducted by Dr Anna Marusiak), indicating that MLK2 plays a role in resistance to PLX4032 in these cells. The mechanism of this effect is not yet clear as no mutations were found in *MAP3K10* (MLK2) and expression was not increased at the mRNA level. It may

be that MLK2 was stabilised or activated upstream to lead to increased activity of the kinase, but this needs to be investigated further once functional MLK2 and phospho-MLK2 antibodies are available.

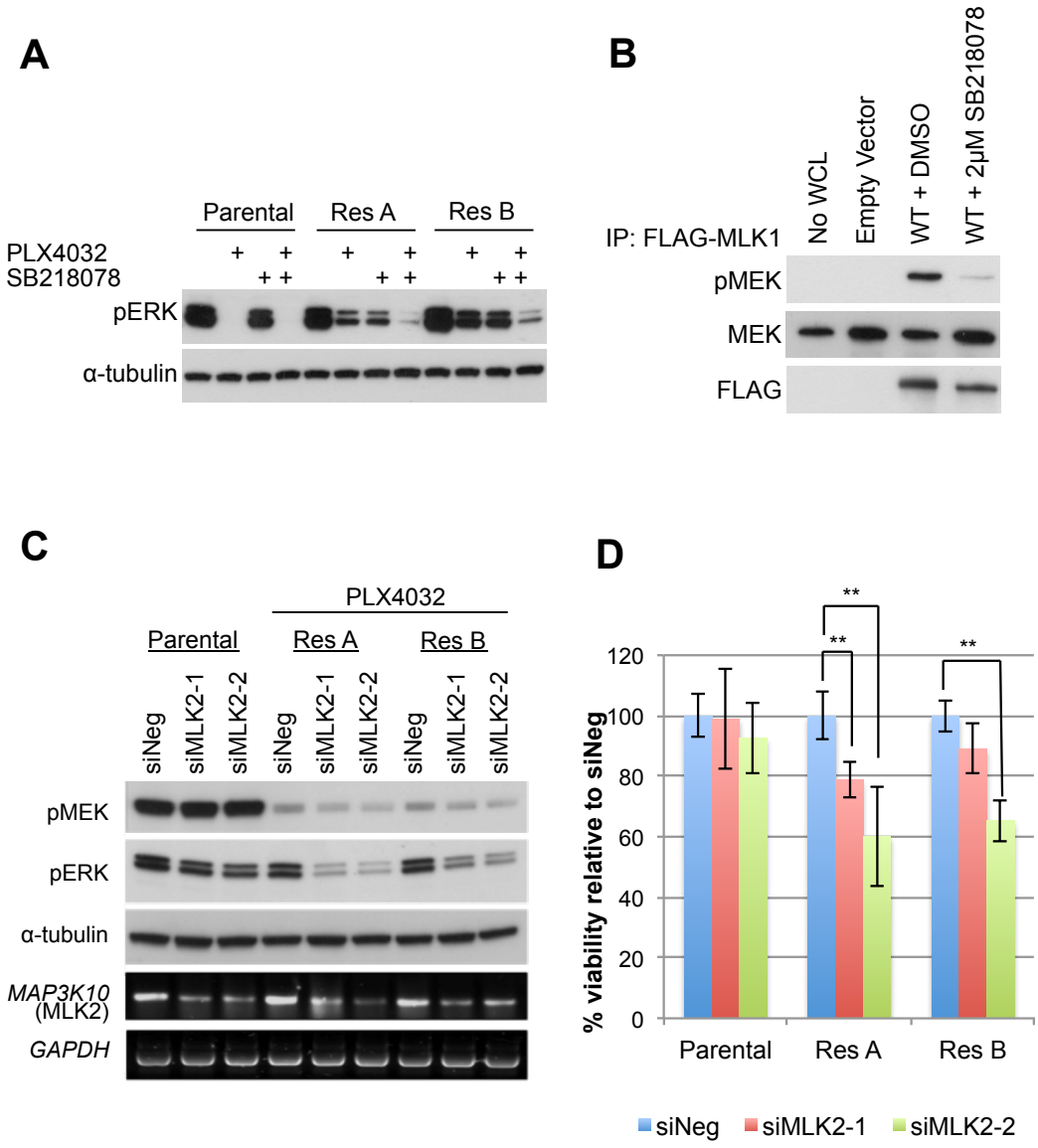

Figure 8: MLK2 contributes to BRAF inhibitor resistance in MDA-MB-435 cells. PLX4032-resistant MDA-MB-435 clones (Res A and Res B) were generated by chronic treatment with 1μM PLX4032. **A:** Resistant MDA-MB-435 are less sensitive to PLX4032 than their parental counterparts. Combination treatment with PLX4032 and SB218078 leads to a greater reduction in pERK levels. **B:** SB218078 can inhibit the activity of MLK proteins. Kinase assay with inactive MEK1 used with or without the addition of 2μM SB218078. Similar results obtained by Dr Ania Marusiak for MLK2–4. **C:** siRNA knockdown of *MAP3K10* (MLK2) reduces pERK levels in resistant cells. **D:** siRNA knockdown of MLK2 reduces viability in resistant cells. Error bars represent ±standard deviation. **two-tailed Student's t-test value of $p<0.05$. Experiment conducted by Dr Anna Marusiak.

3.4.4 MLKs mediate resistance to BRAF inhibitors in mouse models and patient samples (not my work, data shown in Marusiak *et al.*, 2014)

This study was followed up by our collaborators, who investigated the role of MLKs in xenograft models and patient samples. This work is summarised below for completeness of Part One of this thesis; the data are shown in the paper we published in Nature Communications (Marusiak *et al.*, 2014).

My results showed that MLK1 is capable of promoting resistance in cell lines, predominantly in artificial overexpression systems. This was also true for MLK2–4 (Marusiak *et al.*, 2014). To investigate whether MLK overexpression may have a physiological role in resistance to BRAF inhibitors, our collaborators assessed expression of MLK1–4 in patient samples before and after the development of resistance. RNAseq data from the dataset published by Rizos *et al.* were analysed and prepared by Dr Willy Hugo (Division of Dermatology, Jonsson Comprehensive Cancer Center and the University of California). Increased expression of MLKs was detected in 12 of 29 disease progression samples (nine of 21 patients), indicating it could represent a real mechanism of resistance to BRAF inhibitors (Marusiak *et al.*, 2014; Rizos *et al.*, 2014).

To determine whether increased expression of MLKs could mediate resistance *in vivo*, A375 cells with tetracycline-inducible expression of MLK1 were injected subcutaneously into nude mice. This experiment was conducted by Dr Maria Girotti (Molecular Oncology Group, CRUK-MI). Mice were treated with vehicle control or PLX4720 (an analogue of PLX4032 that was reported to have improved bioavailability in mice (Su *et al.*, 2012b)) after three days of tumour establishment. Mice treated with PLX4720 showed significantly reduced tumour growth as compared with the vehicle control group. Two groups were set up to simulate MLK1-induced resistance: an 'acquired resistance' group, which was fed with doxycycline diet from day eight; and a '*de novo* resistance' group, which was pre-treated with doxycycline diet from day one, prior to treatment with PLX4720. Both groups displayed significantly enhanced tumour growth as compared with PLX4720-treated mice, indicating that increased MLK1 expression can promote resistance to BRAF inhibition *in vivo*. A fifth group set up to assess the effects of overexpression of MLK1 alone, without PLX4720 treatment, exhibited reduced tumour growth compared with the vehicle control group. This could be due to pro-apoptotic JNK signalling

activated by overexpression of MLK1 in the tumours, or simply down to the toxic effects of protein overexpression (Marusiak *et al.*, 2014).

3.4.5 MLK1 mutations in melanoma

Recently, mutations in the *MAP3K9* (MLK1) gene were identified in melanoma cell lines and tumour samples (Stark *et al.*, 2012); these mutations were spread along the length of the protein (Fig 9A). Mutants were made by SDM and their impact on MLK1 function, specifically activation of ERK, was assessed by overexpression in H157 and 293T cells (Fig. 9B for H157 results, similar results obtained for 293T cells). Some of the mutations rendered the kinase less active than the WT protein; these were mostly within the kinase domain (P263L, R160C, A246V, E319K). However, several of the mutants led to increased pERK levels, notably D176N, S533Y, S616F, S650L and G769D, suggesting that they were more active in cells than the WT kinase. Densitometry was used to assess the activation of the ERK pathway by a selection of the most activating mutants relative to the WT kinase. This showed that some of these mutants were 1.5- to 2-fold more active towards ERK than WT MLK1 (Fig. 9C). These mutations may confer *de novo* resistance to BRAF inhibitors, or could even be drivers of melanomagenesis themselves. More research needs to be conducted to further characterise these mutants and assess their impact in an endogenous setting.

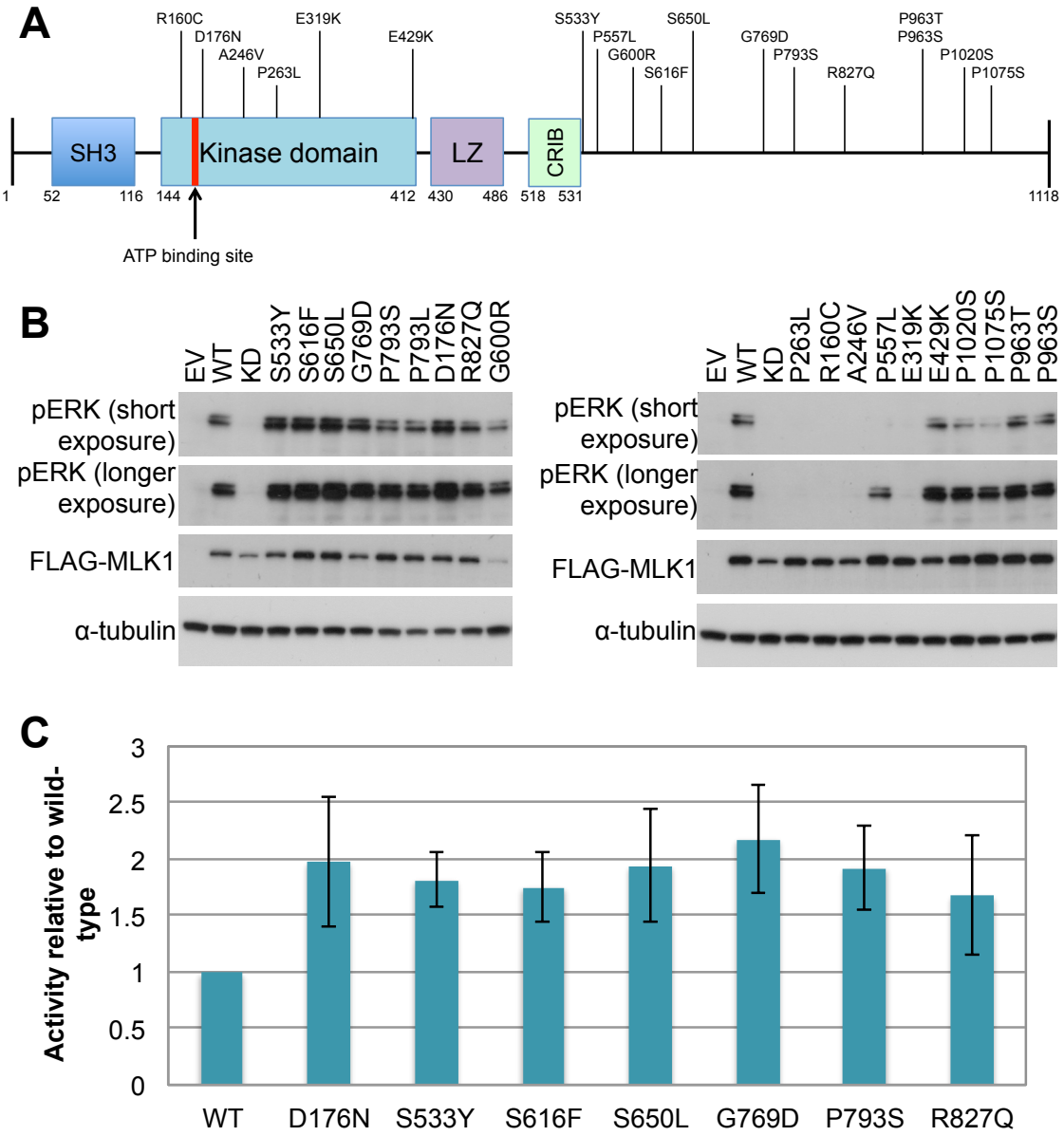

Figure 9: Activation of ERK pathway by MLK1 melanoma mutants. FLAG-tagged MLK1 melanoma mutants were overexpressed in H157 cells. **A:** Schematic representation of MLK1 showing where the mutations reside. **B:** Analysis of lysates by western blot. Some mutants are LOF, some GOF with respect to the ERK pathway. **C:** Activity of mutants towards the ERK pathway relative to wild-type MLK1, assessed by densitometry. Results are normalised for expression and loading. Graph shows average of 3 independent experiments, and error bars represent ±standard deviation.

3.5 Discussion

3.5.1 Overexpression of MLKs promotes resistance to BRAF inhibition in melanoma

MLK family members have been reported to activate the JNK and p38 pathways in response to certain stimuli. Some evidence has implicated MLK3 in activation of the ERK pathway, although results were conflicted as to whether this is a kinase-dependent effect (Hartkamp *et al.*, 1999), or whether MLK3 has a kinase-independent scaffolding function, via formation of a complex with BRAF and CRAF (Chadee and Kyriakis, 2004; Chadee *et al.*, 2006). Since our study commenced, MLK4 was also published to be able to phosphorylate MEK *in vitro* (Martini *et al.*, 2013), but the activity of MLK1 and MLK2 toward the MEK–ERK pathway has not yet been investigated. My results demonstrate that MLK1 can directly phosphorylate MEK1 (Fig. 4E), and activate the ERK pathway when expressed in cells (Fig. 3A). A KD construct of MLK1 did not display these effects, showing that this was a kinase-dependent mechanism of activation rather than a scaffolding effect. Pan-RAF inhibitors did not prevent the phosphorylation of MEK or ERK after MLK1 expression (Fig. 4A–C), demonstrating that this was a RAF-independent mechanism and further supporting the conclusion that MLK1 was not simply acting as a scaffold for RAF proteins. The use of MEK inhibitors prevented downstream activation of ERK (Fig. 4A–B,D), indicating that MLK1 acts on MEK in cells rather than directly on ERK itself. In contrast to MLK1, LZK overexpression did not activate the ERK pathway (Fig. 3B); this is consistent with previous reports (Ikeda *et al.*, 2001a).

The ERK pathway has a growth-promoting role in cells and is frequently upregulated in cancer. It appears to be particularly critical in melanoma development; half of metastatic melanomas are driven by the $BRAF^{V600E}$ activating mutation (Davies *et al.*, 2002), with NRAS mutations also common (20–30% of cases (cBio, 2015)). Selective inhibitors of $BRAF^{V600E}$, such as PLX4032, have improved survival rates for this disease, but within 2–18 months patients become resistant to these drugs and relapse (Flaherty *et al.*, 2010). Tumours from patients who develop resistance to BRAF inhibitors frequently display reactivation of the ERK pathway (Johannessen *et al.*, 2010; Nazarian *et al.*, 2010; Poulikakos *et al.*, 2011).

My results demonstrate that MLK1 could potentially mediate resistance to selective BRAF inhibitors in metastatic melanoma via reactivation of the crucial ERK pathway. The ability

of MLK1 to phosphorylate MEK and activate the ERK pathway was not affected by the presence of RAF inhibitors (Fig. 4); therefore this is a feasible means of resistance. Consistent with previous reports, my results confirmed that PLX4032 ablates activation of the ERK pathway, reduces viability, and promotes apoptosis in A375 and A2058 melanoma cells (Yang *et al.*, 2010a; Su *et al.*, 2012a). Expression of MLK1 in $BRAF^{V600E}$-expressing melanoma cell lines demonstrated that MLK1 was able to rescue ERK pathway activation, cell viability and cell survival after treatment with PLX4032 (Fig. 6). Moreover, xenograft data demonstrated that overexpression of MLK1 can promote resistance to PLX4032 *in vivo* (Marusiak *et al.*, 2014).

Experiments conducted in this laboratory have shown that MLK2, MLK3 and MLK4 were also capable of activating the MEK–ERK pathway and promoting viability despite the presence of RAF inhibitors (Marusiak *et al.*, 2014). It should be noted that MLK3 was one of the kinase ORFs (open reading frames) tested by Johannessen *et al.* in their screen for kinases capable of conferring resistance to selective BRAF inhibitors; however, it was not identified as a potential resistance mechanism (Johannessen *et al.*, 2010). The MLK3 construct used in the study was cloned in this laboratory and found to have an early stop codon at position 346 in the kinase domain. This produces a truncated protein, so it is unsurprising that this construct did not initiate downstream pathway activation. ZAK and DLK were also analysed by Johannessen *et al.*, but MLK1, MLK2, MLK4 and LZK were not part of the screen.

Data from a PLX4032-resistant melanoma cell line provide some evidence that MLKs could mediate endogenous resistance to BRAF inhibitors, as MLK2 was shown to contribute to resistance by reactivation of ERK (Fig. 8). Most compellingly, analysis of RNAseq data showed upregulation of MLKs in nine of 21 patients with disease progression after BRAF inhibitor treatment (Marusiak *et al.*, 2014). Fold-change increases seen for MLKs were similar to that observed for COT kinase, overexpression of which represents an established mechanism of resistance to BRAF inhibitors (Johannessen *et al.*, 2010). This supports the biological relevance of these data, and these patients may benefit from combined treatment with BRAF inhibitors and either MEK or MLK inhibition.

3.5.2 The JNK pathway and MLKs in melanoma

MLK family proteins, including MLK1 and LZK, are well characterised to activate the JNK pathway (Ikeda *et al.*, 2001b; Durkin *et al.*, 2004); my data confirm these results. The JNK pathway has a role in apoptosis under certain conditions. For this reason it was originally thought that JNK signalling would need to be lost for tumours to develop. MLKs activate JNK via MKK4/MKK7 (Teramoto *et al.*, 1996), and the majority of MKK4 mutations in cancer are LOF (Kan *et al.*, 2010; Ahn *et al.*, 2011); therefore it could be expected that MLK proteins would play a tumour suppressive role. However, JNK also has important roles in migration and proliferation, and particularly can promote invasive phenotypes and metastasis (Wagner and Nebreda, 2009; Tournier, 2013). It is apparent that cancer cells will need to find some means to attenuate apoptotic JNK signalling, but that other aspects of JNK signalling are required for tumourigenesis and maintenance of a cancerous phenotype in certain tissue types. The apoptotic pathway appears to be a specific one controlled by particular components and scaffolding proteins (Ghosh *et al.*, 2011). It is possible that loss of MKK4 or DLK, for example, may enable shutdown of the apoptotic JNK pathway, while mutational activation or overexpression of MLK1–4 could instead promote ERK or migratory JNK targets. MLK3 has been shown to promote metastasis in breast cancer xenografts by activation of the JNK–cJUN pathway (Chen and Gallo, 2012; Cronan *et al.*, 2012). Additionally, MLK3 was recently shown to be elevated in metastatic melanomas compared to primary melanomas, and was proposed to promote invasion via JNK activation (Zhang *et al.*, 2014). Given our results (Marusiak *et al.*, 2014), it is tempting to speculate that melanoma patients with overexpression of MLK3 could be among those that show *de novo* resistance to BRAF inhibitors (Flaherty *et al.*, 2010; Chapman *et al.*, 2011).

Endogenous JNK activation is low in the A375 cell line; however, ectopic expression of MLK1 was capable of activating JNK in these cells (Fig. 7A). In our xenograft mouse model, overexpression of MLK1 alone reduced tumour burden compared to the control group (Marusiak *et al.*, 2014). While this might be due to non-specific toxicities arising from ectopic expression of large amounts of protein, it could also be the result of pro-apoptotic JNK signalling activated by MLK1 overexpression in the tumours. This could be determined by overexpression of a KD form of MLK1. If the latter was the case it may be that MLK1 overexpression is only advantageous to tumour cells in the setting of BRAF inhibition, where MLK1 signalling is instead directed towards activation of MEK. A similar phenotype has been observed with EGFR overexpression; in the context of BRAF

inhibition it promoted drug resistance and survival, whereas when $BRAF^{V600E}$ was not inhibited, EGFR expression reduced proliferation of melanoma cells and growth of tumours *in vivo* (Sun *et al.*, 2014).

Experiments using a JNK inhibitor in combination with PLX4032 demonstrated that activation of the JNK pathway was not responsible for the rescue effects conferred by MLK1 after BRAF inhibition (Fig. 7B), supporting the hypothesis that rescue is mediated via ERK pathway reactivation. Interestingly, JNK inhibition led to a reduction in MLK1 expression (Fig. 7A), which could indicate a novel mode of regulation of MLK1. DLK is subject to a positive feedback loop on activation of JNK signalling, whereby JNK directly phosphorylates DLK to enhance its stability (Huntwork-Rodriguez *et al.*, 2013). JNK has also been shown to phosphorylate MLK2 (Phelan *et al.*, 2001) and MLK3 (Schachter *et al.*, 2006) to promote continued signalling downstream; my data suggest this could potentially be the case for MLK1. Despite the observed reduction in MLK1 after JNK inhibition, levels of phosphorylated MEK were sufficient to rescue the effect of PLX4032 on cellular viability. This is consistent with reports that over 80% inhibition of ERK activation is required to achieve tumour regression in patients (Bollag *et al.*, 2010).

3.5.3 MLK1 mutants in melanoma

Interestingly, MLK1 was found to be frequently mutated in melanoma; 15% of 85 melanoma cell lines from patients had mutations in the *MAP3K9* gene (Stark *et al.*, 2012). These mutations were made using SDM, and analysis of ERK pathway activation upon overexpression revealed that a number of these mutants were more active than the WT protein (Fig. 9). In fact, of 12 patients with MLK1 mutations, nine had potential GOF mutants.

These results need to be verified by knockdown experiments in the melanoma cell lines that express mutant MLK1, to determine if these mutants can endogenously regulate the ERK pathway. If they were found to be bona fide GOF mutants then patients harbouring these mutations may be inherently resistant to treatment with BRAF inhibitors, or at least may be predisposed to developing resistance through MLK1. To test this, PLX4032-resistant cell lines would need to be generated from the cells with $BRAF^{V600E}$ and GOF MLK1 mutants, and tested by knockdown and inhibition of MLK1.

In addition, ~40% of MLK1 GOF mutations occur in tumours without $BRAF^{V600E}$, opening up the possibility that MLK1 GOF mutants may themselves be drivers of tumourigenesis in some patients. Again, this would need to be tested in the relevant cell lines, to elucidate whether MLK1 mutants promote viability in these cells.

At present it is not clear what mechanisms are responsible for the observed GOF phenotype of the various mutants. Since a number of the mutants involve loss of a serine residue (S533Y, S616F and S650L) it could be that these sites can be phosphorylated in cells to cause inhibition of the protein. For example, S616 is predicted to be a site for phosphorylation by CDK5 (Scansite, 2012), which can phosphorylate and inhibit another MAP3K, namely PAK1 (Rashid *et al.*, 2001). Phosphorylation of MLK1 on these serine residues could mediate inhibition of the protein via an autoinhibitory interaction with the SH3 domain of MLK1, or by promoting binding to scaffolding or regulatory proteins. This possibility could be elucidated by the use of phosphomimetic mutants (e.g. S616D), which would be LOF towards the ERK pathway if these were sites of inhibitory phosphorylation. In addition, the D176N mutant is close to K171, the critical lysine that binds the negatively-charged phosphates of ATP. Therefore it is possible that the change from a negatively-charged aspartate to an asparagine at the nearby position 176 could aid binding of ATP by removing any repellent effect.

Additionally, the importance of the LOF MLK1 mutations has yet to be investigated further; for example, R160C and P263L displayed a complete loss of ability to act downstream, comparable to the KD construct (Fig. 9B). The majority of LOF mutations reside within the kinase domain of the protein, so it is not surprising that this function has been lost. The specific mutational profile of a tumour varies between patients, and it may be that the loss of MLK1 function in these patients is favoured as a method of deactivating the apoptotic JNK response to DNA damage. Alternatively these may be one of many coincidental mutations that a tumour cell acquires as it evolves. It should also be noted that these patients have not yet been treated with BRAF inhibitors (Stark *et al.*, 2012), thus have no need to achieve reactivation of the ERK pathway.

3.5.4 Conclusions

Tumour cells are very adaptable to changes in environment; despite inhibition of BRAF they will find another way to promote growth. Resistance mechanisms seen in the clinic so

far have involved reactivation of the ERK pathway by various means (Johannessen *et al.*, 2010; Nazarian *et al.*, 2010; Poulikakos *et al.*, 2011). Our results suggest that overexpression of MLKs is a bona fide mechanism of resistance and provides another means of reactivating the ERK pathway after BRAF inhibition. Endogenous overexpression of MLKs promotes resistance to RAF inhibition *in vitro* and *in vivo*. Most convincingly, increased expression of MLKs was observed in tumours from patients who developed resistance to RAF inhibitors. These patients may potentially benefit from combination treatment of BRAF inhibitors and MLK inhibition, which could prevent recurrence of melanoma. Since MLKs promote resistance by phosphorylation of MEK, the combination of BRAF and MEK inhibitors may prevent the emergence of resistance by upregulation of MLKs, but this remains to be tested.

In 2013 the above work was submitted for publication (Marusiak *et al.*, 2014), and I moved on to work on my main project, looking at the role of LZK in HNSCC (see Part Two).

4 Part Two: The role of LZK in SCC

4.1 Abstract

Squamous cell carcinoma (SCC) originates from squamous epithelial cells of various anatomical sites, including the lung, head and neck, oesophagus and cervix. Head and neck SCC (HNSCC) includes epithelial cancers of the oral and nasal cavity, larynx and pharynx, and accounts for ~650,000 cases/year worldwide. Smoking-related HNSCC has a similar profile to lung SCC (LSCC), where targetable mutations are rare compared to adenocarcinomas. On the other hand, copy number alterations are frequently observed in SCCs, the most common of which is copy number gain at 3q. SOX2 is becoming established as a key driver on this amplicon for LSCC; however, critical target genes have not been conclusively determined for HNSCC and it is likely that multiple oncogenes cooperate to promote tumourigenesis.

MAP3K13 (the gene encoding leucine zipper-bearing kinase, LZK) resides on the 3q amplicon. LZK belongs to the mixed lineage kinase (MLK) family of MAP3Ks, and can activate the JNK, p38, and NFκB pathways. Data presented here suggest that amplification of LZK may contribute to tumourigenesis in HNSCC. Copy number gain at 3q was shown to lead to an increase in *MAP3K13* mRNA in HNSCC tumour samples and cell lines. Knockdown of LZK by siRNA reduced cell viability and survival of HNSCC cell lines but not normal control cells. Validating these data, inducible knockdown of LZK by shRNA reduced cell survival, viability and proliferation of two HNSCC lines with 3q gain, but not control cell lines. Additionally, inducible knockdown of LZK caused a near complete loss of colony forming ability of cells with 3q gain. The mechanism behind these effects has not been fully elucidated but may involve regulation of AKT and GOF p53. In summary, this project has identified LZK as a potential driver that promotes proliferation in HNSCC cells with 3q amplification.

4.2 Introduction: HNSCC and the 3q amplicon

Squamous cell carcinoma (SCC) originates from squamous epithelial cells of various anatomical sites, including the lung, head and neck, oesophagus and cervix. Head and neck SCC (HNSCC) accounts for 90% of cancers of the head and neck region (Culliney *et al.*, 2008), and includes epithelial tumours of the oral and nasal cavities, larynx and pharynx. There are approximately 650,000 cases and 350,000 deaths per year worldwide due to HNSCC (Parkin *et al.*, 2005). The main causal factors for HNSCC are smoking and alcohol consumption, although human papillomavirus (HPV) infection is a causal factor in ~20% of cases (Molinolo *et al.*, 2012).

Patients who present with early stage HNSCC can be treated by surgical resection or radiotherapy, with success rates of 90% for stage I and 70% for stage II disease (Argiris *et al.*, 2008). However, a majority of patients present with stage III or IV disease, when local advancement to nearby tissue or lymph nodes has already occurred. After treatment, 50% of these patients will experience disease progression within two years, either due to local recurrence or metastasis, commonly to the lung (Argiris *et al.*, 2008; Haddad and Shin, 2008). Five year survival rates for patients who present with advanced disease are under 50% (Carvalho *et al.*, 2005).

At present, the current treatment regimens for later stages involve surgical resection, where possible, followed by radiotherapy or chemoradiotherapy, which carry significant toxicities (Haddad and Shin, 2008; Suh *et al.*, 2014). Chemoradiotherapy improves rates of progression-free and overall survival as compared with radiotherapy alone (Bernier *et al.*, 2004). Efficacy of radiotherapy can also be enhanced by combination with cetuximab, which targets EGFR, in advanced stages of the disease (Bonner *et al.*, 2006). EGFR is overexpressed in ~90% of HNSCC; however, only a small subset (13%) of patients respond to cetuximab monotherapy (Vermorken *et al.*, 2007), and it is not yet known what determines its efficacy in this subset of patients (Cassell and Grandis, 2010; Ang *et al.*, 2014). Addition of cetuximab to a regimen of chemoradiotherapy was not found to have any additional benefit, regardless of EGFR expression levels (Ang *et al.*, 2014), and it is thought to be most useful as a combination with radiotherapy for patients who cannot tolerate chemoradiotherapy (Argiris *et al.*, 2008; Haddad and Shin, 2008). Therefore, no truly ‘targeted’ therapy, based upon assessment of biomarkers, is currently in use for the treatment of HNSCC.

HNSCC tumours have a high mutational burden. Genetic alterations resulting in loss of the Rb (retinoblastoma protein) and p53 tumour suppressor pathways are very common, often via inactivation of *CDKN2A* (CDK inhibitor 2A, the gene locus encoding $p16^{INK4A}$ and $p14^{ARF}$), amplification of *CCND1* (cyclin D1) and loss of wild-type p53 function (Cancer Genome Atlas Network, 2015). These changes allow cancer cells to escape cell cycle regulation and senescence, thus obtaining limitless replicative capacity, a hallmark of tumourigenesis (Hanahan and Weinberg, 2011).

Similarly to LSCC, targetable mutations are relatively rare in HNSCC (Cancer Genome Atlas Network, 2012; Cancer Genome Atlas Network, 2015), although 10–20% of tumours have mutations in *PIK3CA* (Du *et al.*, 2012; Lui *et al.*, 2013; Cancer Genome Atlas Network, 2015), representing a cohort of patients that may benefit from treatment with PI3K (phosphatidylinositol 3-kinase) or mTOR (mammalian target of rapamycin) inhibitors. Copy number alterations (CNA), on the other hand, are frequently observed in SCCs as compared to other tumours, the most common of which is copy number gain at 3q (Cancer Genome Atlas Network, 2012; Cancer Genome Atlas Network, 2015). SOX2 is becoming established as a key target on this amplicon for LSCC (Bass *et al.*, 2009); however, it is clear that multiple genes on the 3q amplicon can promote tumourigenic phenotypes. Leucine zipper-bearing kinase (LZK), or *MAP3K13*, resides on the 3q amplicon. LZK belongs to the mixed lineage kinase (MLK) family of MAP3Ks, which activate various signalling pathways that have roles in SCC.

4.2.1 The 3q amplicon in squamous cell carcinoma

4.2.1.1 Introduction

CNA is commonly seen in cancer cell DNA, particularly in carcinomas. This can involve focal amplifications, which include one or a few genes, as well as amplification or deletion of large chromosomal regions (Knowles, 2005). Amplification or deletion of particular genes or regions occurs frequently across cancer types, suggesting that there may be a growth advantage associated with possessing CNA at these regions (Hanahan and Weinberg, 2011). Copy number gains of large regions have been observed with multiple subpeaks of amplification, and it is thought that these regions likely harbour multiple driver genes (Knowles, 2005).

The long arm of chromosome 3 is subject to copy number gain in a variety of cancers, including SCCs of the lung, head and neck, and cervix, as well as ovarian cancer (Qian and Massion, 2008). 3q amplification is an early event in the development of SCC and is maintained throughout disease progression (Ma *et al.*, 2000; Qian and Massion, 2008). The amplicon correlates with increased malignancy, becoming more frequent as tumour stage progresses (Qian and Massion, 2008). A number of genes have been nominated as potential drivers, although many studies have been based solely upon genomic analysis and no functional validation has yet been completed. This section will review some of the genes for which functional data is available, including the most compelling targets: *PIK3CA*, *SOX2* and *TP63*. It will encompass research on 3q in different squamous cancer types, with a focus on HNSCC where data are available.

4.2.1.2 *PIK3CA* and the AKT pathway

PIK3CA encodes the p110α subunit of PI3K, which acts upstream of AKT, a critical mediator of cell survival that is frequently dysregulated in cancer (Du *et al.*, 2012). RTKs such as EGFR and IGFR initiate PI3K/AKT signalling cascades, by a range of different mechanisms (Fig. 10). Binding of the appropriate growth factors to RTKs instigates receptor dimerisation and autophosphorylation of tyrosine residues in their cytoplasmic domains. This recruits the p85 regulatory subunit of PI3K to the membrane, either via binding of the SH2 domain of p85 directly to receptor phospho-tyrosine (pTyr) residues, or via adaptor proteins such as IRS1 (insulin receptor substrate 1) or GRB2 which bind to RTKs. GRB2 has an SH3 domain, recruiting GAB1 (GRB2-associated binding protein 1), which in turn recruits the p85 subunit of PI3K via binding of the SH2 domain of p85 to a pleckstrin homology (PH) domain on GAB1. Binding of p85 to GRB2-GAB1 or IRS1, or to pTyr residues on an RTK, relieves inhibition of the p110α catalytic subunit of PI3K. Alternatively, GRB2 can bind to SOS, activating RAS, which can also promote activation of p110α (reviewed in Carracedo and Pandolfi, 2008; Castellano and Downward, 2011).

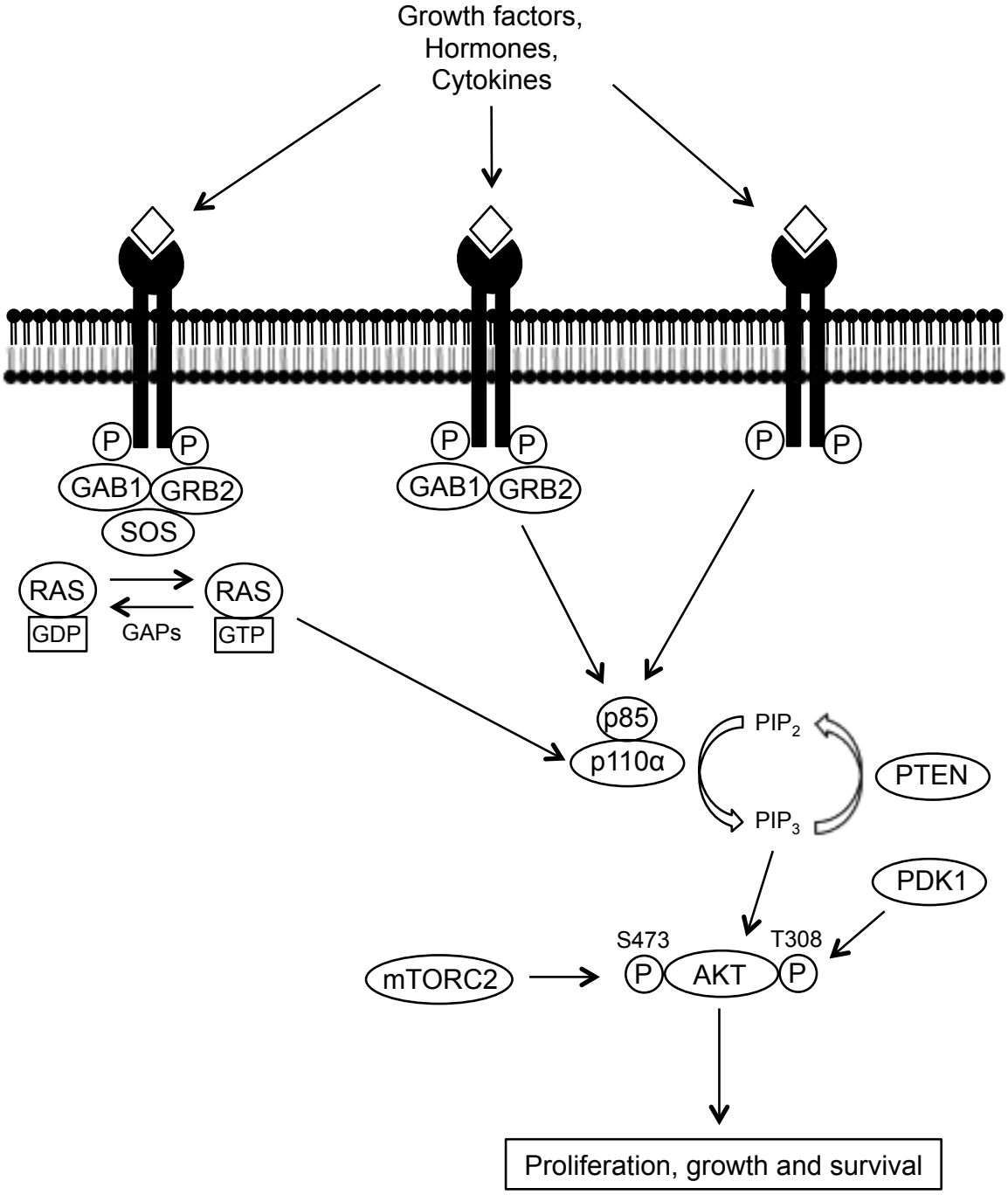

Figure 10: Schematic illustrating activation of PI3K/AKT pathway. Simplified diagram illustrating three mechanisms of activation of PI3K/AKT downstream of RTKs. Binding of ligand to RTKs initiates receptor dimerisation and autophosphorylation of tyrosine residues in the cytoplasmic domain. This recruits the p85 regulatory subunit of PI3K, either via binding of p85 directly to phospho-tyrosine residues, or via adaptor proteins such as GRB2 which bind to RTKs. GRB2 recruits GAB1, which recruits the p85 subunit of PI3K. Binding of p85 promotes activation of the p110α catalytic subunit of PI3K. Alternatively, GRB2 can bind to SOS, activating RAS, which can also activate p110α. p110α converts PIP_2 to PIP_3, recruiting AKT to the plasma membrane. AKT is activated by phosphorylation at Thr308 by PDK1 and at Ser473 by mTORC2. Adapted from figures in Castellano and Downward, 2011.

Once activated, the p110α subunit of PI3K phosphorylates the 3' hydroxyl position of phosphatidylinositols such as PIP_2 (phosphatidylinositol-4,5-bisphosphate [$PI(4,5)P_2$]) to produce PIP_3 (phosphatidylinositol-3,4,5-trisphosphate [$PI(3,4,5)P_3$]). PIP_3 recruits PH domain-containing proteins including AKT and PDK1 (PIP_3-dependent kinase 1) to the plasma membrane (Du *et al.*, 2012). This enables phosphorylation of AKT at Thr308 in the activation loop by PDK1 (Alessi *et al.*, 1997). Full activation of AKT requires phosphorylation at Ser473 in its hydrophobic motif by mTOR complex 2 (mTORC2) (Hresko and Mueckler, 2005; Sarbassov *et al.*, 2005). AKT activation has a wide range of pro-survival, pro-growth and pro-proliferative downstream effects, including inhibition of pro-apoptotic proteins such as FOXO, BAD and GSK3, phosphorylation of MDM2 leading to a reduction in levels of p53, downregulation of the cell cycle inhibitor p27, and activation of the mTORC1 complex, which regulates growth and cell cycle progression. Activation of mTORC1 occurs via inhibitory phosphorylation of its negative regulators, TSC2 (tuberous sclerosis 2) and PRAS40 (proline-rich AKT substrate of 40kDa), by AKT. Phosphorylation of TSC2 inhibits the GTPase-activating protein (GAP) activity of the TSC1/TSC2 complex, allowing downstream GTP-bound RHEB (RAS homologue enriched in brain) to activate mTORC1. PRAS40 binds to the RAPTOR (regulatory-associated protein of mTOR) component of the mTORC1 complex and prevents recruitment of downstream substrates. Phosphorylation of PRAS40 by AKT promotes its dissociation from the mTORC1 complex, allowing signalling to proceed (reviewed in Manning and Cantley, 2007; Hemmings and Restuccia, 2012).

The PI3K/AKT pathway is frequently altered in HNSCC by a variety of mechanisms (reviewed in Du *et al.*, 2012); 30% of HNSCC tumours were found to harbour mutations in this pathway (Lui *et al.*, 2013). *PIK3CA* is on the 3q amplicon, while 10–20% of HNSCC have mutations in this gene that cause constitutive activation (Du *et al.*, 2012; Lui *et al.*, 2013; cBio, 2015). Other mechanisms that activate the pathway include loss of the negative regulator PTEN, a lipid phosphatase which dephosphorylates PIP_3 to yield PIP_2 and attenuate PI3K/AKT signalling, and mutation of the gene encoding p85α which weakens its inhibition of p110α (Du *et al.*, 2012). These were observed at lower frequencies of 3% and 1% in HNSCC tumours (cBio, 2015).

Preliminary evidence suggested that amplification of *PIK3CA* correlated with increased PI3K activity: lung cells with amplified *PIK3CA* had higher levels of pAKT as compared with normal controls, and immunoprecipitation of p85 from a cell line with *PIK3CA* copy

number gain showed PI3K activity was higher than in non-amplified cells (Yamamoto *et al.*, 2008). The PI3K inhibitor LY294002 reduced growth of cell lines from ovarian (Shayesteh *et al.*, 1999) and cervical carcinomas (Ma *et al.*, 2000) with 3q gain as compared with normal control cells. Constitutively active PIK3CA transformed NIH3T3 cells (Singh *et al.*, 2002); however, this active form of the protein did not transform primary ovarian cells. Importantly, expression of active PIK3CA in the epithelium of the murine female reproductive tract caused hyperplasia but not malignant disease, suggesting that, at least in ovarian cancer, *PIK3CA* amplification alone is not sufficient for tumourigenesis (Liang *et al.*, 2009). Additionally, *PIK3CA* mutations occur at equal frequencies in TCGA (The Cancer Genome Atlas) samples with and without 3q amplification across multiple tumour types, including HNSCC (Hagerstrand *et al.*, 2013; cBio, 2015). Furthermore, while HNSCC cell lines with *PIK3CA* mutations were sensitive to treatment with PI3K/AKT pathway inhibitors, amplification of *PIK3CA* did not predict sensitivity to these inhibitors (Lui *et al.*, 2013; Mazumdar *et al.*, 2014). This suggests that mutation of *PIK3CA* is a more effective oncogenic event and that *PIK3CA* may not be an important target of 3q amplification.

4.2.1.3 SOX2

The most well-studied 3q target in LSCC is SOX2, a transcription factor that regulates self-renewal and differentiation of embryonic stem cells. SOX2 overexpression is proposed to confer a stem-like phenotype on squamous tumour cells (Hussenet *et al.*, 2010). *SOX2* was found in a narrow peak of amplification in LSCC samples, and knockdown of SOX2 reduced proliferation and anchorage-independent growth in lung and oesophageal SCC cells. The effects of knockdown in this study were greater for *SOX2* than for 10 of its neighbouring genes, as well as *PIK3CA* and *TP63*. However, SOX2 overexpression was insufficient to transform immortalised epithelial cells (Bass *et al.*, 2009). The authors followed up this study in mouse models with conditional overexpression of SOX2 in the basal cells of the oesophagus and forestomach. This led to carcinomas in the forestomach, but only hyperplasia in the oesophagus. SOX2 expression in the forestomach caused an increased immune infiltrate, with higher numbers of myeloid cells and expression of inflammatory cytokines including interleukins IL-1β and IL-6, which activate STAT3 (signal transducer and activator of transcription 3). This was associated with a loss of differentiated suprabasal cells and exposure of basal progenitor cells to gastric acid (Liu *et al.*, 2013). This inflammation was not seen in the oesophagus,

while the squamous forestomach is not present in humans (Bass and Wang, 2013), calling into question the broader relevance of these findings.

SOX2 overexpression was insufficient to transform tracheobronchial immortalised epithelial cells (Bass *et al.*, 2009) or oesophageal progenitor cells (Liu *et al.*, 2013). However, SOX2 was able to transform cells and promote oesophageal tumour formation in mice when coexpressed with activated STAT3 (Liu *et al.*, 2013). Additionally, knockdown of either SOX2 or STAT3 reduced tumour growth of an engrafted oesophageal cell line. In humans, oesophageal SCC is mostly caused by smoking, which is well documented to promote inflammation, thus it is likely that this inflammatory environment cooperates with *SOX2* amplification in some cases. Analysis of oesophageal SCC tumour samples showed that 31 of 83 samples had high levels of both SOX2 and STAT3, although other samples had overexpressed SOX2 without high STAT3 (Liu *et al.*, 2013), which may mean that other factors can cooperate with SOX2 to promote tumourigenesis. In LSCC, PKCι, (protein kinase C iota) which is also on the 3q amplicon, and SOX2 are both involved in the Hedgehog signalling pathway. Knockdown of either reduced cell growth, and it was suggested that they might cooperate to promote LSCC growth, although transformation ability was not tested (Justilien *et al.*, 2014). In contrast to the studies by Bass *et al.* and Liu *et al.*, SOX2 overexpression alone led to increased growth of BEAS2B immortalised bronchial epithelial cells in soft agar, and enabled growth of the cell line *in vivo*. However, BEAS2B cells are not typical immortalised cells in that they already exhibit weak growth on soft agar. Additionally, tumours formed in mice grew slowly, leading the authors to speculate that other factors would be required for full transformation of cells (Hussenet 2010).

The role of SOX2 in HNSCC has been less extensively investigated, but a recent study has revealed a possible tumourigenic role. SOX2 protein expression was detected in 45% of 69 HNSCC tumours. Ectopic expression of SOX2 in HNSCC lines promoted stem cell-like properties and induced expression of cyclin B1 to promote proliferation. Expression of SOX2 was enriched in cancer stem cells (CSCs) isolated from HNSCC tumours, and knockdown in these cells reduced formation of tumour spheres and tumourigenicity of CSCs in xenograft models (Lee *et al.*, 2014). A larger study of 449 tumour samples found that amplification of SOX2 did lead to significantly increased protein levels that was not specific to CSCs. Interestingly, 25% of samples without amplification had detectable SOX2 protein, while in 18% of samples with amplification, SOX2 protein could not be

detected, suggesting that other mechanisms exist to increase SOX2 protein levels in HNSCC (Schröck *et al.*, 2014).

4.2.1.4 p63

The transcription factor p63 (tumour protein p63, encoded by *TP63*) is required for normal epithelial development, and is proposed to be involved in the development of SCC. p63 is expressed as two isoforms: TAp63, the full-length protein that has a tumour suppressive role; and ΔNp63, which lacks the N-terminal p53-like transactivation domain, and is the form that is predominantly expressed in squamous carcinomas (Rocco *et al.*, 2006). Various anti-apoptotic mechanisms of amplified *TP63* have been proposed: ΔNp63 was demonstrated to inhibit transactivation by the tumour suppressor protein p73 (DeYoung *et al.*, 2006; Rocco *et al.*, 2006); it was shown to interact with HDAC1/2 (histone deacetylase 1/2) to form a transcriptional repressor complex that inhibits expression of pro-apoptotic genes including *BBC3* (the gene encoding PUMA, p53-upregulated modulator of apoptosis) and *PMAIP1* (phorbol-12-myristate-13-acetate-induced protein 1, encoding NOXA) (Rocco *et al.*, 2006; Ramsey *et al.*, 2011); and expression of ΔNp63 induced FGFR2 (FGF receptor 2), which was then activated by secretion of FGF7 from tumour-associated fibroblasts in a mouse model of oral SCC (Ramsey *et al.*, 2013). Knockdown of p63 in HNSCC lines caused apoptosis (DeYoung *et al.*, 2006; Rocco *et al.*, 2006), and excision of *TP63* from SCC cells of mice with carcinogen-induced oral tumours led to tumour regression (Ramsey *et al.*, 2013), implying an oncogenic role. However, mRNA expression of *TP63* did not correlate with copy number in HNSCC, suggesting that it may have an important role in HNSCC development, but that it is overexpressed by mechanisms other than 3q amplification (Redon *et al.*, 2001).

Interestingly, SOX2 and ΔNp63 have been shown to associate with each other, specifically in SCC cells, to enhance transcription of genes such *ETV4* (ETS variant 4). Combined knockdown of p63 and SOX2 in oesophageal and LSCC lines had a synergistic anti-proliferative effect (Watanabe *et al.*, 2014), highlighting the fact that different genes on 3q may cooperate to promote tumourigenesis. However, coexpression of SOX2 and ΔNp63 did not transform immortalised lung epithelial cells, suggesting that additional factors are required (Watanabe *et al.*, 2014).

4.2.1.5 Other potential 3q drivers

Other candidate drivers that have been identified on the 3q amplicon include the novel protein DCUN1D1 (DCN1(defective in cullin neddylation 1)-like protein 1), which was found in a subpeak of amplification in head and neck cancer cell lines. Increased protein levels correlated with copy number gains in lung and head and neck cell lines and tumours. Knockdown of DCUN1D1 caused death of cell lines with amplification of *DCUN1D1* but not of those whose 3q amplicon did not include this gene (Sarkaria *et al.*, 2006). Overexpression of DCUN1D1 transformed NIH3T3 cells (Sarkaria *et al.*, 2006) and improved their invasive capacity via upregulation of MMP2 (O-charoenrat *et al.*, 2008). However, upregulation of MMP2 levels required WT p53 (O-charoenrat *et al.*, 2008); p53 is mutated in the majority of SCC so the physiological relevance of this pro-invasive phenotype is debatable. Knockdown studies have been very limited for this gene and further study is warranted to examine its potential role in the maintenance and development of SCC.

Various studies have looked for minimal regions of amplification across a range of tumour or cell line samples and proposed targets based on this (Guan *et al.*, 2001; Tjia *et al.*, 2005; McCaughan *et al.*, 2010). However, the 'minimal region' varies between sample sets and it remains probable that a number of different genes on this chromosome have an oncogenic role. For example, a recent study used data from Tumorscape to find samples with 3q amplification that did not include the typical candidate oncogenes *TP63*, *PIK3CA* or *SOX2*. They screened genes in their minimal region by knockdown and overexpression assays in breast and lung cell lines, and found two genes, *TLOC1* (SEC62 homologue, pre-protein translocation factor) and *SKIL* (SKI-like proto-oncogene), that promote proliferation and invasion, respectively. Knockdown of each protein in cell lines inhibited these phenotypic abilities, while overexpression of the two genes synergistically promoted anchorage-independent growth in primary mammary cells. Importantly, PIK3CA or SOX2 were also able to transform the primary mammary epithelial cells utilised in this study, highlighting the fact that various 3q oncogenes may be able to confer a tumourigenic phenotype (Hagerstrand *et al.*, 2013).

4.2.1.6 Conclusions

The region of amplification of 3q found in tumours is often large, encompassing many genes, several of which have been proposed to possess tumourigenic capabilities. Some studies have used fine mapping techniques to identify subpeaks of focal amplification within the amplicon. Multiple subpeaks have been found within the same tumour samples, providing further evidence that more than one gene confers a survival advantage on these tumour cells. However, the subpeaks that have been identified vary between cancer sites and sample sets (Singh *et al.*, 2002; Sarkaria *et al.*, 2006; Sparano *et al.*, 2006), and more work needs to be done to further stratify patients and identify important drivers. The focus needs to be on identifying targetable oncogenes within this amplicon that would enable treatment of a significant proportion of SCC patients.

4.2.2 p53 mutations in HNSCC

4.2.2.1 Introduction

Mutation or deletion of the *TP53* (tumour protein p53) gene is a frequent and early event in the development of HNSCC (Boyle *et al.*, 1993). In TCGA dataset, 72% of HNSCC tumours had alterations in the gene (Cancer Genome Atlas Network, 2015). Hotspots of mutation include R175, G245, R248, R249, R273 and R282 (Muller and Vousden, 2013).

The transcription factor p53 functions as a critical tumour suppressor, with well-characterised functions. In response to stress or DNA damage, WT p53 transactivates the gene encoding p21 (*CDKN1A*, CDK inhibitor 1A), leading to cell cycle arrest and enabling DNA repair by p53-regulated processes. If DNA repair cannot be completed, p53 promotes apoptosis by transactivation of pro-apoptotic genes such as *BAX* and *BBC3* (encoding PUMA) (reviewed in Bieging *et al.*, 2014). Discovery of these functions led to the hypothesis that the *TP53* mutants frequently observed in cancer were all LOF, and it is true that *TP53* cancer mutants lose the tumour suppressor abilities of the WT protein, usually by disrupting the DNA binding domain (Oren and Rotter, 2010; Ota *et al.*, 2012). However, many *TP53* mutations produce a full-length protein, which is highly expressed in cancer cell lines (Burns *et al.*, 1993). This suggested that the mutant protein may have some additional function, and while in some cases heterozygous mutants simply act in a dominant-negative manner, binding to WT p53 to abrogate its activity (Duan *et al.*, 2008), several have been demonstrated to have additional oncogenic capabilities (reviewed in

Oren and Rotter, 2010; Muller and Vousden, 2013). These include the ability to transform p53-null cells and promote tumour growth in mice (Dittmer *et al.*, 1993).

4.2.2.2 Functions of oncogenic p53 mutants

Mutant p53 proteins have been demonstrated to have a range of tumourigenic abilities. GOF p53 mutants are associated with anti-apoptotic (Vikhanskaya *et al.*, 2007; Weisz *et al.*, 2007; Alexandrova *et al.*, 2015), pro-proliferative (Bossi *et al.*, 2006; Acin *et al.*, 2011; Li *et al.*, 2011) and pro-invasive phenotypes (Dong *et al.*, 2009; Li *et al.*, 2011; Zhou *et al.*, 2014), as well as with resistance to chemotherapy (Bossi *et al.*, 2006; Wong *et al.*, 2007).

Several studies have demonstrated GOF abilities for mutant p53 by utilising overexpression in p53-null cells or transgenic mice (Dittmer *et al.*, 1993; Dong *et al.*, 2009; Acin *et al.*, 2011; Sano *et al.*, 2011). For example, expression of $p53^{R172H}$ in murine oral epithelium promoted growth of oral tumours initiated by $KRAS^{G12D}$. This was the case even in the absence of a WT allele, confirming that these effects were due to a true GOF mutant rather than dominant-negative effects over the WT protein. 15% of these tumours progressed to form carcinomas, while mice with deletion of p53 never progressed beyond benign papillomas (Acin *et al.*, 2011), illustrating the oncogenic ability of p53 mutants. Others have utilised RNAi of endogenous mutant p53 to confirm GOF phenotypes, and shown that knockdown of mutant p53 reduces growth, proliferation, invasion and tumourigenicity of cancer cells (Bossi *et al.*, 2006; Li *et al.*, 2011; Zhou *et al.*, 2014; Zhu *et al.*, 2015).

4.2.2.3 Mechanisms of p53 GOF activity

Several mechanisms have been elucidated for p53 GOF activity, the nature of which likely varies depending on the specific mutation and tissue type (reviewed in Muller and Vousden, 2013). GOF p53 cannot bind to WT p53-type promoters or transactivate typical WT targets, such as *CDKN1A* (p21) or *MDM2* (mouse double minute homologue) (Scian *et al.*, 2004a; Vikhanskaya *et al.*, 2007; Zhou *et al.*, 2014), but have an alternative gene expression signature. GOF p53 mutants have been shown to upregulate cyclins A and B1 (Di Agostino *et al.*, 2006; Acin *et al.*, 2011), telomerase reverse transcriptase (hTERT) (Scian *et al.*, 2004a), multi-drug resistance 1 (MDR1) (Dittmer *et al.*, 1993), NFκB2 and

MYC (Scian *et al.*, 2004b), and downregulate p21, PTEN, BAX (Vikhanskaya *et al.*, 2007) and caspase-3 (Wong *et al.*, 2007).

Modulation of gene expression by GOF p53 can occur in various different ways. The majority of p53 mutations in cancer are found in the DNA binding domain, abolishing binding to typical p53 response sites, but leaving the transactivation domain intact. This may enable GOF p53 to transactivate an alternative set of genes compared to the WT protein, either by binding to different promoter sites or via interaction with other transcription factors. p53 GOF mutants are divided into two main categories: DNA contact mutants (including R248 and R273 mutants) that disrupt the ability of the protein to bind its consensus DNA sequences; and conformational mutants (these include mutations at R175, G245, R249 and R282) that cause large scale changes in p53 protein structure. This structural change allows an altered spectrum of protein–protein interactions compared with WT p53. These include modulation of transcriptional activities of the sister proteins of p53, p63 and p73, which share some of the transcriptional targets of p53 but also have distinct target genes. The full-length isoforms, TAp63 and TAp73, have tumour suppressor abilities including promotion of apoptosis and inhibition of invasion, and can be inhibited in a dominant-negative fashion by binding to GOF p53 (reviewed in Muller and Vousden, 2013). GOF p53 can also interact with nuclear transcription factor Y (NF-Y), upregulating factors involved in cell cycle progression, including cyclin A, cyclin B1, CDK1 and CDC25, in response to DNA damage (Di Agostino *et al.*, 2006). Recently, GOF p53 has been shown to bind to another transcription factor, ETS2, leading to modulation of chromatin regulatory genes, including methyltransferases *MLL1* and *MLL2*, and the histone acetyltransferase *MOZ* (Zhu *et al.*, 2015).

A recent study has demonstrated that mutant p53 can interact with and inhibit AMP-activated protein kinase (AMPK) in HNSCC (Zhou *et al.*, 2014). AMPK is a critical regulator of cellular homeostasis; it modulates metabolic processes in response to metabolic stresses. AMPK is activated when cellular energy levels are low and functions as a crucial checkpoint to restrain growth and proliferation. It exists as a heterotrimeric complex comprising the α catalytic subunit, and β and γ regulatory subunits. AMPK acts in part by phosphorylation of RAPTOR and TSC2 to inhibit the mTORC1 complex, which would otherwise promote growth and cell cycle progression. Other downstream substrates of AMPK include acetyl-coA carboxylase (ACC1/2), phosphorylation of which attenuates fatty acid synthesis (reviewed in Shackelford and Shaw, 2009). In normal cells, AMPK

activity also helps to restrict proliferation by activation of WT p53, and is involved in a positive feedback loop that is key to tumour suppression as WT p53 transactivates the gene that encodes AMPKβ. However, in HNSCC cells GOF p53 was shown to inhibit activation of AMPK. Knockdown of GOF p53 enhanced AMPK activity, increasing ACC phosphorylation and reducing mTOR signalling. Energy stress such as glucose deprivation promoted a direct interaction of mutant p53 with AMPK, inhibiting phosphorylation of AMPKα at Thr172 by the upstream kinase LKB1 (liver kinase B1). This was likely due to the altered conformation of GOF p53 as WT p53 could also interact with AMPK but could not inhibit its activation (Zhou *et al.*, 2014).

4.2.2.4 Elevated stability of GOF p53 in cancer cells

Expression of WT p53 is kept at a low level in cells, until its activity is required under conditions of cellular stress. This occurs primarily via an interaction with MDM2, which inhibits p53 function through transcriptional repression as well as via its activity as an E3 ligase that marks p53 for degradation. This is enhanced by negative feedback from p53, which transactivates *MDM2*. WT p53 is stabilised in response to cellular stresses by various mechanisms. For example, DNA damage activates ATR and ATM serine/threonine kinases, which phosphorylate MDM2, promoting its degradation. ATR and ATM also activate CHK1 and CHK2, respectively; all four of these kinases can phosphorylate p53 to reduce its affinity for MDM2, contributing to p53 stabilisation. p53 is also subject to regulation by ARF (the alternate reading frame product of the *CDKN2A* locus, $p14^{ARF}$ in humans and $p19^{ARF}$ in mice), which antagonises MDM2 to promote p53 stability (reviewed in Bieging *et al.*, 2014).

In contrast to the WT protein, GOF p53 mutants are found at constitutively high levels in cancer cells. In an analysis of mutational status and protein expression of p53 in HNSCC tumours and cell lines, samples with high protein expression were found to have missense mutations or in-frame deletions (50% of 16 cases), whereas samples with WT p53 (12.5%) or nonsense mutations (37.5%) had no detectable p53 protein expression (Burns *et al.*, 1993). This observation could be explained by the inability of mutant p53 to transactivate its negative regulator *MDM2* (Oren and Rotter, 2010). However, the mutant proteins are not inherently more stable than the WT, as demonstrated by expression in normal tissue compared with tumour tissue in transgenic mice (Terzian *et al.*, 2008); this suggests that

basal levels of MDM2 are sufficient to maintain low expression of mutant p53 in normal tissue (Li *et al.*, 2011), and that mutants are stabilised by tumour cell-specific factors.

Various potential mechanisms have been proposed for this effect, some of which utilise the traditional means of enhanced p53 stability seen in response to stress stimuli. For example, GOF p53 can still be regulated by MDM2 and deletion of *MDM2* in mice allowed enhanced stability of GOF p53 (Terzian *et al.*, 2008). Alterations in the $p16^{INK4A}$–Rb pathway can also enhance GOF p53 stability. $p16^{INK4A}$ inhibits cyclin D1/CDK activity; when $p16^{INK4A}$ is lost, cyclin D1/CDK phosphorylate Rb, releasing E2F transcription factors. E2F can transactivate *ARF* to promote p53 stability (Sherr and McCormick, 2002). Loss of $p16^{INK4A}$ enhanced GOF p53 expression in normal cells, and loss of $p16^{INK4A}$ was observed in tumours from transgenic mice. Similarly, upregulation of cyclin D1 was found in tumours from these mice (Terzian *et al.*, 2008). GOF p53 could also be stabilised by exposure of mice to ionising radiation; this was sustained for a longer period than WT p53, likely due to the lack of transactivation of *MDM2* by GOF p53 (Terzian *et al.*, 2008). Other DNA damaging agents, including reactive oxygen species (ROS) and doxorubicin, which is commonly used as a chemotherapeutic agent, could also stabilise GOF p53 (Suh *et al.*, 2011). Expression of oncogenes, such as MYC or activated KRAS, also enhanced GOF p53 stability in transgenic mice; this may also occur via pathways seen in normal cells, whereby aberrant growth signals lead to activation of WT p53 as a tumour suppressive mechanism (Suh *et al.*, 2011).

Recent studies have elucidated a new mechanism of enhanced GOF p53 stability via the HSP90 chaperone, a heat shock response complex which functions to prevent misfolding and aggregation of aberrant proteins. This includes mutant p53, which was found in a stable complex with HSP90 in cancer cells. In cancer cell lines, HSP90 has been shown to prevent ubiquitination and consequent degradation of GOF p53 by MDM2 and CHIP (C terminus of HSC70-interacting protein), a component of the HSP90 complex. Interference with this pathway, by HSP90 inhibition or knockdown of HSF1 (heat shock transcription factor 1), the transcriptional regulator of the heat shock response, destabilised p53; this effect could be reversed by knockdown of MDM2 and CHIP (Li *et al.*, 2011). Importantly, inhibition of HSP90 destabilised mutant p53 and improved survival of mice with T-cell lymphomas that harboured mutant p53 tumours, but not those with p53 deletion (Alexandrova *et al.*, 2015).

4.2.3 LZK (*MAP3K13*) in SCC

LZK is a member of the MLK family of Ser/Thr protein kinases (Dorow *et al.*, 1993). MLKs are MAP3Ks that can activate the JNK (Teramoto *et al.*, 1996; Sakuma *et al.*, 1997; Liu *et al.*, 2000a), p38 (Tibbles *et al.*, 1996; Cuenda and Dorow, 1998) and ERK (Marusiak *et al.*, 2014) pathways. The MLK family is reviewed in detail in section 1, and LZK-specific functions are summarised below.

Overexpression of LZK activated MKK4/7–JNK and further downstream cJUN (Sakuma *et al.*, 1997). Association with the scaffold JIP1 enhanced this activation (Ikeda *et al.*, 2001a). LZK was also reportedly able to activate p38 on overexpression in COS7 cells; however, data were not shown to illustrate this (Ikeda *et al.*, 2001a). In addition, LZK could weakly activate NFκB in cells, and this activation was increased upon coexpression with PRDX3. LZK associated with and activated IKKβ; however, it could not directly phosphorylate IKKβ and the downstream substrate that connects LZK to IKKβ is not yet known. Activation of NFκB protects cells from apoptosis by inducing expression of BCL2 proteins and inhibitors of JNK signalling, thus PRDX3 may promote activation of NFκB by LZK as a way to avoid JNK-mediated apoptosis (Masaki *et al.*, 2003). The ability to associate with JIP1 or PRDX3 suggests that these regulatory proteins may be important in determining the outcome of LZK activation in response to different stimuli. Data shown in Part One of this thesis demonstrated that overexpression of LZK does not activate ERK (Marusiak *et al.*, 2014). Pathways activated downstream of LZK are summarised in Figure 1B.

MAP3K13 (LZK) resides at 3q27.2 and is frequently amplified in SCC. LZK has not previously been proposed to be an oncogene; however, its ability to activate three pathways that might have roles in HNSCC warrants investigation into whether it has a role in promoting this cancer. JNK activity was reportedly increased in HNSCC and inhibition of JNK with SP600125 reduced growth in an HNSCC xenograft model. Use of this compound should be treated with caution as it was used at a high concentration of 20μM in cellular assays and will likely inhibit other kinases or cause general cytotoxic effects; however, siRNA knockdown of JNK1/2 reduced proliferation and expression of EGFR *in vitro*, replicating the results obtained with SP600125 (Gross *et al.*, 2007). p38 was also found to be activated in HNSCC tumours; inhibition of p38 with SB203580 reduced proliferation *in vitro*, and decreased growth and angiogenesis in xenografts (Junttila *et al.*, 2007; Leelahavanichkul *et al.*, 2014). Again, these results were confirmed using RNAi;

stable knockdown of p38 or expression of a dominant-negative form of the protein reduced growth in a xenograft model (Leelahavanichkul *et al.*, 2014). Finally, NFκB has anti-apoptotic, pro-proliferative and pro-invasive roles in HNSCC via transactivation of a range of downstream targets (reviewed in Allen *et al.*, 2007); NFκB can be activated in HNSCC tumours by overexpression of IKKα and IKKβ (Nottingham *et al.*, 2014).

4.2.4 Conclusions and project aims

HNSCC, like other SCCs, is characterised by the relatively low frequency of targetable mutations, with the exception of the 10–20% of patients that harbour *PIK3CA* activating mutations. As such, treatment currently relies on chemo- and radiotherapeutic approaches. Copy number alteration is common in squamous cell carcinomas, including HNSCC, the most common of which is copy number gain of the long arm of chromosome 3. This is a large amplicon that frequently involves copy number gain of the whole of 3q. SOX2 has been established as a key tumourigenic target on the 3q amplicon for LSCC; however, several other genes have been shown to confer a survival advantage, and it is likely that multiple genes cooperate to promote cell growth and survival. At present SOX2 is not a druggable target, and research needs to be focused on identifying critical survival genes that may be targeted with small molecule inhibitors. *MAP3K13* (LZK) is a MAP3K that resides on the 3q amplicon, but its role in SCC has not been investigated. This research has focused on determining whether LZK may be a targetable protein that promotes survival in HNSCC with 3q amplification.

- Aim 1: Determine whether copy number gain of *MAP3K13* correlates with increased expression of LZK in cell lines.
- Aim 2: If a correlation is found, investigate whether amplified *MAP3K13* might have a tumour-promoting role. This will be assessed by knockdown experiments in cell lines with copy number gain.
- Aim 3: Elucidate the mechanisms of any effects by analysis of signalling pathways downstream.

4.3 Materials and Methods

For general procedures, including molecular cloning, western blot analysis and assay procedures please see section 2.

4.3.1 Cell culture

BEAS2B, DETROIT562, 293T and NCIH520 cells were obtained from ATCC; CAL33 cells were purchased from DMSZ; MSK921 cells were bought from Memorial Sloan-Kettering Cancer Center; OKF6/TERT2 cells were obtained from Harvard Skin Disease Research Center; and BICR6, BICR16, BICR18, BICR22, BICR56, PE-CA/PJ15 (hereafter PJ15) and PE-CA/PJ34 (hereafter PJ34) cells were purchased from Public Health England. 293FT cells were provided by Invitrogen as part of the ViraPower HiPerform T-Rex Gateway Expression System (Invitrogen).

293T, CAL33 and DETROIT562 cells were maintained in DMEM D6546 (Sigma Aldrich) supplemented with 10% FBS (Lonza), 1% pen-strep (Gibco, equivalent to 100Units/ml penicillin and 100µg/ml streptomycin) and 2mM L-glutamine (Gibco). BICR6, BICR16, BICR18, BICR22 and BICR56 cells were grown in DMEM D6546 supplemented with 10% FBS, 1% pen-strep, 0.4µg/ml hydrocortisone (Sigma Aldrich) and 2mM L-glutamine. MSK921, BEAS2B, KYSE70, LUDLU1 and NCIH520 cells were maintained in RPMI 1640 + GlutaMAX (Gibco) with 10% FBS and 1% pen-strep. PE-CA/PJ15 and PE-CA/PJ34 were cultured in IDMEM supplemented with 10% FBS, 1% pen-strep and 2mM L-glutamine. 293FT were maintained in DMEM with 10% FBS, 4mM L-Glutamine, 1mM sodium pyruvate (Gibco) and 0.1mM NEAA (Gibco).

OKF6/TERT2 cells were seeded in keratinocyte serum-free medium (K-sfm) (Gibco) with accompanying supplements: 25µg/ml bovine pituitary extract, 0.2ng/ml EGF, 0.3mM $CaCl_2$ and 1% pen-strep. At 30% confluency medium was changed for 1:1 K-sfm:DFK to allow growth to full confluence. DFK was composed of DMEM/F12 (Gibco) with 2mM L-glutamine, 25µg/ml bovine pituitary extract (Gibco), 0.2ng/ml EGF (Gibco), 0.3mM $CaCl_2$ (Lonza) and 1% pen-strep.

Incubation was at 37°C and 5% CO_2 for all cells. Upon reaching confluency, or when required for experiments, medium was aspirated and plates washed with PBS (Sigma

Aldrich) before being trypsinised (0.5% trypsin-EDTA (Gibco) in PBS) for 10–15min at 37°C.

4.3.2 Generation of inducible cell lines

4.3.2.1 Generation of doxycycline-inducible knockdown cell lines

CAL33 and BICR56 inducible knockdown cells were generated by Sirion Biotech. Initially, 10 shRNA sequences were tested for their ability to target LZK by transfection into NIH3T3 cells followed by qRT-PCR. The two best sequences were selected, these were: CGGAATGAACCTGTCTCTGAA (sh1) and GATGTAGATTCTTCAGCCATT (sh2). The lentiviral expression plasmid was pCLVi(3G)-MCS-Puro, which expresses a dox-responsive transactivator and the shRNA from the same vector. Expression of the transactivator is constitutive, while expression of shRNA is dependent on a dox-inducible promoter. Binding of doxycycline to the transactivator allows it to bind the dox-inducible promoter and promote expression of the shRNA.

Lentiviral stocks of the inducible knockdown constructs were then ordered from Sirion (generated by transfection of 293TN cells with expression vectors and lentiviral packaging plasmids), and used to generate inducible knockdown in MSK921 and BICR22 cells. Firstly, cells were treated with a range of concentrations of puromycin and observed daily to determine the lowest concentration that effectively killed all cells within one week. The transduction procedure was as follows: 140,000 cells/well were seeded in a 6-well plate. The next day, lentiviral stock was added at multiplicity of infection (MOI) 5 (=5 IP/cell ≈ 250 VP/cell) plus 8μg/ml polybrene to promote transduction. After 24h, medium was replaced with fresh medium containing 0.5μg/ml puromycin (Invitrogen) to select for cells that had been effectively transduced. Medium was refreshed every 48h until all cells in the puromycin control wells for each cell line were dead. Puromycin-resistant cells containing the inducible shRNA constructs were continually selected for using puromycin and transferred to a 10cm dish once cells had grown sufficiently. Colonies of single cell clones were selected using sterile cloning disks (Sigma Aldrich), and expanded into 12-well plates, then 10cm dishes until enough cells were present to freeze down vials. The rest of the cells were pooled. Pooled cells were used for experiments, and the clones kept in case knockdown could not be verified for the pools.

4.3.2.2 Generation of tetracycline-inducible expression cell lines

Stable inducible expression cell lines were generated using the ViraPower HiPerform T-Rex Gateway Expression System (Invitrogen). Cells were transduced with pLenti3.3/TR vector (for tetracycline repressor expression), and then LZK or SOX2 in pLenti/TO/V5-DEST vector (constructs cloned from pDONR221 vector by LR clonase reaction, as section 2.2.2) in a stepwise manner. Effective expression of TetR was checked by western blot before moving on to transduction with the vector containing the protein of interest.

The protocol was as follows: 293FT cells were seeded in 10cm dishes so that confluency was ~80% the next day. Cells were transfected with pLenti/TO/V5-DEST vector or pLenti3.3/TR vector, using Lipofectamine2000. In tube 1, 36µl Lipofectamine2000 was diluted in 1.5ml optimum. Tube 2 contained 9µg Virapack plus 3µg pLenti vector diluted in 1.5ml optimum. Each tube was incubated for 5min at RT and then tubes were mixed and incubated for 20min at RT before dropwise addition to the dish of cells. The day after transfection, medium was removed and 5ml medium added (to concentrate viral stock. Note: for transduction of OKF6/TERT2 cells medium used was 1:1 K-sfm:DFK as these cells undergo growth arrest when exposed to FBS). Two days later, viral stock was collected and spun at 2000xg for 15min at 4°C. Stock was filtered through a 0.45µm filter (Millipore) and stored in working aliquots at -80°C.

Target cell lines were seeded in 6-well plates (200,000/well for BEAS2B and 140,000 for OKF6/TERT2), including an extra well as a control for the selection antibiotic. The next day, medium was removed and replaced with 1ml lentiviral stock plus polybrene (6µg/ml for BEAS2B and 2µg/ml for OKF6/TERT2). The following day, viral stock was replaced with complete growth medium. 24h later, fresh growth medium with selection antibiotic was added. Geneticin (Gibco) selects for cells containing the pLenti3.3/TR vector and was used at 500µg/ml for BEAS2B and 200µg/ml for OKF6/TERT2. Blasticidin (Invitrogen) selects for cells containing the pLenti/TO/V5-DEST vector (with LZK or SOX2 inserted) and was used at 10µg/ml for BEAS2B and 3µg/ml for OKF6/TERT2. Medium with antibiotics was changed every 2–3 days until all cells in the antibiotic control well had died.

4.3.3 Copy number analysis

DNA from cell lines used in this project was prepared using a Qiagen Blood & Tissue kit, according to manufacturer's instructions. Briefly, protocol was as follows: cells from one 10cm dish were spun for 5min at 190rpm and resuspended in 400µl PBS. 40µl proteinase K was added, then 4µl RNase A (100mg/ml solution), then 400µl Buffer AL (lysis buffer). Eppendorfs were incubated in a 56°C water bath for 10min. 400µl ethanol (Fisher) was added to each tube and mixed thoroughly by vortexing. The mixture was divided between two DNeasy Mini spin columns and spun at 8000rpm for 1min. Collection tubes were discarded, and spin columns placed in fresh collection tubes. 500µl Buffer AW1 (wash buffer 1) was added to spin column and spun for 1min at 8000rpm. Collection tubes were discarded and spin columns placed in new collection tubes. 500µl Buffer AW2 (wash buffer 2) was added to spin columns and spun for 3min at 14,000rpm. Collection tubes were again discarded and spin columns transferred to a new Eppendorf. DNA was eluted by addition of 200µl Buffer AE (elution buffer) to the spin columns and incubation for 1min at RT. Columns were then spun for 1min at 8000rpm.

DNA was sent to Dr Henry Wood in the Pre-Cancer Genomics Group at the Leeds Institute of Molecular Medicine for copy number analysis by paired-end whole genome sequencing (2 x 100bp reads) on an Illumina HiSeq 2000. 30million pairs per samples were generated, which gave ~two-fold coverage of the genome. The most common ploidy was defined as 'normal' for the purposes of assessing copy number gain and loss. Analysis was run according to previously published procedures (Samman *et al.*, 2014). No viral genomes were detected in any sample, so cell lines were determined to be HPV negative with 95% confidence.

DNA from recently obtained cell lines (MSK921 and DETROIT562) was processed by the MBCF at CRUK-MI using the procedures described above. Data were analysed as above by Sudhakar Sahoo at CRUK-MI.

4.3.4 RT-PCR

RNA extraction and RT-PCR protocols are described in section 2.3. 20ng/µl RNA solutions were prepared from stocks. For LZK, 10µl (200ng) was added plus 0.5µl water.

For GAPDH, 1µl (20ng) plus 9.5µl water was used in the reaction. 25 cycles of amplification were used for both genes. Primers detailed in Appendix I.

4.3.5 Real-time quantitative reverse transcription PCR (qRT-PCR)

Primer validation had been carried out previously for reference genes (*ACTB* and *B2M*) by the CRUK-MI MBCF. qRT-PCR for *MAP3K13* was optimised by Dr Eleanor Trotter. Briefly, efficiency of the primers was tested using a serial dilution of RNA. The average C_T value for each data point was plotted against the log of the RNA concentration. The R^2 value for the resulting graph was 0.98.

The Power SYBR® Green RNA-to-C_T 1-Step Kit (Invitrogen) was used for qRT-PCR. From RNA preparations, 50ng/µl stocks were made. From this, 1µl RNA was added in triplicate to a 384-well qRT-PCR plate. A master mix was made for the remaining components, comprising the following quantities per well: 0.2µl 10µM F primer, 0.2µl R 10µM primer, 0.08µl RT enzyme mix, 5µl Power SYBR® Green RT-PCR Mix and 3.52µl water. Samples were run on an ABI 7900 HT real-time PCR instrument, with the following program:

- Reverse transcription: 48°C, 30min
- Amplification of DNA polymerase: 95°C, 10min
- Cycling (40 cycles):
  - Denature: 95°C, 15s
  - Anneal/Extend: 60°C, 1min

SDS software was used to compute C_T values. Graphs display relative expression of *MAP3K13* compared to a reference gene and a control sample. Calculations were as follows:

$$\Delta C_T = C_T(LZK) - C_T(reference\ gene)$$

$$\Delta\Delta C_T = \Delta C_T(sample) - \Delta C_T(control\ sample)$$

$$Relative\ expression = 2^{-\Delta\Delta CT}$$

4.3.6 Transient knockdown experiments

For transient knockdown in BEAS2B, MSK921, CAL33 and BICR56, cells were seeded at 160,000/well in 12-well plates or 16,000/well in 96-well plates. Cells were reverse

transfected with siRNA using DharmaFECT1 (0.5µl/well for 96-well plates, 5µl/well for 12-well plates), as section 2.5.1.2.

OKF6/TERT2 cells were seeded at 350,000 cells/well in 12-well plates and 35,000/well in 96-well plates. The following day, medium was changed and cells transfected with siRNA using DharmaFECT1 (0.5µl/well for 96-well plates, 5µl/well for 12-well plates, as above).

12-well plates were set up for collection of RNA or protein. Lysates were collected for protein (section 2.4.1) or RNA preparation (section 2.3.1) 48h after transfection. RT-PCR was performed as section 2.3.2.

Crystal violet assays were conducted in 12-well plates and stained 72h after transfection (see section 2.5.2.2 for staining).

MTT viability assays were conducted in triplicate in 96-well plates (see section 2.5.2.1) and analysed 72h after transfection.

siRNA used for LZK was obtained from Origene and used at 10nM. Sequences were as follows: GGAACACGAUGAAUCAGAGACGGCG (siLZKA), GGCGAAUAAUUUAUACAUGGAAUTG (siLZKB) and AGAACAGAAUGAGACGGAUAUCAAG (siLZKC). siRNA to p53 was ordered as a SMARTpool from Dharmacon (L-003329-00-0020) and used at 100nM. Non-targeting siRNA control was also ordered from Dharmacon (D-001810-01-20), and used at the same concentration as siRNA to the appropriate target.

4.3.7 Inducible knockdown experiments

4.3.7.1 Doxycycline

Doxycycline was obtained from Sigma Aldrich as a sterile 100mg/ml solution in DMSO. From this, 1mg/ml working stock solutions were prepared by 1:100 dilution in ddH_2O for use in cell culture experiments. The half-life of doxycycline in culture is 48h so for assays that continued beyond this point media was replaced at 48h intervals to add fresh doxycycline.

4.3.7.2 Collection of lysates

Cells were seeded in 6-well plates for collection of RNA or protein. 100,000/well was used for CAL33, and 50,000/well for BICR56, BICR22 and MSK921. The day after seeding, 1μg/ml doxycycline was added to appropriate wells and cells incubated for a further 48h. Protein or RNA was collected from 6-well plates 48h after induction using cold lysis buffer (see section 2.4.1) or RLT buffer (see section 2.3.1), respectively. See section 2.4.3 for phosphoarray-specific details.

4.3.7.3 MTT viability assays

Cells were seeded in triplicate at 2000 cells/well in 96-well plates for MTT assays. The following day medium was refreshed and cells treated with 1μg/ml doxycycline where appropriate. Cells were treated for 72h before analysis (see section 2.5.2.1).

4.3.7.4 Short-term growth and survival assays by crystal violet staining

Crystal violet assays were used to assess relative cell growth and survival after treatment. Cells were seeded in triplicate in 6-well plates at 100,000/well for CAL33, and 50,000/well for BICR56, BICR22 and MSK921. The day after seeding, 1μg/ml doxycycline was added to appropriate wells. Cells were incubated for 72h before staining (see section 2.5.2.2).

4.3.7.5 Colony formation assays

Cells were seeded at 1000/well in triplicate in 6-well plates. Half the wells were treated the next day with 1μg/ml doxycycline. Medium was refreshed every 2–3 days to add fresh doxycycline. Plates were incubated for 14 days before crystal violet staining (section 2.5.2.2).

4.3.7.6 Matrigel

The '3D on-top assay' (Lee *et al.*, 2007) was used to assess growth in matrigel. Matrigel used was Growth Factor Reduced, Phenol Red-Free Basement Membrane Matrix from mouse EHS tumour (Corning). Matrigel was thawed at 4°C overnight. Plates and tips were

pre-chilled prior to experiment, and experiment was conducted on ice, except where specified. 12-well plates were coated with 200µl matrigel and incubated at 37°C for 30min. Cells were plated at 80,000/well in 0.5ml medium and left to settle for 30min at 37°C. 0.5ml 5% matrigel in medium was added gently to each well. The following day, cells were treated with 1µg/ml doxycycline where required. After 72h treatment, plates were observed with an Axiovert 40 CFL Inverted Microscope, and photographs taken with the aid of AxioVision software. The 'Color Threshold' tool in ImageJ was used to assess average colony size. Three images per condition were used for measurement, and average colony size calculated for each condition.

4.3.7.7 BrdU proliferation assays

Cells were seeded in triplicate at 2000 cell/well in 96-well plates for BrdU assays. The following day medium was refreshed and cells treated with 1µg/ml doxycycline where appropriate. Cells were incubated for 48h before addition of BrdU label, then a further 24h before analysis (as described in section 2.5.2.3).

4.3.7.8 Cell cycle

For cell cycle analysis, cells were seeded in 6-well plates at 50,000/well for BICR56 and MSK921 and 100,000/well for CAL33. Plates were treated with 1µg/ml doxycycline the following day, and incubated for 48h before collection. Cell cycle samples were collected from 6-well plates 48h after induction and analysed as described in section 2.5.2.4.

4.3.7.9 Inhibitor treatments

BKM120 and GDC0941 were bought from Selleck Chemicals and dissolved in DMSO (Fisher). For western blot, cells were lysed 48h after induction and inhibitors were added to cells 1h before lysis. For BrdU assays, inhibitors were added (with doxycycline were appropriate) 24h after cell seeding and plates incubated for 48h before addition of BrdU label. A further 24h later media was removed and cells fixed for later analysis (section 2.5.2.3).

4.3.7.10 Rescue experiments

For rescue experiments, mutations were introduced into the WT LZK cDNA construct within the region targeted by LZK-sh1. This was conducted by Dr Eleanor Trotter. Mutations that do not change the amino acid sequence produced were made in each codon within this region to reduce the binding of the shRNA sequence to the cDNA (see Appendix I, section 6.1.4, for mutation details).

For CAL33, 200,000 cells/well were seeded in 6-well plates. The following day, medium was changed to add 1μg/ml doxycycline to half the wells. Cells were then transfected using Attractene (1.6μg DNA, 9μl Attractene in 100μl Opti-MEM), see section 2.5.1.1 for protocol. Medium was changed after 8h to reduce toxicity due to transfection, and fresh doxycycline added where appropriate. Cell lysate was collected 48h later, and crystal violet staining, as section 2.5.2.2, conducted 72h after transfection.

For BICR56, 150,000 cells were seeded in each well of a 6-well plate. The following day, medium was changed to add 1μg/ml doxycycline to half of the wells. Then cells were transfected using Lipofectamine LTX as section 2.5.1.4. Medium was changed after 8h to reduce toxicity caused by transfection. Cell lysate was collected 48h later, and crystal violet staining, as described in section 2.5.2.2, 72h after induction.

4.3.8 Transient overexpression

For overexpression assays in 293T and BEAS2B, cells were seeded into 12-well plates. After 24h they were transiently transfected using Attractene (0.8μg DNA, 3μl Attractene in 80μl Opti-MEM) as section 2.5.1.1. After 48h cells were lysed on ice using cold lysis buffer (section 2.4.1).

4.3.9 Inducible overexpression experiments

4.3.9.1 Tetracycline

Tetracycline was supplied as a 10mg/ml solution in water with the ViraPower HiPerform T-Rex Gateway Expression System (Invitrogen). This stock solution was diluted 1:10 in water for use in experiments.

4.3.9.2 Short-term growth and survival by crystal violet staining

50,000 cells/well were seeded in triplicate in 6-well plates and treated with 1μg/ml tetracycline the following day. Cells were incubated for 72h before crystal violet staining (section 2.5.2.2).

4.3.9.3 Colony formation assays

200 cells/well were seeded in triplicate in 6-well plates and treated with 1μg/ml tetracycline, where appropriate, every 2–3 days. For BEAS2B, plates were treated for 11 days after induction; for OKF6/TERT2, plates were treated for 14 days before staining with crystal violet (section 2.5.2.2).

4.3.10 Statistics

Error bars shown on graphs represent ±standard deviation. Two-tailed Student's t-test (with unequal standard deviation assumed) was used to assess significance of differences between groups for assays.

Analysis of variance (ANOVA) analysis was conducted by Phil Chapman to assess the significance of differences in mRNA expression between groups based on GISTIC (Genomic Identification of Significant Targets in Cancer algorithm) copy numbers.

4.4 Results

4.4.1 *MAP3K13* (LZK) is amplified in SCC

Examination of data from The Cancer Genome Atlas (TCGA) revealed that *MAP3K13* (LZK) was amplified in a considerable number of squamous cell tumours. For HNSCC, high-level amplification was present in 20% of TCGA dataset (Fig. 11A), while a further 56% had copy number gain of the gene (cBio, 2015). In the LSCC dataset, 36% had amplification and another 46% had copy number gain. In summary, for the two predominantly smoking-related SCCs with datasets available in the cBio portal, approximately 80% of patients had copy number gain of *MAP3K13*.

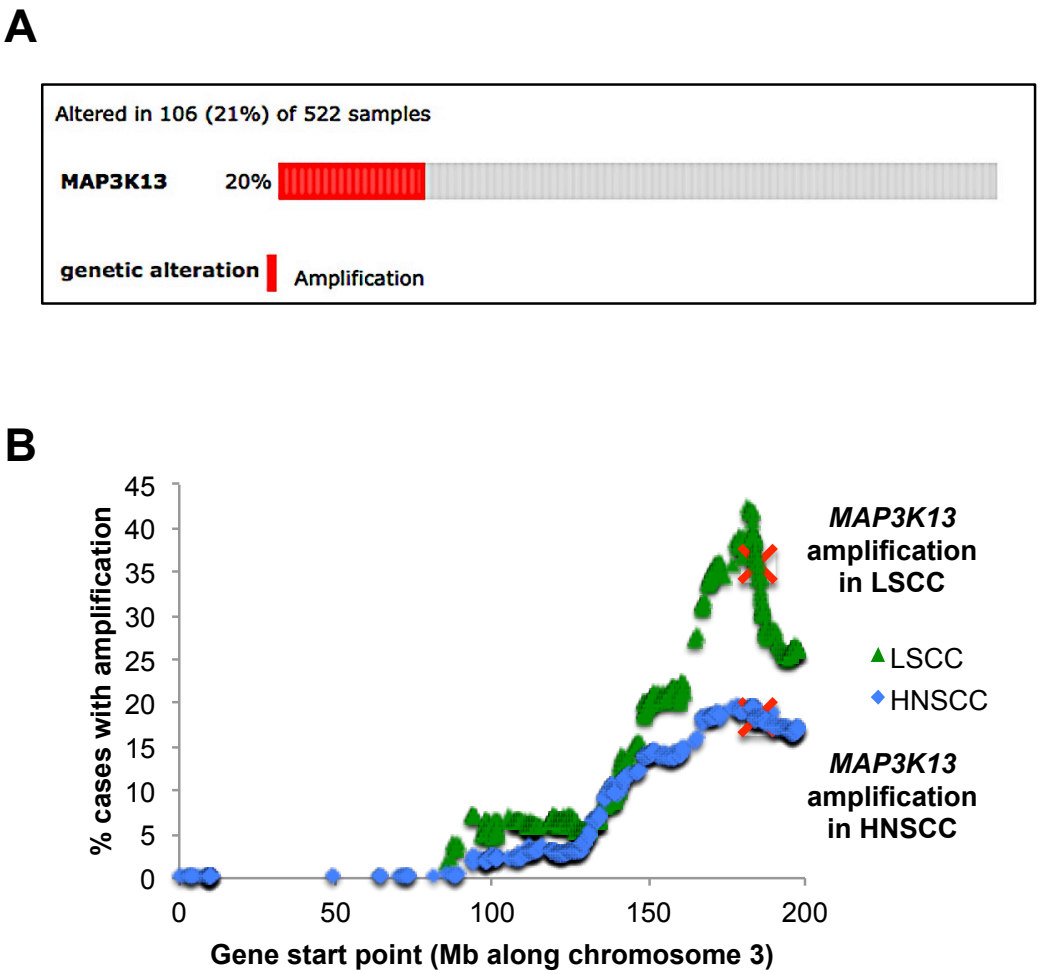

Figure 11: *MAP3K13* (LZK) is amplified in HNSCC and LSCC. A: Amplification of *MAP3K13* in 20% of HNSCC tumour samples from TCGA dataset. Graphic from cBio Portal. **B:** Graph representing % of HNSCC and LSCC patients with amplification of each gene on chromosome 3, according to TCGA. *MAP3K13* is marked with a red cross. Analysis conducted by Phil Chapman.

A

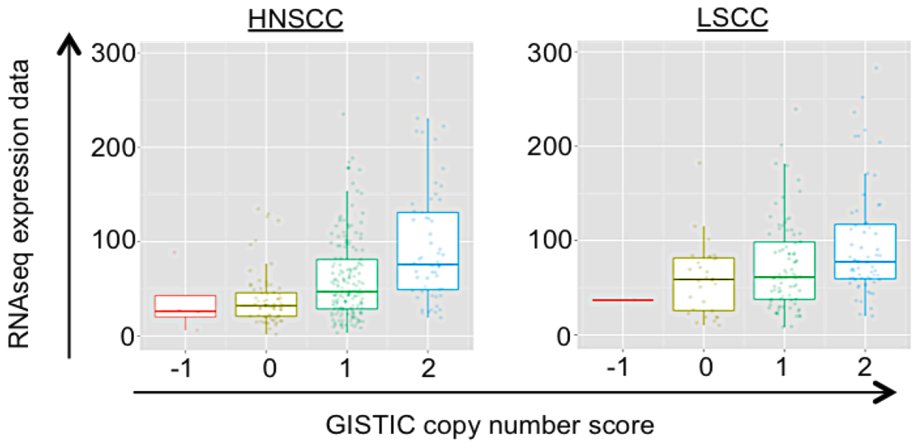

B

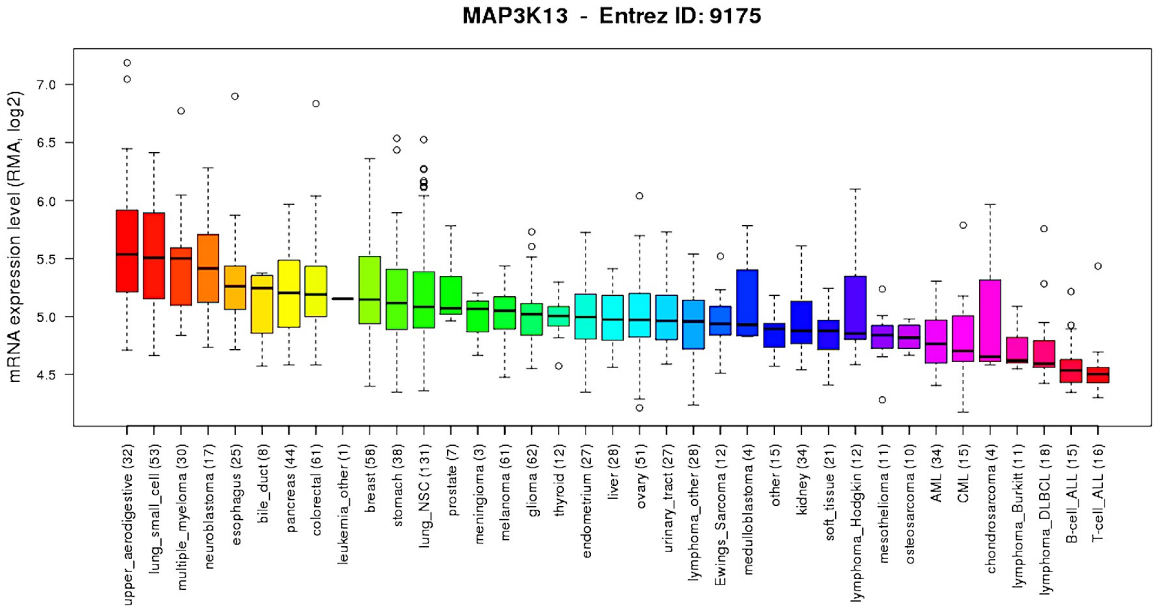

Figure 12: *MAP3K13* (LZK) mRNA expression in HNSCC and LSCC. A: Increased copy number of *MAP3K13* leads to an increase in mRNA expression levels. RNAseq expression data and GISTIC copy number scores were extracted from the cBio portal. Box plots compare expression of *MAP3K13* across different GISTIC copy number scores where -2=deletion, -1=loss of heterozygosity, 0=diploid, 1=gain and 2=amplification. Left panel shows HNSCC (ANOVA *p*-value 2.3e-11), right panel shows LSCC (ANOVA *p*-value=2.7e-4). Data prepared by Phil Chapman. **B:** Figure from CCLE showing that upper aerodigestive tract (UADT) cell lines have the highest expression of *MAP3K13* compared with other cancer cell lines. The vast majority of these UADT cell lines are HNSCC.

Analysis of the full length of chromosome 3 conducted by Phil Chapman (Drug Discovery Unit, CRUK-MI) using the cBio Portal revealed that *MAP3K13* was within the top 100 most frequently amplified genes in this region in LSCC and HNSCC (Fig. 11B). Further

analysis of data from TCGA tumour samples indicated that higher *MAP3K13* copy number was associated with significantly increased mRNA expression (Fig. 12A). This was true for LSCC and HNSCC, although the difference in mRNA expression between diploid and amplified tumour samples was more significant for HNSCC (t-test *p*-value: 2.93×10^{-4} for LSCC, 1.562×10^{-8} for HNSCC). In addition, data from the Cancer Cell Line Encyclopaedia (CCLE) have shown that upper aerodigestive tract (UADT) cell lines have the highest levels of *MAP3K13* mRNA compared with other cancer cell lines (Fig. 12B; note the vast majority of UADT cell lines are HNSCC) (CCLE, 2015). I decided to focus on HNSCC (rather than LSCC) in the first instance in part because of these factors, alongside the fact that a wider range of HNSCC lines were more readily available. Additionally, SOX2 has now been established as a critical tumourigenic target of the 3q amplicon in LSCC. Initial experiments comparing SOX2 protein expression in HNSCC and LSCC lines indicated that HNSCC cell lines frequently did not express SOX2, suggesting different genes on the 3q amplicon might promote tumourigenesis in HNSCC (see section 4.4.2.3).

4.4.2 Amplification of *MAP3K13* (LZK) correlates with increased expression in HNSCC cell lines

4.4.2.1 Copy number

A panel of SCC lines with 3q gain based on data from the CCLE was obtained to assess copy number gain and LZK expression levels. Normal cell lines used as controls included BEAS2B immortalised bronchial epithelial cells and OKF6/TERT2 immortalised normal oral keratinocytes. DNA was prepared from the cell lines and sent to Dr Henry Wood at the Leeds Institute of Molecular Medicine for copy number analysis by whole genome sequencing. Full genome strips are shown in Appendix II. A more detailed view of chromosome 3 is shown in Figure 13 to illustrate more clearly the position of *MAP3K13*. These data confirmed the presence of copy number gain including the 3q amplicon in almost all SCC cell lines tested (BICR6, BICR16, BICR22, BICR56, CAL33, PJ15, PJ34 and SCC15 HNSCC lines; NCIH520 LSCC line; KYSE70 oesophageal SCC line. LUDLU1 was obtained from Dr Wood and had already been verified in his lab to have amplification at 3q (Wood *et al.*, 2010)). MSK921 was the only SCC cell line tested that had no CNA at 3q. Many of the cell lines, including CAL33 and BICR56, had no specific amplicon but instead showed copy number gain of the entire 3q arm.

BICR22 was notable for the fact that its region of copy number gain did not encompass *MAP3K13*. Thus it was chosen as an additional control cell line alongside MSK921, which lacked CNA at 3q (Fig. 13; Singh *et al.*, 2001). The immortalised normal control cell lines, BEAS2B and OKF6/TERT2, were broadly diploid with no change at 3q, and thus confirmed to be appropriate normal tissue controls for this study.

4.4.2.2 mRNA expression

As described in section 4.4.1, RNAseq data from TCGA indicated that higher copy numbers of *MAP3K13* correlated with increased mRNA expression. Reverse transcription PCR (RT-PCR) was conducted to determine whether HNSCC cell lines with 3q gain would mimic primary tumours and display increased *MAP3K13* mRNA expression. Initially, semi-quantitative RT-PCR was carried out to analyse relative expression of *MAP3K13* compared with control cell lines. RT-PCR indicated that levels of *MAP3K13* mRNA were elevated in cell lines with 3q gain as compared with control lines (BEAS2B cells, OKF6/TERT2 immortalised oral keratinocytes and HNSCC lines that lacked copy number gain of *MAP3K13* (MSK921 and BICR22)) (Fig. 14A–B).

To verify and quantify these results, real-time quantitative RT-PCR (qRT-PCR) was conducted by my colleague, Dr Eleanor Trotter. *MAP3K13* cycle threshold (C_T) values were normalised to the β-actin reference gene (*ACTB*), and fold-change of these values expressed relative to that of the OKF6/TERT2 control cell line (Fig. 14C). A majority of the cell lines with copy number gain of *MAP3K13* had increased mRNA expression. CAL33 and BICR56 cell lines were part of the initial cell line panel, obtained based on CCLE data that these cell lines expressed high levels of *MAP3K13* mRNA, and they have been used extensively to evaluate the importance of LZK in HNSCC. For the BICR56 and CAL33 cell lines, mRNA expression was increased approximately four-fold as compared with OKF6/TERT2, BEAS2B and MSK921, which all have normal copy number at 3q. The increase as compared with BICR22, which has a 3q amplicon that does not include *MAP3K13*, was approximately two-fold. Results were similar for BICR16 and PJ15, while BICR6 and DETROIT562 had even higher expression relative to controls. In contrast, expression levels in PJ34 were similar to, or lower than, the control cell lines.

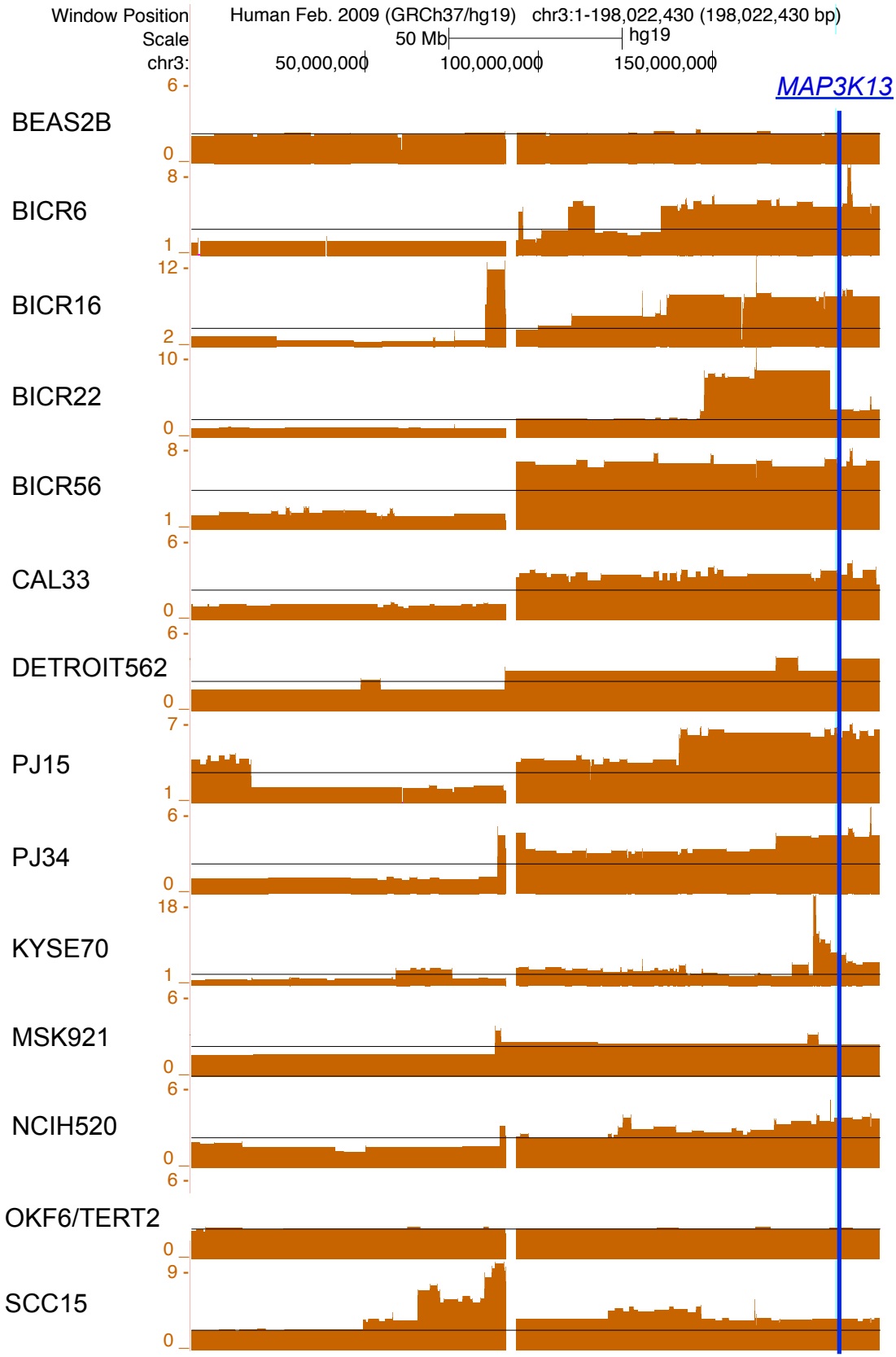

Figure 13: Copy number gain of *MAP3K13* (LZK) in SCC cell lines. Copy number analysis was conducted by whole genome sequencing to determine which cell lines harboured the 3q amplicon. Data for chromosome 3 are shown (for full genome strips see Appendix II). Most SCC lines have amplification of 3q (as compared with the overall average ploidy of each cell line, shown by black y-indicator line), whereas control cell lines do not (BEAS2B immortalised bronchial epithelial cells, OKF6/TERT2 immortalised oral keratinocytes, and MSK921 HNSCC cells). Other lines shown are HNSCC except KYSE70 (oesophageal SCC) and NCIH520 (LSCC).

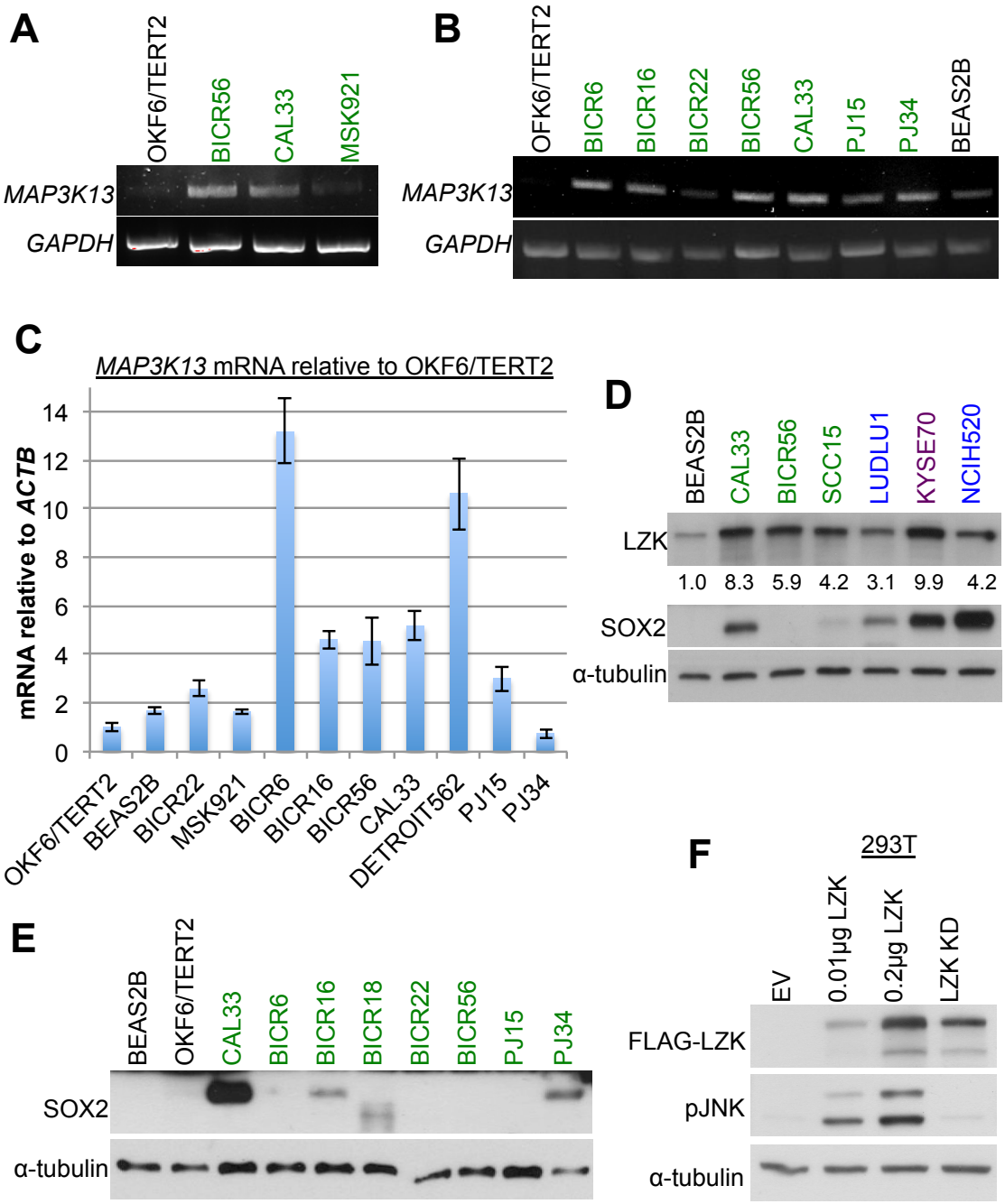

Figure 14: Expression of *MAP3K13*/LZK in HNSCC. A-B: Semi-quantitative RT-PCR shows increased *MAP3K13* mRNA expression in HNSCC lines with 3q copy number gain compared with OKF6/TERT2 immortalised normal oral keratinocytes, BEAS2B immortalised bronchial epithelial cells and MSK921 and BICR22 cells that lack copy number gain of *MAP3K13*. **C:** qRT-PCR shows increased *MAP3K13* mRNA expression in HNSCC lines with 3q copy number gain relative to controls. Results were normalised to *ACTB* (β-actin) control gene and then to OKF6/TERT2 control cell line. Conducted by Dr Eleanor Trotter. **D:** Protein levels of LZK in SCC cell lines as compared with BEAS2B cells. HNSCC cell lines are in green, LSCC in blue and oesophageal in purple. Quantification of LZK was assessed by densitometry using ImageJ, results were normalised for loading and are expressed relative to BEAS2B under the LZK blot. **E:** Low SOX2 protein expression in many HNSCC lines despite copy number gain of the *SOX2* gene. **F:** Transfection of 293T cells with a higher concentration of LZK cDNA increases downstream activation of JNK.

4.4.2.3 LZK protein expression

Western blot analysis was used to determine whether the increase in *MAP3K13* mRNA in cells with amplification of the gene led to an increase in protein levels of LZK. Western blots comparing LZK expression between BEAS2B cells and SCC cell lines from the initial cell line panel (CAL33, BICR56 and SCC15 HNSCC lines, LUDLU1 and NCIH520 LSCC lines, and KYSE70 oesophageal cells) indicated that there was an increase in expression at the protein level in cells with 3q gain (Fig. 14D). These experiments were conducted using a commercial antibody that was specific for detecting endogenous LZK (as verified by knockdown studies) and overexpressed LZK. Unfortunately, this specificity was lost in subsequent batches of the antibody (see Appendix III for details) and we were not able to confirm this observation for a wider panel of cell lines. A panel of additional commercial and custom made antibodies have been tested, but none have displayed specificity for detecting endogenous LZK levels (similar results obtained by Genentech, personal communication from Dr Mike Siu and Dr Joe Lewcock).

In summary, my results are consistent with primary tumour data where *MAP3K13* copy number gain in SCC cell lines correlates with increased expression of LZK.

Interestingly, SOX2 protein expression was not detected in many of the HNSCC lines, despite amplification of the *SOX2* gene (Fig. 14D–E), suggesting that SOX2 may not play the same oncogenic role as it does for LSCC. Additionally, LZK levels were lower in the LSCC lines (LUDLU1 and NCIH520) than the HNSCC lines (CAL33, BICR56 and SCC15), which provided a further reason to focus on HNSCC for this study (Fig. 14D).

In an attempt to recapitulate *MAP3K13* amplification in HNSCC, varying amounts of cDNA were transfected into 293T cells. As determined by densitometry using ImageJ, the fold-change between levels of protein expression after transfection was within the range of that between BEAS2B and the SCC lines shown in Figure 14D (Fig. 14F: 5-fold increase in FLAG-tagged LZK). Transfection of the higher quantity of cDNA further increased JNK activation as compared with transfection of the lower quantity of cDNA (Fig. 14F). This suggests that amplification of *MAP3K13* could theoretically increase downstream pathway activation in SCC, although these levels are likely to be higher than endogenous protein.

4.4.3 siRNA knockdown of LZK reduces viability and survival of HNSCC cells with 3q copy number gain

To determine whether LZK is important for maintaining tumourigenic phenotypes in HNSCC, siRNA-mediated knockdown was conducted in the HNSCC cell lines. Three individual siRNAs targeting LZK effectively depleted protein levels in CAL33 and BICR56 HNSCC cells, as well as in the OKF6/TERT2 and BEAS2B control cell lines (Fig. 15A). These experiments were conducted when the LZK antibody was still effectively detecting the endogenous protein (Appendix III). Upon establishing that later batches of the antibody were no longer able to detect endogenous LZK, knockdown was verified for each experiment by semi-quantitative RT-PCR, using *GAPDH* to verify equal RNA loading. The three LZK siRNAs effectively depleted mRNA levels in CAL33 and BICR56 HNSCC cells, as well as in the OKF6/TERT2 control cell line (Fig. 15B).

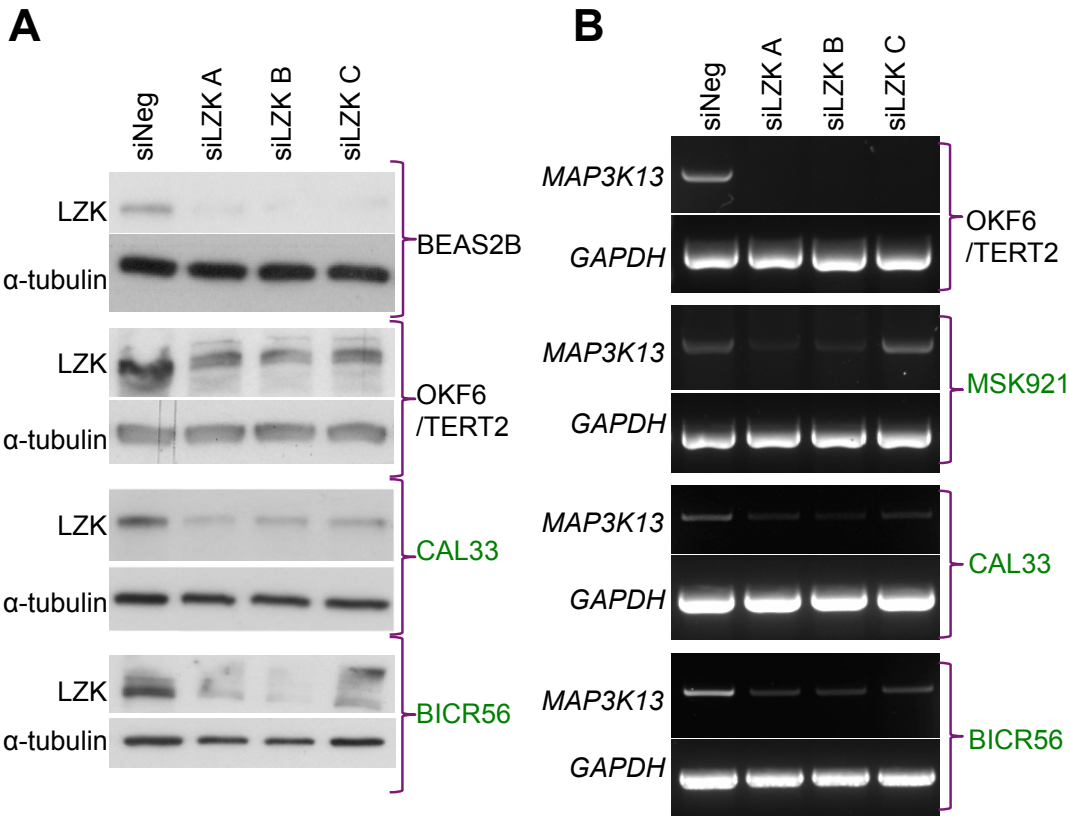

Figure 15: *MAP3K13*/LZK knockdown by siRNA. LZK is knocked down in HNSCC and normal control cell lines by three separate siRNAs. Cells were reverse transfected for 24h (CAL33 and BICR56) or 48h (BEAS2B and MSK921) with 10nM LZK or non-targeting control siRNA. Forward transfection for 72h was used for OKF6/TERT2 cells. **A:** Knockdown of LZK protein by western blot. **B:** Knockdown of *MAP3K13* mRNA by RT-PCR.

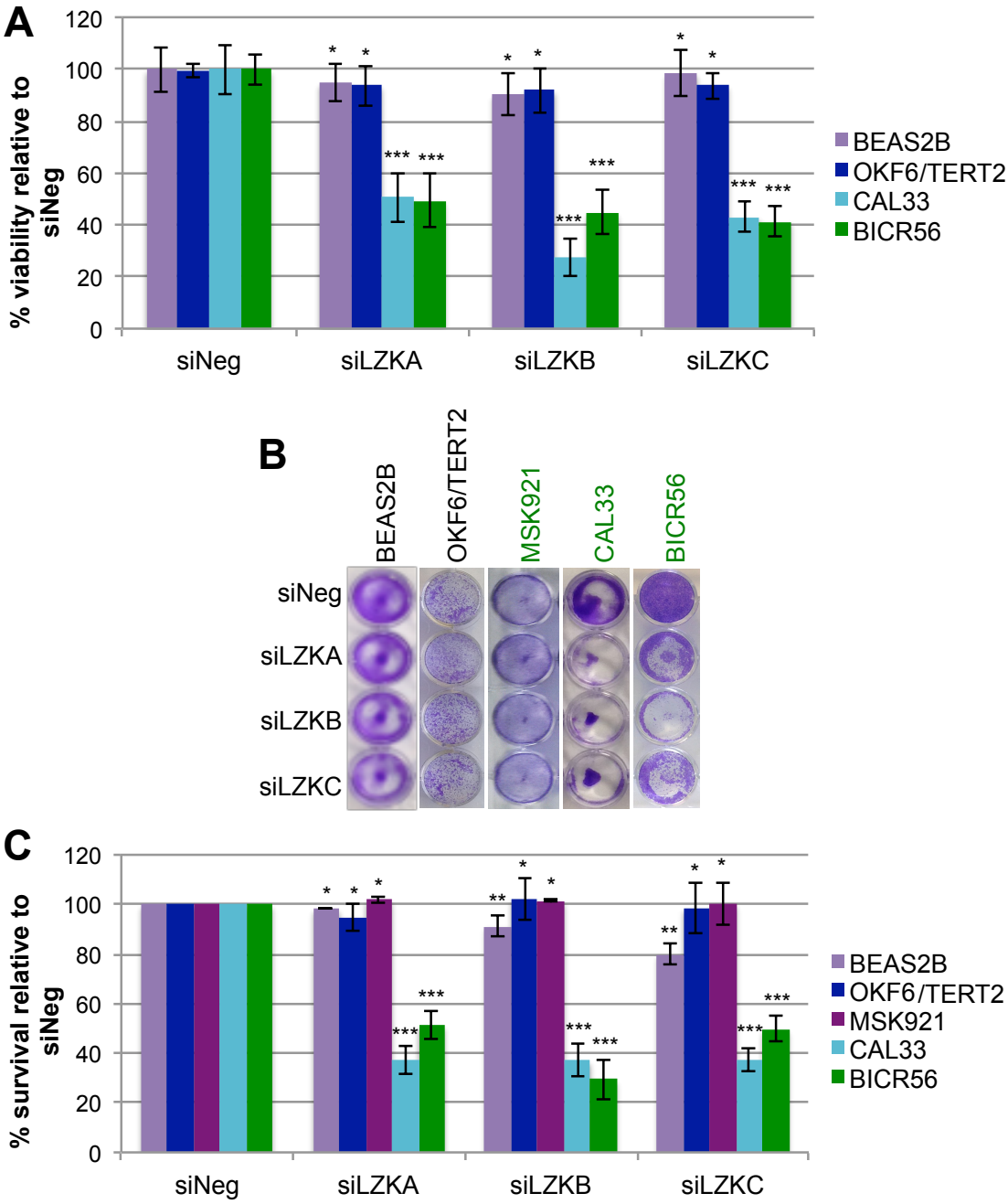

Figure 16: Transient LZK knockdown reduces viability and survival of HNSCC cells with 3q gain. A: Knockdown of LZK reduces viability of CAL33 and BICR56 HNSCC cell lines, but has no effect on BEAS2B immortalised bronchial cells or OKF6/TERT2 immortalised oral keratinocytes. Cells were transfected in triplicate and analysed by MTT assay 72h later. Graph shows average of at least three independent experiments and error bars indicate ±standard deviation. **B:** Knockdown of LZK reduces survival of CAL33 and BICR56 cells as compared with BEAS2B, OKF6/TERT2 and MSK921 controls. Cells were incubated for 72h after transfection, fixed with methanol and stained with crystal violet solution. **C:** Crystal violet was solubilised in 10% acetic acid and read at 595nm to quantify results. Results averaged from at least three independent experiments and expressed relative to siNeg. Error bars represent ±standard deviation. ***t-test *p*-value of <0.001 compared with relevant negative control result. **t-test 0.05>*p*-value>0.001 compared with relevant negative control. *non-significant t-test *p*-value of >0.05 compared with relevant negative control. Two-tailed Student's t-test used.

These siRNAs were used in an MTT assay to assess their effect on cellular viability. All three LZK siRNAs caused a highly significant reduction in viability in CAL33 and BICR56 cells, but had no effect on BEAS2B and OKF6/TERT2 control cell lines (Fig. 16A). To confirm MTT results, crystal violet staining was used to estimate relative cell proliferation and survival after LZK knockdown. Knockdown of LZK decreased survival of CAL33 and BICR56 cells. The effect on control cell lines was significantly less, although some toxicity, which reached significance, was seen for BEAS2B cells with B and C siRNAs (Fig. 16B–C).

Crystal violet assays were also conducted for the MSK921 cell line that lacks 3q gain. Knockdown was assessed by RT-PCR to detect LZK. A limited degree of knockdown was achieved in MSK921 for LZK A and B siRNAs, but siLZKC was not effective in this cell line (Fig. 15B). No toxicity was seen with LZK siRNAs for MSK921 by crystal violet assay (Fig. 16B–C); however, since knockdown was not very efficient under these conditions and by this point in time an inducible knockdown system had been set up, it was decided to proceed directly to inducible knockdown for this cell line.

In summary, siRNA experiments indicated that LZK was important for maintaining viability of HNSCC cell lines with 3q copy number gain; therefore I proceeded to shRNA inducible cell lines to validate these results further.

4.4.4 shRNA knockdown of LZK

To validate these viability effects, CAL33 and BICR56 cell lines with doxycycline-inducible expression of shRNA targeting *MAP3K13* were ordered from Sirion Biotech. After confirmation of effective knockdown in these cells, lentiviral stocks were ordered to enable in-house generation of inducible knockdown of LZK in a wider panel of cell lines. This system could not be utilised for the OKF6/TERT2 normal oral keratinocyte cell line, as it was already resistant to the selection marker puromycin because of the vector introduced during the immortalisation process (OKF6/TERT2 was immortalised by ectopic expression of hTERT (Dickson *et al.*, 2000)). The control cell line selected instead was MSK921, which has no CNA at 3q and no copy number gain of *MAP3K13*. An additional control used was BICR22, which had 3q gain, but *MAP3K13* was not included in its region of amplification.

4.4.4.1 Validating knockdown by RT-PCR and qRT-PCR

To test knockdown, cells were induced with doxycycline for 48h before collection of RNA. Sirion Biotech previously demonstrated ~80% knockdown with each shRNA after addition of doxycycline in CAL33 and BICR56 inducible cells by qRT-PCR relative to topoisomerase 1 (*TOP1*) (Fig. 17A). Knockdown was first verified by semi-quantitative RT-PCR. *GAPDH* was used as a control to verify equal total RNA concentration between samples. This demonstrated effective knockdown of LZK after addition of doxycycline in the inducible cell lines (Fig. 17B).

qRT-PCR was then conducted to quantify levels of inducible knockdown for each of the cell lines. *ACTB* was used as a control gene for this purpose. For CAL33, MSK921 and BICR22 inducible knockdown cell lines, knockdown of ~40–60% was observed by qRT-PCR relative to *ACTB* (Fig. 17C).

For BICR56 cell lines, *ACTB* levels were increased after addition of doxycycline, so *ACTB* could not be used as a control gene. Since this was not the case for any of the other inducible knockdown cell lines, it may be that this was an off-target effect of the doxycycline in BICR56 cells. Instead, β2-microglobulin (*B2M*) was used as a control to assess levels of *MAP3K13* knockdown by qRT-PCR (Fig. 17D). No change in *B2M* levels was observed after addition of doxycycline, as was the case for the *TOP1* control used by Sirion. In addition, when calculations were completed without comparison to a control gene, a reduction was seen in *MAP3K13* mRNA levels after knockdown (Fig. 17E). These data indicated that LZK was knocked down at the mRNA level in BICR56 cells with doxycycline-inducible knockdown of *MAP3K13*.

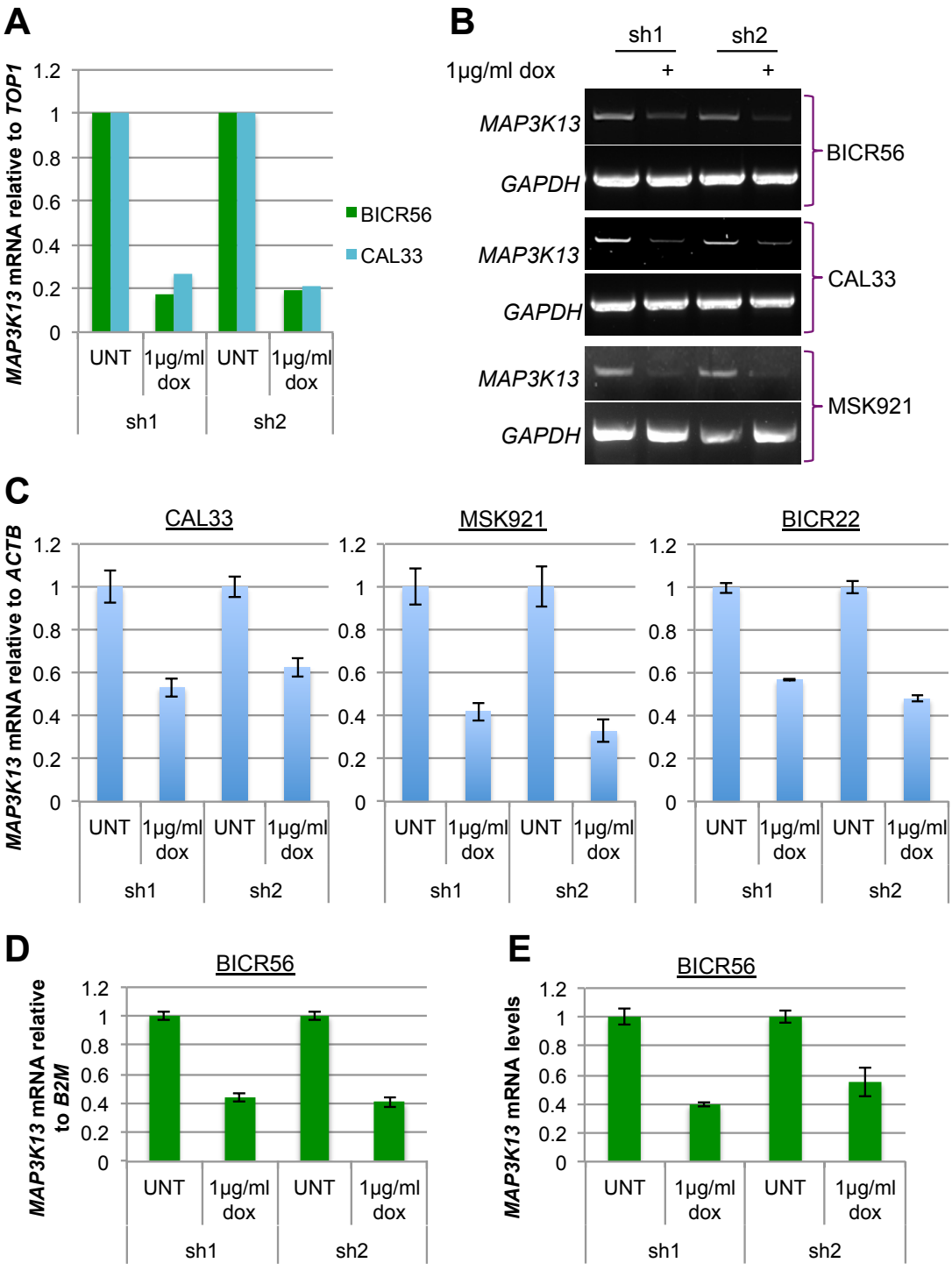

Figure 17: *MAP3K13* (LZK) knockdown by doxycycline-inducible shRNA. CAL33 and BICR56 inducible knockdown cell lines were generated by Sirion. I generated the MSK921 and BICR22 inducible lines using lentiviral stocks provided by Sirion. **A:** qRT-PCR data from Sirion shows knockdown of *MAP3K13* in BICR56 and CAL33 inducible knockdown lines, as compared with topoisomerase (*TOP1*) control gene. **B:** Induction by doxycycline reduces *MAP3K13* mRNA in BICR56, CAL33 and MSK921 inducible knockdown cells. Knockdown assessed by RT-PCR. **C:** qRT-PCR shows knockdown of *MAP3K13* (relative to *ACTB* control gene) relative to untreated in CAL33, MSK921 and BICR22 cell lines. **D:** qRT-PCR demonstrates knockdown of *MAP3K13* relative to the *B2M* control gene in BICR56 inducible knockdown cells. **E:** qRT-PCR shows knockdown of *MAP3K13* in BICR56 inducible knockdown cells – without reference to a control gene.

4.4.4.2 Survival and viability

Initially, short-term survival assays were used to validate the effects seen with LZK siRNA in these cell lines. Induction of knockdown by doxycycline was conducted for 72h before analysis by crystal violet staining. Induced knockdown of LZK led to a ~50% decrease in cell survival in BICR56 and CAL33 cells, but had no effect on MSK921 and BICR22 cells that lack *MAP3K13* copy number gain (Fig. 18A–B).

MTT assays were conducted after 72h induction to verify these data. The MTT assay produced very similar results for CAL33 and BICR56 inducible knockdown cells, showing a 40–50% reduction in viability of cells after LZK knockdown by doxycycline induction. For MSK921, there was no significant effect on viability after LZK knockdown (Fig. 18C).

To confirm these effects in a 3D setting that more closely replicates the tumour microenvironment, two different methods were explored. Initially, attempts were made to grow the cells in soft agar; however, neither BICR56 nor CAL33 cells grew in soft agar at 10,000 or 15,000 cells/well. The second method tested was the '3D on-top' matrigel method (Lee *et al.*, 2007). The matrigel used was Engelbreth-Holm-Swarm (EHS) extracellular matrix extract, which contains the main components of the basement membrane and thus better represents the tumour microenvironment than 2D culture on plastic. Cells were seeded on top of a layer of matrigel, coated with a dilute solution of matrigel and treated with doxycycline the following day. After 72h, cells were visualised using an inverted light microscope and pictures were taken for analysis (Fig. 19A). Images were analysed using the 'Color Threshold' tool in ImageJ, which enabled calculation of average colony size for each picture taken. The three main cell lines utilised in this study grew well on matrigel. CAL33 and BICR56 had reduced colony sizes after LZK knockdown, whereas no significant effect was seen for MSK921 (Fig. 19B).

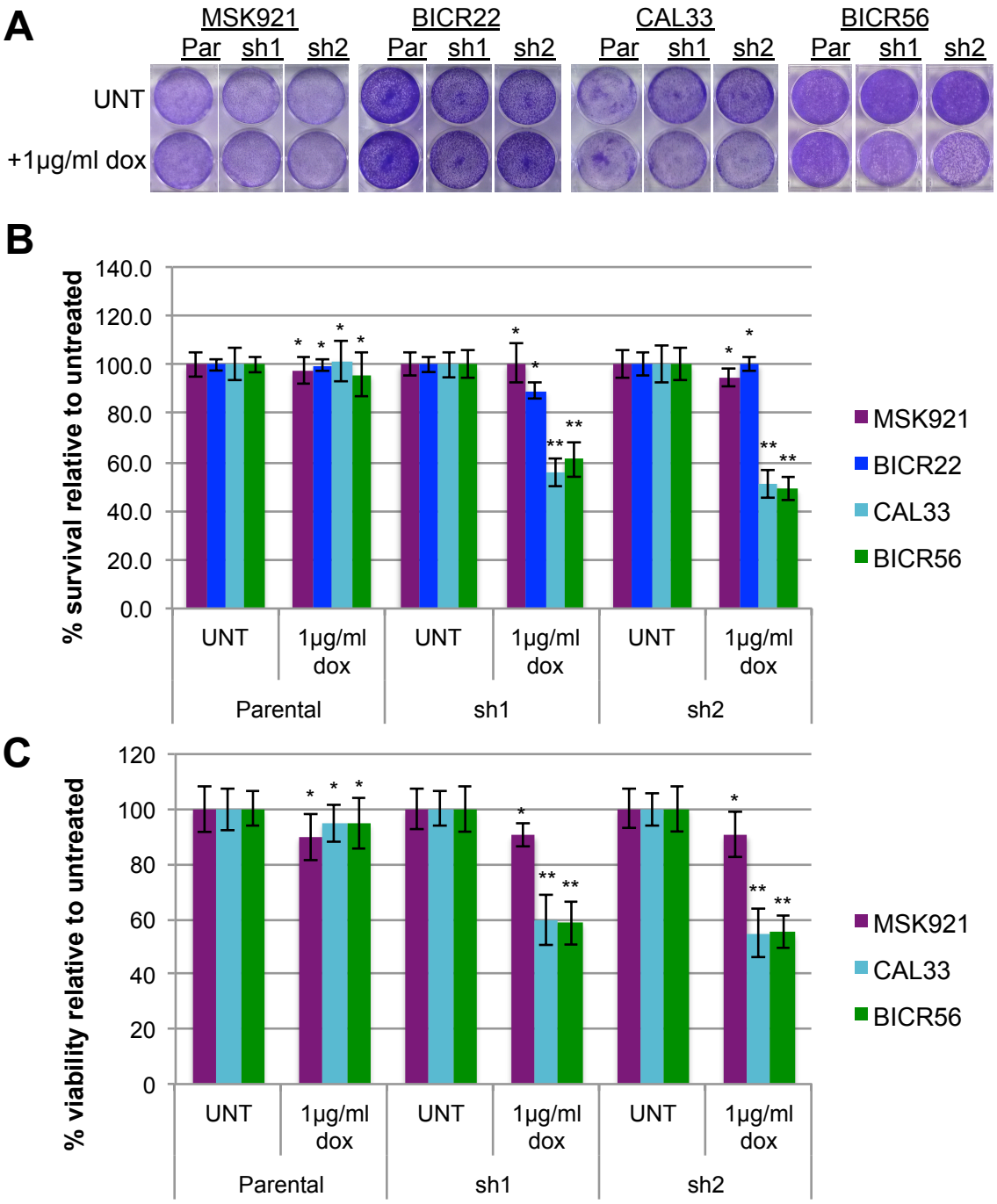

Figure 18: LZK knockdown by doxycycline-inducible shRNA reduces survival and viability of HNSCC cells with copy number gain. A: Knockdown of LZK reduces cell survival of CAL33 and BICR56 cells as compared with BICR22 and MSK921 controls. Cells were seeded in triplicate, incubated for 72h after doxycycline treatment, fixed with methanol and stained with crystal violet solution. **B:** Quantification of survival assay. Crystal violet was solubilised in 10% acetic acid and read at 595nm to quantify results. Results expressed relative to untreated wells. Graph shows average of at least three independent experiments and error bars represent ±standard deviation. **C:** Knockdown of LZK reduces viability of CAL33 and BICR56 HNSCC cell lines, but has no effect on MSK921 cells. Cells were induced in triplicate and analysed by MTT assay 72h later. Graph shows average of at least three independent experiments and error bars indicate ±standard deviation. **t-test *p*-value of <0.05 compared with relevant untreated control result. *non-significant t-test *p*-value of >0.05 compared with relevant untreated control. Two-tailed Student's t-test used.

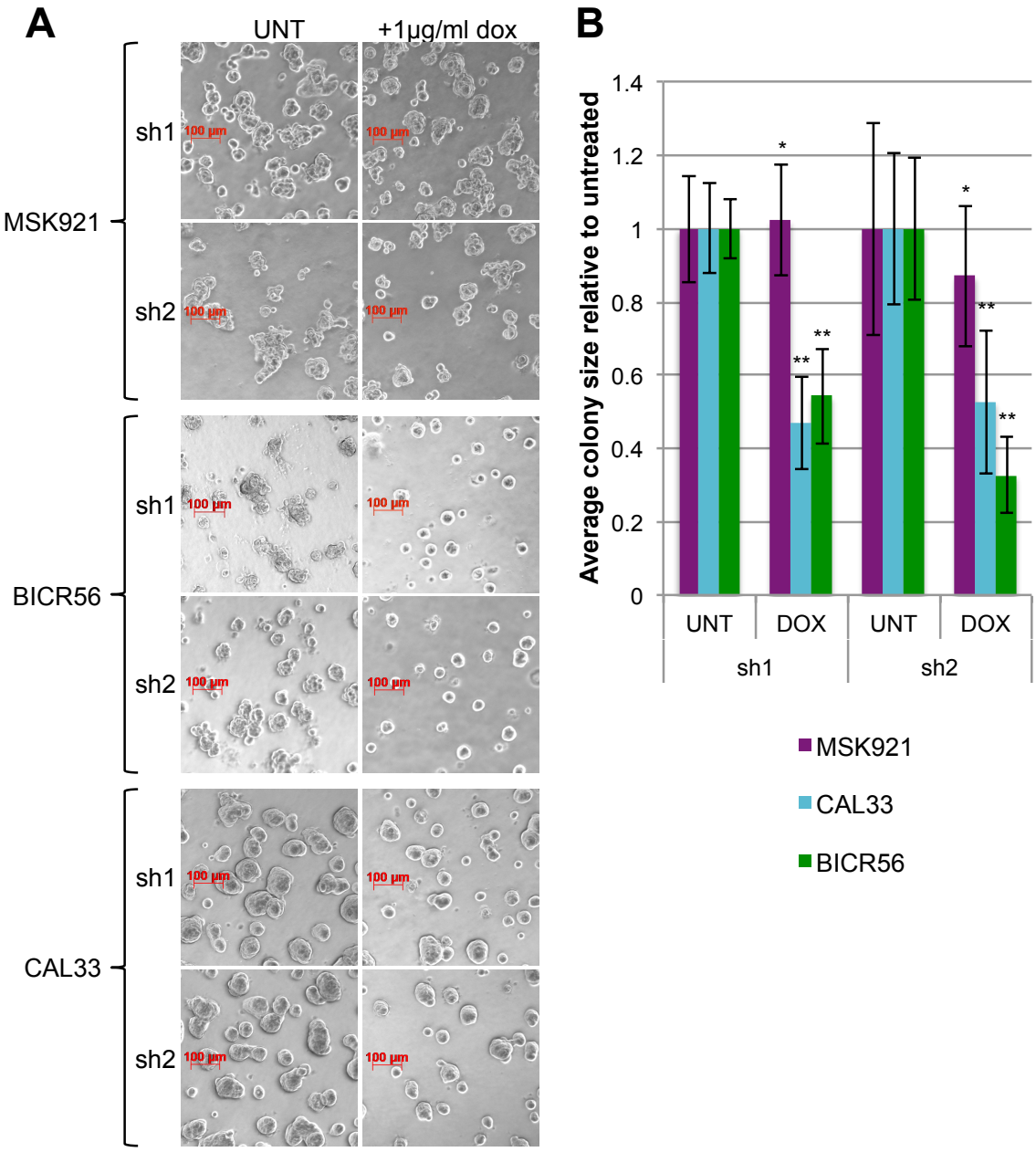

Figure 19: LZK knockdown by doxycycline-inducible shRNA reduces growth of cells in matrigel. A: Knockdown of LZK reduces cell growth of CAL33 and BICR56 cells in EHS matrigel as compared with MSK921 controls. Cells were incubated for 72h after doxycycline treatment, and visualised using an inverted light microscope. **B:** Quantification of results. The 'Color Threshold' tool in ImageJ was used to assess average colony size. Three images per condition were used for measurement, and average colony size for each calculated. Values expressed relative to untreated control. Error bars represent ±standard deviation. **t-test *p*-value of <0.05 compared with relevant untreated control result. *non-significant t-test *p*-value of >0.05 compared with relevant untreated control. Two-tailed Student's t-test used.

4.4.4.3 Colony formation assays

Colony formation assays were then used to assess the importance of LZK in clonogenicity. Cells were seeded at low density and induced with doxycycline for two weeks before crystal violet staining. A near complete ablation of colony forming ability was observed for CAL33 and BICR56 cells after induced knockdown of LZK (Fig. 20A–B). For BICR22 (experiment conducted by Dr Pedro Torres), no effect on colony formation was seen for the sh1 cell line; however, for sh2, colony formation was actually increased by doxycycline treatment (Fig. 20A,C). Since this only occurred for one construct, it was unlikely to be due to LZK knockdown, and may have been an off-target effect of this construct in BICR22 cells.

The MSK921 cells did show a reduction in colony formation after doxycycline treatment (Fig. 20A). This effect occurred at least in part due to the toxicity of doxycycline on this cell line, as the parental cells showed a reduction of ~20% that was significant (Fig. 20C). Discrepancies observed between parental and selected LZK inducible knockdown cell lines are likely attributable to the fact that selected knockdown cells appeared to proliferate at a reduced rate compared to parental cells. However, at this stage it cannot be ruled out that LZK may play a minor role in promoting colony formation in the MSK921 cells. Regardless of whether LZK has a role in the MSK921 cells, it is clear that knockdown had a much more marked effect on cells with copy number gain of the gene.

In summary, the striking effects observed in the CAL33 and BICR56 cells, whereby no visible colonies were present after doxycycline treatment, highlight that LZK is essential for colony formation in these HNSCC cell lines with 3q copy number gain.

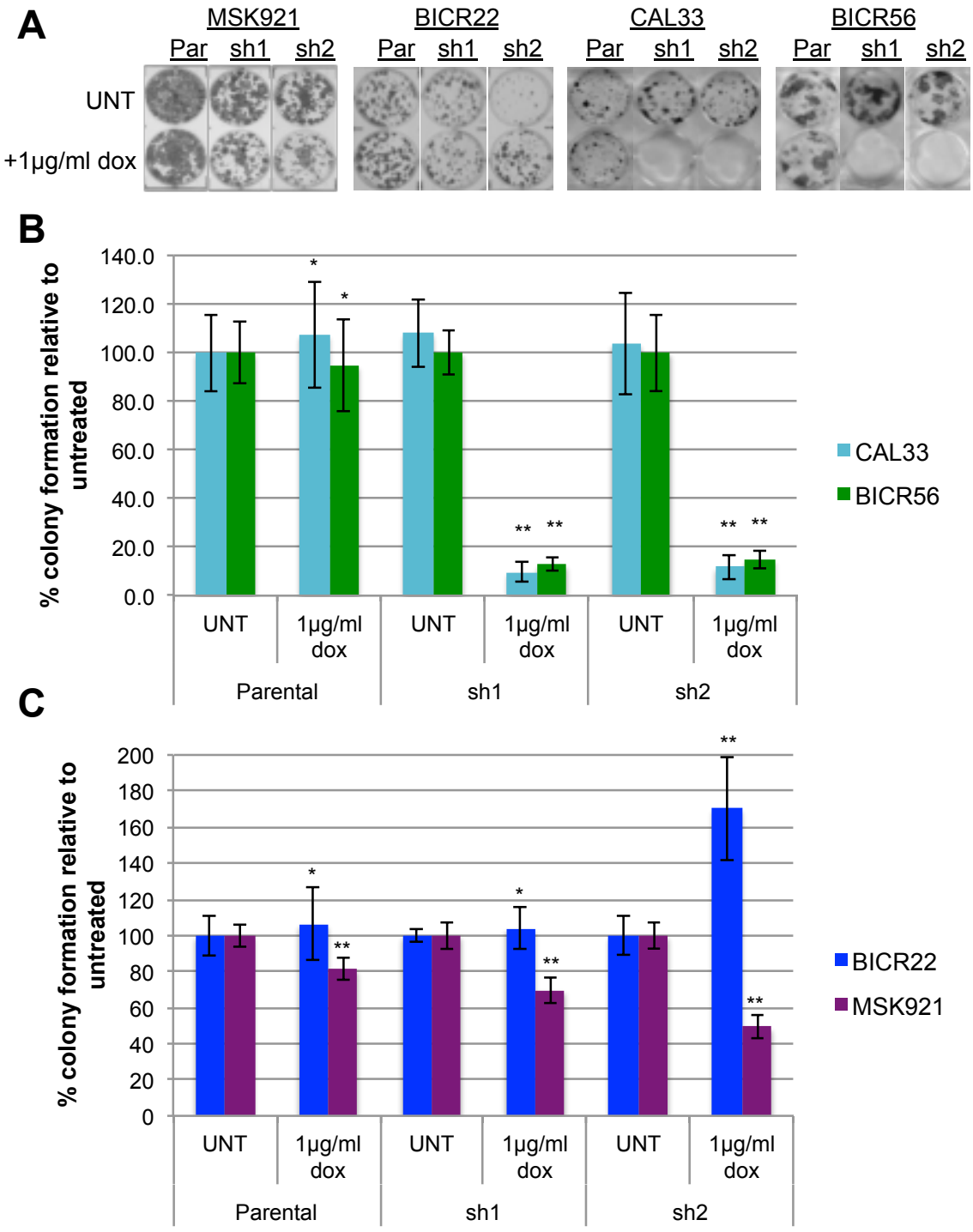

Figure 20: LZK knockdown by doxycycline-inducible shRNA ablates colony formation of cells with 3q gain. A: Knockdown of LZK reduces colony forming ability of CAL33 and BICR56 cells as compared with BICR22 and MSK921 controls. Cells were seeded at 1000/well in triplicate and treated with doxycycline for 14 days before fixing with methanol and staining with crystal violet. BICR22 experiments conducted by Dr Pedro Torres. **B-C:** Quantification of results. **B**=cells with gain of *MAP3K13*, **C**=cells without gain of this gene. Crystal violet was solubilised in 10% acetic acid and read at 595nm to quantify results. Graphs show an average of at least three independent experiments and error bars represent ±standard deviation. **t-test *p*-value of <0.05 compared with relevant untreated control result. *non-significant t-test *p*-value of >0.05 compared with relevant untreated control. Two-tailed Student's t-test used.

4.4.4.4 Phenotypic assays

To investigate potential mechanisms of reduced viability, phenotypic assays were carried out. First, a BrdU assay was utilised to assess proliferation. Doxycycline-induced knockdown had no effect on proliferation of BICR22 control cells (Fig. 21A). For MSK921, doxycycline had a very minor, but significant, effect on proliferation after 72h, but this was true for the parental cells as well as the inducible knockdown lines, indicating that this result was not due to LZK knockdown. The difference between doxycycline-treated parental MSK921 cells and doxycycline-treated shRNA-inducible cells was not significant (Fig. 21B).

For CAL33 and BICR56 cells, a significant decrease in proliferation was observed after induction of shRNA targeting *MAP3K13* (Fig. 21A). The decrease seen was to a similar extent as the reduction observed for viability and survival assays, suggesting that this proliferative decrease may be the main mechanism underpinning these effects. This was supported by observation of the cells under the microscope after doxycycline treatment; cells were not visibly floating after induced knockdown, providing an initial indication that the reduction in viability and survival resulted from altered regulation of proliferation rather than apoptosis, anoikis, or other mechanisms.

To support this hypothesis, western blots were run after a longer period of inducible knockdown. Cells were set up for 72h and 96h doxycycline-induction, and lysates were run to identify any PARP cleavage, a marker of apoptosis. No cleaved PARP was observed after doxycycline-induced knockdown in CAL33 or BICR56 cells (Fig. 22).

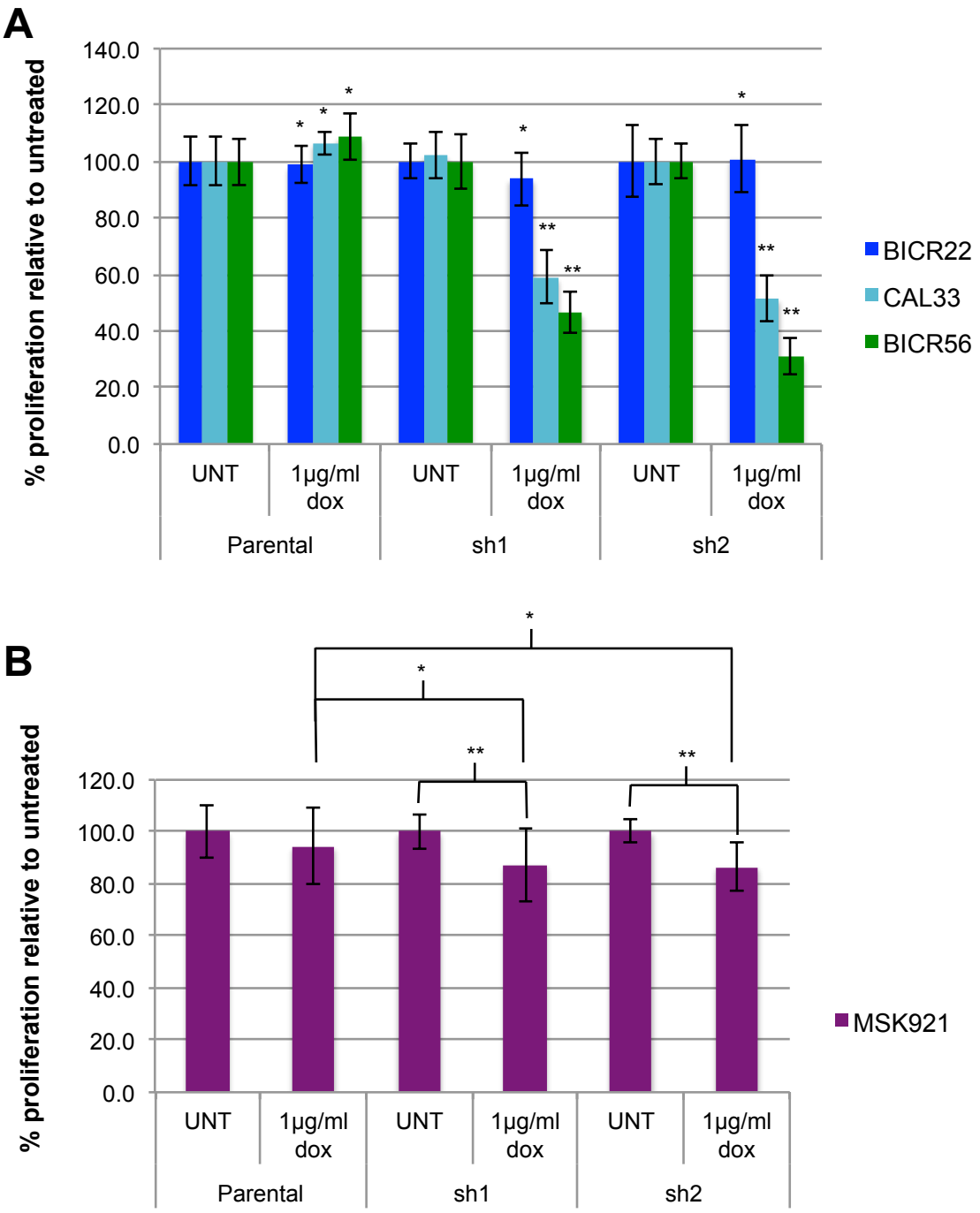

Figure 21: LZK knockdown by doxycycline-inducible shRNA reduces proliferation of HNSCC cells with copy number gain. A: Knockdown of LZK reduces proliferation of CAL33 and BICR56 cells as compared with BICR22 control. Cells were incubated for 48h after doxycycline treatment, then BrdU label was added for a further 24h before being fixed for later analysis. Graph shows average of at least three independent experiments and error bars indicate ±standard deviation. **t-test *p*-value of <0.05 compared with relevant untreated control result. *non-significant t-test *p*-value of >0.05 compared to relevant untreated control. Two-tailed Student's t-test used. **B:** BrdU assay conducted as (**A**) for MSK921 control cells. Minor but significant effect of doxycycline is seen for inducible knockdown cells, but this is not significant when compared with dox-treated parental cells. **t-test *p*-value of <0.05. *non-significant t-test *p*-value of >0.05. Two-tailed Student's t-test used.

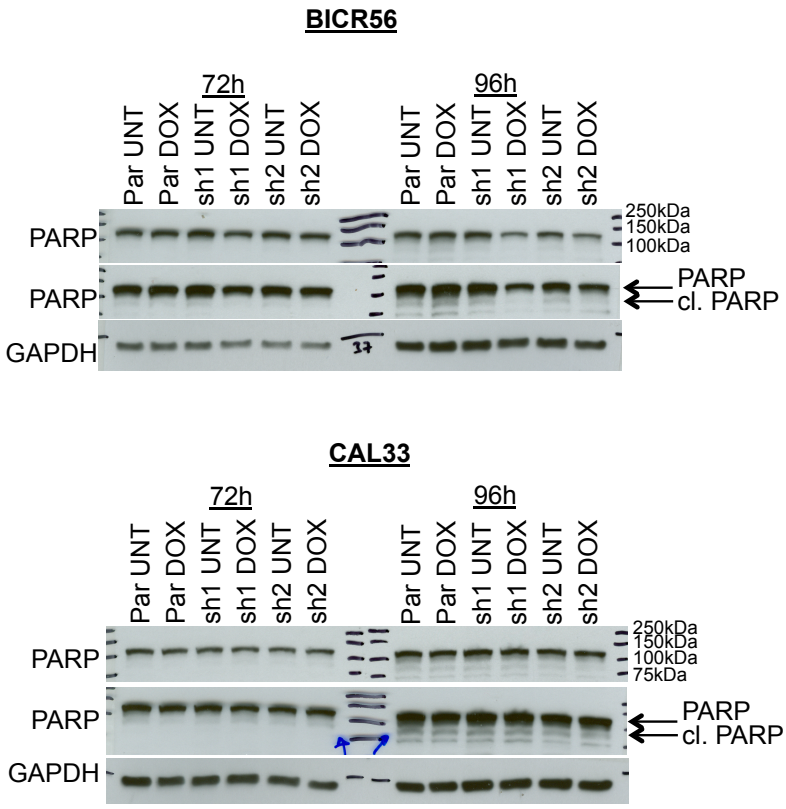

Figure 22: LZK knockdown does not promote PARP cleavage. PARP cleavage assay. Cells were induced with doxycycline for 72 or 96h before lysis. No increase is observed at the expected size for cleaved PARP after doxycycline treatment. Uncleaved PARP appears above the 100kDa marker, cleaved PARP should appear underneath the 100kDa marker.

Propidium iodide assays were then used to assess the effect of LZK knockdown on progression through the cell cycle. An increase in the percentage of cells in G1 phase and concomitant decrease in cells in S, G2 and M stages was observed for CAL33 and BICR56 inducible knockdown cells, but not for MSK921 (Fig. 23A). This led to an increase in G1/S ratio, a measure of cell cycle arrest, of approximately three-fold for CAL33 and two-fold for BICR56 (Fig. 23B).

Also of note are the unusual sub-G1 peaks for BICR56 and CAL33. These do not look like typical apoptotic cells, which usually have a less defined peak. Whether these peaks represent apoptotic cells is unclear, and they may instead be due to DNA aneuploidy in these cell lines. DNA aneuploidy should not occur in clonal cell lines; however, inducible knockdown cells are a collection of cells pooled following the introduction of shRNA, so there could be a subclone growing in the cells. Further work would need to be performed to understand the identity of this peak. To test the presence of aneuploidy, cells with known DNA content could be spiked into the samples to assess linearity of the system and assign peaks. Clones could be selected from early cell passages of inducible knockdown

cells to determine whether a subclone with differing DNA content has been selected. There was no consistent difference in the percentage of cells in this peak after LZK knockdown and the most striking change was the G1/S ratio (Fig. 23).

Preliminary cell cycle analysis (n=2) was consistent with the BrdU proliferation results. Overall, these results indicate that LZK knockdown has a cytostatic effect rather than a cytotoxic effect.

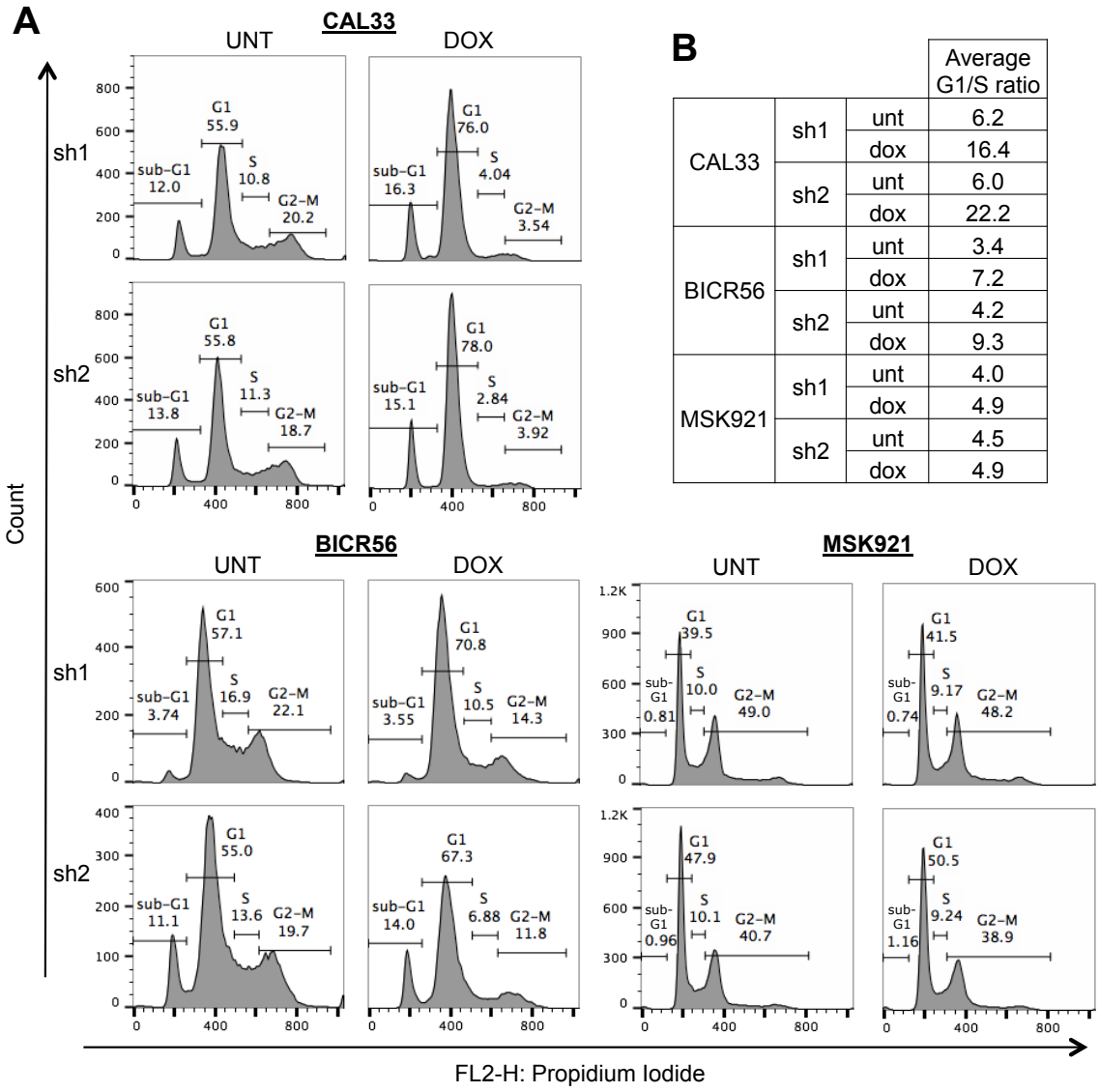

			Average G1/S ratio
CAL33	sh1	unt	6.2
		dox	16.4
	sh2	unt	6.0
		dox	22.2
BICR56	sh1	unt	3.4
		dox	7.2
	sh2	unt	4.2
		dox	9.3
MSK921	sh1	unt	4.0
		dox	4.9
	sh2	unt	4.5
		dox	4.9

Figure 23: LZK knockdown by doxycycline-inducible shRNA leads to cell cycle arrest in G1. A: Histograms showing cell count vs FL2-H (propidium iodide) for inducible knockdown cells. Cells were induced with 1µg/ml doxycycline 24h after seeding and incubated for 48h before collection. Media were collected before trypsinisation of adherent cells, to include any floating cells in the analysis. Once stained, cells were analysed on a 3-colour FACSCalibur. For CAL33 and BICR56 (but not MSK921), the percentage of cells in G1 increased, and percentage of cells in S and G2/M decreased, upon doxycycline induction. **B:** Average G1/S ratio over two independent experiments for each cell line. G1/S ratio is increased for CAL33 and BICR56 cells after doxycycline-induced LZK knockdown.

4.4.5 Elucidation of signalling pathways downstream of LZK

4.4.5.1 Signalling pathways activated upon overexpression of LZK

To identify the pathways activated by LZK, a FLAG-tagged construct was overexpressed in 293T cells. LZK overexpression led to increased activation of the expected downstream JNK pathway, as compared with the EV control (Fig. 24A). This was not the case for a KD construct of LZK, made by mutation of the invariant ATP-binding lysine in the VAIK motif to a methionine (K195M), indicating that JNK activation was a kinase-dependent effect. In contrast, no further activation of the p38 pathway was apparent, nor the NFκB pathway, as assessed by IκBα (inhibitor of NFκB alpha) phosphorylation (Fig. 24A).

These results were further verified with control cell lines (BEAS2B and OKF6/TERT2) that were engineered to induce expression of LZK upon treatment with tetracycline. These LZK tetracycline-inducible cell lines were generated by stepwise lentiviral transduction of pLenti3.3/TR vector (for tetracycline repressor (TR) expression), followed by LZK in pLenti/TO/V5-DEST vector. Induction of *MAP3K13* expression after addition of tetracycline was confirmed by RT-PCR in both cell lines (Fig. 24B–C). Analysis of downstream signalling after induction confirmed that LZK activated the JNK pathway, but not the p38 pathway in both cell lines (Fig. 24B–C). Phosphorylation of IκBα was not detected in either line (data not shown).

A phospho-kinase array was then performed to reveal other pathways that may be activated by LZK; this confirmed that induction of LZK by tetracycline in OKF6/TERT2 cells led to increased levels of pJNK and p-cJUN, indicating activation of the JNK–cJUN pathway, but did not reveal any additional downstream targets (Fig. 24D). A MAPK array was then used to elucidate the specific isoforms activated downstream of LZK; this showed that LZK induction activated JNK1 and JNK2, but not JNK3 (Fig. 24E). No activation of any ERK or p38 isoform, nor a wide range of other kinase targets, was observed (see Appendix IV for full list).

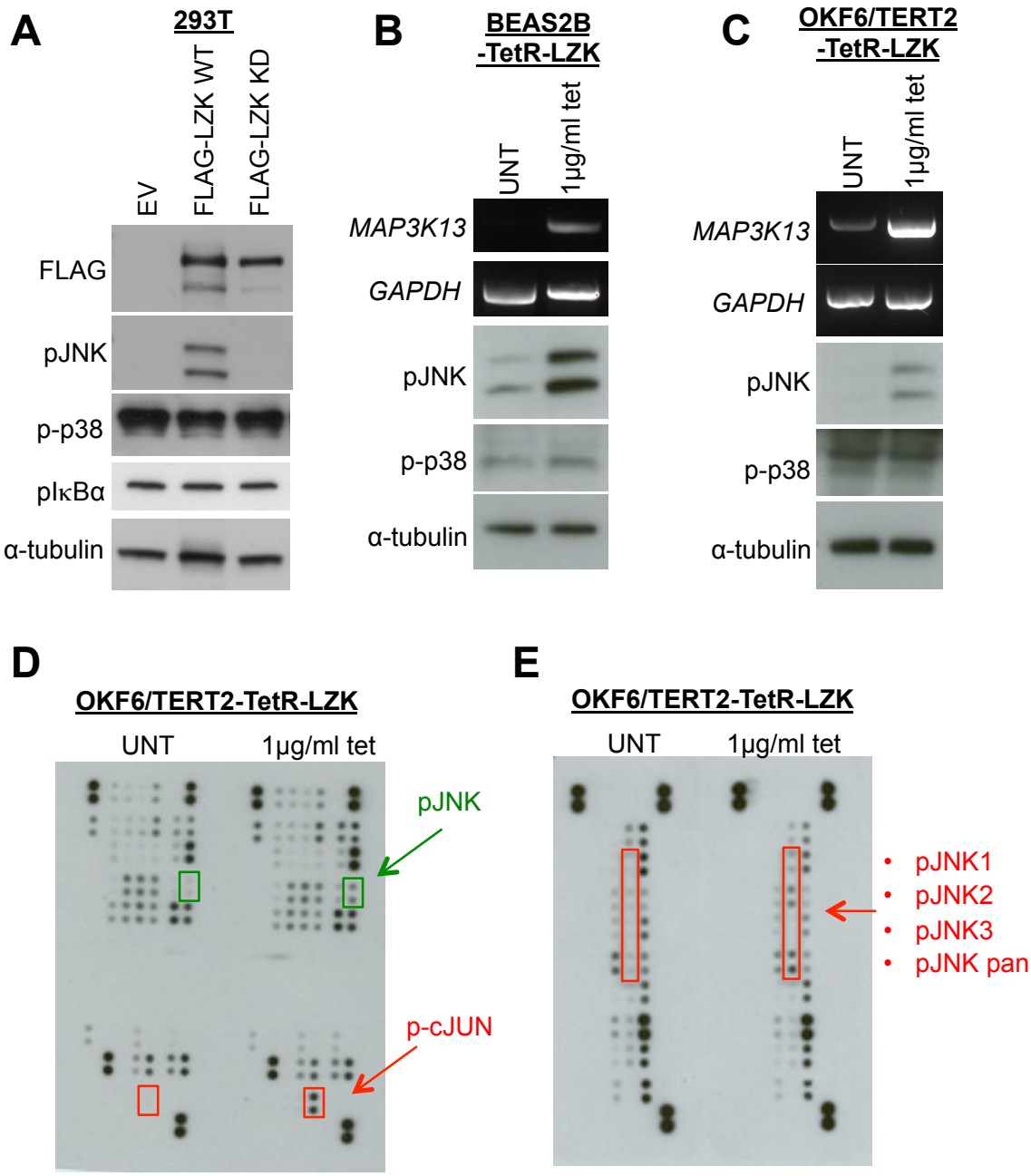

Figure 24: Activation of cellular pathways upon LZK overexpression. A: FLAG-tagged LZK constructs were overexpressed in 293T cells. Lysates were resolved by SDS-PAGE and analysed by western blot using antibodies for downstream phospho-proteins. α-tubulin was used to assess loading. LZK WT (but not KD) activates the JNK pathway, but not the NFκB (as assessed by pIκBα levels) or p38 pathways. **B-C:** Tetracycline-inducible expression of LZK in BEAS2B or OKF6/TERT2 cells was introduced by lentiviral transduction. Treatment with tetracycline for 48h induced *MAP3K13* (LZK) expression, leading to activation of the JNK but not the p38 pathway. Induction was checked by RT-PCR due to unreliable antibodies. **D:** Analysis of a wider range of possible downstream substrates was conducted by phospho-kinase array using LZK-inducible OKF6/TERT2 cells. LZK expression was induced by incubation with tetracycline for 48h; only pJNK and p-cJUN show increased levels after induction. **E:** A MAPK-specific phosphoarray was used to delineate the specific isoforms activated downstream of LZK. After 48h induction, only JNK1 and JNK2 show increased activation.

4.4.5.2 Investigation of pathways downstream of LZK after knockdown

Overexpression experiments indicated that LZK activates the JNK pathway, but did not reveal any other downstream targets for this kinase in normal control cells. However, in a tumour cell context, different interactions may be favoured that could enable activation of a distinct range of pathways than is observed upon overexpression in normal control cells. Therefore, pathways regulated downstream of LZK were investigated by western blot after inducible knockdown of LZK in HNSCC cells.

Results of investigations into the expected downstream signalling pathways are shown in Figure 25. In BICR56 cells, endogenous levels of pJNK and p-p38 were very low, and there was no decrease in pJNK or p-p38 after doxycycline induction (Fig. 25A), while it was not possible to detect either pJNK or p-p38 in CAL33 cells. This suggested that neither of these pathways was responsible for the reduced survival observed after LZK knockdown in these cells. For MSK921, there was a small decrease in pJNK levels after knockdown (Fig. 25B), but this was true for the parental cells too, suggesting that this occured because of doxycycline treatment rather than LZK knockdown. There may have been a minor reduction in p-p38 after LZK knockdown in MSK921 cells (Fig. 25B). Overall these data indicate that the pro-proliferative effect of LZK is not mediated by signalling through the JNK or p38 pathways.

The effect of LZK knockdown on the NFκB pathway was also investigated. TNFα was used as a positive control for NFκB activation to verify that the antibodies function correctly. Phospho-IκBα was not detected at the expected molecular weight even after TNFα treatment (data not shown), so degradation of total IκBα was used to assess NFκB activation instead. After 30min TNFα treatment, levels of total IκBα were significantly reduced in CAL33, BICR56 and MSK921 lines, demonstrating activation of NFκB (Fig. 25C–E). Upon doxycycline-induced knockdown of LZK, no significant change was observed in total IκBα levels in BICR56 and CAL33 cells, indicating that LZK does not endogenously regulate NFκB in these cells (Fig. 25C–D). Additionally, there was a reduction in IκBα levels in the MSK921 control cell line after LZK knockdown, suggesting that LZK potentially inhibits NFκB activation in these cells (Fig. 25E). Overall, these results suggest that other downstream substrates are responsible for the pro-proliferative role of LZK.

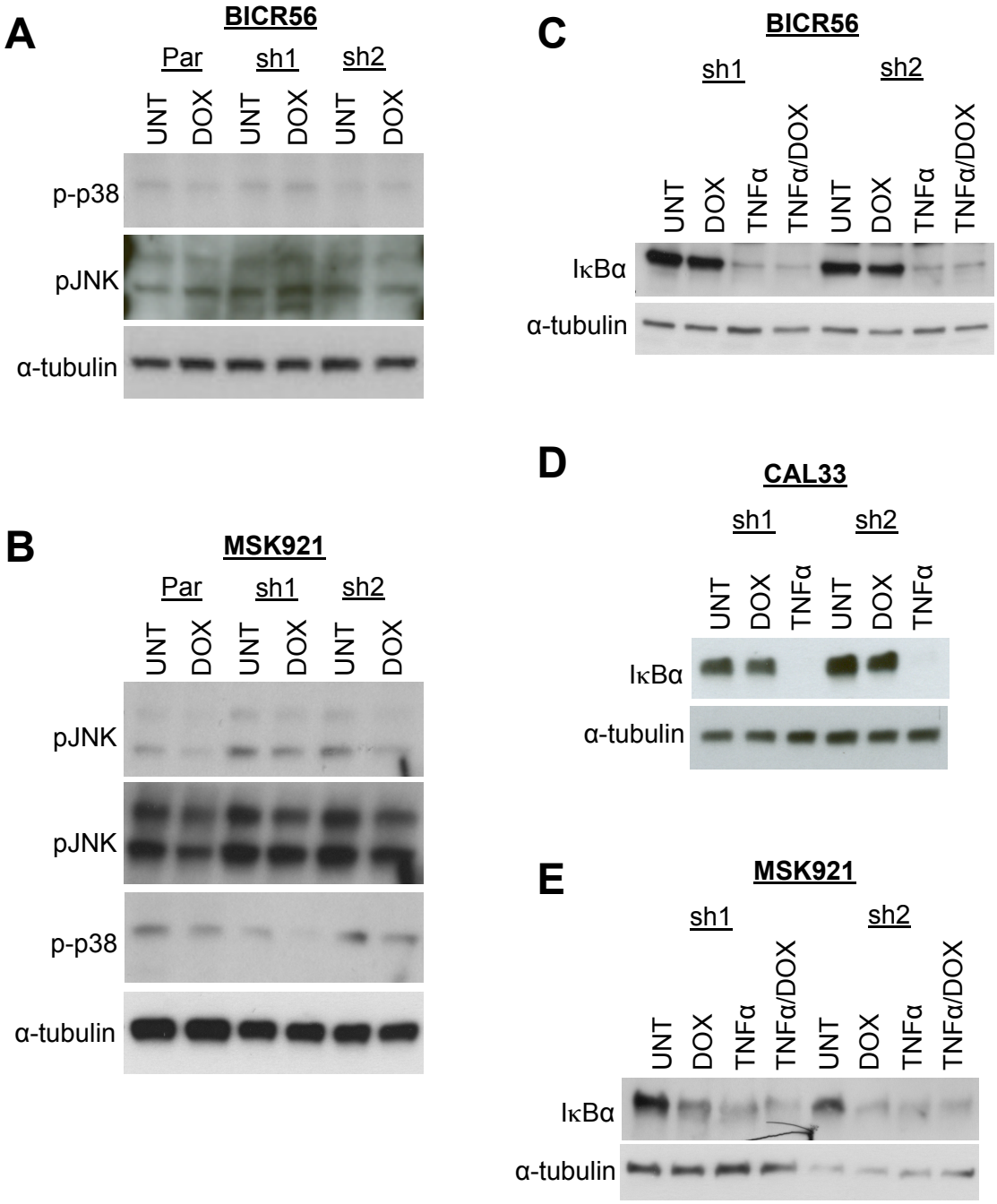

Figure 25: Expected signalling pathways after LZK knockdown. A-B: Knockdown of LZK has no effect on levels of expected downstream pathways pJNK and p-p38 in BICR56 cells. Minor effects are observed in MSK921 cells. Cells were treated with 1µg/ml doxycycline for 48h before lysis. pJNK and p-p38 could not be detected in CAL33 cells. **C-D:** Induced knockdown of LZK has no effect on NFκB activation in CAL33 and BICR56 cells, as assessed by degradation of IκBα. TNFα treatment was used to verify that the antibody was detecting the correct protein. Cells were treated with 1µg/ml doxycycline for 48h before lysis. TNFα treatment was at 30ng/ml for 30min prior to lysis. **E:** As (**C-D**) but using MSK921 cells. Results suggest that LZK may negatively regulate NFκB in the MSK921 control cell line.

To identify other potential proteins regulated by LZK, a phospho-kinase array was conducted using the CAL33 inducible knockdown cell lines. Lysates were normalised by protein concentration and incubated with membranes dotted with phospho-antibodies for a range of possible downstream substrates. A range of exposures was taken for these membranes to allow observation of differences in phospho-protein levels. The most obvious differences seen were for pAKT(S473) (Fig. 26A) and three different p53 phosphorylation sites (S15, S46 and S392) (Fig. 26B). Western blot analysis was then completed for these substrates to validate results seen by phosphoarray. This confirmed the reduction in pAKT(S473) in CAL33 cells, with a clear decrease noted after LZK knockdown (Fig. 27A). A decrease was also observed in levels of pAKT(T308). Total AKT levels were not affected by knockdown. The phospho-p53 results were also validated by western blot for the S392 phospho-site; however, in this case it was found that total p53 levels were reduced after LZK knockdown, which likely accounts for the observed decrease in p-p53 at three different phosphorylation sites (Fig. 27A).

Effects on p53, pAKT(S473), and pAKT(T308) were then investigated in the BICR56 inducible knockdown cells; all were also markedly reduced in this cell line background after depletion of LZK (Fig. 27B). For the MSK921 control cell line, no reductions in pAKT(S473) or total p53 were observed (Fig. 27C).

Mutations in *TP53* are very common in HNSCC. Notably, CAL33 has a known GOF mutation in p53 (R175H), so a decrease in total p53 would be expected to lead to reduced proliferation. BICR56 also has a mutation in p53 (Y126_splice), which leads to the exclusion of seven amino acids (Y126–K132) from the protein at the beginning of exon 5. To date, this mutant has not been characterised and it is not clear whether it is GOF, but my results suggest that it may also possess pro-proliferative properties. From DNA and RNA sequencing data available on the CCLE database, there is no evidence that a WT allele is expressed in either CAL33 or BICR56 cells (CCLE, 2015). This is in agreement with a study by Burns *et al.*, which found no expression of the WT allele in BICR56 cells (Burns *et al.*, 1993). MSK921 has two heterozygous mutations in the *TP53* gene, leading to protein changes of P191L and I232T (Anderson *et al.*, 2013), neither of which has yet been characterised. My data suggest that *TP53* mutations in BICR56, CAL33 and MSK921 may be GOF (for further details see p53 knockdown data in section 4.4.5.3.2). The fact that no decrease in p53 was seen in MSK921 cells after LZK knockdown

suggests that some kind of threshold level of LZK exists to allow stabilisation of mutant p53, and that copy number gain of *MAP3K13* is required to enable these effects.

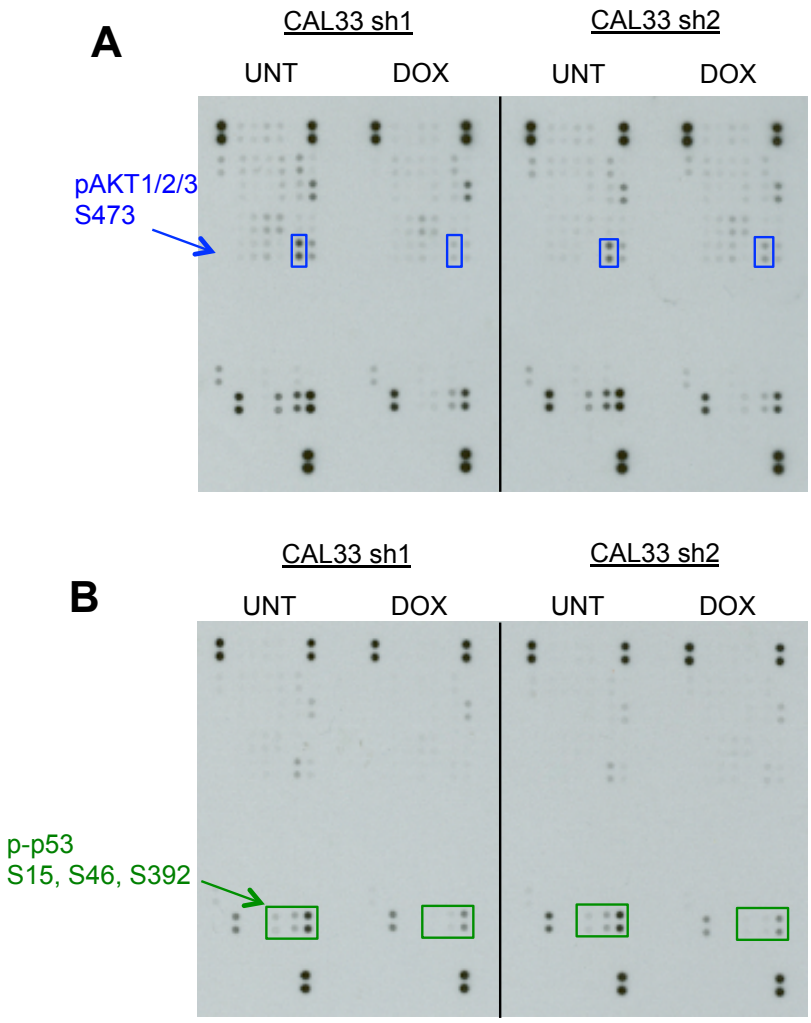

Figure 26: Pathways altered after inducible knockdown of LZK. A-B: Phosphoarray conducted after inducible knockdown of LZK in CAL33 cells indicates reductions in pAKT(S473) and p-p53 at three different phosphorylation sites. Cells were treated with 1µg/ml doxycycline for 48h before lysis. **A** and **B** show two different exposures to illustrate relevant results clearly. Full table of phospho-antibodies included in array shown in Appendix IV.

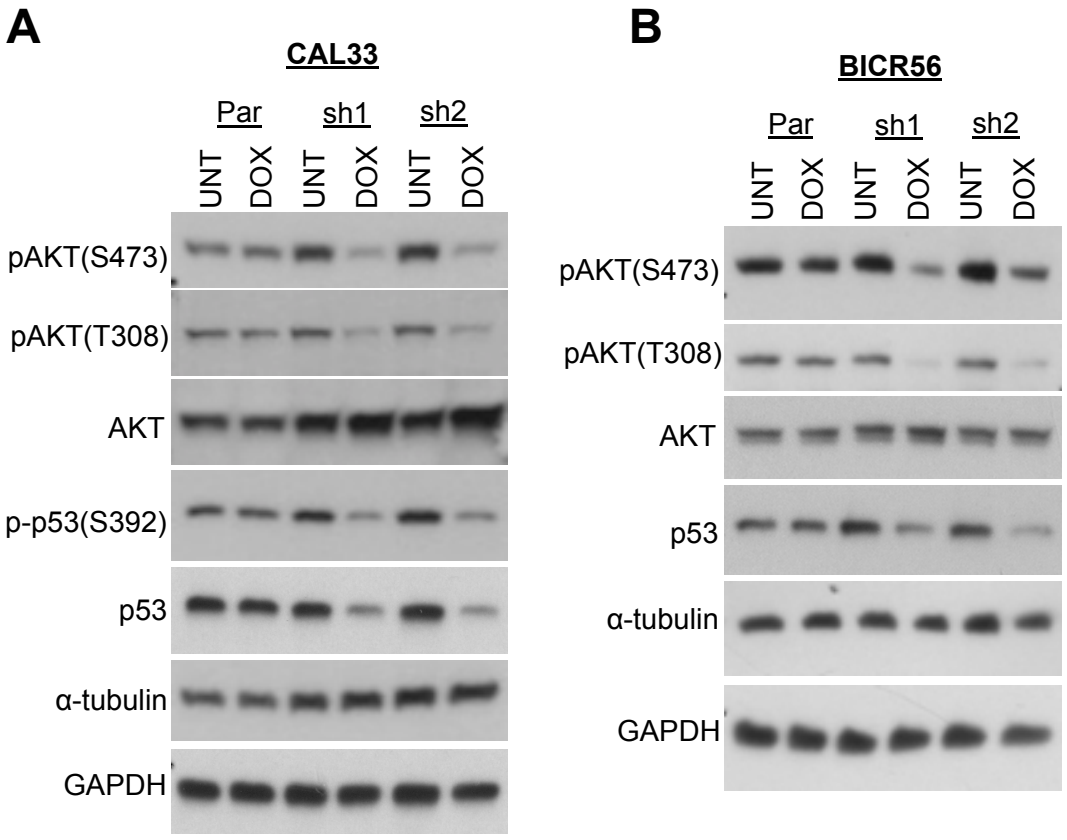

Figure 27: p53 and pAKT levels are reduced after knockdown of LZK. A: Validation of phosphoarray results in CAL33 cells. pAKT levels are confirmed to be reduced. p-p53 reduction found to be due to a decrease in total p53 levels. Cells were treated with 1µg/ml doxycycline for 48h before lysis. **B-C:** Extension of experiment to further inducible knockdown cell lines. BICR56 also show a clear decrease in pAKT and p53 after LZK knockdown (**B**), while there is no effect in MSK921 cells (**C**).

4.4.5.3 Preliminary investigations into downstream pathways

4.4.5.3.1 AKT pathway

To investigate further the role that pAKT may have in the pro-proliferative effects of LZK, western blots were run for downstream AKT substrates. As expected, these downstream pathways were not affected in MSK921 cells (Fig. 28A), where pAKT levels were not reduced after LZK knockdown. For BICR56, a clear reduction in pPRAS40 was seen after LZK knockdown, as well as a more minor decrease in pGSK3β (Fig. 28B). Phosphorylation of PRAS40 promotes its dissociation from RAPTOR, leading to activation of mTORC1, which promotes cell growth and proliferation. GSK3β has pro-apoptotic and anti-proliferative roles, and is inhibited by its phosphorylation by AKT (Manning and Cantley, 2007), so either of these pathways could potentially explain the phenotype of LZK knockdown.

For CAL33, no change was seen for pPRAS40, while a slight increase was observed in phosphorylation of GSK3β (Fig. 28C). This is phosphorylated downstream of AKT, and as such would be expected to show reduced phosphorylation in response to a decrease in pAKT. Interestingly, an increase was seen in total p27 levels after LZK knockdown in CAL33 cells (Fig. 28C). p27 was investigated due to the observed effects on cell cycle progression. p27 can promote cell cycle arrest (Chu *et al.*, 2008), so this is a potential mechanism that may play a role in the phenotype of G1 arrest seen after LZK knockdown.

Western blots were also utilised to determine whether LZK might activate the AKT pathway by degradation of the negative regulator PTEN; however, no change was observed in PTEN levels after LZK knockdown for any of the cell lines (Fig. 28D).

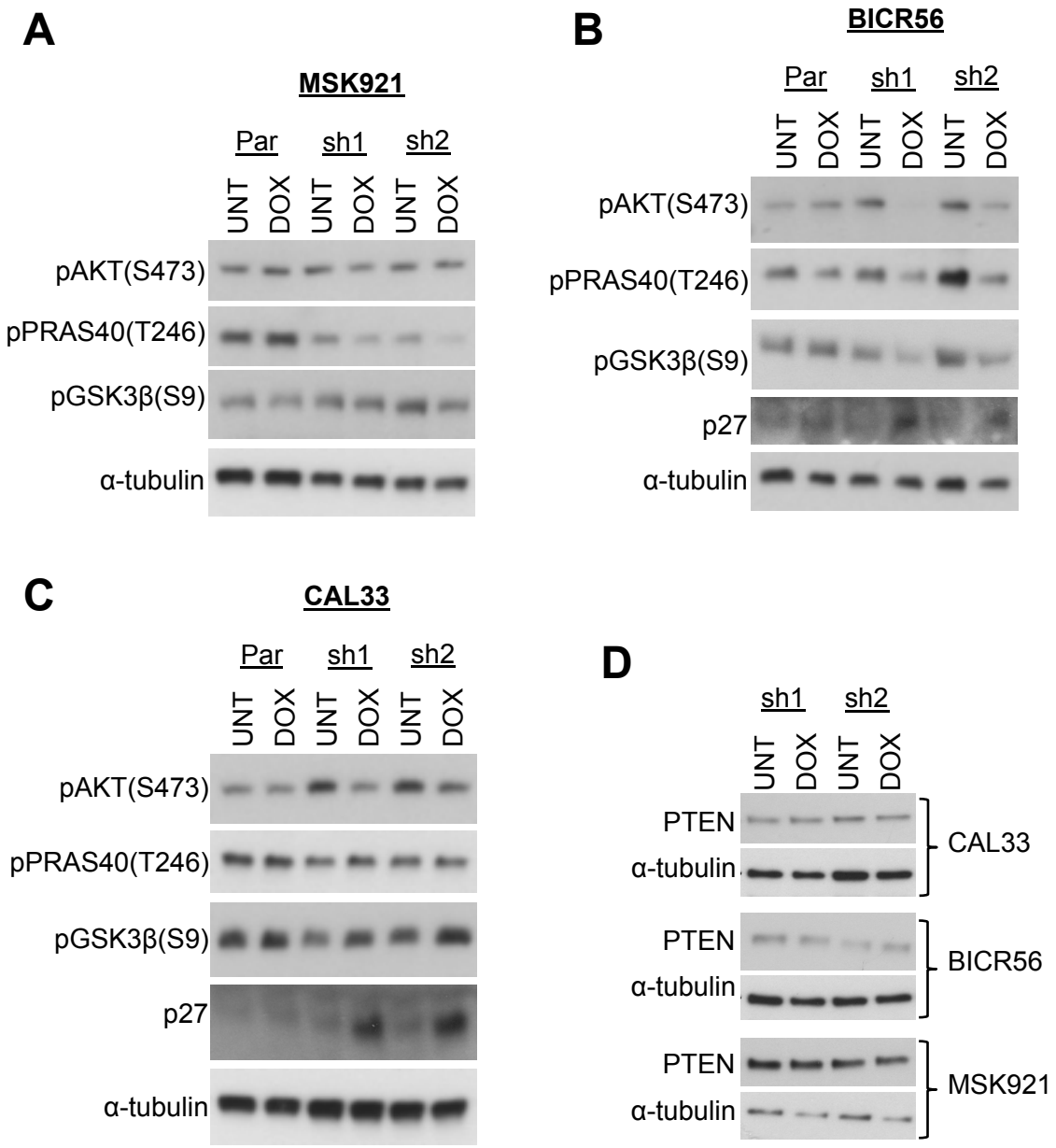

Figure 28: Initial investigations of AKT signalling after induction of LZK knockdown. Investigation of substrates downstream of AKT after induced LZK knockdown. All cells were induced with 1µg/ml doxycycline for 48h before lysis. **A:** MSK921 control cells: no significant effects observed on AKT downstream substrates. Total p27 could not be detected in these lysates. **B:** BICR56 cells; reductions observed in pPRAS40 and pGSK3β after doxycycline induction. **C:** CAL33 cells; an increase is seen in p27 after LZK knockdown. **D:** LZK knockdown has no effect on PTEN levels.

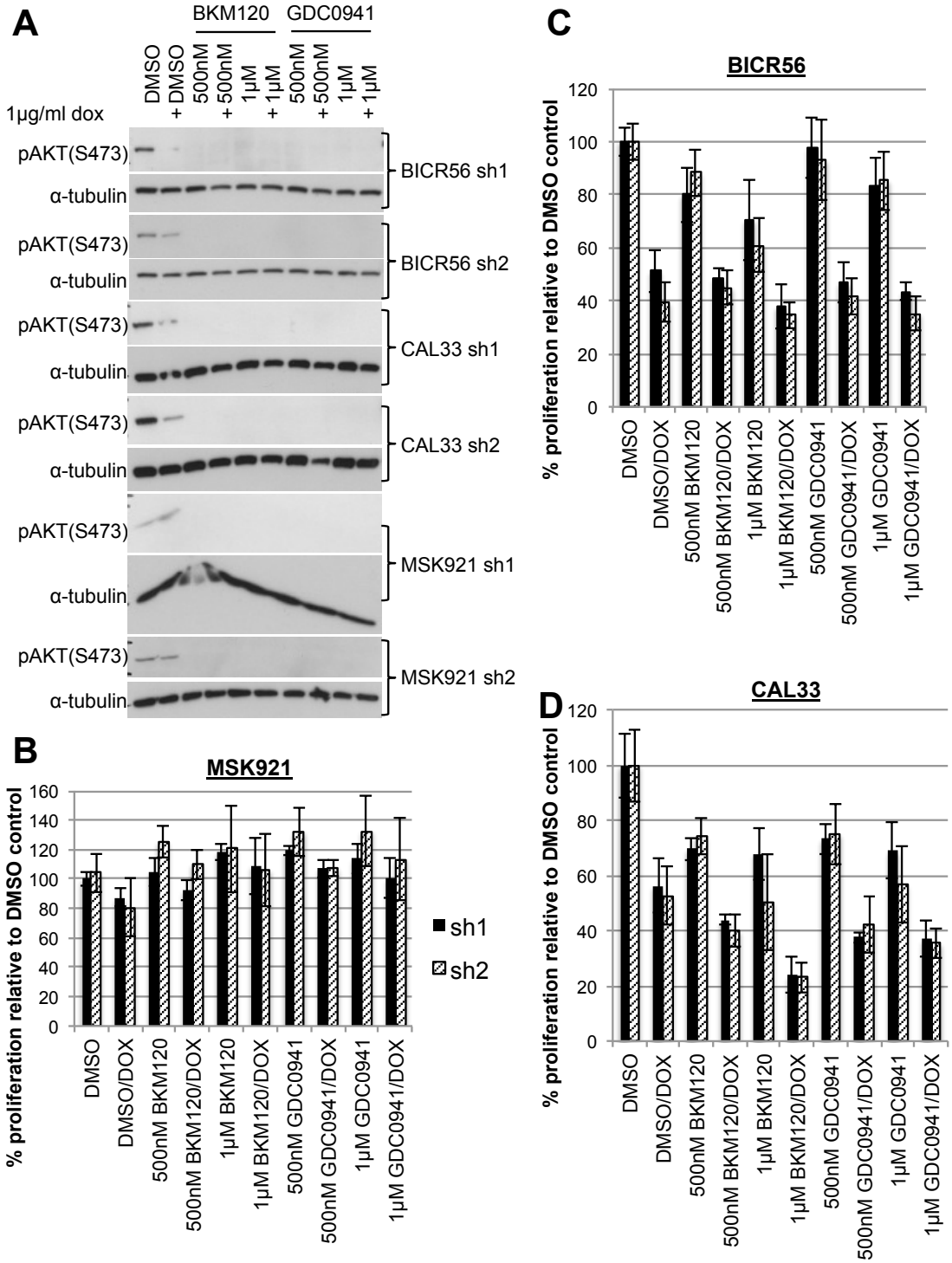

Figure 29: Combined PI3K inhibition and induced LZK knockdown. A: Treatment of cells with ≥500nM BKM120 or GDC0941 p110 inhibitors ablates AKT activation. Cells were treated with doxycycline for 48h, and PI3K inhibitors for 1h before lysis. **B-D:** PI3K inhibitors have no effect on MSK921 cells, but do reduce proliferation of CAL33 and BICR56. Combined knockdown of LZK and inhibition of PI3K in these cells has an additive effect on proliferation. Cells were treated with doxycycline and/or PI3K inhibitors for 48h before addition of BrdU label. Cells were then incubated for a further 24h before analysis.

PI3K inhibitors were used in combination with doxycycline induction to test the effects of dual LZK knockdown and inhibition of the PI3K pathway. Two different PI3K inhibitors were used, BKM120 and GDC0941; both can inhibit all p110 isoforms (p110α/β/δ/γ),

although GDC0941 has modest selectivity for p110α/β over p110δ/γ. Interestingly, MSK921 cells were not sensitive to these inhibitors, showing no decrease in proliferation despite complete shutdown of the AKT pathway (Fig. 29A–B). On the other hand, CAL33 and BICR56 cells were sensitive to both PI3K inhibitors at 500nM and above. Addition of doxycycline to these cells further reduced proliferation after PI3K inhibition (Fig. 29C–D), despite effective shutdown of the AKT pathway with inhibitors alone (Fig. 29A), suggesting that the reduction in pAKT is not solely responsible for the reduced proliferation after LZK knockdown.

4.4.5.3.2 p53 pathway

As detailed in section 4.4.5.2, all of the three main cell lines have mutations in *TP53*. Mutations in *TP53* are very common in HNSCC, at 72% of cases in TCGA dataset (Cancer Genome Atlas Network, 2015), and while some of these are LOF or dominant-negative mutants that simply abolish the tumour suppressor activities of p53, some mutants have been demonstrated to have oncogenic properties (Muller and Vousden, 2013). GOF p53 mutants have been found to have a pro-proliferative role (Bossi *et al.*, 2006), so reduction in p53 could account for the decreased proliferation seen after LZK knockdown. GOF p53 mutations disrupt the typical DNA binding activity of p53. This leads to the loss of WT p53 tumour suppressive activity, such as transactivation of genes encoding MDM2 and p21, and potentially gains of new transactivation targets. GOF mutants also cause large changes in p53 protein structure, leading to altered protein–protein interactions, and therefore a wide range of new functions (Muller and Vousden, 2013). Mechanisms proposed for p53 oncogenic activity include a dominant-negative effect over its sister proteins p63 and p73, ability to complex with NF-Y (Muller and Vousden, 2013), and inhibition of AMPK activation (Zhou *et al.*, 2014).

CAL33 cells have a mutation in p53 at R175H, a hotspot mutation that is known to be GOF. Recently published work has shown that one of the mechanisms of activity of GOF p53 in HNSCC lines is inhibition of phosphorylation of the tumour suppressor AMPKα at its activation site, T172 (Zhou *et al.*, 2014). Western blots were therefore run to assess pAMPKα(T172) levels after inducible knockdown of LZK. In CAL33 and BICR56 cells, an increase was observed in pAMPKα after knockdown of LZK, while no effect was seen in MSK921 control cells (Fig. 30). This suggests that the increase in pAMPKα may play a role in the reduced proliferation after LZK knockdown. LZK could potentially regulate

AMPK by promoting the stability of GOF p53, which leads to inhibition of AMPK activity (Zhou *et al.*, 2014), or by regulation of AKT activity that can also inhibit AMPK downstream (Kovacic *et al.*, 2003).

AMPK is a master regulator of cellular homeostasis, which is activated when ATP levels are reduced and acts as a checkpoint to restrain the growth of cells. Low cellular energy levels will often be the case in hypoxic tumour environments (Shackelford and Shaw, 2009). Substrates phosphorylated downstream of AMPK include ACC, ULK1 and RAPTOR. ACC is a metabolic enzyme that is involved in biosynthesis of fatty acids and is inhibited by its phosphorylation by AMPK. Phosphorylation of RAPTOR by AMPK leads to inhibition of the mTORC1 complex (Shackelford and Shaw, 2009). ULK1 is phosphorylated by AMPK and can promote autophagy (Mao and Klionsky, 2011).

Investigation of these downstream pathways after inducible knockdown of LZK was conducted by western blot. As expected, no changes in levels of pACC or pRAPTOR were observed in MSK921 control cells (note: pULK1 could not be detected in MSK921) (Fig. 30A). In CAL33, no changes were observed in levels of pULK1, pRAPTOR or pACC (Fig. 30B). For BICR56, decreases in pACC and pULK1 were seen, while they would be expected to increase along with pAMPKα (Fig. 30C). It is therefore not clear what substrates are regulated downstream of AMPK in these cells, and further work needs to be conducted examining different time points and further downstream substrates.

To investigate the function of p53 in the three main cell lines, transient knockdown was conducted using siRNA. Knockdown of p53 was very effective in all three cell lines (Fig. 31A). Knockdown of p53 led to a small but significant decrease in viability of ~20% in CAL33, BICR56 and MSK921 cell lines (Fig. 31B), suggesting that these cells possess GOF p53 mutations. However, despite near complete knockdown of p53 protein, reductions in survival seen in BICR56 and CAL33 after p53 knockdown were less marked than the effect of LZK knockdown. This indicates that promotion of p53 stability might contribute to, but cannot fully account for, the proliferative effects of LZK.

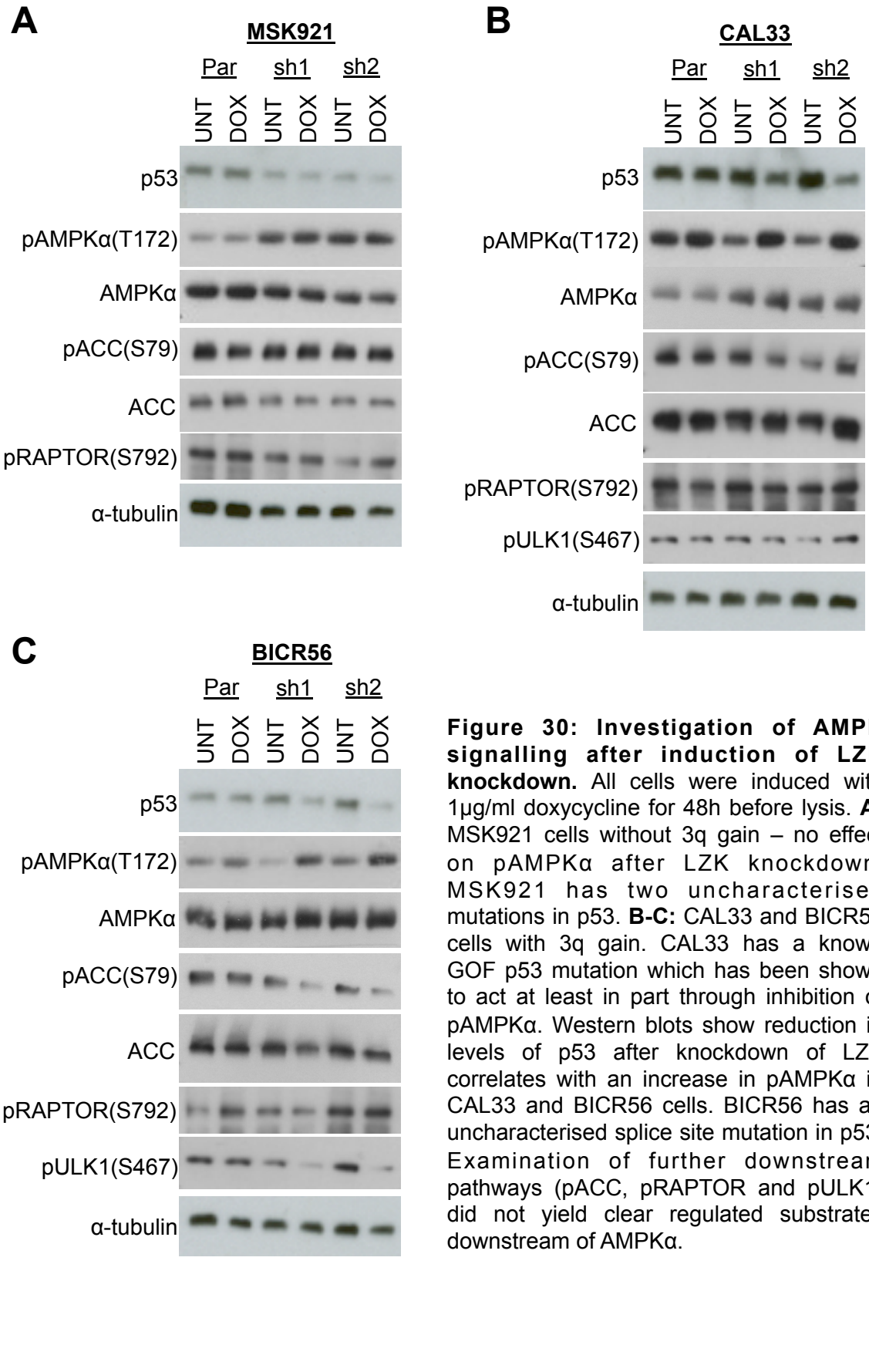

Figure 30: Investigation of AMPK signalling after induction of LZK knockdown. All cells were induced with 1µg/ml doxycycline for 48h before lysis. **A:** MSK921 cells without 3q gain – no effect on pAMPKα after LZK knockdown. MSK921 has two uncharacterised mutations in p53. **B-C:** CAL33 and BICR56 cells with 3q gain. CAL33 has a known GOF p53 mutation which has been shown to act at least in part through inhibition of pAMPKα. Western blots show reduction in levels of p53 after knockdown of LZK correlates with an increase in pAMPKα in CAL33 and BICR56 cells. BICR56 has an uncharacterised splice site mutation in p53. Examination of further downstream pathways (pACC, pRAPTOR and pULK1) did not yield clear regulated substrates downstream of AMPKα.

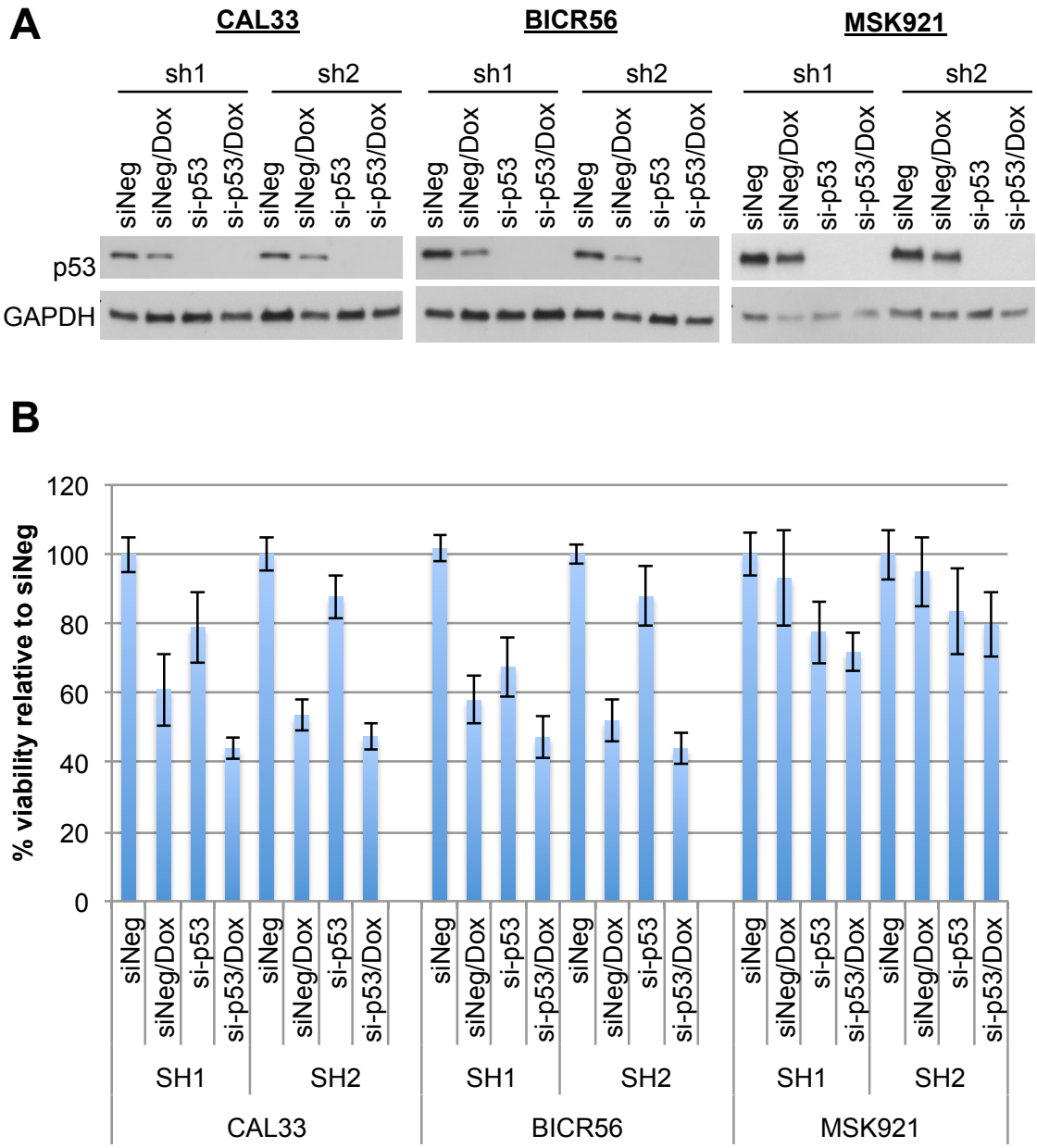

Figure 31: Transient p53 knockdown in cells with inducible knockdown of LZK. A: Western blots show effective knockdown of p53 with siRNA. **B:** MTT assay to assess viability of cells after combination of doxycycline-induced LZK knockdown and transient p53 knockdown. p53 knockdown reduces viability of cells, but not to the same extent as knockdown of LZK for cells with 3q gain. Cells were reverse transfected in triplicate with 100nM siRNA to p53 or non-targeting control, and induced with 1µg/ml doxycycline (where appropriate) at the same time. Protein plate was lysed after 48h, MTT was read after 72h.

4.4.5.4 Rescue of LZK knockdown by expression of shRNA-resistant cDNA

To confirm that the observed reduction in cell survival was specifically because of depletion of LZK, rescue experiments were performed by overexpression of shRNA-resistant LZK. Re-expression of the sh1-resistant LZK construct into CAL33-sh1 and BICR56-sh1 cells rescued the effect of LZK knockdown on cell survival over 72h, confirming that these effects were specific to LZK knockdown. For CAL33, full rescue was achieved (Fig. 32A), while for BICR56, rescue was partial but significant (Fig. 32B). It should be noted that without an antibody for LZK it is unclear how the expression relates to endogenous protein levels. Expression achieved in BICR56 cells may not have fully restored protein expression to endogenous levels, which could explain why rescue was only partial.

Western blots from these experiments demonstrated that the reduction in p53 after knockdown was rescued by re-expression of shRNA-resistant LZK. However, rescue of pAKT was not seen in CAL33 cells (Fig. 32C), and was only minimal for the BICR56 line (Fig. 32D). It could be that p53 is a more direct downstream substrate, and that AKT is phosphorylated further downstream of this effect. The $p53^{R175H}$ mutant present in CAL33 cells has been shown to promote AKT activation in endometrial cancer cells (Dong *et al.*, 2009).

No increase was seen in pAKT or p53 after overexpression of LZK in BICR56 or CAL33 cells without doxycycline treatment (Fig. 32C–D). It is likely that these were already at their maximal levels in these cells; GOF p53 has enhanced stability and pAKT is also high in HNSCC, particularly in cells that harbour activating *PIK3CA* mutations, as do CAL33 cells.

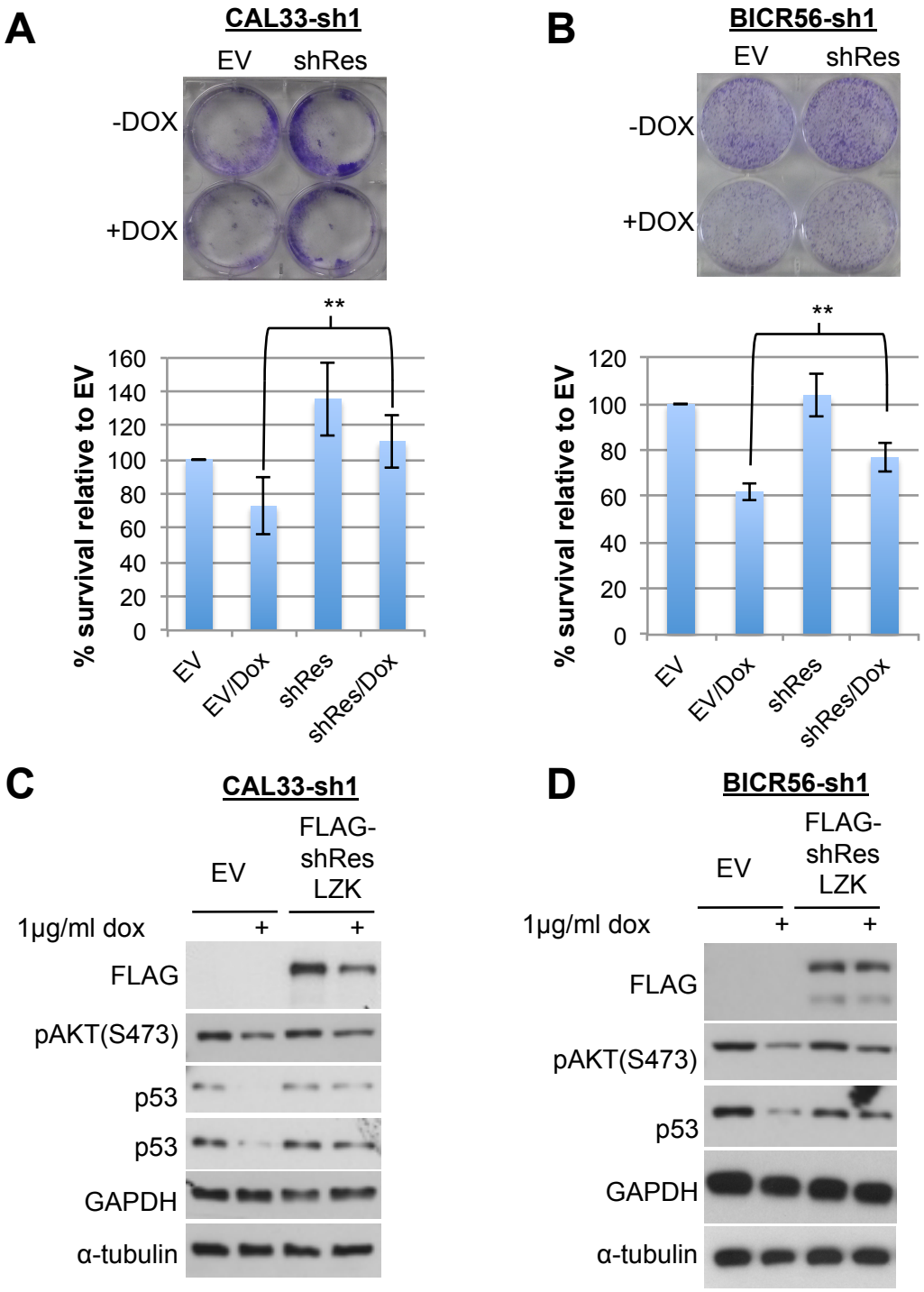

Figure 32: Rescue of LZK knockdown by expression of shRNA-resistant LZK. Cells with inducible sh1 construct were transiently transfected 24h after seeding with FLAG-tagged shRNA-resistant LZK (shRes) or empty vector (EV) control. Eight hours after transfection, medium was changed and 1µg/ml doxycycline added where required. Cells were lysed for protein 48h after transfection, and stained for crystal violet 72h after transfection. **A-B:** Results from crystal violet assay (Upper=picture of plates, lower=quantification by dissolution of crystal violet in 10% acetic acid and reading at 595nm). Reduced survival after LZK knockdown is rescued by expression of shRNA-resistant LZK. Full rescue achieved for CAL33 but only partial rescue for BICR56. **Student's two-tailed t-test *p*-value of <0.05. **C-D:** Western blots looking at pAKT(S473) and p53 after rescue with shRNA-resistant LZK show partial rescue of p53 but only minimal restoration of pAKT levels.

4.4.5.5 Summary

Total p53 and phospho-AKT levels were reduced in cells with 3q gain after knockdown of LZK. The mechanisms of activation of AKT and stabilisation of p53 by LZK are not yet clear, and it is not known whether these effects are directly caused by LZK. Preliminary investigations of downstream pathways have suggested some potentially important downstream substrates, including inhibition of AMPKα by GOF p53, and suppression of p27 expression, but more work needs to be completed to elucidate the exact mechanisms involved.

Knockdown of p53, or inhibition of PI3K, caused a decrease in viability and proliferation, respectively, in cells with 3q gain. However, in both cases, combination with LZK knockdown had a synergistic effect, suggesting that the effect of LZK knockdown is not due to either AKT or p53 alone. A combination of the two pathways may account for the survival effects of knockdown, and dual p53 knockdown and PI3K inhibition could be tested to determine whether this may be the case. Alternatively, there may be other substrates regulated by LZK that mediate its effects.

4.4.6 LZK overexpression reduces growth of immortalised normal cells

To determine whether increased expression of LZK can promote growth, crystal violet assays were conducted in the tetracycline-inducible OKF6/TERT2 immortalised oral keratinocyte line. After 72h of LZK induction by tetracycline (Fig. 33A), cell survival was partially, but significantly, reduced in the inducible OKF6/TERT2 cells, but not in the parental cell line, indicating that LZK induction was responsible for reduced survival (Fig. 33B). Colony formation assays conducted with these cells showed a greater reduction in survival due to LZK expression over a longer period of time (Fig. 33C–D). It is likely that JNK activation caused by induction of LZK (Fig. 24C) led to apoptosis in the inducible OKF6/TERT2 cells. OKF6/TERT2 cells with inducible KD LZK should be generated to test whether JNK activation is responsible for this phenotype. In addition, it is possible that enhanced LZK expression promotes increased expression of WT p53 and suppresses cell viability through this mechanism.

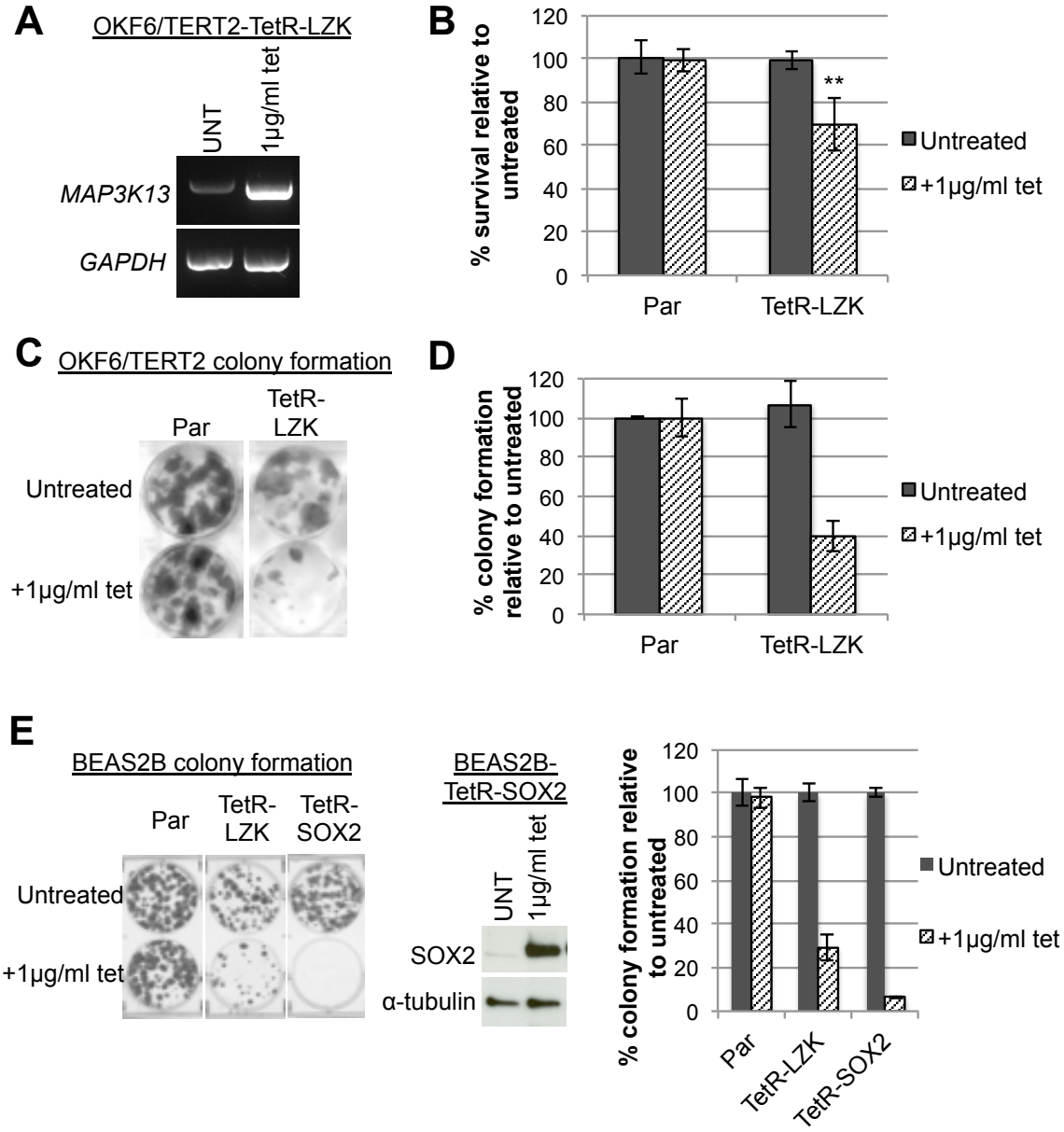

Figure 33: Induction of LZK expression reduces survival of normal cells. A: Keratinocyte cell line OKF6/TERT2 was transduced with tetracycline repressor followed by LZK in pLenti vector, enabling tetracycline-inducible expression of *MAP3K13*/LZK. Induced expression of *MAP3K13* shown by RT-PCR (48h induction). **B:** Parental OKF6/TERT2 cells and OKF6/TERT2 with inducible LZK (OKF6/TERT2-TetR-LZK) were treated with 1µg/ml tetracycline for 72h, fixed with methanol and stained with crystal violet solution to assess cell survival. Crystal violet was dissolved in 10% acetic acid and read at 595nm. **significant t-test result of $p<0.05$ relative to untreated control. Tetracycline treatment causes death where LZK is induced, but not in parental cells. **C:** Colony formation assay. 200 cells/well were treated with tetracycline for 2 weeks before crystal violet staining. **D:** Quantification of (**C**) by dissolution in 10% acetic acid. **E:** BEAS2B cells with tet-inducible expression of LZK or SOX2 were generated as (**A**). Western blot demonstrates induced expression of SOX2 after tetracycline addition. LZK induction in BEAS2B shown in Fig. 24B. Colony formation assays were conducted and analysed by crystal violet staining after 11 days tetracycline treatment. Induction of SOX2 or LZK causes a large reduction in colony formation ability.

Colony formation assays were also conducted in the tetracycline-inducible BEAS2B cells. In addition to the BEAS2B-TetR-LZK cells (Fig. 24B), BEAS2B cells with inducible

expression of SOX2 were generated (Fig. 33E). BEAS2B is an immortalised cell line that exhibits weak growth on soft agar (Maeno *et al.*, 2006; Hussenet *et al.*, 2010). SOX2 overexpression in BEAS2B cells has been shown to promote growth on soft agar (Hussenet *et al.*, 2010), but this is reportedly not the case in 2D culture (seminar given by Dr Frank McCaughan at the Wolfson Molecular Imaging Centre, 3rd July 2014). In our hands, SOX2 overexpression caused a major reduction in the colony forming ability of BEAS2B cells on plastic (Fig. 33E). Induction of LZK decreased survival to a lesser extent than SOX2 (Fig. 33E). The fact that SOX2 overexpression causes death in 2D culture but is reported to transform cells in 3D culture suggests that it is worth testing whether induction of LZK could also promote anchorage-independent growth in soft agar and organoid assays, which are thought to be more representative of colony formation *in vivo*.

4.5 Discussion

4.5.1 Copy number gain of *MAP3K13* (LZK) plays a pro-proliferative role in HNSCC lines

MAP3K13 (LZK) is frequently amplified in SCC tumours, as part of the 3q amplicon; 76% of HNSCC patients have copy number gain of this gene (cBio, 2015). Increased copy number of *MAP3K13* correlated with an increase in its mRNA expression in primary tumours (Fig. 12A) and cell lines (Fig. 14C). A corresponding increase in LZK protein expression was observed in a limited range of SCC cell lines as compared with BEAS2B immortalised bronchial epithelial cells (Fig. 14D). My results indicate that LZK may play a role in HNSCC tumourigenesis. siRNA knockdown (Fig. 15) of LZK in two HNSCC cell lines with 3q copy number gain reduced cell viability and survival (Fig. 16). These effects were not seen for BEAS2B cells, OKF6/TERT2 immortalised normal oral keratinocytes or an HNSCC cell line without 3q gain. Confirming these results, inducible shRNA knockdown of LZK also led to a reduction in viability and survival in two cell lines with copy number gain of *MAP3K13* (CAL33 and BICR56), but had no effect on two control cell lines that lack gain of the gene (MSK921 and BICR22) (Fig. 18).

In longer-term colony formation assays, a striking reduction in number of colonies was observed in CAL33 and BICR56 cells after LZK knockdown by shRNA (Fig. 20). No such decrease was observed in BICR22 cells, supporting the hypothesis that LZK plays a role in HNSCC when subject to copy number gain. MSK921 inducible LZK knockdown cells did show a reduction in colony formation, which was significant but much less marked than for the cells with copy number gain. This effect was at least in part because of the toxicity of doxycycline on this cell line, as the parental counterparts also showed a reduction in colony formation after doxycycline treatment. Doxycycline has been reported to have toxic effects on some cell lines (Xie *et al.*, 2008; Shen *et al.*, 2010), and this toxicity is likely more pronounced when cells are seeded at a low density (Ermak *et al.*, 2003), which could explain why these effects were not seen in short-term assays. However, there was a larger effect of doxycycline on the inducible knockdown cell lines compared with the parental line, and LZK may play a minor role in promoting colony formation in MSK921 cells. Alternatively, it should be noted that the inducible knockdown cell lines did not proliferate as quickly as the parental cell line in this assay, and it could be that doxycycline had enhanced toxicity as a result of the higher effective concentration per cell. To be certain of the role of LZK in these cells in longer-term

colony formation assays, further testing with the inducible knockdown constructs needs to be completed to identify clones that grow at a similar rate to the parental cells in this assay.

Critically, re-expression of an shRNA-resistant cDNA for LZK rescued the effects of LZK knockdown for the sh1 inducible knockdown cell lines (Fig. 32). This confirmed that survival effects seen were specific to LZK knockdown. For CAL33, full rescue of survival was achieved. For BICR56, rescue was only partial but was significant. In future studies, rescue experiments will be performed for the sh2 knockdown cell line to confirm these data. Additionally, re-expression of kinase-dead shRNA-resistant LZK will be tested to determine whether the role of LZK is kinase-dependent or due to scaffolding effects.

Investigation of phenotypic effects downstream of LZK knockdown revealed a reduction in proliferation in cells with 3q gain (Fig. 21). Consistent with these data, preliminary cell cycle analysis showed an increase in the percentage of cells in G1 phase after LZK knockdown (Fig. 23). These data indicate that LZK has a pro-proliferative effect, and that inhibition of the protein would have a cytostatic rather than a cytotoxic effect.

The role of LZK in HNSCC has not been studied previously. My results indicate that LZK may play a tumourigenic role in HNSCC tumours with copy number gain of *MAP3K13*. The described knockdown experiments need to be conducted for a wider range of cell lines to verify the importance of LZK as a 3q driver for HNSCC.

4.5.2 Signalling pathways behind the pro-proliferative effect of LZK

4.5.2.1 Expected downstream signalling pathways of LZK

Overexpression data convincingly demonstrated that LZK activates the JNK pathway in a kinase-dependent fashion (Fig. 24), consistent with previous reports (Sakuma *et al.*, 1997; Ikeda *et al.*, 2001a). However, pJNK was not detected in CAL33 cells, and no decrease was observed after LZK knockdown in BICR56 cells (Fig. 25A), indicating that LZK does not mediate its pro-proliferative effect via activation of JNK. LZK was also reportedly able to activate p38 when overexpressed in COS7 cells; however, no data were shown to support this finding (Ikeda *et al.*, 2001a) and my data demonstrated that overexpression of LZK does not lead to activation of this pathway in three different cell lines. Knockdown

of LZK led to a minor decrease in p-p38 in the MSK921 cell lines (Fig. 25B), supporting a potential role for endogenous activation of the pathway by LZK in some cellular contexts. However, no decrease in p-p38 was seen in the two cell lines that showed reduced proliferation after knockdown of LZK, confirming that this pathway is not involved in the pro-proliferative phenotype of LZK.

In contrast to previous reports (Masaki *et al.*, 2003), no detectable activation of NFκB was seen after overexpression of LZK in 293T, BEAS2B or OKF6/TERT2 cells. The canonical NFκB pathway is initiated by cytokines such as TNFα, which leads to activation of the IKK complex. The IKKα or IKKβ component of this complex phosphorylates IκBα, an NFκB inhibitor, promoting its degradation and release of NFκB. Masaki *et al.* were only able to show a minor increase in activation of NFκB when LZK was expressed alone, and coexpression with PRDX3 or IKKβ was required to detect significant activation of NFκB or phosphorylation of IκBα (Masaki *et al.*, 2003). It is likely that the 293T, BEAS2B and OKF6/TERT2 cells did not recapitulate conditions of PRDX3 or IKKβ overexpression; this could explain why LZK did not activate NFκB in these cells. However, no increase was observed in total IκBα after LZK knockdown in HNSCC cells with 3q gain (Fig. 25C–D); thus I found no evidence that LZK endogenously regulates NFκB in this context. In MSK921 cells, decreases were seen in IκBα after depletion of LZK, which could suggest that LZK is able to inhibit NFκB activation in these cells (Fig. 25E). The importance of this is not clear and the pathway would need to be examined in a more comprehensive manner to confirm this finding.

4.5.2.2 The role of AKT and p53

LZK is an under-researched kinase, so a phosphoarray was utilised to identify novel downstream targets. Marked reductions in phospho-AKT and total p53 levels were observed after knockdown of LZK in CAL33 and BICR56 cells, but not in the MSK921 cell line that lacks copy number gain of *MAP3K13* (Fig. 27).

The AKT pathway mediates well-characterised pro-survival and pro-proliferative effects, and is frequently activated in HNSCC (Du *et al.*, 2012). Consistent with this, inhibition of PI3K with two different inhibitors reduced proliferation of BICR56 and CAL33 cells, verifying the dependence of these cells on PI3K/AKT signalling (Fig. 29). AKT needs to be phosphorylated at two sites to allow full activation: at Thr308 by PDK1 (Alessi *et al.*,

1997) and at Ser473 by mTORC2 (Hresko and Mueckler, 2005; Sarbassov *et al.*, 2005). Decreases in phosphorylation were observed at both the T308 and S473 sites after LZK knockdown. T308 is in the activation loop of AKT and its phosphorylation is required for catalytic activity; S473 is in the hydrophobic motif in the C terminal domain, and crystal structures suggest that phosphorylation at S473 stabilises AKT in its active conformation (Yang *et al.*, 2002a; Yang *et al.*, 2002b). Some reports have presented conflicting evidence regarding the regulation of AKT activity at these two sites (reviewed in Bhaskar and Hay, 2007). While phosphorylation of both sites is required for significant activity *in vitro* (Alessi *et al.*, 1996), phosphorylation of T308 alone allows activation of some of the downstream substrates of AKT (Guertin *et al.*, 2006). It is thought that these sites are phosphorylated independently of one another (Alessi *et al.*, 1996), and genetic deletion of *RICTOR* (rapamycin-insensitive companion of mTOR) or *PDK1* does not preclude phosphorylation at T308 or S473, respectively (Williams *et al.*, 2000; Guertin *et al.*, 2006). However, knockdown of the RICTOR component of mTORC2 reduces phosphorylation of both T308 and S473 (Hresko and Mueckler, 2005; Sarbassov *et al.*, 2005). Unlike WT AKT, the phosphomimetic mutant AKT^{S473D} could still be phosphorylated on T308 after knockdown of RICTOR, supporting the hypothesis that activation of S473 facilitates enhanced phosphorylation of T308 (Wheeler *et al.*, 2015).

The mechanism behind the observation that pAKT is reduced after LZK knockdown has not been elucidated; at present it is not clear whether this effect is direct or because of altered signalling further downstream. PTEN negatively regulates AKT activation by conversion of PIP_3 to PIP_2, leading to reduced phosphorylation of both T308 and S473 (Carracedo and Pandolfi, 2008). No change in expression of PTEN was observed after LZK knockdown, suggesting that degradation of PTEN is not the mechanism utilised. As discussed above, the fact that knockdown of RICTOR reduces phosphorylation of T308 as well as S473 suggests that regulation of mTORC2 by LZK represents a potential mechanism of regulation. Another mechanism worth exploring is modulation of RAB35 activity by LZK; RAB35 is a RAS-related small GTPase that was recently discovered as a novel positive regulator of AKT activity upstream of PDK1 and mTORC2, including in cell lines with activating *PIK3CA* mutations. Activated RAB35 associates with and can promote the activity of PI3K; LZK could potentially activate RAB35 to regulate the AKT pathway (Wheeler *et al.*, 2015). Regulation of PI3K by LZK is possible, but less likely, because of the presence of a mutation in the kinase domain of PIK3CA at H1047R in CAL33 cells (Lui *et al.*, 2013; CCLE, 2015). This mutant has a higher basal activity than

WT, which is thought to occur due to an increased membrane affinity (Mandelker *et al.*, 2009; Burke *et al.*, 2012). Interestingly, BICR56 contains a homologous mutation at H1304R in *PIK3C2G* (encoding PI3K-C2γ) (CCLE, 2015), although the function of this class II PI3K isoform is not yet known (Thorpe *et al.*, 2015). Further work will be required to understand the role of LZK in regulating the PI3K/AKT pathway. If an effective antibody can be generated, immunoprecipitation of LZK from CAL33 or BICR56 cells could help to reveal whether LZK interacts with any of these key components and help to determine how LZK regulates this pathway. Identification of direct downstream phosphorylation targets of LZK via a protein microarray could also aid elucidation of important novel substrates.

The reduction in p53 seen after LZK depletion in cells with 3q gain provides an interesting theory as to how LZK could mediate its pro-proliferative effects in HNSCC. CAL33 has a mutation in p53 at R175H. This mutant has been characterised as GOF, and has been shown to promote proliferation *in vitro* (Bossi *et al.*, 2006; Zhou *et al.*, 2014) and *in vivo* (Zhou *et al.*, 2014). My results confirm these studies, as knockdown of p53 in CAL33 cells led to diminished viability. BICR56 has a p53 mutation at a splice site, which removes seven amino acids from Y126–K132 of the protein (Burns *et al.*, 1993; CCLE, 2015). Knockdown experiments suggested that this is also an oncogenic form of p53 (Fig. 31); this could be verified by overexpression of the mutant in p53-null cells, to ensure than any transformative activity observed results from a true GOF phenotype rather than simply from dominant-negative effects on WT p53 (Dittmer *et al.*, 1993; Oren and Rotter, 2010). However, there is no evidence of expression of a WT p53 allele in BICR56 cells based on DNA (CCLE, 2015) and RNA sequencing (Burns *et al.*, 1993; CCLE, 2015), suggesting it could be a true GOF mutation.

Reduction in p53 levels could explain the phenotype of cell cycle arrest observed in these cell lines. GOF p53 has been shown to promote progression through the cell cycle at least in part via upregulation of cyclins A and B1. Expression of GOF p53 was found to promote accelerated transition through the G2/M checkpoint, facilitating entry to mitosis (Acin *et al.*, 2011). G2 and M phase percentages cannot be distinguished by propidium iodide assay alone, and would need to be examined by dual staining with a marker of M phase entry such as phospho-histone H3. Acin *et al.* did not investigate the G1/S transition, presumably due to pathway analysis that suggested the involvement of GOF p53 in mitosis (Acin *et al.*, 2011), so it is possible that GOF p53 mutants can regulate the

cell cycle in multiple ways by transactivation of alternative cyclins or other pathways. For example, mutant p53 can repress expression of p21 (Vikhanskaya *et al.*, 2007), an inhibitor of the G1/S transition. GOF p53 can also interact with and inhibit the anti-proliferative protein BTG2 (B-cell translocation gene 2); in this study it was demonstrated that BTG2 inhibition by GOF p53 upregulates HRAS activity by preventing interaction of BTG2 with HRAS (Solomon *et al.*, 2012). However, BTG2 is also a cell cycle regulator that can induce G1 arrest by reducing expression of cyclin D1 (Guardavaccaro *et al.*, 2000) and cyclin E (Lim *et al.*, 1998) via as yet unexplained mechanisms. Cell cycle analysis after p53 knockdown with and without induced LZK depletion would help to determine whether the reduction in p53 after LZK knockdown is the likely cause of cell cycle arrest.

GOF p53 mutant proteins have enhanced expression in cancer cells as compared with the WT protein, despite the fact that the mutants themselves are not inherently more stable than the WT. Some mechanisms for this enhanced stability have been suggested, including loss of *MDM2* or $p16^{INK4A}$ (Terzian *et al.*, 2008), DNA damage (Suh *et al.*, 2011) and inhibition of p53 ubiquitination by the HSP90 chaperone complex (Li *et al.*, 2011; Alexandrova *et al.*, 2015). It is possible that amplified LZK is able to promote stability of p53 mutants, either via one of these pathways or by a novel mechanism. Interestingly, LZK was one of 36 kinase genes whose mRNA expression correlated with the presence of p53 mutations in the CCLE database in a recent *in silico* study (Wang and Simon, 2013), although this category also includes cell lines with nonsense p53 mutations, which are unlikely to be GOF. The mechanism of the effect of LZK on GOF p53 could be investigated using a sequence of experiments. The main mediator of p53 stability is MDM2, which ubiquitinates p53 to initiate its degradation. Use of the nutlin compound, which inhibits the MDM2–p53 interaction, would rescue the effects of LZK knockdown if mechanisms utilised were dependent on MDM2. However, in some cancer cells MDM2 and p53 have been found in a complex with HSP90 that prevents the ubiquitination of p53 by MDM2. Thus another mechanism worth exploring is regulation of the heat shock response, possibly via HSP90 or the transcriptional regulator HSF1 (Li *et al.*, 2011). To determine whether LZK regulates p53 at the transcriptional level, RT-PCR for p53 could be conducted after LZK knockdown. Alternatively, regulation may occur by direct phosphorylation of p53. To investigate this possibility, LZK knockdown should be performed for a variety of shorter time points to identify the time point at which LZK is knocked down, but before p53 depletion is observed. This would enable examination of

various phosphorylation sites on p53. Known p-p53 sites could be investigated by western blot analysis; if this failed to yield regulated phosphorylation sites then p53 could be immunoprecipitated after LZK knockdown and subjected to mass spectrometry to identify potential novel phosphorylation sites.

Knockdown of p53 in MSK921 control cells that lack copy number gain of *MAP3K13* had a minor but significant effect on cell viability (Fig. 31). This indicates that one or both of the *TP53* mutations in MSK921 (P191L and I232T) may have GOF abilities. However, these mutants are heterozygous and it is not known whether they reside on different alleles, or whether there is still a WT allele present in these cells, complicating interpretation of knockdown data. In contrast, there is no evidence of the WT allele in CAL33 or BICR56 cells (CCLE, 2015), so knockdown in these cells will only target the mutant. Regardless of whether MSK921 p53 mutants are GOF, no changes were seen in levels of p53 or pAKT after LZK knockdown in MSK921 cells (Fig. 27C). This suggests that a threshold level of LZK exists to allow stabilisation of mutant p53 and phosphorylation of AKT, and that copy number gain of *MAP3K13* is required to enable these effects. However, it remains possible that the specific p53 mutations in MSK921 may alter the structure in a way that prevents regulation of protein stability by LZK, which would indicate that LZK is more generally able to regulate p53, and that sensitivity to knockdown is dependent only on presence of a GOF mutation in p53. A wider range of cell lines needs to be investigated to confirm which factors determine sensitivity to LZK knockdown. Testing on the following categories of cell lines would aid elucidation of determinants of sensitivity: cells with amplification of *MAP3K13* but WT p53, and cells without amplification of *MAP3K13* but with GOF p53 mutations.

It is not clear whether p53 or AKT are regulated directly by LZK. Furthermore, it is not yet evident whether regulation of either or both pathways accounts for the phenotype observed after LZK knockdown, as both are capable of promoting growth and proliferation. Inhibition of PI3K reduced proliferation of CAL33 and BICR56 cells, but combining PI3K inhibitors with LZK knockdown had an even greater effect, indicating that regulation of the AKT pathway was not the sole mediator of LZK pro-proliferative activity (Fig. 29). Rescue experiments suggest it is more likely that stabilisation of p53 is the more direct downstream effector of LZK (Fig. 32). Interestingly, $p53^{R175H}$ has been shown to be capable of regulation of AKT; overexpression of $p53^{R175H}$ led to an increase in pAKT(S473) while knockdown of the p53 mutant in an HNSCC line reduced

pAKT(S473) (Dong *et al.*, 2009). This suggested a mechanism whereby LZK promotes stability of GOF p53, which leads to activation of AKT downstream. However, in my studies knockdown of p53 in cells with 3q gain did not reduce cell viability to the same extent as knockdown of LZK, despite near complete ablation of p53 protein levels (Fig. 31). This suggests that stabilisation of GOF p53 is not the only mechanism of LZK activity either. Further work needs to be completed to understand the mechanisms involved, including expression of potential direct downstream targets to attempt phenotypic rescue after induced LZK knockdown. For example, GOF p53 or constitutively active AKT could be expressed in conjunction with LZK knockdown to see which is able to rescue survival effects. Additionally, other pathways may play a contributory role in the pro-proliferative effect of LZK.

4.5.2.3 Pathways downstream of p53 and AKT

Investigation of pathways downstream of p53 and AKT yielded some interesting potential mechanisms, but as yet no clear pathways. Figure 34 illustrates some of the pathways downstream of AKT and GOF p53 that have been investigated here.

In CAL33 and BICR56 cells, an increase in pAMPKα was observed after LZK knockdown (Fig. 30). This is consistent with the finding that AMPK activation, by phosphorylation on T172, is inhibited by GOF p53 in HNSCC cells (Zhou *et al.*, 2014). Additionally, AKT signalling may negatively regulate AMPK by currently undefined mechanisms, as overexpression of constitutively active AKT has been shown to reduce pAMPK levels (Kovacic *et al.*, 2003). AMPK is a critical metabolic regulator that is activated in response to low cellular energy levels; elevated AMP binds to AMPK to allow its activation by upstream kinases such as LKB1. AMPK suppresses cell growth, in part through inhibition of mTOR signalling. The RAPTOR component of mTORC1 is responsible for recruiting downstream substrates, such as 4EBP1 (eIF4E-binding protein 1) and S6K (ribosomal protein S6 kinase); AMPK phosphorylates RAPTOR, promoting binding of 14-3-3 and inhibition of the mTORC1 complex (Gwinn *et al.*, 2008). Phosphorylation of RAPTOR was not observed after LZK knockdown; however, AMPK can also inhibit mTORC1 by activating phosphorylation of TSC2, which is yet to be investigated. The AMPK TSC2 phosphorylation sites are distinct from those subject to inhibitory phosphorylation by AKT (Huang and Manning, 2008). Other substrates phosphorylated by AMPK include ULK1, whose phosphorylation promotes autophagy

(Mao and Klionsky, 2011), and ACC, which regulates fatty acid metabolism (Shackelford and Shaw, 2009). However, no change was observed in pULK1 or pACC in CAL33 cells, while unexpected decreases in phosphorylation of both proteins were seen in BICR56 cells. Therefore, it is unclear which pathways are regulated downstream of AMPK after LZK knockdown in HNSCC cells. Inhibition of AMPK using Compound C should be tested to see whether this could rescue the phenotypic effect of LZK knockdown and confirm the importance of this pathway.

Initial investigation into signalling downstream of AKT has yielded other possible mechanisms of LZK activity. Due to the phenotype of G1 arrest seen after LZK knockdown, effects on the cell cycle inhibitor p27 were explored. Downstream of AKT, FOXO family proteins can promote transcriptional activation of p27. AKT signalling inhibits FOXO by phosphorylation, which leads to sequestration of FOXO in the cytoplasm and so reduces transactivation of *CDKN1B* (CDK inhibitor 1B, p27) and other target genes. p27 inhibits the cyclin E/CDK2 complex, promoting cell cycle arrest in G1 (Medema *et al.*, 2000). Additionally, AMPK can phosphorylate FOXO proteins at alternative phosphorylation sites; this does not affect localisation but does enhance transcription of FOXO target genes (Greer *et al.*, 2007). Thus the increase in pAMPKα and decrease in pAKT seen after LZK knockdown could synergise to promote transcription of p27. An increase was seen in total p27 levels after LZK knockdown in CAL33 cells (Fig. 28); there may also have been a slight increase in p27 in BICR56 cells, although this is much less clear. AKT can also inhibit the activity of p27 by phosphorylation at T157, leading to sequestration in the cytosol (Manning and Cantley, 2007; Chu *et al.*, 2008); this is worth exploring after LZK knockdown particularly in BICR56 cells. Western blots were used to probe lysates for pFOXO1/O3a after LZK depletion, but no bands were detected at the expected molecular weight in any of these cell lines and further work needs to be conducted to find suitable antibodies to illuminate this potentially important pathway.

For BICR56, more convincing results were observed for pPRAS40, a negative regulator of mTORC1, and pGSK3β, both of which were reduced after LZK knockdown. Either of these effects could explain the phenotype of G1 arrest. Activated GSK3β has multiple effects downstream, one of which is promotion of degradation of cyclins involved in the G1/S transition (Manning and Cantley, 2007). PRAS40 binds to the RAPTOR component of the mTORC1 complex and prevents recruitment of downstream substrates.

Phosphorylation of PRAS40 allows binding of 14-3-3, promoting the dissociation of PRAS40 from the mTORC1 complex and allowing signalling to proceed. In addition to its role in cellular growth, mTORC1 signalling is important in regulating cellular proliferation, including via promotion of MYC and cyclin D1 expression; this is illustrated by the fact that mTORC1 inhibitors cause G1 arrest (Manning and Cantley, 2007). This pathway has not yet been comprehensively examined; AKT signalling has a range of pro-proliferative effects, and other substrates, such as p21 and TSC2, have yet to be investigated. However, so far my results provide some potential mechanisms that can be correlated with effects downstream of LZK.

4.5.2.4 Conclusions

The mechanism behind the anti-proliferative phenotype of LZK knockdown has not been fully elucidated. I have confirmed that this phenotype cannot be explained by previously published signalling pathways activated downstream of LZK and have revealed a potential role for GOF p53 and the AKT cascade. However, the exact mechanisms of LZK activity towards GOF p53 and AKT are not known, and at present it is not clear whether these effects are direct or due to cross-talk further downstream.

My data suggest that neither the AKT nor p53 pathway is solely responsible for the phenotypic effects of LZK knockdown. It may be that regulation of both pathways is involved in the mechanism of LZK activity in HNSCC. Combined knockdown of p53 and inhibition of PI3K/AKT would determine whether this is the case. Both AKT and GOF p53 can promote proliferation but as yet investigation of the key substrates downstream of these proteins have not revealed any clearly defined pathways. The most striking result was an increase in pAMPKα, which could be explained by the observed reduction in GOF p53 levels. The AMPK and AKT pathways interact at various points to integrate a response to varying nutrient levels, by parallel and opposing regulation of mTOR and FOXO proteins. It is possible that the effects of activated AMPK and reduced pAKT synergise to decrease proliferation after knockdown of LZK. High throughput kinase activity assays could be used to discover novel direct downstream phosphorylation targets for LZK, which may help to elucidate mechanisms by which LZK could regulate these pathways.

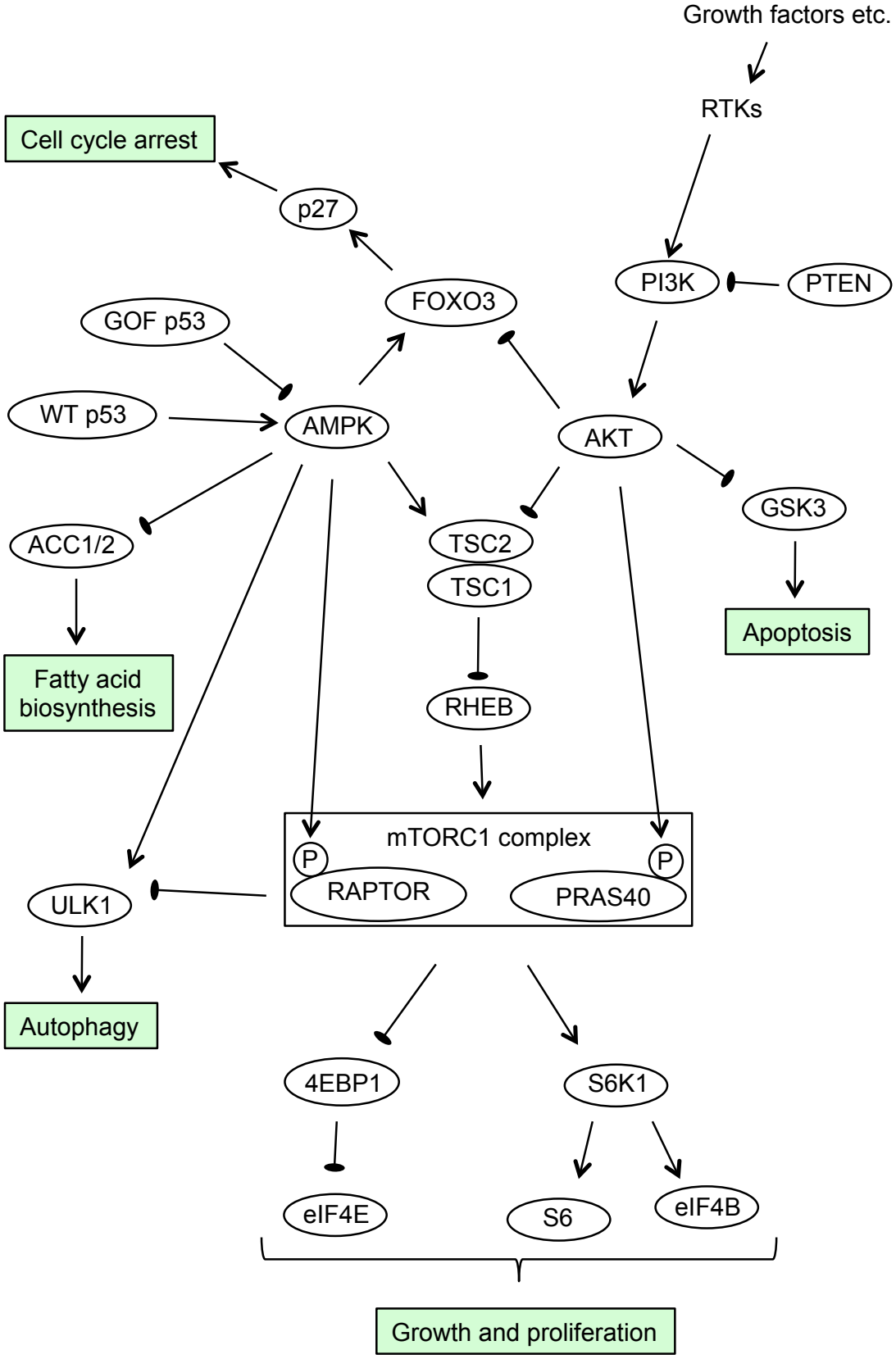

Figure 34: Schematic illustrating pathways investigated downstream of AMPK and AKT. Adapted from Shackleford *et al.*, 2009.

4.5.3 Importance of LZK in the 3q amplicon

Copy number gain of 3q has been identified in a range of squamous cell carcinomas, including HNSCC, LSCC and oesophageal SCC, and other cancers including small cell lung cancer (SCLC). The two SCC cell lines utilised here are both HNSCC lines derived from tongue tumours. Preliminary data suggested that LZK may be a more important target in HNSCC than in LSCC, as protein levels were higher in HNSCC cell lines (Fig. 14D). Additionally, higher copy number led to a more significant increase in mRNA expression in HNSCC as compared with LSCC tumours (Fig. 12A). In future work, knockdown of LZK will be tested in a range of cancer cell lines, to determine whether it plays a wider role in maintaining tumours with 3q copy number gain.

The 3q amplicon on which *MAP3K13* resides is broad and encompasses many genes. Compelling target genes include *SOX2*, *TP63* and *PIK3CA*. The majority of research in this area has focused on LSCC, for which SOX2 is emerging as a promising driver (Bass *et al.*, 2009; Liu *et al.*, 2013). However, in contrast to LZK, expression of SOX2 protein was not detected in several HNSCC lines, despite amplification of the *SOX2* gene (Fig. 14D–E). The role of SOX2 has not been studied in as much detail in HNSCC, although since this project was initiated one study has demonstrated an increase in its protein expression in tumour samples with 3q copy number gain (Schröck *et al.*, 2014). This was determined by IHC of tumour samples, and results were variable; 18% of samples with *SOX2* amplification had low SOX2 protein levels, so it is possible that cell lines utilised in this project may represent this subset of tumour samples. It could be that SOX2 protein expression in tumours is not well represented by culture of tumour cell lines in these conditions, as SOX2 levels were reported to be reduced by exposure to serum (Lim *et al.*, 2011); however, enhanced SOX2 could be detected in three lung and oesophageal cell lines (Fig. 14D), which were grown in the same serum-containing conditions as the HNSCC lines and analysed at similar passage numbers.

The 3q region likely harbours multiple genes that have a role in promoting and maintaining the tumour. Various studies have identified different 3q genes that can promote tumourigenic phenotypes in HNSCC, including *SOX2* (Lee *et al.*, 2014), *PIK3CA* (Singh *et al.*, 2002), *TP63* (DeYoung *et al.*, 2006; Rocco *et al.*, 2006; Ramsey *et al.*, 2013) and *DCUN1D1* (Sarkaria *et al.*, 2006). Some of these are not currently druggable, including SOX2. Several PI3K inhibitors have been developed, although preliminary

evidence suggests that these may not be as effective in cancer cells with amplification of *PIK3CA* as compared to those with mutationally activated *PIK3CA* (Lui *et al.*, 2013; Mazumdar *et al.*, 2014). Further research, in particular utilising LZK inhibitors *in vivo*, will determine whether LZK is a clinically actionable driver in tumours with copy number gain of 3q.

4.5.4 LZK overexpression does not transform immortalised normal control cells

Inducible overexpression of LZK in BEAS2B immortalised bronchial epithelial cells or the OKF6/TERT2 immortalised oral keratinocyte line reduced clonogenicity (Fig. 33), suggesting that amplification of *MAP3K13* alone is not oncogenic. Several well-characterised tumour-promoting genes, including $BRAF^{V600E}$ (Michaloglou *et al.*, 2005; Zhuang *et al.*, 2008) and activated *RAS* (Serrano *et al.*, 1997; Zhuang *et al.*, 2008), cause senescence when overexpressed in normal cells. Senescence is a process caused in normal cells by telomere erosion over many DNA replication cycles, but can also be activated prematurely in response to cellular stresses such as DNA damage or oncogene activation. This process is termed oncogene-induced senescence, and is an important tumour-suppressive mechanism that prevents benign lesions from undergoing malignant transformation. It is associated with activation of ARF–p53–$p21^{Cip1}$ and $p16^{INK4A}$–Rb pathways, and leads to stable cell cycle arrest (reviewed in Bringold and Serrano, 2000; Mooi and Peeper, 2006).

Oncogene-induced senescence is one possible explanation for the reduced clonogenicity observed after LZK overexpression. However, it must be noted that OKF6/TERT2 and BEAS2B cells are immortalised lines rather than true 'normal' cells and as such they will have lost functionality of some of the pathways involved in oncogene-induced senescence. OKF6/TERT2 has been immortalised by expression of hTERT (the catalytic subunit of telomerase); it retains a functional p53 pathway but lacks $p16^{INK4A}$ expression (Dickson *et al.*, 2000). In rodent cells, $p16^{INK4A}$ is required for oncogene-induced senescence (Serrano *et al.*, 1997); however, in human cells these mechanisms are less clear and are thought to vary by cellular context and oncogene (Bianchi-Smiraglia and Nikiforov, 2012). For example, fibroblasts with low expression of $p16^{INK4A}$ were found to be resistant to RAS-induced senescence, while those with high expression of $p16^{INK4A}$ were sensitive (Benanti and Galloway, 2004). In contrast, depletion of $p16^{INK4A}$ from melanocytes did not prevent oncogene-induced senescence due to expression of $NRAS^{Q61R}$ (Zhuang *et al.*, 2008) or

$BRAF^{V600E}$ (Michaloglou *et al.*, 2005; Zhuang *et al.*, 2008). BEAS2B was immortalised by Adenovirus12-Simian virus 40 (Ad12-SV40) hybrid virus and expresses SV40 T antigen (Reddel *et al.*, 1988). Expression of SV40 T antigen functions in part by inactivation of the p53 and Rb pathways (reviewed in Ahuja *et al.*, 2005) and expression of SV40 allows melanocytes to avoid $BRAF^{V600E}$-induced senescence (Michaloglou *et al.*, 2005). However, BEAS2B was reported to retain WT p53 activity, including increased p-p53, p21 and induction of apoptosis in response to DNA damage induced by carcinogens (Oya *et al.*, 2011) or heavy metals (Park *et al.*, 2015). Regardless, activated RAS was reported to transform BEAS2B cells, so these cells appear to be resistant to oncogene-induced senescence at least in the context of this particular oncogene (Reddel *et al.*, 1995). Additionally, oncogene-induced senescence occurs after an initial period of increased proliferation over a few population doublings (Mooi and Peeper, 2006). This is not the case with overexpression of LZK, which reduced survival of immortalised keratinocytes after only three days in culture. In contrast, expression of $BRAF^{V600E}$ in melanocytes caused increased proliferation at this time point, before causing the cells to undergo oncogene-induced senescence (Michaloglou *et al.*, 2005). The potential role of oncogene-induced senescence in LZK overexpression could be determined by examination of senescence-associated markers such as β-galactosidase and the Rb and p53 pathways.

A more likely explanation for the observed reduction in cell proliferation after LZK expression is direct activation of downstream signalling pathways by LZK, such as the apoptotic JNK pathway. It is also possible that LZK is able to stabilise WT p53; if this were the case then overexpression of LZK in a WT p53 background would be expected to promote cell cycle arrest and apoptosis due to the tumour suppressor functions of WT p53.

There are many genetic abnormalities in HNSCC cells, which might enable the cells to tolerate overexpression of LZK and maintain cell proliferation. This has been seen with SOX2, which requires coexpression with other proteins such as FGFR2 or FOXE1 (forkhead box E1) to transform immortalised tracheobronchial epithelial cells (Bass *et al.*, 2009), or activated STAT3 to transform oesophageal progenitor cells (Liu *et al.*, 2013). The 3q amplicon is broad and likely harbours multiple genes that have roles in promoting and maintaining the tumour; this region is not amplified in BEAS2B or OKF6/TERT2 cells, and other genes on this chromosome could be required to transform cells in combination with LZK. Based on my inducible knockdown data, it may be that GOF mutant p53 would need to be coexpressed with LZK to promote tumourigenic phenotypes.

It is worth testing whether LZK overexpression would cooperate with expression of GOF mutant p53 to promote tumourigenic phenotypes.

4.5.5 Conclusions and future directions

My data indicate that LZK promotes proliferation in HNSCC cell lines with copy number gain of *MAP3K13*. However, overexpression data suggest that LZK overexpression alone is not enough to promote cellular transformation, and may require the presence of mutation or amplification of other genes to exert a pro-tumourigenic effect. The crucial mechanisms downstream of LZK have not yet been clarified; there is a potential role for regulation of AKT and/or GOF p53 but neither of these alone can fully account for the phenotype of LZK knockdown. A larger range of cell lines needs to be utilised to determine whether LZK has a wider role in promoting proliferation in cells with 3q gain and/or GOF p53.

Genentech has developed a DLK inhibitor (Patel *et al.*, 2015) that they report to inhibit LZK at 300nM (personal confidential communication from Dr Mike Siu and Dr Joe Lewcock). In a continuation of this study, the inhibitor will be tested in cell lines with and without 3q copy number gain to confirm knockdown data. If effects seen replicate those observed with knockdown experiments, a drug-resistant LZK construct will be expressed to attempt to rescue the phenotype. Longer-term, mouse models would be used to test this inhibitor *in vivo*. Ideally, patient samples with 3q gain would be obtained and transplanted into mice, followed by treatment with the drug to assess whether inhibition of LZK could be a viable treatment option for HNSCC patients. Proliferation and cell cycle data indicate that inhibition of the protein would have a cytostatic rather than a cytotoxic effect. If this is the case, LZK inhibition may need to be combined with another agent to promote tumour cell death in patients. GOF p53 can promote resistance to common chemotherapeutic drugs (Bossi *et al.*, 2006), so it is possible that LZK inhibition could sensitise cancer cells to these treatments. However, since chemotherapy targets cells that proliferate rapidly, the anti-proliferative phenotype of LZK knockdown might counteract such an effect. Alternatively, dual inhibition of LZK and PI3K could prove effective, as knockdown of LZK synergised with PI3K inhibition in cell lines with 3q gain. Future studies will determine whether inhibition of LZK, possibly in combination with other agents, could be efficacious in the treatment of HNSCC with 3q amplification.

5 References

Acin, S., Li, Z., Mejia, O., Roop, D. R., El-Naggar, A. K. & Caulin, C. (2011) Gain-of-function mutant p53 but not p53 deletion promotes head and neck cancer progression in response to oncogenic K-ras. *The Journal of Pathology,* 225(4)**,** 479-89.

Ahn, Y. H., Yang, Y., Gibbons, D. L., Creighton, C. J., Yang, F., Wistuba, II, Lin, W., Thilaganathan, N., Alvarez, C. A., Roybal, J., Goldsmith, E. J., Tournier, C. & Kurie, J. M. (2011) Map2k4 functions as a tumor suppressor in lung adenocarcinoma and inhibits tumor cell invasion by decreasing peroxisome proliferator-activated receptor gamma2 expression. *Molecular and Cellular Biology,* 31(21)**,** 4270-85.

Ahuja, D., Sáenz-Robles, M. T. & Pipas, J. M. (2005) SV40 large T antigen targets multiple cellular pathways to elicit cellular transformation. *Oncogene,* 24(52)**,** 7729-45.

Alessi, D. R., Andjelkovic, M., Caudwell, B., Cron, P., Morrice, N., Cohen, P. & Hemmings, B. A. (1996) Mechanism of activation of protein kinase B by insulin and IGF-1. *The EMBO Journal,* 15(23)**,** 6541-51.

Alessi, D. R., James, S. R., Downes, C. P., Holmes, A. B., Gaffney, P. R., Reese, C. B. & Cohen, P. (1997) Characterization of a 3-phosphoinositide-dependent protein kinase which phosphorylates and activates protein kinase Balpha. *Current Biology,* 7(4)**,** 261-9.

Alexandrova, E. M., Yallowitz, A. R., Li, D., Xu, S., Schulz, R., Proia, D. A., Lozano, G., Dobbelstein, M. & Moll, U. M. (2015) Improving survival by exploiting tumour dependence on stabilized mutant p53 for treatment. *Nature,* 523(7560)**,** 352-6.

Allen, C. T., Ricker, J. L., Chen, Z. & Van Waes, C. (2007) Role of activated nuclear factor-kappaB in the pathogenesis and therapy of squamous cell carcinoma of the head and neck. *Head & Neck,* 29(10)**,** 959-71.

Anastassiadis, T., Deacon, S. W., Devarajan, K., Ma, H. & Peterson, J. R. (2011) Comprehensive assay of kinase catalytic activity reveals features of kinase inhibitor selectivity. *Nature Biotechnology,* 29(11)**,** 1039-45.

Anderson, R. T., Keysar, S. B., Bowles, D. W., Glogowska, M. J., Astling, D. P., Morton, J. J., Le, P., Umpierrez, A., Eagles-Soukup, J., Gan, G. N., Vogler, B. W., Sehrt, D., Takimoto, S. M., Aisner, D. L., Wilhelm, F., Frederick, B. A., Varella-Garcia, M., Tan, A. C. & Jimeno, A. (2013) The dual pathway inhibitor rigosertib is effective in direct patient tumor xenografts of head and neck squamous cell carcinomas. *Molecular Cancer Therapeutics,* 12(10)**,** 1994-2005.

Ang, K. K., Zhang, Q., Rosenthal, D. I., Nguyen-Tan, P. F., Sherman, E. J., Weber, R. S., Galvin, J. M., Bonner, J. A., Harris, J., El-Naggar, A. K., Gillison, M. L., Jordan, R. C., Konski, A. A., Thorstad, W. L., Trotti, A., Beitler, J. J., Garden, A. S., Spanos, W. J., Yom, S. S. & Axelrod, R. S. (2014) Randomized phase III trial of concurrent accelerated radiation plus cisplatin with or without cetuximab for stage III to IV head and neck carcinoma: RTOG 0522. *Journal of Clinical Oncology,* 32(27)**,** 2940-50.

Argiris, A., Karamouzis, M. V., Raben, D. & Ferris, R. L. (2008) Head and neck cancer. *Lancet,* 371(9625)**,** 1695-709.

Aronov, A. M., Tang, Q., Martinez-Botella, G., Bemis, G. W., Cao, J., Chen, G., Ewing, N. P., Ford, P. J., Germann, U. A., Green, J., Hale, M. R., Jacobs, M., Janetka, J. W., Maltais, F., Markland, W., Namchuk, M. N., Nanthakumar, S., Poondru, S., Straub, J., ter Haar, E. & Xie, X. (2009) Structure-guided design of potent and selective pyrimidylpyrrole inhibitors of extracellular signal-regulated kinase (ERK) using conformational control. *Journal of Medicinal Chemistry,* 52(20)**,** 6362-8.

Basile, K. J., Le, K., Hartsough, E. J. & Aplin, A. E. (2014) Inhibition of mutant BRAF splice variant signaling by next-generation, selective RAF inhibitors. *Pigment Cell & Melanoma Research,* 27(3)**,** 479-84.

Bass, A. J. & Wang, T. C. (2013) An inflammatory situation: SOX2 and STAT3 cooperate in squamous cell carcinoma initiation. *Cell Stem Cell,* 12(3)**,** 266-8.

Bass, A. J., Watanabe, H., Mermel, C. H., Yu, S., Perner, S., Verhaak, R. G., Kim, S. Y., Wardwell, L., Tamayo, P., Gat-Viks, I., Ramos, A. H., Woo, M. S., Weir, B. A., Getz, G., Beroukhim, R., O'Kelly, M., Dutt, A., Rozenblatt-Rosen, O., Dziunycz, P., Komisarof, J., Chirieac, L. R., Lafargue, C. J., Scheble, V., Wilbertz, T., Ma, C., Rao, S., Nakagawa, H., Stairs, D. B., Lin, L., Giordano, T. J., Wagner, P., Minna, J. D., Gazdar, A. F., Zhu, C. Q., Brose, M. S., Cecconello, I., Jr, U. R., Marie, S. K., Dahl, O., Shivdasani, R. A., Tsao, M. S., Rubin, M. A., Wong, K. K., Regev, A., Hahn, W. C., Beer, D. G., Rustgi, A. K. & Meyerson, M. (2009) SOX2 is an amplified lineage-survival oncogene in lung and esophageal squamous cell carcinomas. *Nature Genetics,* 41(11)**,** 1238-42.

Benanti, J. A. & Galloway, D. A. (2004) Normal human fibroblasts are resistant to RAS-induced senescence. *Molecular and Cellular Biology,* 24(7)**,** 2842-52.

Bernier, J., Domenge, C., Ozsahin, M., Matuszewska, K., Lefebvre, J. L., Greiner, R. H., Giralt, J., Maingon, P., Rolland, F., Bolla, M., Cognetti, F., Bourhis, J., Kirkpatrick, A., van Glabbeke, M., European Organization for, R. & Treatment of Cancer, T. (2004) Postoperative irradiation with or without concomitant chemotherapy for locally advanced head and neck cancer. *The New England Journal of Medicine,* 350(19)**,** 1945-52.

Bhaskar, P. T. & Hay, N. (2007) The two TORCs and Akt. *Developmental Cell,* 12(4)**,** 487-502.

Bianchi-Smiraglia, A. & Nikiforov, M. A. (2012) Controversial aspects of oncogene-induced senescence. *Cell Cycle,* 11(22)**,** 4147-51.

Bieging, K. T., Mello, S. S. & Attardi, L. D. (2014) Unravelling mechanisms of p53-mediated tumour suppression. *Nature Reviews Cancer,* 14(5)**,** 359-70.

Bisson, N., Tremblay, M., Robinson, F., Kaplan, D. R., Trusko, S. P. & Moss, T. (2008) Mice lacking both mixed-lineage kinase genes Mlk1 and Mlk2 retain a wild type phenotype. *Cell Cycle,* 7(7)**,** 909-16.

Bock, B. C., Vacratsis, P. O., Qamirani, E. & Gallo, K. A. (2000) Cdc42-induced activation of the mixed-lineage kinase SPRK in vivo. Requirement of the Cdc42/Rac interactive binding motif and changes in phosphorylation. *The Journal of Biological Chemistry,* 275(19)**,** 14231-41.

Bollag, G., Hirth, P., Tsai, J., Zhang, J., Ibrahim, P. N., Cho, H., Spevak, W., Zhang, C., Zhang, Y., Habets, G., Burton, E. A., Wong, B., Tsang, G., West, B. L., Powell, B., Shellooe, R., Marimuthu, A., Nguyen, H., Zhang, K. Y., Artis, D. R., Schlessinger, J., Su,

F., Higgins, B., Iyer, R., D'Andrea, K., Koehler, A., Stumm, M., Lin, P. S., Lee, R. J., Grippo, J., Puzanov, I., Kim, K. B., Ribas, A., McArthur, G. A., Sosman, J. A., Chapman, P. B., Flaherty, K. T., Xu, X., Nathanson, K. L. & Nolop, K. (2010) Clinical efficacy of a RAF inhibitor needs broad target blockade in BRAF-mutant melanoma. *Nature,* 467(7315)**,** 596-9.

Bonner, J. A., Harari, P. M., Giralt, J., Azarnia, N., Shin, D. M., Cohen, R. B., Jones, C. U., Sur, R., Raben, D., Jassem, J., Ove, R., Kies, M. S., Baselga, J., Youssoufian, H., Amellal, N., Rowinsky, E. K. & Ang, K. K. (2006) Radiotherapy plus cetuximab for squamous-cell carcinoma of the head and neck. *The New England Journal of Medicine,* 354(6)**,** 567-78.

Bossi, G., Lapi, E., Strano, S., Rinaldo, C., Blandino, G. & Sacchi, A. (2006) Mutant p53 gain of function: reduction of tumor malignancy of human cancer cell lines through abrogation of mutant p53 expression. *Oncogene,* 25(2)**,** 304-9.

Boyle, J. O., Hakim, J., Koch, W., van der Riet, P., Hruban, R. H., Roa, R. A., Correo, R., Eby, Y. J., Ruppert, J. M. & Sidransky, D. (1993) The incidence of p53 mutations increases with progression of head and neck cancer. *Cancer Research,* 53(19)**,** 4477-80.

Brancho, D., Ventura, J. J., Jaeschke, A., Doran, B., Flavell, R. A. & Davis, R. J. (2005) Role of MLK3 in the regulation of mitogen-activated protein kinase signaling cascades. *Molecular and Cellular Biology,* 25(9)**,** 3670-81.

Bringold, F. & Serrano, M. (2000) Tumor suppressors and oncogenes in cellular senescence. *Experimental Gerontology,* 35(3)**,** 317-29.

Brognard, J. & Hunter, T. (2011) Protein kinase signaling networks in cancer. *Current Opinion in Genetics & Development,* 21(1)**,** 4-11.

Bubici, C. & Papa, S. (2014) JNK signalling in cancer: in need of new, smarter therapeutic targets. *British Journal of Pharmacology,* 171(1)**,** 24-37.

Buchsbaum, R. J., Connolly, B. A. & Feig, L. A. (2002) Interaction of Rac exchange factors Tiam1 and Ras-GRF1 with a scaffold for the p38 mitogen-activated protein kinase cascade. *Molecular and Cellular Biology,* 22(12)**,** 4073-85.

Burke, J. E., Perisic, O., Masson, G. R., Vadas, O. & Williams, R. L. (2012) Oncogenic mutations mimic and enhance dynamic events in the natural activation of phosphoinositide 3-kinase p110α (PIK3CA). *Proceedings of the National Academy of Sciences of the United States of America,* 109(38)**,** 15259-64.

Burns, J. E., Baird, M. C., Clark, L. J., Burns, P. A., Edington, K., Chapman, C., Mitchell, R., Robertson, G., Soutar, D. & Parkinson, E. K. (1993) Gene mutations and increased levels of p53 protein in human squamous cell carcinomas and their cell lines. *British Journal of Cancer,* 67(6)**,** 1274-84.

Cancer Genome Atlas Network. (2012) Comprehensive genomic characterization of squamous cell lung cancers. *Nature,* 489(7417)**,** 519-25.

Cancer Genome Atlas Network. (2015) Comprehensive genomic characterization of head and neck squamous cell carcinomas. *Nature,* 517(7536)**,** 576-82.

Carracedo, A. & Pandolfi, P. P. (2008) The PTEN-PI3K pathway: of feedbacks and cross-talks. *Oncogene,* 27(41)**,** 5527-41.

Carvalho, A. L., Nishimoto, I. N., Califano, J. A. & Kowalski, L. P. (2005) Trends in incidence and prognosis for head and neck cancer in the United States: a site-specific analysis of the SEER database. *International Journal of Cancer,* 114(5)**,** 806-16.

Cassell, A. & Grandis, J. R. (2010) Investigational EGFR-targeted therapy in head and neck squamous cell carcinoma. *Expert Opinion on Investigational Drugs,* 19(6)**,** 709-22.

Castellano, E. & Downward, J. (2011) RAS Interaction with PI3K: More Than Just Another Effector Pathway. *Genes & Cancer,* 2(3)**,** 261-74.

cBio. (2015) *cBio Cancer Genomics Portal* [Online]. Available: http://www.cbioportal.org/public-portal/ [Accessed 29th June 2015].

CCLE. (2015) *Cancer Cell Line Encyclopedia* [Online]. Available: http://www.broadinstitute.org/ccle/ [Accessed 16th July 2015].

Cha, H., Dangi, S., Machamer, C. E. & Shapiro, P. (2006) Inhibition of mixed-lineage kinase (MLK) activity during G2-phase disrupts microtubule formation and mitotic progression in HeLa cells. *Cellular Signalling,* 18(1)**,** 93-104.

Chadee, D. N. & Kyriakis, J. M. (2004) MLK3 is required for mitogen activation of B-Raf, ERK and cell proliferation. *Nature Cell Biology,* 6(8)**,** 770-6.

Chadee, D. N., Xu, D., Hung, G., Andalibi, A., Lim, D. J., Luo, Z., Gutmann, D. H. & Kyriakis, J. M. (2006) Mixed-lineage kinase 3 regulates B-Raf through maintenance of the B-Raf/Raf-1 complex and inhibition by the NF2 tumor suppressor protein. *Proceedings of the National Academy of Sciences of the United States of America,* 103(12)**,** 4463-8.

Chapman, P. B., Hauschild, A., Robert, C., Haanen, J. B., Ascierto, P., Larkin, J., Dummer, R., Garbe, C., Testori, A., Maio, M., Hogg, D., Lorigan, P., Lebbe, C., Jouary, T., Schadendorf, D., Ribas, A., O'Day, S. J., Sosman, J. A., Kirkwood, J. M., Eggermont, A. M., Dreno, B., Nolop, K., Li, J., Nelson, B., Hou, J., Lee, R. J., Flaherty, K. T. & McArthur, G. A. (2011) Improved survival with vemurafenib in melanoma with BRAF V600E mutation. *The New England Journal of Medicine,* 364(26)**,** 2507-16.

Chen, J. & Gallo, K. A. (2012) MLK3 regulates paxillin phosphorylation in chemokine-mediated breast cancer cell migration and invasion to drive metastasis. *Cancer Research,* 72(16)**,** 4130-40.

Chen, J., Miller, E. M. & Gallo, K. A. (2010) MLK3 is critical for breast cancer cell migration and promotes a malignant phenotype in mammary epithelial cells. *Oncogene,* 29(31)**,** 4399-411.

Chu, I. M., Hengst, L. & Slingerland, J. M. (2008) The Cdk inhibitor p27 in human cancer: prognostic potential and relevance to anticancer therapy. *Nature Reviews Cancer,* 8(4)**,** 253-67.

ClinicalTrials.gov. (2015). Available: https://clinicaltrials.gov [Accessed 6th Aug 2015].

Corcoran, R. B., Dias-Santagata, D., Bergethon, K., Iafrate, A. J., Settleman, J. & Engelman, J. A. (2010) BRAF gene amplification can promote acquired resistance to

MEK inhibitors in cancer cells harboring the BRAF V600E mutation. *Science Signaling,* 3(149)**,** ra84.

Corcoran, R. B., Ebi, H., Turke, A. B., Coffee, E. M., Nishino, M., Cogdill, A. P., Brown, R. D., Della Pelle, P., Dias-Santagata, D., Hung, K. E., Flaherty, K. T., Piris, A., Wargo, J. A., Settleman, J., Mino-Kenudson, M. & Engelman, J. A. (2012) EGFR-mediated re-activation of MAPK signaling contributes to insensitivity of BRAF mutant colorectal cancers to RAF inhibition with vemurafenib. *Cancer Discovery,* 2(3)**,** 227-35.

Corso, G., Velho, S., Paredes, J., Pedrazzani, C., Martins, D., Milanezi, F., Pascale, V., Vindigni, C., Pinheiro, H., Leite, M., Marrelli, D., Sousa, S., Carneiro, F., Oliveira, C., Roviello, F. & Seruca, R. (2011) Oncogenic mutations in gastric cancer with microsatellite instability. *European Journal of Cancer,* 47(3)**,** 443-51.

Cronan, M. R., Nakamura, K., Johnson, N. L., Granger, D. A., Cuevas, B. D., Wang, J. G., Mackman, N., Scott, J. E., Dohlman, H. G. & Johnson, G. L. (2012) Defining MAP3 kinases required for MDA-MB-231 cell tumor growth and metastasis. *Oncogene,* 31(34)**,** 3889-900.

Cuenda, A. & Dorow, D. S. (1998) Differential activation of stress-activated protein kinase kinases SKK4/MKK7 and SKK1/MKK4 by the mixed-lineage kinase-2 and mitogen-activated protein kinase kinase (MKK) kinase-1. *The Biochemical Journal,* 333 (Pt 1)**,** 11-5.

Culliney, B., Birhan, A., Young, A. V., Choi, W., Shulimovich, M. & Blum, R. H. (2008) Management of locally advanced or unresectable head and neck cancer. *Oncology (Williston Park),* 22(10)**,** 1152-61; discussion 1162-6, 1171-2.

Davies, H., Bignell, G. R., Cox, C., Stephens, P., Edkins, S., Clegg, S., Teague, J., Woffendin, H., Garnett, M. J., Bottomley, W., Davis, N., Dicks, E., Ewing, R., Floyd, Y., Gray, K., Hall, S., Hawes, R., Hughes, J., Kosmidou, V., Menzies, A., Mould, C., Parker, A., Stevens, C., Watt, S., Hooper, S., Wilson, R., Jayatilake, H., Gusterson, B. A., Cooper, C., Shipley, J., Hargrave, D., Pritchard-Jones, K., Maitland, N., Chenevix-Trench, G., Riggins, G. J., Bigner, D. D., Palmieri, G., Cossu, A., Flanagan, A., Nicholson, A., Ho, J. W., Leung, S. Y., Yuen, S. T., Weber, B. L., Seigler, H. F., Darrow, T. L., Paterson, H., Marais, R., Marshall, C. J., Wooster, R., Stratton, M. R. & Futreal, P. A. (2002) Mutations of the BRAF gene in human cancer. *Nature,* 417(6892)**,** 949-54.

Davis, M. I., Hunt, J. P., Herrgard, S., Ciceri, P., Wodicka, L. M., Pallares, G., Hocker, M., Treiber, D. K. & Zarrinkar, P. P. (2011) Comprehensive analysis of kinase inhibitor selectivity. *Nature Biotechnology,* 29(11)**,** 1046-51.

DeYoung, M. P., Johannessen, C. M., Leong, C. O., Faquin, W., Rocco, J. W. & Ellisen, L. W. (2006) Tumor-specific p73 up-regulation mediates p63 dependence in squamous cell carcinoma. *Cancer Research,* 66(19)**,** 9362-8.

Di Agostino, S., Strano, S., Emiliozzi, V., Zerbini, V., Mottolese, M., Sacchi, A., Blandino, G. & Piaggio, G. (2006) Gain of function of mutant p53: the mutant p53/NF-Y protein complex reveals an aberrant transcriptional mechanism of cell cycle regulation. *Cancer Cell,* 10(3)**,** 191-202.

Dickson, H. M., Zurawski, J., Zhang, H., Turner, D. L. & Vojtek, A. B. (2010) POSH is an intracellular signal transducer for the axon outgrowth inhibitor Nogo66. *The Journal of Neuroscience,* 30(40)**,** 13319-25.

Dickson, M. A., Hahn, W. C., Ino, Y., Ronfard, V., Wu, J. Y., Weinberg, R. A., Louis, D. N., Li, F. P. & Rheinwald, J. G. (2000) Human keratinocytes that express hTERT and also bypass a p16(INK4a)-enforced mechanism that limits life span become immortal yet retain normal growth and differentiation characteristics. *Molecular and Cellular Biology,* 20(4)**,** 1436-47.

Dittmer, D., Pati, S., Zambetti, G., Chu, S., Teresky, A. K., Moore, M., Finlay, C. & Levine, A. J. (1993) Gain of function mutations in p53. *Nature Genetics,* 4(1)**,** 42-6.

Dong, P., Xu, Z., Jia, N., Li, D. & Feng, Y. (2009) Elevated expression of p53 gain-of-function mutation R175H in endometrial cancer cells can increase the invasive phenotypes by activation of the EGFR/PI3K/AKT pathway. *Molecular Cancer,* 8**,** 103.

Dorow, D. S., Devereux, L., Dietzsch, E. & De Kretser, T. (1993) Identification of a new family of human epithelial protein kinases containing two leucine/isoleucine-zipper domains. *European Journal of Biochemistry / FEBS,* 213(2)**,** 701-10.

Dorow, D. S., Devereux, L., Tu, G. F., Price, G., Nicholl, J. K., Sutherland, G. R. & Simpson, R. J. (1995) Complete nucleotide sequence, expression, and chromosomal localisation of human mixed-lineage kinase 2. *European Journal of Biochemistry / FEBS,* 234(2)**,** 492-500.

Du, L., Shen, J., Weems, A. & Lu, S. L. (2012) Role of phosphatidylinositol-3-kinase pathway in head and neck squamous cell carcinoma. *Journal of Oncology,* 2012**,** 450179.

Duan, W., Gao, L., Jin, D., Otterson, G. A. & Villalona-Calero, M. A. (2008) Lung specific expression of a human mutant p53 affects cell proliferation in transgenic mice. *Transgenic Research,* 17(3)**,** 355-66.

Durkin, J. T., Holskin, B. P., Kopec, K. K., Reed, M. S., Spais, C. M., Steffy, B. M., Gessner, G., Angeles, T. S., Pohl, J., Ator, M. A. & Meyer, S. L. (2004) Phosphoregulation of mixed-lineage kinase 1 activity by multiple phosphorylation in the activation loop. *Biochemistry,* 43(51)**,** 16348-55.

EMA. (2012) *European Medicines Agency* [Online]. Available: http://www.ema.europa.eu/ema/ [Accessed 2nd July 2012].

Ermak, G., Cancasci, V. J. & Davies, K. J. (2003) Cytotoxic effect of doxycycline and its implications for tet-on gene expression systems. *Analytical Biochemistry,* 318(1)**,** 152-4.

Fan, G., Merritt, S. E., Kortenjann, M., Shaw, P. E. & Holzman, L. B. (1996) Dual leucine zipper-bearing kinase (DLK) activates p46SAPK and p38mapk but not ERK2. *The Journal of Biological Chemistry,* 271(40)**,** 24788-93.

FDA. (2012) *U.S. Food and Drug Administration* [Online]. Available: http://www.fda.gov/ [Accessed 2nd July 2012].

Finegan, K. G. & Tournier, C. (2010) The mitogen-activated protein kinase kinase 4 has a pro-oncogenic role in skin cancer. *Cancer Research,* 70(14)**,** 5797-806.

Flaherty, K. T., Puzanov, I., Kim, K. B., Ribas, A., McArthur, G. A., Sosman, J. A., O'Dwyer, P. J., Lee, R. J., Grippo, J. F., Nolop, K. & Chapman, P. B. (2010) Inhibition of mutated, activated BRAF in metastatic melanoma. *The New England Journal of Medicine,* 363(9)**,** 809-19.

Gallo, K. A. & Johnson, G. L. (2002) Mixed-lineage kinase control of JNK and p38 MAPK pathways. *Nature Reviews Molecular Cell Biology,* 3(9)**,** 663-72.

Gallo, K. A., Mark, M. R., Scadden, D. T., Wang, Z., Gu, Q. & Godowski, P. J. (1994) Identification and characterization of SPRK, a novel src-homology 3 domain-containing proline-rich kinase with serine/threonine kinase activity. *The Journal of Biological Chemistry,* 269(21)**,** 15092-100.

Garlena, R. A., Gonda, R. L., Green, A. B., Pileggi, R. M. & Stronach, B. (2010) Regulation of mixed-lineage kinase activation in JNK-dependent morphogenesis. *Journal of Cell Science,* 123(Pt 18)**,** 3177-88.

Ghosh, A. S., Wang, B., Pozniak, C. D., Chen, M., Watts, R. J. & Lewcock, J. W. (2011) DLK induces developmental neuronal degeneration via selective regulation of proapoptotic JNK activity. *The Journal of Cell Biology,* 194(5)**,** 751-64.

Gibney, G. T., Messina, J. L., Fedorenko, I. V., Sondak, V. K. & Smalley, K. S. (2013) Paradoxical oncogenesis--the long-term effects of BRAF inhibition in melanoma. *Nature Reviews Clinical Oncology,* 10(7)**,** 390-9.

Gillies, R. J., Didier, N. & Denton, M. (1986) Determination of cell number in monolayer cultures. *Analytical Biochem,* 159(1)**,** 109-13.

Girotti, M. R., Lopes, F., Preece, N., Niculescu-Duvaz, D., Zambon, A., Davies, L., Whittaker, S., Saturno, G., Viros, A., Pedersen, M., Suijkerbuijk, B. M., Menard, D., McLeary, R., Johnson, L., Fish, L., Ejiama, S., Sanchez-Laorden, B., Hohloch, J., Carragher, N., Macleod, K., Ashton, G., Marusiak, A. A., Fusi, A., Brognard, J., Frame, M., Lorigan, P., Marais, R. & Springer, C. (2015) Paradox-breaking RAF inhibitors that also target SRC are effective in drug-resistant BRAF mutant melanoma. *Cancer Cell,* 27(1)**,** 85-96.

Girotti, M. R., Pedersen, M., Sanchez-Laorden, B., Viros, A., Turajlic, S., Niculescu-Duvaz, D., Zambon, A., Sinclair, J., Hayes, A., Gore, M., Lorigan, P., Springer, C., Larkin, J., Jorgensen, C. & Marais, R. (2013) Inhibiting EGF receptor or SRC family kinase signaling overcomes BRAF inhibitor resistance in melanoma. *Cancer Discovery,* 3(2)**,** 158-67.

Gopal, Y. N., Deng, W., Woodman, S. E., Komurov, K., Ram, P., Smith, P. D. & Davies, M. A. (2010) Basal and treatment-induced activation of AKT mediates resistance to cell death by AZD6244 (ARRY-142886) in Braf-mutant human cutaneous melanoma cells. *Cancer Research,* 70(21)**,** 8736-47.

Greer, E. L., Oskoui, P. R., Banko, M. R., Maniar, J. M., Gygi, M. P., Gygi, S. P. & Brunet, A. (2007) The energy sensor AMP-activated protein kinase directly regulates the mammalian FOXO3 transcription factor. *The Journal of Biological Chemistry,* 282(41)**,** 30107-19.

Gross, N. D., Boyle, J. O., Du, B., Kekatpure, V. D., Lantowski, A., Thaler, H. T., Weksler, B. B., Subbaramaiah, K. & Dannenberg, A. J. (2007) Inhibition of Jun NH2-terminal kinases suppresses the growth of experimental head and neck squamous cell carcinoma. *Clinical Cancer Research,* 13(19)**,** 5910-7.

Guan, X. Y., Sham, J. S., Tang, T. C., Fang, Y., Huo, K. K. & Yang, J. M. (2001) Isolation of a novel candidate oncogene within a frequently amplified region at 3q26 in ovarian cancer. *Cancer Research,* 61(9)**,** 3806-9.

Guardavaccaro, D., Corrente, G., Covone, F., Micheli, L., D'Agnano, I., Starace, G., Caruso, M. & Tirone, F. (2000) Arrest of G(1)-S progression by the p53-inducible gene PC3 is Rb dependent and relies on the inhibition of cyclin D1 transcription. *Molecular and Cellular Biology,* 20(5)**,** 1797-815.

Guertin, D. A., Stevens, D. M., Thoreen, C. C., Burds, A. A., Kalaany, N. Y., Moffat, J., Brown, M., Fitzgerald, K. J. & Sabatini, D. M. (2006) Ablation in mice of the mTORC components raptor, rictor, or mLST8 reveals that mTORC2 is required for signaling to Akt-FOXO and PKCalpha, but not S6K1. *Developmental Cell,* 11(6)**,** 859-71.

Gwinn, D. M., Shackelford, D. B., Egan, D. F., Mihaylova, M. M., Mery, A., Vasquez, D. S., Turk, B. E. & Shaw, R. J. (2008) AMPK phosphorylation of raptor mediates a metabolic checkpoint. *Molecular Cell,* 30(2)**,** 214-26.

Haddad, R. I. & Shin, D. M. (2008) Recent advances in head and neck cancer. *The New England Journal of Medicine,* 359(11)**,** 1143-54.

Hagerstrand, D., Tong, A., Schumacher, S. E., Ilic, N., Shen, R. R., Cheung, H. W., Vazquez, F., Shrestha, Y., Kim, S. Y., Giacomelli, A. O., Rosenbluh, J., Schinzel, A. C., Spardy, N. A., Barbie, D. A., Mermel, C. H., Weir, B. A., Garraway, L. A., Tamayo, P., Mesirov, J. P., Beroukhim, R. & Hahn, W. C. (2013) Systematic interrogation of 3q26 identifies TLOC1 and SKIL as cancer drivers. *Cancer Discovery,* 3(9)**,** 1044-57.

Hanahan, D. & Weinberg, R. A. (2011) Hallmarks of cancer: the next generation. *Cell,* 144(5)**,** 646-74.

Handley, M. E., Rasaiyaah, J., Chain, B. M. & Katz, D. R. (2007) Mixed lineage kinases (MLKs): a role in dendritic cells, inflammation and immunity? *International Journal of Experimental Pathology,* 88(2)**,** 111-26.

Haq, R., Yokoyama, S., Hawryluk, E. B., Jonsson, G. B., Frederick, D. T., McHenry, K., Porter, D., Tran, T. N., Love, K. T., Langer, R., Anderson, D. G., Garraway, L. A., Duncan, L. M., Morton, D. L., Hoon, D. S., Wargo, J. A., Song, J. S. & Fisher, D. E. (2013) BCL2A1 is a lineage-specific antiapoptotic melanoma oncogene that confers resistance to BRAF inhibition. *Proceedings of the National Academy of Sciences of the United States of America,* 110(11)**,** 4321-6.

Hartkamp, J., Troppmair, J. & Rapp, U. R. (1999) The JNK/SAPK activator mixed lineage kinase 3 (MLK3) transforms NIH 3T3 cells in a MEK-dependent fashion. *Cancer Research,* 59(9)**,** 2195-202.

Hatzivassiliou, G., Song, K., Yen, I., Brandhuber, B. J., Anderson, D. J., Alvarado, R., Ludlam, M. J., Stokoe, D., Gloor, S. L., Vigers, G., Morales, T., Aliagas, I., Liu, B., Sideris, S., Hoeflich, K. P., Jaiswal, B. S., Seshagiri, S., Koeppen, H., Belvin, M., Friedman, L. S. & Malek, S. (2010) RAF inhibitors prime wild-type RAF to activate the MAPK pathway and enhance growth. *Nature,* 464(7287)**,** 431-5.

Heidorn, S. J., Milagre, C., Whittaker, S., Nourry, A., Niculescu-Duvas, I., Dhomen, N., Hussain, J., Reis-Filho, J. S., Springer, C. J., Pritchard, C. & Marais, R. (2010) Kinase-

dead BRAF and oncogenic RAS cooperate to drive tumor progression through CRAF. *Cell,* 140(2)**,** 209-21.

Hemmings, B. A. & Restuccia, D. F. (2012) PI3K-PKB/Akt pathway. *Cold Spring Harbor Perspectives in Biology,* 4(9)**,** a011189.

Hirai, S., Cui de, F., Miyata, T., Ogawa, M., Kiyonari, H., Suda, Y., Aizawa, S., Banba, Y. & Ohno, S. (2006) The c-Jun N-terminal kinase activator dual leucine zipper kinase regulates axon growth and neuronal migration in the developing cerebral cortex. *The Journal of Neuroscience,* 26(46)**,** 11992-2002.

Hirai, S., Katoh, M., Terada, M., Kyriakis, J. M., Zon, L. I., Rana, A., Avruch, J. & Ohno, S. (1997) MST/MLK2, a member of the mixed lineage kinase family, directly phosphorylates and activates SEK1, an activator of c-Jun N-terminal kinase/stress-activated protein kinase. *The Journal of Biological Chemistry,* 272(24)**,** 15167-73.

Holderfield, M., Merritt, H., Chan, J., Wallroth, M., Tandeske, L., Zhai, H., Tellew, J., Hardy, S., Hekmat-Nejad, M., Stuart, D. D., McCormick, F. & Nagel, T. E. (2013) RAF inhibitors activate the MAPK pathway by relieving inhibitory autophosphorylation. *Cancer Cell,* 23(5)**,** 594-602.

Holderfield, M., Nagel, T. E. & Stuart, D. D. (2014) Mechanism and consequences of RAF kinase activation by small-molecule inhibitors. *British Journal of Cancer,* 111(4)**,** 640-5.

Holzman, L. B., Merritt, S. E. & Fan, G. (1994) Identification, molecular cloning, and characterization of dual leucine zipper bearing kinase. A novel serine/threonine protein kinase that defines a second subfamily of mixed lineage kinases. *The Journal of Biological Chemistry,* 269(49)**,** 30808-17.

Hresko, R. C. & Mueckler, M. (2005) mTOR.RICTOR is the Ser473 kinase for Akt/protein kinase B in 3T3-L1 adipocytes. *The Journal of Biological Chemistry,* 280(49)**,** 40406-16.

Huang, C. Y., Kuo, W. W., Chueh, P. J., Tseng, C. T., Chou, M. Y. & Yang, J. J. (2004) Transforming growth factor-beta induces the expression of ANF and hypertrophic growth in cultured cardiomyoblast cells through ZAK. *Biochemical and Biophysical Research Communications,* 324(1)**,** 424-31.

Huang, J. & Manning, B. D. (2008) The TSC1-TSC2 complex: a molecular switchboard controlling cell growth. *Biochemical Journal,* 412(2)**,** 179-90.

Huntwork-Rodriguez, S., Wang, B., Watkins, T., Ghosh, A. S., Pozniak, C. D., Bustos, D., Newton, K., Kirkpatrick, D. S. & Lewcock, J. W. (2013) JNK-mediated phosphorylation of DLK suppresses its ubiquitination to promote neuronal apoptosis. *The Journal of Cell Biology,* 202(5)**,** 747-63.

Hussenet, T., Dali, S., Exinger, J., Monga, B., Jost, B., Dembele, D., Martinet, N., Thibault, C., Huelsken, J., Brambilla, E. & du Manoir, S. (2010) SOX2 is an oncogene activated by recurrent 3q26.3 amplifications in human lung squamous cell carcinomas. *PLOS ONE,* 5(1)**,** e8960.

Ikeda, A., Hasegawa, K., Masaki, M., Moriguchi, T., Nishida, E., Kozutsumi, Y., Oka, S. & Kawasaki, T. (2001a) Mixed lineage kinase LZK forms a functional signaling complex

with JIP-1, a scaffold protein of the c-Jun NH(2)-terminal kinase pathway. *Journal of Biochemistry,* 130(6)**,** 773-81.

Ikeda, A., Masaki, M., Kozutsumi, Y., Oka, S. & Kawasaki, T. (2001b) Identification and characterization of functional domains in a mixed lineage kinase LZK. *FEBS Letters,* 488(3)**,** 190-5.

Johannessen, C. M., Boehm, J. S., Kim, S. Y., Thomas, S. R., Wardwell, L., Johnson, L. A., Emery, C. M., Stransky, N., Cogdill, A. P., Barretina, J., Caponigro, G., Hieronymus, H., Murray, R. R., Salehi-Ashtiani, K., Hill, D. E., Vidal, M., Zhao, J. J., Yang, X., Alkan, O., Kim, S., Harris, J. L., Wilson, C. J., Myer, V. E., Finan, P. M., Root, D. E., Roberts, T. M., Golub, T., Flaherty, K. T., Dummer, R., Weber, B. L., Sellers, W. R., Schlegel, R., Wargo, J. A., Hahn, W. C. & Garraway, L. A. (2010) COT drives resistance to RAF inhibition through MAP kinase pathway reactivation. *Nature,* 468(7326)**,** 968-72.

Junttila, M. R., Ala-Aho, R., Jokilehto, T., Peltonen, J., Kallajoki, M., Grenman, R., Jaakkola, P., Westermarck, J. & Kahari, V. M. (2007) p38alpha and p38delta mitogen-activated protein kinase isoforms regulate invasion and growth of head and neck squamous carcinoma cells. *Oncogene,* 26(36)**,** 5267-79.

Justilien, V., Walsh, M. P., Ali, S. A., Thompson, E. A., Murray, N. R. & Fields, A. P. (2014) The PRKCI and SOX2 oncogenes are coamplified and cooperate to activate Hedgehog signaling in lung squamous cell carcinoma. *Cancer Cell,* 25(2)**,** 139-51.

Kan, Z., Jaiswal, B. S., Stinson, J., Janakiraman, V., Bhatt, D., Stern, H. M., Yue, P., Haverty, P. M., Bourgon, R., Zheng, J., Moorhead, M., Chaudhuri, S., Tomsho, L. P., Peters, B. A., Pujara, K., Cordes, S., Davis, D. P., Carlton, V. E., Yuan, W., Li, L., Wang, W., Eigenbrot, C., Kaminker, J. S., Eberhard, D. A., Waring, P., Schuster, S. C., Modrusan, Z., Zhang, Z., Stokoe, D., de Sauvage, F. J., Faham, M. & Seshagiri, S. (2010) Diverse somatic mutation patterns and pathway alterations in human cancers. *Nature,* 466(7308)**,** 869-73.

Kant, S., Swat, W., Zhang, S., Zhang, Z. Y., Neel, B. G., Flavell, R. A. & Davis, R. J. (2011) TNF-stimulated MAP kinase activation mediated by a Rho family GTPase signaling pathway. *Genes & Development,* 25(19)**,** 2069-78.

Kashuba, V. I., Grigorieva, E. V., Kvasha, S. M., Pavlova, T. V., Grigoriev, V., Protopopov, A., Kharchenko, O., Gizatullin, R., Rynditch, A. V. & Zabarovsky, E. R. (2011) Cloning and Initial Functional Characterization of Mlk4alpha and Mlk4beta. *Genomics Insights,* 4**,** 1-12.

Kim, C. A. & Bowie, J. U. (2003) SAM domains: uniform structure, diversity of function. *Trends in Biochemical Sciences,* 28(12)**,** 625-8.

Kim, K. Y., Kim, B. C., Xu, Z. & Kim, S. J. (2004) Mixed lineage kinase 3 (MLK3)-activated p38 MAP kinase mediates transforming growth factor-beta-induced apoptosis in hepatoma cells. *The Journal of Biological Chemistry,* 279(28)**,** 29478-84.

Knowles, M. A. (2005). Oncogenes, *in:* Knowles, M. A. & Selby, P. (eds.) *Introduction to the cellular and molecular biology of cancer.* Fourth Edition. Oxford: Oxford University Press, pp. 117-134

Kovacic, S., Soltys, C. L., Barr, A. J., Shiojima, I., Walsh, K. & Dyck, J. R. (2003) Akt activity negatively regulates phosphorylation of AMP-activated protein kinase in the heart. *The Journal of Biological Chemistry,* 278(41)**,** 39422-7.

Kueng, W., Silber, E. & Eppenberger, U. (1989) Quantification of cells cultured on 96-well plates. *Analytical Biochemistry,* 182(1)**,** 16-9.

Le, K., Blomain, E. S., Rodeck, U. & Aplin, A. E. (2013) Selective RAF inhibitor impairs ERK1/2 phosphorylation and growth in mutant NRAS, vemurafenib-resistant melanoma cells. *Pigment Cell & Melanoma Research,* 26(4)**,** 509-17.

Lee, G. Y., Kenny, P. A., Lee, E. H. & Bissell, M. J. (2007) Three-dimensional culture models of normal and malignant breast epithelial cells. *Nature Methods,* 4(4)**,** 359-65.

Lee, S. H., Oh, S. Y., Do, S. I., Lee, H. J., Kang, H. J., Rho, Y. S., Bae, W. J. & Lim, Y. C. (2014) SOX2 regulates self-renewal and tumorigenicity of stem-like cells of head and neck squamous cell carcinoma. *British Journal of Cancer,* 111(11)**,** 2122-30.

Leelahavanichkul, K., Amornphimoltham, P., Molinolo, A. A., Basile, J. R., Koontongkaew, S. & Gutkind, J. S. (2014) A role for p38 MAPK in head and neck cancer cell growth and tumor-induced angiogenesis and lymphangiogenesis. *Molecular Oncology,* 8(1)**,** 105-18.

Leung, I. W. & Lassam, N. (1998) Dimerization via tandem leucine zippers is essential for the activation of the mitogen-activated protein kinase kinase kinase, MLK-3. *The Journal of Biological Chemistry,* 273(49)**,** 32408-15.

Leung, I. W. & Lassam, N. (2001) The kinase activation loop is the key to mixed lineage kinase-3 activation via both autophosphorylation and hematopoietic progenitor kinase 1 phosphorylation. *The Journal of Biological Chemistry,* 276(3)**,** 1961-7.

Li, D., Marchenko, N. D., Schulz, R., Fischer, V., Velasco-Hernandez, T., Talos, F. & Moll, U. M. (2011) Functional inactivation of endogenous MDM2 and CHIP by HSP90 causes aberrant stabilization of mutant p53 in human cancer cells. *Molecular Cancer Research,* 9(5)**,** 577-88.

Liang, S., Yang, N., Pan, Y., Deng, S., Lin, X., Yang, X., Katsaros, D., Roby, K. F., Hamilton, T. C., Connolly, D. C., Coukos, G. & Zhang, L. (2009) Expression of activated PIK3CA in ovarian surface epithelium results in hyperplasia but not tumor formation. *PLOS ONE,* 4(1)**,** e4295.

Lim, I. K., Lee, M. S., Ryu, M. S., Park, T. J., Fujiki, H., Eguchi, H. & Paik, W. K. (1998) Induction of growth inhibition of 293 cells by downregulation of the cyclin E and cyclin-dependent kinase 4 proteins due to overexpression of TIS21. *Molecular Carcinogenesis,* 23(1)**,** 25-35.

Lim, Y. C., Oh, S. Y., Cha, Y. Y., Kim, S. H., Jin, X. & Kim, H. (2011) Cancer stem cell traits in squamospheres derived from primary head and neck squamous cell carcinomas. *Oral Oncology,* 47(2)**,** 83-91.

Liu, K., Jiang, M., Lu, Y., Chen, H., Sun, J., Wu, S., Ku, W. Y., Nakagawa, H., Kita, Y., Natsugoe, S., Peters, J. H., Rustgi, A., Onaitis, M. W., Kiernan, A., Chen, X. & Que, J. (2013) Sox2 cooperates with inflammation-mediated Stat3 activation in the malignant transformation of foregut basal progenitor cells. *Cell Stem Cell,* 12(3)**,** 304-15.

Liu, T. C., Huang, C. J., Chu, Y. C., Wei, C. C., Chou, C. C., Chou, M. Y., Chou, C. K. & Yang, J. J. (2000a) Cloning and expression of ZAK, a mixed lineage kinase-like protein containing a leucine-zipper and a sterile-alpha motif. *Biochemical and Biophysical Research Communications,* 274(3)**,** 811-6.

Liu, Y. F., Dorow, D. & Marshall, J. (2000b) Activation of MLK2-mediated signaling cascades by polyglutamine-expanded huntingtin. *The Journal of Biological Chemistry,* 275(25)**,** 19035-40.

Long, G. V., Stroyakovskiy, D., Gogas, H., Levchenko, E., de Braud, F., Larkin, J., Garbe, C., Jouary, T., Hauschild, A., Grob, J. J., Chiarion Sileni, V., Lebbe, C., Mandala, M., Millward, M., Arance, A., Bondarenko, I., Haanen, J. B., Hansson, J., Utikal, J., Ferraresi, V., Kovalenko, N., Mohr, P., Probachai, V., Schadendorf, D., Nathan, P., Robert, C., Ribas, A., DeMarini, D. J., Irani, J. G., Casey, M., Ouellet, D., Martin, A. M., Le, N., Patel, K. & Flaherty, K. (2014) Combined BRAF and MEK inhibition versus BRAF inhibition alone in melanoma. *The New England Journal of Medicine,* 371(20)**,** 1877-88.

Lui, V. W., Hedberg, M. L., Li, H., Vangara, B. S., Pendleton, K., Zeng, Y., Lu, Y., Zhang, Q., Du, Y., Gilbert, B. R., Freilino, M., Sauerwein, S., Peyser, N. D., Xiao, D., Diergaarde, B., Wang, L., Chiosea, S., Seethala, R., Johnson, J. T., Kim, S., Duvvuri, U., Ferris, R. L., Romkes, M., Nukui, T., Kwok-Shing Ng, P., Garraway, L. A., Hammerman, P. S., Mills, G. B. & Grandis, J. R. (2013) Frequent Mutation of the PI3K Pathway in Head and Neck Cancer Defines Predictive Biomarkers. *Cancer Discovery,* 3(7)**,** 761-769.

Ma, Y. Y., Wei, S. J., Lin, Y. C., Lung, J. C., Chang, T. C., Whang-Peng, J., Liu, J. M., Yang, D. M., Yang, W. K. & Shen, C. Y. (2000) PIK3CA as an oncogene in cervical cancer. *Oncogene,* 19(23)**,** 2739-44.

Maeno, K., Masuda, A., Yanagisawa, K., Konishi, H., Osada, H., Saito, T., Ueda, R. & Takahashi, T. (2006) Altered regulation of c-jun and its involvement in anchorage-independent growth of human lung cancers. *Oncogene,* 25(2)**,** 271-7.

Mandelker, D., Gabelli, S. B., Schmidt-Kittler, O., Zhu, J., Cheong, I., Huang, C. H., Kinzler, K. W., Vogelstein, B. & Amzel, L. M. (2009) A frequent kinase domain mutation that changes the interaction between PI3Kalpha and the membrane. *Proceedings of the National Academy of Sciences of the United States of America,* 106(40)**,** 16996-7001.

Manning, B. D. & Cantley, L. C. (2007) AKT/PKB signaling: navigating downstream. *Cell,* 129(7)**,** 1261-74.

Mao, K. & Klionsky, D. J. (2011) AMPK activates autophagy by phosphorylating ULK1. *Circulation Research,* 108(7)**,** 787-8.

Maroney, A. C., Finn, J. P., Connors, T. J., Durkin, J. T., Angeles, T., Gessner, G., Xu, Z., Meyer, S. L., Savage, M. J., Greene, L. A., Scott, R. W. & Vaught, J. L. (2001) Cep-1347 (KT7515), a semisynthetic inhibitor of the mixed lineage kinase family. *The Journal of Biological Chemistry,* 276(27)**,** 25302-8.

Martini, M., Russo, M., Lamba, S., Vitiello, E., Crowley, E. H., Sassi, F., Romanelli, D., Frattini, M., Marchetti, A. & Bardelli, A. (2013) Mixed lineage kinase MLK4 is activated in colorectal cancers where it synergistically cooperates with activated RAS signaling in driving tumorigenesis. *Cancer Research,* 73(6)**,** 1912-21.

Marusiak, A. A., Edwards, Z. C., Hugo, W., Trotter, E. W., Girotti, M. R., Stephenson, N. L., Kong, X., Gartside, M. G., Fawdar, S., Hudson, A., Breitwieser, W., Hayward, N. K., Marais, R., Lo, R. S. & Brognard, J. (2014) Mixed lineage kinases activate MEK independently of RAF to mediate resistance to RAF inhibitors. *Nature Communications,* 5**,** 3901.

Masaki, M., Ikeda, A., Shiraki, E., Oka, S. & Kawasaki, T. (2003) Mixed lineage kinase LZK and antioxidant protein-1 activate NF-kappaB synergistically. *European Journal of Biochemistry / FEBS,* 270(1)**,** 76-83.

Mazumdar, T., Byers, L. A., Ng, P. K., Mills, G. B., Peng, S., Diao, L., Fan, Y. H., Stemke-Hale, K., Heymach, J. V., Myers, J. N., Glisson, B. S. & Johnson, F. M. (2014) A comprehensive evaluation of biomarkers predictive of response to PI3K inhibitors and of resistance mechanisms in head and neck squamous cell carcinoma. *Molecular Cancer Therapeutics,* 13(11)**,** 2738-50.

McCaughan, F., Pole, J. C., Bankier, A. T., Konfortov, B. A., Carroll, B., Falzon, M., Rabbitts, T. H., George, P. J., Dear, P. H. & Rabbitts, P. H. (2010) Progressive 3q amplification consistently targets SOX2 in preinvasive squamous lung cancer. *American Journal of Respiratory and Critical Care Medicine,* 182(1)**,** 83-91.

McKay, M. M. & Morrison, D. K. (2007) Integrating signals from RTKs to ERK/MAPK. *Oncogene,* 26(22)**,** 3113-21.

Medema, R. H., Kops, G. J., Bos, J. L. & Burgering, B. M. (2000) AFX-like Forkhead transcription factors mediate cell-cycle regulation by Ras and PKB through p27kip1. *Nature,* 404(6779)**,** 782-7.

Menzies, A. M. & Long, G. V. (2014) Dabrafenib and trametinib, alone and in combination for BRAF-mutant metastatic melanoma. *Clinical Cancer Research,* 20(8)**,** 2035-43.

Miao, B., Ji, Z., Tan, L., Taylor, M., Zhang, J., Choi, H. G., Frederick, D. T., Kumar, R., Wargo, J. A., Flaherty, K. T., Gray, N. S. & Tsao, H. (2015) EPHA2 is a mediator of vemurafenib resistance and a novel therapeutic target in melanoma. *Cancer Discovery,* 5(3)**,** 274-87.

Michaloglou, C., Vredeveld, L. C., Soengas, M. S., Denoyelle, C., Kuilman, T., van der Horst, C. M., Majoor, D. M., Shay, J. W., Mooi, W. J. & Peeper, D. S. (2005) BRAFE600-associated senescence-like cell cycle arrest of human naevi. *Nature,* 436(7051)**,** 720-4.

Mishra, P., Senthivinayagam, S., Rangasamy, V., Sondarva, G. & Rana, B. (2010) Mixed lineage kinase-3/JNK1 axis promotes migration of human gastric cancer cells following gastrin stimulation. *Molecular Endocrinology,* 24(3)**,** 598-607.

Mishra, R., Barthwal, M. K., Sondarva, G., Rana, B., Wong, L., Chatterjee, M., Woodgett, J. R. & Rana, A. (2007) Glycogen synthase kinase-3beta induces neuronal cell death via direct phosphorylation of mixed lineage kinase 3. *The Journal of Biological Chemistry,* 282(42)**,** 30393-405.

Molinolo, A. A., Marsh, C., El Dinali, M., Gangane, N., Jennison, K., Hewitt, S., Patel, V., Seiwert, T. Y. & Gutkind, J. S. (2012) mTOR as a molecular target in HPV-associated oral and cervical squamous carcinomas. *Clinical Cancer Research,* 18(9)**,** 2558-68.

Montagut, C., Sharma, S. V., Shioda, T., McDermott, U., Ulman, M., Ulkus, L. E., Dias-Santagata, D., Stubbs, H., Lee, D. Y., Singh, A., Drew, L., Haber, D. A. & Settleman, J. (2008) Elevated CRAF as a potential mechanism of acquired resistance to BRAF inhibition in melanoma. *Cancer Research,* 68(12)**,** 4853-61.

Mooi, W. J. & Peeper, D. S. (2006) Oncogene-induced cell senescence--halting on the road to cancer. *The New England Journal of Medicine,* 355(10)**,** 1037-46.

Morris, E. J., Jha, S., Restaino, C. R., Dayananth, P., Zhu, H., Cooper, A., Carr, D., Deng, Y., Jin, W., Black, S., Long, B., Liu, J., Dinunzio, E., Windsor, W., Zhang, R., Zhao, S., Angagaw, M. H., Pinheiro, E. M., Desai, J., Xiao, L., Shipps, G., Hruza, A., Wang, J., Kelly, J., Paliwal, S., Gao, X., Babu, B. S., Zhu, L., Daublain, P., Zhang, L., Lutterbach, B. A., Pelletier, M. R., Philippar, U., Siliphaivanh, P., Witter, D., Kirschmeier, P., Bishop, W. R., Hicklin, D., Gilliland, D. G., Jayaraman, L., Zawel, L., Fawell, S. & Samatar, A. A. (2013) Discovery of a novel ERK inhibitor with activity in models of acquired resistance to BRAF and MEK inhibitors. *Cancer Discovery,* 3(7)**,** 742-50.

Muller, P. A. & Vousden, K. H. (2013) p53 mutations in cancer. *Nature Cell Biology,* 15(1)**,** 2-8.

Nazarian, R., Shi, H., Wang, Q., Kong, X., Koya, R. C., Lee, H., Chen, Z., Lee, M. K., Attar, N., Sazegar, H., Chodon, T., Nelson, S. F., McArthur, G., Sosman, J. A., Ribas, A. & Lo, R. S. (2010) Melanomas acquire resistance to B-RAF(V600E) inhibition by RTK or N-RAS upregulation. *Nature,* 468(7326)**,** 973-7.

Nheu, T. V., He, H., Hirokawa, Y., Tamaki, K., Florin, L., Schmitz, M. L., Suzuki-Takahashi, I., Jorissen, R. N., Burgess, A. W., Nishimura, S., Wood, J. & Maruta, H. (2002) The K252a derivatives, inhibitors for the PAK/MLK kinase family selectively block the growth of RAS transformants. *Cancer Journal,* 8(4)**,** 328-36.

Nihalani, D., Merritt, S. & Holzman, L. B. (2000) Identification of structural and functional domains in mixed lineage kinase dual leucine zipper-bearing kinase required for complex formation and stress-activated protein kinase activation. *The Journal of Biological Chemistry,* 275(10)**,** 7273-9.

Nihalani, D., Meyer, D., Pajni, S. & Holzman, L. B. (2001) Mixed lineage kinase-dependent JNK activation is governed by interactions of scaffold protein JIP with MAPK module components. *The EMBO Journal,* 20(13)**,** 3447-58.

Nottingham, L. K., Yan, C. H., Yang, X., Si, H., Coupar, J., Bian, Y., Cheng, T. F., Allen, C., Arun, P., Gius, D., Dang, L., Van Waes, C. & Chen, Z. (2014) Aberrant IKKα and IKKβ cooperatively activate NF-κB and induce EGFR/AP1 signaling to promote survival and migration of head and neck cancer. *Oncogene,* 33(9)**,** 1135-47.

O-charoenrat, P., Sarkaria, I., Talbot, S. G., Reddy, P., Dao, S., Ngai, I., Shaha, A., Kraus, D., Shah, J., Rusch, V., Ramanathan, Y. & Singh, B. (2008) SCCRO (DCUN1D1) induces extracellular matrix invasion by activating matrix metalloproteinase 2. *Clinical Cancer Research,* 14(21)**,** 6780-9.

Oren, M. & Rotter, V. (2010) Mutant p53 gain-of-function in cancer. *Cold Spring Harbor Perspectives in Biology,* 2(2)**,** a001107.

Ota, I., Okamoto, N., Yane, K., Takahashi, A., Masui, T., Hosoi, H. & Ohnishi, T. (2012) Therapeutic strategies for head and neck cancer based on p53 status. *Experimental and Therapeutic Medicine,* 3(4)**,** 585-591.

Oya, E., Ovrevik, J., Arlt, V. M., Nagy, E., Phillips, D. H. & Holme, J. A. (2011) DNA damage and DNA damage response in human bronchial epithelial BEAS-2B cells following exposure to 2-nitrobenzanthrone and 3-nitrobenzanthrone: role in apoptosis. *Mutagenesis,* 26(6)**,** 697-708.

Packer, L. M., Rana, S., Hayward, R., O'Hare, T., Eide, C. A., Rebocho, A., Heidorn, S., Zabriskie, M. S., Niculescu-Duvaz, I., Druker, B. J., Springer, C. & Marais, R. (2011) Nilotinib and MEK inhibitors induce synthetic lethality through paradoxical activation of RAF in drug-resistant chronic myeloid leukemia. *Cancer Cell,* 20(6)**,** 715-27.

Paraiso, K. H., Xiang, Y., Rebecca, V. W., Abel, E. V., Chen, Y. A., Munko, A. C., Wood, E., Fedorenko, I. V., Sondak, V. K., Anderson, A. R., Ribas, A., Palma, M. D., Nathanson, K. L., Koomen, J. M., Messina, J. L. & Smalley, K. S. (2011) PTEN loss confers BRAF inhibitor resistance to melanoma cells through the suppression of BIM expression. *Cancer Research,* 71(7)**,** 2750-60.

Park, Y. H., Kim, D., Dai, J. & Zhang, Z. (2015) Human bronchial epithelial BEAS-2B cells, an appropriate in vitro model to study heavy metals induced carcinogenesis. *Toxicology and Applied Pharmacology,* 287(3)**,** 240-5.

Parkin, D. M., Bray, F., Ferlay, J. & Pisani, P. (2005) Global cancer statistics, 2002. *CA: A Cancer Journal for Clinicians,* 55(2)**,** 74-108.

Parkinson Study Group PRECEPT Investigators. (2007) Mixed lineage kinase inhibitor CEP-1347 fails to delay disability in early Parkinson disease. *Neurology,* 69(15)**,** 1480-90.

Patel, S., Cohen, F., Dean, B. J., De La Torre, K., Deshmukh, G., Estrada, A. A., Ghosh, A. S., Gibbons, P., Gustafson, A., Huestis, M. P., Le Pichon, C. E., Lin, H., Liu, W., Liu, X., Liu, Y., Ly, C. Q., Lyssikatos, J. P., Ma, C., Scearce-Levie, K., Shin, Y. G., Solanoy, H., Stark, K. L., Wang, J., Wang, B., Zhao, X., Lewcock, J. W. & Siu, M. (2015) Discovery of dual leucine zipper kinase (DLK, MAP3K12) inhibitors with activity in neurodegeneration models. *Journal of Medicinal Chemistry,* 58(1)**,** 401-18.

Phelan, D. R., Price, G., Liu, Y. F. & Dorow, D. S. (2001) Activated JNK phosphorylates the c-terminal domain of MLK2 that is required for MLK2-induced apoptosis. *The Journal of Biological Chemistry,* 276(14)**,** 10801-10.

Poitras, L., Bisson, N., Islam, N. & Moss, T. (2003) A tissue restricted role for the Xenopus Jun N-terminal kinase kinase kinase MLK2 in cement gland and pronephric tubule differentiation. *Developmental Biology,* 254(2)**,** 200-14.

Poulikakos, P. I., Persaud, Y., Janakiraman, M., Kong, X., Ng, C., Moriceau, G., Shi, H., Atefi, M., Titz, B., Gabay, M. T., Salton, M., Dahlman, K. B., Tadi, M., Wargo, J. A., Flaherty, K. T., Kelley, M. C., Misteli, T., Chapman, P. B., Sosman, J. A., Graeber, T. G., Ribas, A., Lo, R. S., Rosen, N. & Solit, D. B. (2011) RAF inhibitor resistance is mediated by dimerization of aberrantly spliced BRAF(V600E). *Nature,* 480(7377)**,** 387-90.

Poulikakos, P. I., Zhang, C., Bollag, G., Shokat, K. M. & Rosen, N. (2010) RAF inhibitors transactivate RAF dimers and ERK signalling in cells with wild-type BRAF. *Nature,* 464(7287)**,** 427-30.

Pozniak, C. D., Sengupta Ghosh, A., Gogineni, A., Hanson, J. E., Lee, S. H., Larson, J. L., Solanoy, H., Bustos, D., Li, H., Ngu, H., Jubb, A. M., Ayalon, G., Wu, J., Scearce-Levie, K., Zhou, Q., Weimer, R. M., Kirkpatrick, D. S. & Lewcock, J. W. (2013) Dual leucine zipper kinase is required for excitotoxicity-induced neuronal degeneration. *The Journal of Experimental Medicine,* 210(12)**,** 2553-67.

Prahallad, A., Sun, C., Huang, S., Di Nicolantonio, F., Salazar, R., Zecchin, D., Beijersbergen, R. L., Bardelli, A. & Bernards, R. (2012) Unresponsiveness of colon cancer to BRAF(V600E) inhibition through feedback activation of EGFR. *Nature,* 483(7387)**,** 100-3.

Prat, A., Adamo, B., Fan, C., Peg, V., Vidal, M., Galvan, P., Vivancos, A., Nuciforo, P., Palmer, H. G., Dawood, S., Rodon, J., Ramon y Cajal, S., Del Campo, J. M., Felip, E., Tabernero, J. & Cortes, J. (2013) Genomic analyses across six cancer types identify basal-like breast cancer as a unique molecular entity. *Scientific Reports,* 3**,** 3544.

Prat, A., Parker, J. S., Karginova, O., Fan, C., Livasy, C., Herschkowitz, J. I., He, X. & Perou, C. M. (2010) Phenotypic and molecular characterization of the claudin-low intrinsic subtype of breast cancer. *Breast Cancer Research,* 12(5)**,** R68.

Qian, J. & Massion, P. P. (2008) Role of chromosome 3q amplification in lung cancer. *Journal of Thoracic Oncology,* 3(3)**,** 212-5.

Ramsey, M. R., He, L., Forster, N., Ory, B. & Ellisen, L. W. (2011) Physical association of HDAC1 and HDAC2 with p63 mediates transcriptional repression and tumor maintenance in squamous cell carcinoma. *Cancer Research,* 71(13)**,** 4373-9.

Ramsey, M. R., Wilson, C., Ory, B., Rothenberg, S. M., Faquin, W., Mills, A. A. & Ellisen, L. W. (2013) FGFR2 signaling underlies p63 oncogenic function in squamous cell carcinoma. *The Journal of Clinical Investigation*.

Rana, A., Gallo, K., Godowski, P., Hirai, S., Ohno, S., Zon, L., Kyriakis, J. M. & Avruch, J. (1996) The mixed lineage kinase SPRK phosphorylates and activates the stress-activated protein kinase activator, SEK-1. *The Journal of Biological Chemistry,* 271(32)**,** 19025-8.

Rana, A., Rana, B., Mishra, R., Sondarva, G., Rangasamy, V., Das, S., Viswakarma, N. & Kanthasamy, A. (2013) Mixed Lineage Kinase-c-Jun N-Terminal Kinase Axis: A Potential Therapeutic Target in Cancer. *Genes & Cancer,* 4(9-10)**,** 334-41.

Rangasamy, V., Mishra, R., Sondarva, G., Das, S., Lee, T. H., Bakowska, J. C., Tzivion, G., Malter, J. S., Rana, B., Lu, K. P., Kanthasamy, A. & Rana, A. (2012) Mixed-lineage kinase 3 phosphorylates prolyl-isomerase Pin1 to regulate its nuclear translocation and cellular function. *Proceedings of the National Academy of Sciences of the United States of America,* 109(21)**,** 8149-54.

Rashid, T., Banerjee, M. & Nikolic, M. (2001) Phosphorylation of Pak1 by the p35/Cdk5 kinase affects neuronal morphology. *The Journal of Biological Chemistry,* 276(52)**,** 49043-52.

Reddel, R. R., De Silva, R., Duncan, E. L., Rogan, E. M., Whitaker, N. J., Zahra, D. G., Ke, Y., McMenamin, M. G., Gerwin, B. I. & Harris, C. C. (1995) SV40-induced immortalization and ras-transformation of human bronchial epithelial cells. *International Journal of Cancer,* 61(2)**,** 199-205.

Reddel, R. R., Ke, Y., Gerwin, B. I., McMenamin, M. G., Lechner, J. F., Su, R. T., Brash, D. E., Park, J. B., Rhim, J. S. & Harris, C. C. (1988) Transformation of human bronchial epithelial cells by infection with SV40 or adenovirus-12 SV40 hybrid virus, or transfection via strontium phosphate coprecipitation with a plasmid containing SV40 early region genes. *Cancer Research,* 48(7)**,** 1904-9.

Redon, R., Muller, D., Caulee, K., Wanherdrick, K., Abecassis, J. & du Manoir, S. (2001) A simple specific pattern of chromosomal aberrations at early stages of head and neck squamous cell carcinomas: PIK3CA but not p63 gene as a likely target of 3q26-qter gains. *Cancer Research,* 61(10)**,** 4122-9.

Ribas, A., Gonzalez, R., Pavlick, A., Hamid, O., Gajewski, T. F., Daud, A., Flaherty, L., Logan, T., Chmielowski, B., Lewis, K., Kee, D., Boasberg, P., Yin, M., Chan, I., Musib, L., Choong, N., Puzanov, I. & McArthur, G. A. (2014) Combination of vemurafenib and cobimetinib in patients with advanced BRAF(V600)-mutated melanoma: a phase 1b study. *Lancet Oncology,* 15(9)**,** 954-65.

Rizos, H., Menzies, A. M., Pupo, G. M., Carlino, M. S., Fung, C., Hyman, J., Haydu, L. E., Mijatov, B., Becker, T. M., Boyd, S. C., Howle, J., Saw, R., Thompson, J. F., Kefford, R. F., Scolyer, R. A. & Long, G. V. (2014) BRAF inhibitor resistance mechanisms in metastatic melanoma: spectrum and clinical impact. *Clinical Cancer Research,* 20(7)**,** 1965-77.

Robert, C., Karaszewska, B., Schachter, J., Rutkowski, P., Mackiewicz, A., Stroiakovski, D., Lichinitser, M., Dummer, R., Grange, F., Mortier, L., Chiarion-Sileni, V., Drucis, K., Krajsova, I., Hauschild, A., Lorigan, P., Wolter, P., Long, G. V., Flaherty, K., Nathan, P., Ribas, A., Martin, A. M., Sun, P., Crist, W., Legos, J., Rubin, S. D., Little, S. M. & Schadendorf, D. (2015) Improved overall survival in melanoma with combined dabrafenib and trametinib. *The New England Journal of Medicine,* 372(1)**,** 30-9.

Rocco, J. W., Leong, C. O., Kuperwasser, N., DeYoung, M. P. & Ellisen, L. W. (2006) p63 mediates survival in squamous cell carcinoma by suppression of p73-dependent apoptosis. *Cancer Cell,* 9(1)**,** 45-56.

Sabbatino, F., Wang, Y., Wang, X., Flaherty, K. T., Yu, L., Pepin, D., Scognamiglio, G., Pepe, S., Kirkwood, J. M., Cooper, Z. A., Frederick, D. T., Wargo, J. A., Ferrone, S. & Ferrone, C. R. (2014) PDGFRalpha up-regulation mediated by sonic hedgehog pathway activation leads to BRAF inhibitor resistance in melanoma cells with BRAF mutation. *Oncotarget,* 5(7)**,** 1926-41.

Sakuma, H., Ikeda, A., Oka, S., Kozutsumi, Y., Zanetta, J. P. & Kawasaki, T. (1997) Molecular cloning and functional expression of a cDNA encoding a new member of mixed lineage protein kinase from human brain. *The Journal of Biological Chemistry,* 272(45)**,** 28622-9.

Samman, M., Wood, H., Conway, C., Berri, S., Pentenero, M., Gandolfo, S., Cassenti, A., Cassoni, P., Al Ajlan, A., Barrett, A. W., Chengot, P., MacLennan, K., High, A. S. & Rabbitts, P. (2014) Next-generation sequencing analysis for detecting human papillomavirus in oral verrucous carcinoma. *Oral Surgery, Oral Medicine, Oral Pathology and Oral Radiology,* 118(1)**,** 117-125 e1.

Sano, D., Xie, T. X., Ow, T. J., Zhao, M., Pickering, C. R., Zhou, G., Sandulache, V. C., Wheeler, D. A., Gibbs, R. A., Caulin, C. & Myers, J. N. (2011) Disruptive TP53 mutation

is associated with aggressive disease characteristics in an orthotopic murine model of oral tongue cancer. *Clinical Cancer Research,* 17(21)**,** 6658-70.

Sarbassov, D. D., Guertin, D. A., Ali, S. M. & Sabatini, D. M. (2005) Phosphorylation and regulation of Akt/PKB by the rictor-mTOR complex. *Science,* 307(5712)**,** 1098-101.

Sarkaria, I., P, O. c., Talbot, S. G., Reddy, P. G., Ngai, I., Maghami, E., Patel, K. N., Lee, B., Yonekawa, Y., Dudas, M., Kaufman, A., Ryan, R., Ghossein, R., Rao, P. H., Stoffel, A., Ramanathan, Y. & Singh, B. (2006) Squamous cell carcinoma related oncogene/DCUN1D1 is highly conserved and activated by amplification in squamous cell carcinomas. *Cancer Research,* 66(19)**,** 9437-44.

Sathyanarayana, P., Barthwal, M. K., Kundu, C. N., Lane, M. E., Bergmann, A., Tzivion, G. & Rana, A. (2002) Activation of the Drosophila MLK by ceramide reveals TNF-alpha and ceramide as agonists of mammalian MLK3. *Molecular Cell,* 10(6)**,** 1527-33.

Scansite. (2012) *Scansite Motif Scanner* [Online]. Available: http://scansite.mit.edu/ [Accessed 27th June 2012].

Schachter, K. A., Du, Y., Lin, A. & Gallo, K. A. (2006) Dynamic positive feedback phosphorylation of mixed lineage kinase 3 by JNK reversibly regulates its distribution to Triton-soluble domains. *The Journal of Biological Chemistry,* 281(28)**,** 19134-44.

Schröck, A., Bode, M., Göke, F. J., Bareiss, P. M., Schairer, R., Wang, H., Weichert, W., Franzen, A., Kirsten, R., van Bremen, T., Queisser, A., Kristiansen, G., Heasley, L., Bootz, F., Lengerke, C. & Perner, S. (2014) Expression and role of the embryonic protein SOX2 in head and neck squamous cell carcinoma. *Carcinogenesis,* 35(7)**,** 1636-42.

Scian, M. J., Stagliano, K. E., Deb, D., Ellis, M. A., Carchman, E. H., Das, A., Valerie, K., Deb, S. P. & Deb, S. (2004a) Tumor-derived p53 mutants induce oncogenesis by transactivating growth-promoting genes. *Oncogene,* 23(25)**,** 4430-43.

Scian, M. J., Stagliano, K. E., Ellis, M. A., Hassan, S., Bowman, M., Miles, M. F., Deb, S. P. & Deb, S. (2004b) Modulation of gene expression by tumor-derived p53 mutants. *Cancer Research,* 64(20)**,** 7447-54.

Serrano, M., Lin, A. W., McCurrach, M. E., Beach, D. & Lowe, S. W. (1997) Oncogenic ras provokes premature cell senescence associated with accumulation of p53 and p16INK4a. *Cell,* 88(5)**,** 593-602.

Shackelford, D. B. & Shaw, R. J. (2009) The LKB1-AMPK pathway: metabolism and growth control in tumour suppression. *Nature Reviews Cancer,* 9(8)**,** 563-75.

Shao, Y. & Aplin, A. E. (2010) Akt3-mediated resistance to apoptosis in B-RAF-targeted melanoma cells. *Cancer Research,* 70(16)**,** 6670-81.

Shayesteh, L., Lu, Y., Kuo, W. L., Baldocchi, R., Godfrey, T., Collins, C., Pinkel, D., Powell, B., Mills, G. B. & Gray, J. W. (1999) PIK3CA is implicated as an oncogene in ovarian cancer. *Nature Genetics,* 21(1)**,** 99-102.

Shen, L. C., Chen, Y. K., Lin, L. M. & Shaw, S. Y. (2010) Anti-invasion and anti-tumor growth effect of doxycycline treatment for human oral squamous-cell carcinoma--in vitro and in vivo studies. *Oral Oncology,* 46(3)**,** 178-84.

Sherr, C. J. & McCormick, F. (2002) The RB and p53 pathways in cancer. *Cancer Cell,* 2(2)**,** 103-12.

Singh, B., Gogineni, S. K., Sacks, P. G., Shaha, A. R., Shah, J. P., Stoffel, A. & Rao, P. H. (2001) Molecular cytogenetic characterization of head and neck squamous cell carcinoma and refinement of 3q amplification. *Cancer Research,* 61(11)**,** 4506-13.

Singh, B., Reddy, P. G., Goberdhan, A., Walsh, C., Dao, S., Ngai, I., Chou, T. C., P, O. C., Levine, A. J., Rao, P. H. & Stoffel, A. (2002) p53 regulates cell survival by inhibiting PIK3CA in squamous cell carcinomas. *Genes & Development,* 16(8)**,** 984-93.

Solomon, H., Buganim, Y., Kogan-Sakin, I., Pomeraniec, L., Assia, Y., Madar, S., Goldstein, I., Brosh, R., Kalo, E., Beatus, T., Goldfinger, N. & Rotter, V. (2012) Various p53 mutant proteins differently regulate the Ras circuit to induce a cancer-related gene signature. *Journal of Cell Science,* 125(Pt 13)**,** 3144-52.

Sosman, J. A., Kim, K. B., Schuchter, L., Gonzalez, R., Pavlick, A. C., Weber, J. S., McArthur, G. A., Hutson, T. E., Moschos, S. J., Flaherty, K. T., Hersey, P., Kefford, R., Lawrence, D., Puzanov, I., Lewis, K. D., Amaravadi, R. K., Chmielowski, B., Lawrence, H. J., Shyr, Y., Ye, F., Li, J., Nolop, K. B., Lee, R. J., Joe, A. K. & Ribas, A. (2012) Survival in BRAF V600-mutant advanced melanoma treated with vemurafenib. *The New England Journal of Medicine,* 366(8)**,** 707-14.

Sparano, A., Quesnelle, K. M., Kumar, M. S., Wang, Y., Sylvester, A. J., Feldman, M., Sewell, D. A., Weinstein, G. S. & Brose, M. S. (2006) Genome-wide profiling of oral squamous cell carcinoma by array-based comparative genomic hybridization. *The Laryngoscope,* 116(5)**,** 735-41.

Stark, M. S., Woods, S. L., Gartside, M. G., Bonazzi, V. F., Dutton-Regester, K., Aoude, L. G., Chow, D., Sereduk, C., Niemi, N. M., Tang, N., Ellis, J. J., Reid, J., Zismann, V., Tyagi, S., Muzny, D., Newsham, I., Wu, Y., Palmer, J. M., Pollak, T., Youngkin, D., Brooks, B. R., Lanagan, C., Schmidt, C. W., Kobe, B., MacKeigan, J. P., Yin, H., Brown, K. M., Gibbs, R., Trent, J. & Hayward, N. K. (2012) Frequent somatic mutations in MAP3K5 and MAP3K9 in metastatic melanoma identified by exome sequencing. *Nature Genetics,* 44(2)**,** 165-9.

Stephens, P. J., Tarpey, P. S., Davies, H., Van Loo, P., Greenman, C., Wedge, D. C., Nik-Zainal, S., Martin, S., Varela, I., Bignell, G. R., Yates, L. R., Papaemmanuil, E., Beare, D., Butler, A., Cheverton, A., Gamble, J., Hinton, J., Jia, M., Jayakumar, A., Jones, D., Latimer, C., Lau, K. W., McLaren, S., McBride, D. J., Menzies, A., Mudie, L., Raine, K., Rad, R., Chapman, M. S., Teague, J., Easton, D., Langerod, A., Lee, M. T., Shen, C. Y., Tee, B. T., Huimin, B. W., Broeks, A., Vargas, A. C., Turashvili, G., Martens, J., Fatima, A., Miron, P., Chin, S. F., Thomas, G., Boyault, S., Mariani, O., Lakhani, S. R., van de Vijver, M., van 't Veer, L., Foekens, J., Desmedt, C., Sotiriou, C., Tutt, A., Caldas, C., Reis-Filho, J. S., Aparicio, S. A., Salomon, A. V., Borresen-Dale, A. L., Richardson, A. L., Campbell, P. J., Futreal, P. A. & Stratton, M. R. (2012) The landscape of cancer genes and mutational processes in breast cancer. *Nature,* 486(7403)**,** 400-4.

Straussman, R., Morikawa, T., Shee, K., Barzily-Rokni, M., Qian, Z. R., Du, J., Davis, A., Mongare, M. M., Gould, J., Frederick, D. T., Cooper, Z. A., Chapman, P. B., Solit, D. B., Ribas, A., Lo, R. S., Flaherty, K. T., Ogino, S., Wargo, J. A. & Golub, T. R. (2012) Tumour micro-environment elicits innate resistance to RAF inhibitors through HGF secretion. *Nature,* 487(7408)**,** 500-4.

Stronach, B. & Perrimon, N. (2002) Activation of the JNK pathway during dorsal closure in Drosophila requires the mixed lineage kinase, slipper. *Genes & Development,* 16(3)**,** 377-87.

Su, F., Bradley, W. D., Wang, Q., Yang, H., Xu, L., Higgins, B., Kolinsky, K., Packman, K., Kim, M. J., Trunzer, K., Lee, R. J., Schostack, K., Carter, J., Albert, T., Germer, S., Rosinski, J., Martin, M., Simcox, M. E., Lestini, B., Heimbrook, D. & Bollag, G. (2012a) Resistance to selective BRAF inhibition can be mediated by modest upstream pathway activation. *Cancer Research,* 72(4)**,** 969-78.

Su, F., Viros, A., Milagre, C., Trunzer, K., Bollag, G., Spleiss, O., Reis-Filho, J. S., Kong, X., Koya, R. C., Flaherty, K. T., Chapman, P. B., Kim, M. J., Hayward, R., Martin, M., Yang, H., Wang, Q., Hilton, H., Hang, J. S., Noe, J., Lambros, M., Geyer, F., Dhomen, N., Niculescu-Duvaz, I., Zambon, A., Niculescu-Duvaz, D., Preece, N., Robert, L., Otte, N. J., Mok, S., Kee, D., Ma, Y., Zhang, C., Habets, G., Burton, E. A., Wong, B., Nguyen, H., Kockx, M., Andries, L., Lestini, B., Nolop, K. B., Lee, R. J., Joe, A. K., Troy, J. L., Gonzalez, R., Hutson, T. E., Puzanov, I., Chmielowski, B., Springer, C. J., McArthur, G. A., Sosman, J. A., Lo, R. S., Ribas, A. & Marais, R. (2012b) RAS mutations in cutaneous squamous-cell carcinomas in patients treated with BRAF inhibitors. *The New England Journal of Medicine,* 366(3)**,** 207-15.

Suh, Y., Amelio, I., Guerrero Urbano, T. & Tavassoli, M. (2014) Clinical update on cancer: molecular oncology of head and neck cancer. *Cell Death & Disease,* 5**,** e1018.

Suh, Y. A., Post, S. M., Elizondo-Fraire, A. C., Maccio, D. R., Jackson, J. G., El-Naggar, A. K., Van Pelt, C., Terzian, T. & Lozano, G. (2011) Multiple stress signals activate mutant p53 in vivo. *Cancer Research,* 71(23)**,** 7168-75.

Sun, C., Wang, L., Huang, S., Heynen, G. J., Prahallad, A., Robert, C., Haanen, J., Blank, C., Wesseling, J., Willems, S. M., Zecchin, D., Hobor, S., Bajpe, P. K., Lieftink, C., Mateus, C., Vagner, S., Grernrum, W., Hofland, I., Schlicker, A., Wessels, L. F., Beijersbergen, R. L., Bardelli, A., Di Nicolantonio, F., Eggermont, A. M. & Bernards, R. (2014) Reversible and adaptive resistance to BRAF(V600E) inhibition in melanoma. *Nature,* 508(7494)**,** 118-22.

Swenson, K. I., Winkler, K. E. & Means, A. R. (2003) A new identity for MLK3 as an NIMA-related, cell cycle-regulated kinase that is localized near centrosomes and influences microtubule organization. *Molecular Biology of the Cell,* 14(1)**,** 156-72.

Swenson-Fields, K. I., Sandquist, J. C., Rossol-Allison, J., Blat, I. C., Wennerberg, K., Burridge, K. & Means, A. R. (2008) MLK3 limits activated Galphaq signaling to Rho by binding to p63RhoGEF. *Molecular Cell,* 32(1)**,** 43-56.

Tedeschi, A. & Bradke, F. (2013) The DLK signalling pathway--a double-edged sword in neural development and regeneration. *EMBO Reports,* 14(7)**,** 605-14.

Teramoto, H., Coso, O. A., Miyata, H., Igishi, T., Miki, T. & Gutkind, J. S. (1996) Signaling from the small GTP-binding proteins Rac1 and Cdc42 to the c-Jun N-terminal kinase/stress-activated protein kinase pathway. A role for mixed lineage kinase 3/protein-tyrosine kinase 1, a novel member of the mixed lineage kinase family. *The Journal of Biological Chemistry,* 271(44)**,** 27225-8.

Terzian, T., Suh, Y. A., Iwakuma, T., Post, S. M., Neumann, M., Lang, G. A., Van Pelt, C. S. & Lozano, G. (2008) The inherent instability of mutant p53 is alleviated by Mdm2 or p16INK4a loss. *Genes & Development,* 22(10)**,** 1337-44.

Thorpe, L. M., Yuzugullu, H. & Zhao, J. J. (2015) PI3K in cancer: divergent roles of isoforms, modes of activation and therapeutic targeting. *Nature Reviews Cancer,* 15(1)**,** 7-24.

Thylur, R. P., Senthivinayagam, S., Campbell, E. M., Rangasamy, V., Thorenoor, N., Sondarva, G., Mehrotra, S., Mishra, P., Zook, E., Le, P. T., Rana, A. & Rana, B. (2011) Mixed Lineage Kinase 3 Modulates {beta}-Catenin Signaling in Cancer Cells. *The Journal of Biological Chemistry,* 286(43)**,** 37470-82.

Tibbles, L. A., Ing, Y. L., Kiefer, F., Chan, J., Iscove, N., Woodgett, J. R. & Lassam, N. J. (1996) MLK-3 activates the SAPK/JNK and p38/RK pathways via SEK1 and MKK3/6. *The EMBO Journal,* 15(24)**,** 7026-35.

Tjia, W. M., Sham, J. S., Hu, L., Tai, A. L. & Guan, X. Y. (2005) Characterization of 3p, 5p, and 3q in two nasopharyngeal carcinoma cell lines, using region-specific multiplex fluorescence in situ hybridization probes. *Cancer Genetics and Cytogenetics,* 158(1)**,** 61-6.

Tournier, C. (2013) The 2 Faces of JNK Signaling in Cancer. *Genes & Cancer,* 4(9-10)**,** 397-400.

Tuma, R. S. (2011) Getting around PLX4032: studies turn up unusual mechanisms of resistance to melanoma drug. *Journal of the National Cancer Institute,* 103(3)**,** 170-1, 177.

Udayakumar, D., Zhang, G., Ji, Z., Njauw, C. N., Mroz, P. & Tsao, H. (2011) EphA2 is a critical oncogene in melanoma. *Oncogene,* 30(50)**,** 4921-9.

Vacratsis, P. O., Phinney, B. S., Gage, D. A. & Gallo, K. A. (2002) Identification of in vivo phosphorylation sites of MLK3 by mass spectrometry and phosphopeptide mapping. *Biochemistry,* 41(17)**,** 5613-24.

Velho, S., Oliveira, C., Paredes, J., Sousa, S., Leite, M., Matos, P., Milanezi, F., Ribeiro, A. S., Mendes, N., Licastro, D., Karhu, A., Oliveira, M. J., Ligtenberg, M., Hamelin, R., Carneiro, F., Lindblom, A., Peltomaki, P., Castedo, S., Schwartz, S., Jr., Jordan, P., Aaltonen, L. A., Hofstra, R. M., Suriano, G., Stupka, E., Fialho, A. M. & Seruca, R. (2010) Mixed lineage kinase 3 gene mutations in mismatch repair deficient gastrointestinal tumours. *Human Molecular Genetics,* 19(4)**,** 697-706.

Vermorken, J. B., Trigo, J., Hitt, R., Koralewski, P., Diaz-Rubio, E., Rolland, F., Knecht, R., Amellal, N., Schueler, A. & Baselga, J. (2007) Open-label, uncontrolled, multicenter phase II study to evaluate the efficacy and toxicity of cetuximab as a single agent in patients with recurrent and/or metastatic squamous cell carcinoma of the head and neck who failed to respond to platinum-based therapy. *Journal of Clinical Oncology,* 25(16)**,** 2171-7.

Vikhanskaya, F., Lee, M. K., Mazzoletti, M., Broggini, M. & Sabapathy, K. (2007) Cancer-derived p53 mutants suppress p53-target gene expression--potential mechanism for gain of function of mutant p53. *Nucleic Acids Research,* 35(6)**,** 2093-104.

Villanueva, J., Vultur, A., Lee, J. T., Somasundaram, R., Fukunaga-Kalabis, M., Cipolla, A. K., Wubbenhorst, B., Xu, X., Gimotty, P. A., Kee, D., Santiago-Walker, A. E., Letrero, R., D'Andrea, K., Pushparajan, A., Hayden, J. E., Brown, K. D., Laquerre, S., McArthur, G. A., Sosman, J. A., Nathanson, K. L. & Herlyn, M. (2010) Acquired resistance to BRAF inhibitors mediated by a RAF kinase switch in melanoma can be overcome by cotargeting MEK and IGF-1R/PI3K. *Cancer Cell,* 18(6)**,** 683-95.

Wagner, E. F. & Nebreda, A. R. (2009) Signal integration by JNK and p38 MAPK pathways in cancer development. *Nature Reviews Cancer,* 9(8)**,** 537-49.

Waldmeier, P., Bozyczko-Coyne, D., Williams, M. & Vaught, J. L. (2006) Recent clinical failures in Parkinson's disease with apoptosis inhibitors underline the need for a paradigm shift in drug discovery for neurodegenerative diseases. *Biochemical Pharmacology,* 72(10)**,** 1197-206.

Wang, H., Daouti, S., Li, W. H., Wen, Y., Rizzo, C., Higgins, B., Packman, K., Rosen, N., Boylan, J. F., Heimbrook, D. & Niu, H. (2011) Identification of the MEK1(F129L) activating mutation as a potential mechanism of acquired resistance to MEK inhibition in human cancers carrying the B-RafV600E mutation. *Cancer Research,* 71(16)**,** 5535-45.

Wang, X. & Simon, R. (2013) Identification of potential synthetic lethal genes to p53 using a computational biology approach. *BMC Medical Genomics,* 6**,** 30.

Ward, R. A., Colclough, N., Challinor, M., Debreczeni, J. E., Eckersley, K., Fairley, G., Feron, L., Flemington, V., Graham, M. A., Greenwood, R., Hopcroft, P., Howard, T. D., James, M., Jones, C. D., Jones, C. R., Renshaw, J., Roberts, K., Snow, L., Tonge, M. & Yeung, K. (2015) Structure-Guided Design of Highly Selective and Potent Covalent Inhibitors of ERK1/2. *Journal of Medicinal Chemistry,* 58(11)**,** 4790-801.

Watanabe, H., Ma, Q., Peng, S., Adelmant, G., Swain, D., Song, W., Fox, C., Francis, J. M., Pedamallu, C. S., DeLuca, D. S., Brooks, A. N., Wang, S., Que, J., Rustgi, A. K., Wong, K. K., Ligon, K. L., Liu, X. S., Marto, J. A., Meyerson, M. & Bass, A. J. (2014) SOX2 and p63 colocalize at genetic loci in squamous cell carcinomas. *Journal of Clinical Investigation,* 124(4)**,** 1636-45.

Watkins, T. A., Wang, B., Huntwork-Rodriguez, S., Yang, J., Jiang, Z., Eastham-Anderson, J., Modrusan, Z., Kaminker, J. S., Tessier-Lavigne, M. & Lewcock, J. W. (2013) DLK initiates a transcriptional program that couples apoptotic and regenerative responses to axonal injury. *Proceedings of the National Academy of Sciences of the United States of America,* 110(10)**,** 4039-44.

Weisz, L., Damalas, A., Liontos, M., Karakaidos, P., Fontemaggi, G., Maor-Aloni, R., Kalis, M., Levrero, M., Strano, S., Gorgoulis, V. G., Rotter, V., Blandino, G. & Oren, M. (2007) Mutant p53 enhances nuclear factor kappaB activation by tumor necrosis factor alpha in cancer cells. *Cancer Research,* 67(6)**,** 2396-401.

Welsbie, D. S., Yang, Z., Ge, Y., Mitchell, K. L., Zhou, X., Martin, S. E., Berlinicke, C. A., Hackler, L., Jr., Fuller, J., Fu, J., Cao, L. H., Han, B., Auld, D., Xue, T., Hirai, S., Germain, L., Simard-Bisson, C., Blouin, R., Nguyen, J. V., Davis, C. H., Enke, R. A., Boye, S. L., Merbs, S. L., Marsh-Armstrong, N., Hauswirth, W. W., DiAntonio, A., Nickells, R. W., Inglese, J., Hanes, J., Yau, K. W., Quigley, H. A. & Zack, D. J. (2013) Functional genomic screening identifies dual leucine zipper kinase as a key mediator of retinal ganglion cell death. *Proceedings of the National Academy of Sciences of the United States of America,* 110(10)**,** 4045-50.

Wheeler, D. B., Zoncu, R., Root, D. E., Sabatini, D. M. & Sawyers, C. L. (2015) Identification of an oncogenic RAB protein. *Science,* 350(6257)**,** 211-7.

Whittaker, S., Kirk, R., Hayward, R., Zambon, A., Viros, A., Cantarino, N., Affolter, A., Nourry, A., Niculescu-Duvaz, D., Springer, C. & Marais, R. (2010) Gatekeeper mutations mediate resistance to BRAF-targeted therapies. *Science Translational Medicine,* 2(35)**,** 35ra41.

Williams, M. R., Arthur, J. S., Balendran, A., van der Kaay, J., Poli, V., Cohen, P. & Alessi, D. R. (2000) The role of 3-phosphoinositide-dependent protein kinase 1 in activating AGC kinases defined in embryonic stem cells. *Current Biology,* 10(8)**,** 439-48.

Wilson, T. R., Fridlyand, J., Yan, Y., Penuel, E., Burton, L., Chan, E., Peng, J., Lin, E., Wang, Y., Sosman, J., Ribas, A., Li, J., Moffat, J., Sutherlin, D. P., Koeppen, H., Merchant, M., Neve, R. & Settleman, J. (2012) Widespread potential for growth-factor-driven resistance to anticancer kinase inhibitors. *Nature,* 487(7408)**,** 505-9.

Wong, R. P., Tsang, W. P., Chau, P. Y., Co, N. N., Tsang, T. Y. & Kwok, T. T. (2007) p53-R273H gains new function in induction of drug resistance through down-regulation of procaspase-3. *Molecular Cancer Therapeutics,* 6(3)**,** 1054-61.

Wood, H. M., Belvedere, O., Conway, C., Daly, C., Chalkley, R., Bickerdike, M., McKinley, C., Egan, P., Ross, L., Hayward, B., Morgan, J., Davidson, L., MacLennan, K., Ong, T. K., Papagiannopoulos, K., Cook, I., Adams, D. J., Taylor, G. R. & Rabbitts, P. (2010) Using next-generation sequencing for high resolution multiplex analysis of copy number variation from nanogram quantities of DNA from formalin-fixed paraffin-embedded specimens. *Nucleic Acids Research,* 38(14)**,** e151.

Wortzel, I. & Seger, R. (2011) The ERK Cascade: Distinct Functions within Various Subcellular Organelles. *Genes & Cancer,* 2(3)**,** 195-209.

Xie, J., Nair, A. & Hermiston, T. W. (2008) A comparative study examining the cytotoxicity of inducible gene expression system ligands in different cell types. *Toxicology in Vitro,* 22(1)**,** 261-6.

Xu, Z., Maroney, A. C., Dobrzanski, P., Kukekov, N. V. & Greene, L. A. (2001) The MLK family mediates c-Jun N-terminal kinase activation in neuronal apoptosis. *Molecular and Cellular Biology,* 21(14)**,** 4713-24.

Yamamoto, H., Shigematsu, H., Nomura, M., Lockwood, W. W., Sato, M., Okumura, N., Soh, J., Suzuki, M., Wistuba, II, Fong, K. M., Lee, H., Toyooka, S., Date, H., Lam, W. L., Minna, J. D. & Gazdar, A. F. (2008) PIK3CA mutations and copy number gains in human lung cancers. *Cancer Research,* 68(17)**,** 6913-21.

Yan, M. & Templeton, D. J. (1994) Identification of 2 serine residues of MEK-1 that are differentially phosphorylated during activation by raf and MEK kinase. *The Journal of Biological Chemistry,* 269(29)**,** 19067-73.

Yang, H., Higgins, B., Kolinsky, K., Packman, K., Go, Z., Iyer, R., Kolis, S., Zhao, S., Lee, R., Grippo, J. F., Schostack, K., Simcox, M. E., Heimbrook, D., Bollag, G. & Su, F. (2010a) RG7204 (PLX4032), a selective BRAFV600E inhibitor, displays potent antitumor activity in preclinical melanoma models. *Cancer Research,* 70(13)**,** 5518-27.

Yang, J., Cron, P., Good, V. M., Thompson, V., Hemmings, B. A. & Barford, D. (2002a) Crystal structure of an activated Akt/protein kinase B ternary complex with GSK3-peptide and AMP-PNP. *Nature Structural & Molecular Biology,* 9(12)**,** 940-4.

Yang, J., Cron, P., Thompson, V., Good, V. M., Hess, D., Hemmings, B. A. & Barford, D. (2002b) Molecular mechanism for the regulation of protein kinase B/Akt by hydrophobic motif phosphorylation. *Molecular Cell,* 9(6)**,** 1227-40.

Yang, J. J., Lee, Y. J., Hung, H. H., Tseng, W. P., Tu, C. C., Lee, H. & Wu, W. J. (2010b) ZAK inhibits human lung cancer cell growth via ERK and JNK activation in an AP-1-dependent manner. *Cancer Science,* 101(6)**,** 1374-81.

Yasuda, J., Whitmarsh, A. J., Cavanagh, J., Sharma, M. & Davis, R. J. (1999) The JIP group of mitogen-activated protein kinase scaffold proteins. *Molecular and Cellular Biology,* 19(10)**,** 7245-54.

Zhan, Y., Abi Saab, W. F., Modi, N., Stewart, A. M., Liu, J. & Chadee, D. N. (2012) Mixed lineage kinase 3 is required for matrix metalloproteinase expression and invasion in ovarian cancer cells. *Experimental Cell Research,* 318(14)**,** 1641-8.

Zhang, H. & Gallo, K. A. (2001) Autoinhibition of mixed lineage kinase 3 through its Src homology 3 domain. *The Journal of Biological Chemistry,* 276(49)**,** 45598-603.

Zhang, J., Lu, L., Xiong, Y., Qin, W., Zhang, Y., Qian, Y., Jiang, H. & Liu, W. (2014) MLK3 promotes melanoma proliferation and invasion and is a target of microRNA-125b. *Clinical and Experimental Dermatology,* 39(3)**,** 376-84.

Zhao, J., Jitkaew, S., Cai, Z., Choksi, S., Li, Q., Luo, J. & Liu, Z. G. (2012) Mixed lineage kinase domain-like is a key receptor interacting protein 3 downstream component of TNF-induced necrosis. *Proceedings of the National Academy of Sciences of the United States of America,* 109(14)**,** 5322-7.

Zhou, G., Wang, J., Zhao, M., Xie, T. X., Tanaka, N., Sano, D., Patel, A. A., Ward, A. M., Sandulache, V. C., Jasser, S. A., Skinner, H. D., Fitzgerald, A. L., Osman, A. A., Wei, Y., Xia, X., Songyang, Z., Mills, G. B., Hung, M. C., Caulin, C., Liang, J. & Myers, J. N. (2014) Gain-of-function mutant p53 promotes cell growth and cancer cell metabolism via inhibition of AMPK activation. *Molecular Cell,* 54(6)**,** 960-74.

Zhu, J., Sammons, M. A., Donahue, G., Dou, Z., Vedadi, M., Getlik, M., Barsyte-Lovejoy, D., Al-awar, R., Katona, B. W., Shilatifard, A., Huang, J., Hua, X., Arrowsmith, C. H. & Berger, S. L. (2015) Gain-of-function p53 mutants co-opt chromatin pathways to drive cancer growth. *Nature,* 525(7568)**,** 206-11.

Zhuang, D., Mannava, S., Grachtchouk, V., Tang, W. H., Patil, S., Wawrzyniak, J. A., Berman, A. E., Giordano, T. J., Prochownik, E. V., Soengas, M. S. & Nikiforov, M. A. (2008) C-MYC overexpression is required for continuous suppression of oncogene-induced senescence in melanoma cells. *Oncogene,* 27(52)**,** 6623-34.

6 Appendices

6.1 Appendix I: Primers

6.1.1 PCR primers

6.1.1.1 LZK

LZKattBF GGGGACAAGTTTGTACAAAAAAGCAGGCTTCatggccaactttcagga
LZKattBR GGGGACCACTTTGTACAAGAAAGCTGGGTCttaccaggtagcagagc

6.1.1.2 MLK1

MLK1attBF GGGGACAAGTTTGTACAAAAAAGCAGGCTTCgagccctccagagcgctt
MLK1attBR GGGGACCACTTTGTACAAGAAAGCTGGGTCctaagaccagaactcctgc

6.1.1.3 SOX2

Sox2attBF GGGGACAAGTTTGTACAAAAAAGCAGGCTTCatgtacaacatgatggagacgg
Sox2attBR GGGGACCACTTTGTACAAGAAAGCTGGGTCtcacatgtgtgagaggggcagt

6.1.2 RT-PCR primers

Gene	Primer	Sequence (5'-3')	Amplicon size (bp)
GAPDH	Forward	CCATGGAGAAGGCTGGGG	668
	Reverse	GTCCACCACCCTGTTGCTGTA	
LZK	Forward	AACTGATTCGAAGGCGCAGA	954
	Reverse	GGGCGTTTTCCAAGAGAGGA	
MLK2	Forward	GAACGTGAGATGGACATCGTGGAA	184
	Reverse	AGGCCTGGACTGTGATCTTATGCT	

6.1.3 qPCR primers

Gene	Primer	Sequence (5'-3')	Amplicon size (bp)
ACTB	Forward	CCAACCGCGAGAAGATGA	97
	Reverse	CCAGAGGCGTACAGGGATAG	
B2M	Forward	TTCTGGCCTGGAGGCTATC	86
	Reverse	TCAGGAAATTTGACTTTCCATTC	
LZK	Forward	CCTTTGTCCGGAAGTCCCAAAATGTC	188
	Reverse	GAAGGGTATTGGGATTGAGCTTGGTG	

6.1.4 Mutagenesis primers

6.1.4.1 LZK

LZK_K195MF GGAAGAGGTGGCCATCATGAAAGTGAGAGAACAGA
LZK_K195MR TCTGTTCTCTCACTTTCATGATGGCCACCTCTTCC

sh1-resistant mutations: g978t_t981c_a984g_t987a_c990g_t993c_a996g
F1267shrescue F
ACTCCAAAAGACCATATATCAACTTTCTCGGACACTGGCTCGTTACGTATCAC
CTCTGGCGCCATCCATG
R1267shrescue R
CATGGATGGCGCCAGAGGTGATACGTAACGAGCCAGTGTCCGAGAAAGTTGA
TATATGGTCTTTTGGAGT

6.1.4.2 MLK1

MLK1R160C GGCTTTGGGAAGGTCTATTGTGCTTTCTGGATAGG
MLK1R160C_antisense CCTATCCAGAAAGCACAATAGACCTTCCCAAAGCC

MLK1D176N AAGCAGCTCGCCACAACCCTGATGAGGAC
MLK1D176N_antisense GTCCTCATCAGGGTTGTGGCGAGCTGCTT

MLK1A246V CATCCTGGTGAATTGGGTTGTGCAGATTGCCAGAG
MLK1A246Vantisense CTCTGGCAATCTGCACAACCCAATTCACCAGGATG

MLK1P263L GATGAGGCAATTGTTCTCATCATCCACCGCGAC
MLK1P263L_antisense GTCGCGGTGGATGATGAGAACAATTGCCTCATC

MLK1D294A GATTCTGAAGATCACTGCTTTTGGCCTGGCTCGGG
MLK1D294Aantisense CCCGAGCCAGGCCAAAAGCAGTGATCTTCAGAATC

MLK1E319K CTTGGATGGCACCCAAAGTCATCCGGGCC
MLK1E319K_antisense GGCCCGGATGACTTTGGGTGCCATCCAAG

MLK1E429K CAGGACAACTGGAAACACAAGATTCAGGAGATGTTTG
MLK1E429K_antisense CAAACATCTCCTGAATCTTGTGTTTCCAGTTGTCCTG

MLK1P496A GTGCCAGGAGAAGGCCCGGGTGAAGAA
MLK1P496Aantisense TTCTTCACCCGGGCCTTCTCCTGGCAC

MLK1S533Y CAAGTTCACGGTGCAGGCCTATCCTACCATGGATAAAAG
MLK1S533Y_antisense CTTTTATCCATGGTAGGATAGGCCTGCACCGTGAACTTG

MLK1P557L AGCCCCACCATCATTCTTCGCCTTCGAGC
MLK1P557L_antisense GCTCGAAGGCGAAGAATGATGGTGGGGCT

MLK1G600R GACGGACGTGGAGGCCAGGGACG
MLK1G600R_antisense CGTCCCTGGCCTCCACGTCCGTC

MLK1S616F GCCTCGGGAGATGAAGGATTCCCTCAGAGA
MLK1S616F_antisense TCTCTGAGGGAATCCTTCATCTCCCGAGGC

MLK1S650L GGATATAAGCAGTGGTTGTCCAGTGCCCCCAAC
MLK1S650L_antisense GTTGGGGGCACTGGACAACCACTGCTTATATCC

MLK1G769D GTGGCTCTGCTCGACTGTGGGGCTGTT
MLK1G769D_antisense AACAGCCCCACAGTCGAGCAGAGCCAC

MLK1P793S GGCAAGTGCCAGCTGCTTAGCCTGGAGGAG
MLK1P793S_antisense CTCCTCCAGGCTAAGCAGCTGGCACTTGCC

MLK1R827Q ACCAGCCCCCCATCCCAAAAGCTTTTCAAGAAG
MLK1R827Q_antisense CTTCTTGAAAAGCTTTTGGGATGGGGGGCTGGT

MLK1P963S CAGGAATGTTGAAAACCAGCAGTCCCAGCCGAGACC
MLK1P963S_antisense GGTCTCGGCTGGGACTGCTGGTTTTCAACATTCCTG

MLK1P963T AGGAATGTTGAAAACCACCAGTCCCAGCCGAG
MLK1P963T_antisense CTCGGCTGGGACTGGTGGTTTTCAACATTCCT

MLK1P1020S CGGCAACGGCTGGACAGTTGGTGGTTTGTGTCC
MLK1P1020S_antisense GGACACAAACCACCAACTGTCCAGCCGTTGCCG

6.1.4.3 MLK4

MLK4_K151MF AGGAGGTGGCCGTGATGGCGGCGC
MLK4_K151MR GCGCCGCCATCACGGCCACCTCCT

6.1.5 Sequencing primers

6.1.5.1 LZK

LZKseq1 ATTTGGATGCTTAAGGCCTG
LZKseq2 AGTGACCCACACAGATG
LZKseq3 AAGAGCTCAGGCATGCG
LZKseq4 AACCAGCCAGCCCAGGAAA
LZKseq5 CCCTGACCTTTCCAAGT
LZKseq6 CCATTGACATATCCTCACAC

6.1.5.2 MLK1

MLK1seq1 AGGTGCTGTCCAAGGACT
MLK1seq2 CTGAAGGAGCCCAACCTCT
MLK1seq3 CTGACTGGTGAGGTGCCCTT
MLK1seq4 GAGCGGGAGATTGACATCCT
MLK1seq5 GGTCAGAAGGAGCTTGCCTCG
MLK1seq6 ACCCCAGTCAACTCGGCCA
MLK1seq7 GACAGCGATGAAATTGTCGTG
MLK1seq8 GAGAGACCCAAGACTCTGGA

6.1.5.3 MLK2

MLK2seqR1 TAGACCTTGCCAAAGCC
MLK2 seqF1 AGAGGAGATCATCGGTGT
MLK2seqF2 TCAAGTCCATCAACATCC
MLK2seqF3 TGCCCCGAGCCCTTTGC
MLK2seqF4 TCAGCCTGCCCTCTGGCTTT
MLK2seqF5 CTTTGCCAGCCTCAATGAGA
MLK2seqF6 CGCTCTGACAGTGACGAGG
MLK2seqF7 CCGCTTGGACCCCTGGAA

6.1.5.4 MLK3

MLK3seqFP1 ATGGAGCCCTTGAAGAGCCTCTTC
MLK3seqFP2 GCTGTGTGCCTGGAGGAGCCCA
MLK3seqFP3 GCCTATGGCGTAGCTGTTAACAAGC
MLK3seqFP4 CGCATCACCGTGCAGGCCTCACCCG
MLK3seqFP5 CGGCACCGCCCTGCTCGCCTCGCTG
MLK3seqRP ATGATGTTGGGGTGTGCCAGCATGG

6.1.5.5 MLK4

MLK4FP1 AGCTGGTGGAGGTGCTGT
MLK4RP2 ATGAGCTCCTTCAGCTCCAG
MLK4FP3 CACCCCAACATCATCGAGCT
MLK4FP4 ATGAGCACAGCAGGCACCTA
MLK4FP5 CAGTGATGACTGAGATGCCT
MLK4FP6 GATGGACATCGAATCAGTTTACC
MLK4FP7 GGATAAGACCTCTCTCCGATGG
MLK4FP9 CATCCTCTCCACACCTTCTT
MLK4FP10 GACCATGTCTGATGGAAATC

6.1.5.6 SOX2

SOX2SEQ1 CCGTTCATCGACGAGGCTAA

6.2 Appendix II: Copy number analysis

Cell lines used in this project were sent to Dr Henry Wood for copy number analysis by whole genome sequencing. Figure 13 in the main text shows a detailed view of chromosome 3 with the position of MAP3K13 marked. Full genome strips are shown in Appendix Figure 1.

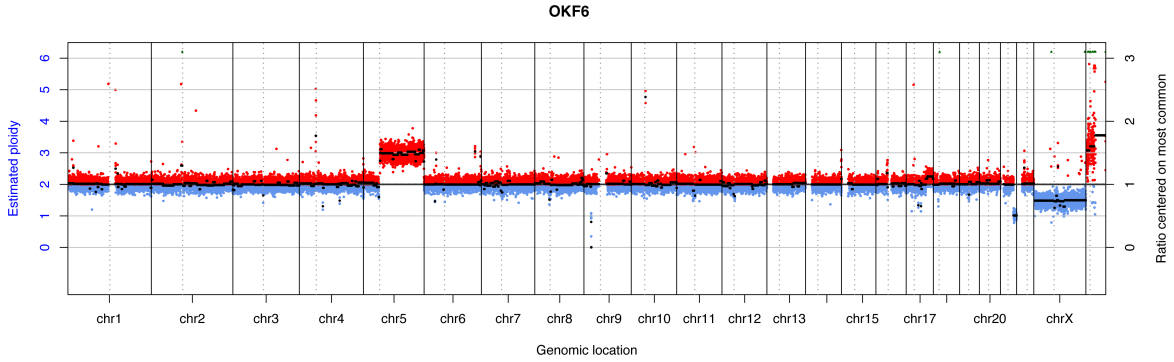
OKF6
Estimated ploidy
Ratio centered on most common
chr1 chr2 chr3 chr4 chr5 chr6 chr7 chr8 chr9 chr10 chr11 chr12 chr13 chr15 chr17 chr20 chrX
Genomic location

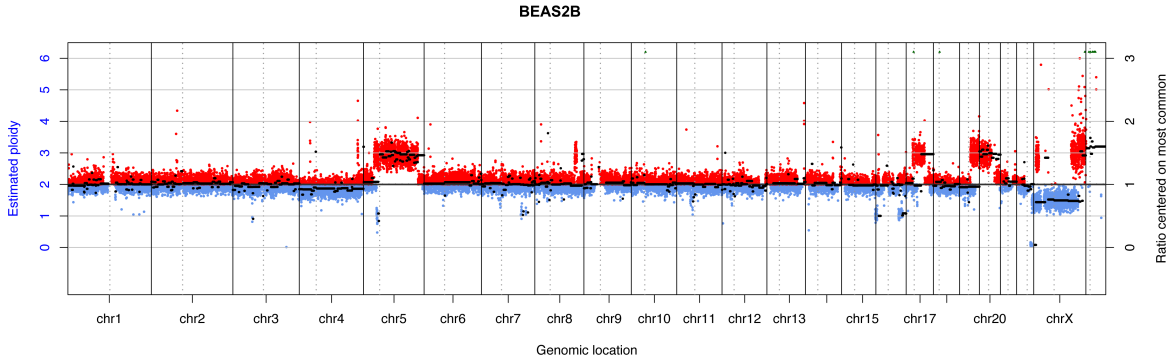
BEAS2B
Estimated ploidy
Ratio centered on most common
chr1 chr2 chr3 chr4 chr5 chr6 chr7 chr8 chr9 chr10 chr11 chr12 chr13 chr15 chr17 chr20 chrX
Genomic location

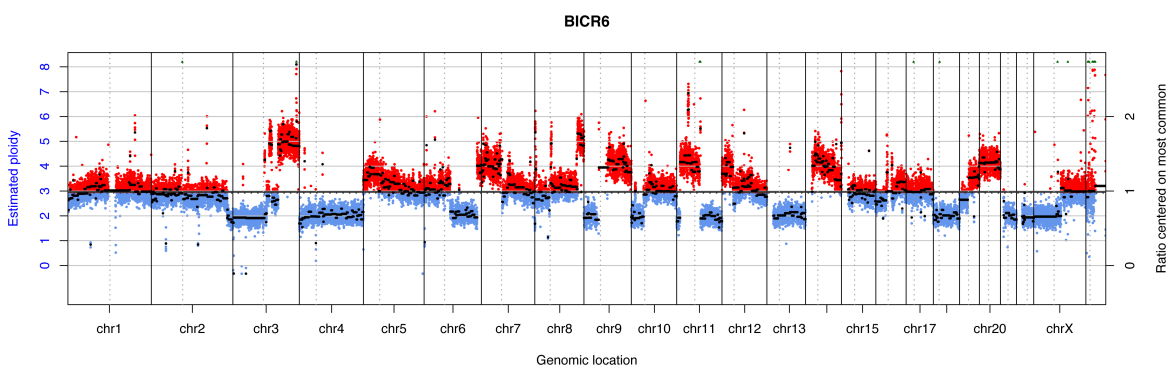
BICR6
Estimated ploidy
Ratio centered on most common
chr1 chr2 chr3 chr4 chr5 chr6 chr7 chr8 chr9 chr10 chr11 chr12 chr13 chr15 chr17 chr20 chrX
Genomic location

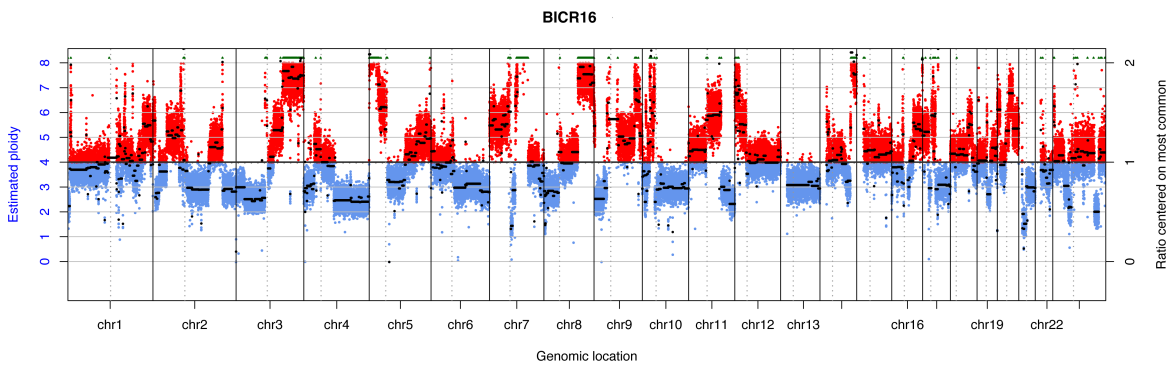
BICR16
Estimated ploidy
Ratio centered on most common
chr1 chr2 chr3 chr4 chr5 chr6 chr7 chr8 chr9 chr10 chr11 chr12 chr13 chr16 chr19 chr22
Genomic location

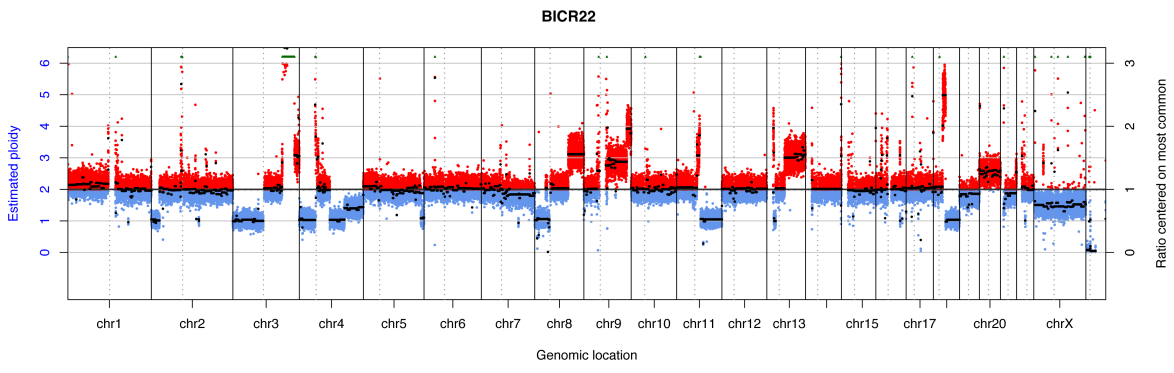
BICR22
Estimated ploidy
Ratio centered on most common
chr1 chr2 chr3 chr4 chr5 chr6 chr7 chr8 chr9 chr10 chr11 chr12 chr13 chr15 chr17 chr20 chrX
Genomic location

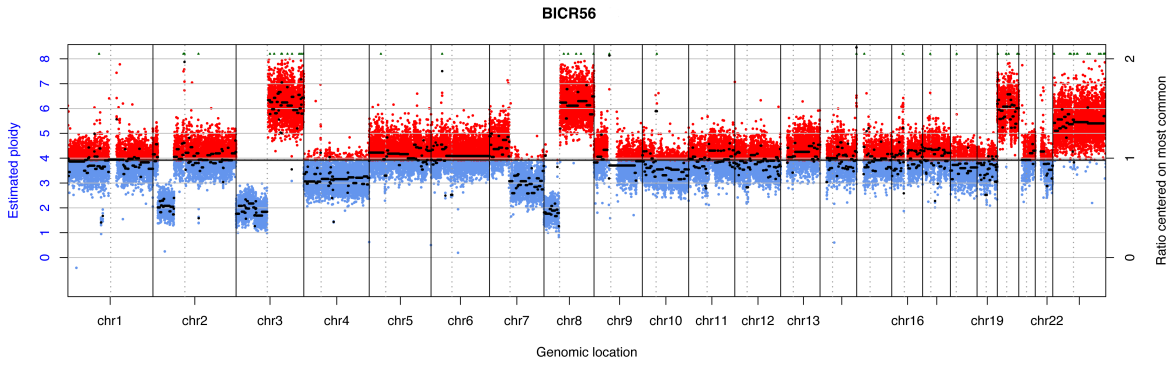
BICR56
Estimated ploidy
Ratio centered on most common
chr1 chr2 chr3 chr4 chr5 chr6 chr7 chr8 chr9 chr10 chr11 chr12 chr13 chr16 chr19 chr22
Genomic location

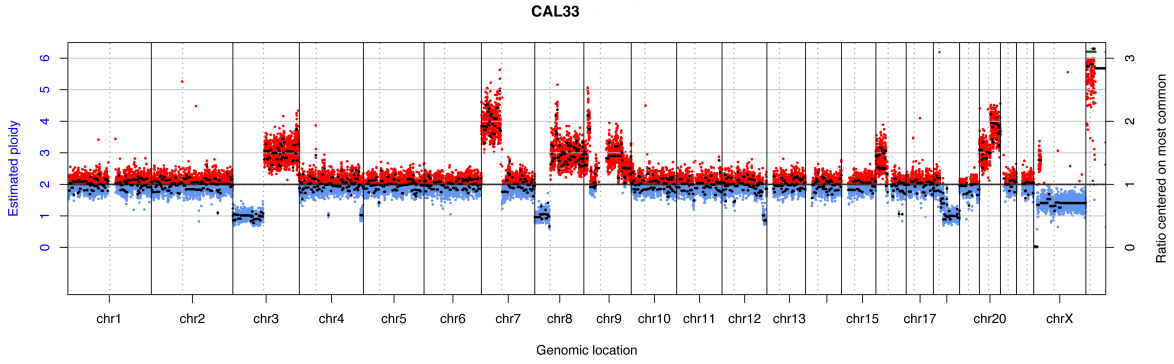
CAL33
Estimated ploidy
Ratio centered on most common
chr1 chr2 chr3 chr4 chr5 chr6 chr7 chr8 chr9 chr10 chr11 chr12 chr13 chr15 chr17 chr20 chrX
Genomic location

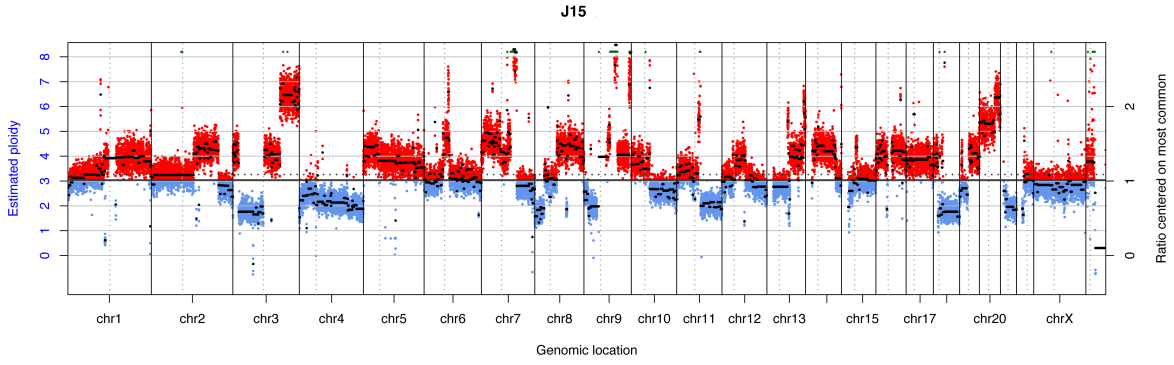
J15
Estimated ploidy
Ratio centered on most common
chr1 chr2 chr3 chr4 chr5 chr6 chr7 chr8 chr9 chr10 chr11 chr12 chr13 chr15 chr17 chr20 chrX
Genomic location

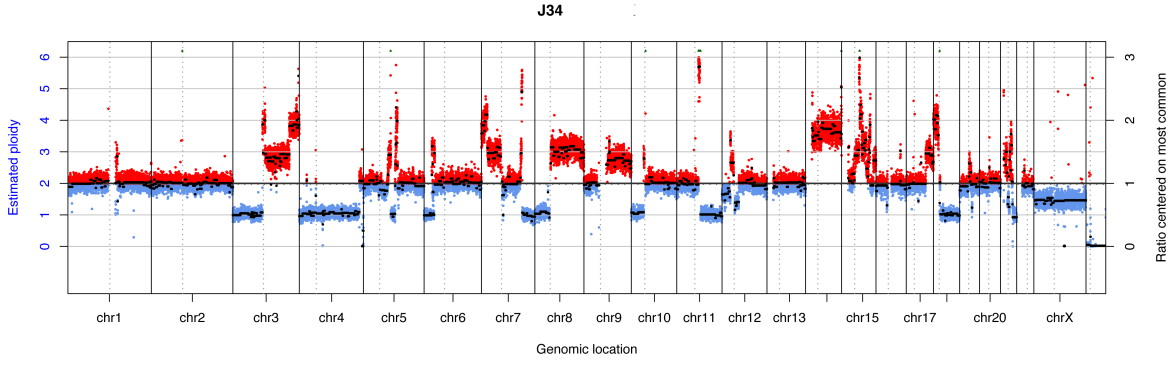
J34
Estimated ploidy
Ratio centered on most common
chr1 chr2 chr3 chr4 chr5 chr6 chr7 chr8 chr9 chr10 chr11 chr12 chr13 chr15 chr17 chr20 chrX
Genomic location

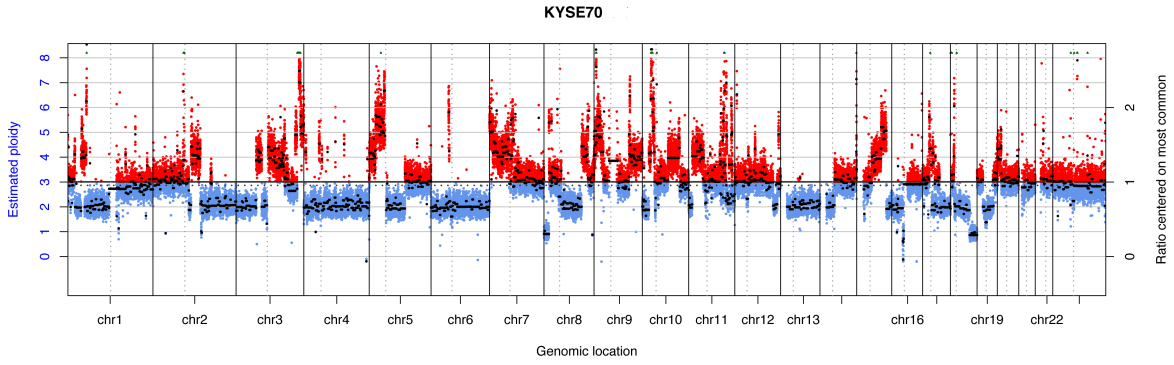
KYSE70
Estimated ploidy
Ratio centered on most common
chr1 chr2 chr3 chr4 chr5 chr6 chr7 chr8 chr9 chr10 chr11 chr12 chr13 chr16 chr19 chr22
Genomic location

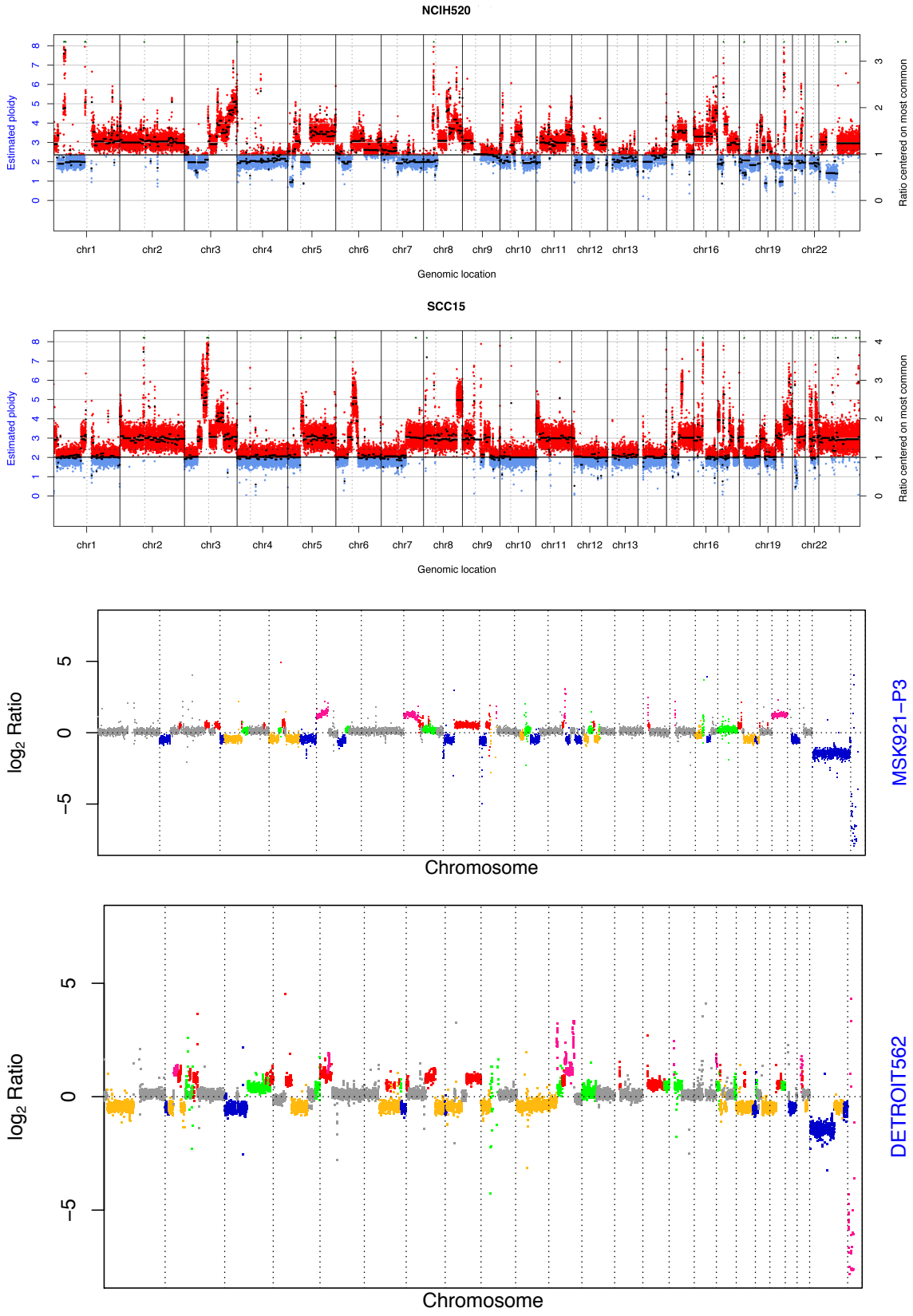

Appendix Figure 1: Copy number analysis of cell lines utilised in this project. Data analysed and generated by Dr Henry Wood, except for MSK921 and DETROIT562 cell lines, which were analysed by Sudhakar Sahoo. For MSK921 and DETROIT562, colour scheme as follows: blue = 0 copies, homozygous deletion; yellow = 1 copy, heterozygous deletion; grey = 2 copies, neutral; green = 3 copies, gain; red = 4 copies, amplification; deep pink ≥5 copies, high-level of amplification.

6.3 Appendix III: Details of antibody issues experienced

As discussed, it became clear during the course of this project that the LZK antibody used was no longer capable of detecting endogenous LZK. While making cell lines with inducible expression of LZK, no increases were seen in LZK protein levels after addition of tetracycline. When no defects in the lentiviral construct were found, generation of LZK-inducible BEAS2B cells was attempted in parallel with generation of MLK1-inducible BEAS2B (this has previously been successfully generated in this laboratory). While tetracycline addition caused a clear increase in MLK1 protein levels in the MLK1-inducible BEAS2B cells, no effect was seen on apparent LZK protein levels in the LZK-inducible cells using the monoclonal antibody from Abcam that we had used previously (Appendix Fig. 2A). However, further analyses revealed that mRNA levels of *MAP3K13* were increased after tetracycline addition (Appendix Fig. 2B), as were levels of pJNK (Appendix Fig. 2C), suggesting that LZK protein levels were elevated after tetracycline treatment but this was not detected because the antibody was no longer specific to LZK. BEAS2B cells with inducible kinase-dead LZK were generated as an additional control in case kinase-active LZK is a toxic gene product that is rapidly degraded in these cells; these also showed no increases in LZK protein levels after tetracycline addition (Appendix Fig. 2C). Similar results were obtained when OKF6 cells with tetracycline-inducible LZK were generated; increases in mRNA (Appendix Fig. 2D) and pJNK (Appendix Fig. 2E) were clear, but no difference was seen in LZK protein levels (Appendix Fig. 2E).

Initially, the LZK antibody utilised in this project was tested after transient overexpression in 293T cells; this antibody detected FLAG-tagged LZK (Appendix Fig. 2F). Additionally, reductions in the LZK band detected were observed after knockdown of *MAP3K13* (Fig. 14A). Samples that were previously used for analysis (Appendix Fig. 2F) were re-analysed recently; this showed that the antibody was no longer functioning as it used to, as only a marginal increase was seen in the sample with overexpression of LZK as compared with the empty vector control (Appendix Fig. 2G), suggesting that the antibody specific to LZK was depleted in samples from later batches. Until a better antibody can be obtained, RT-PCR has been used to validate results seen for LZK expression and knockdown.

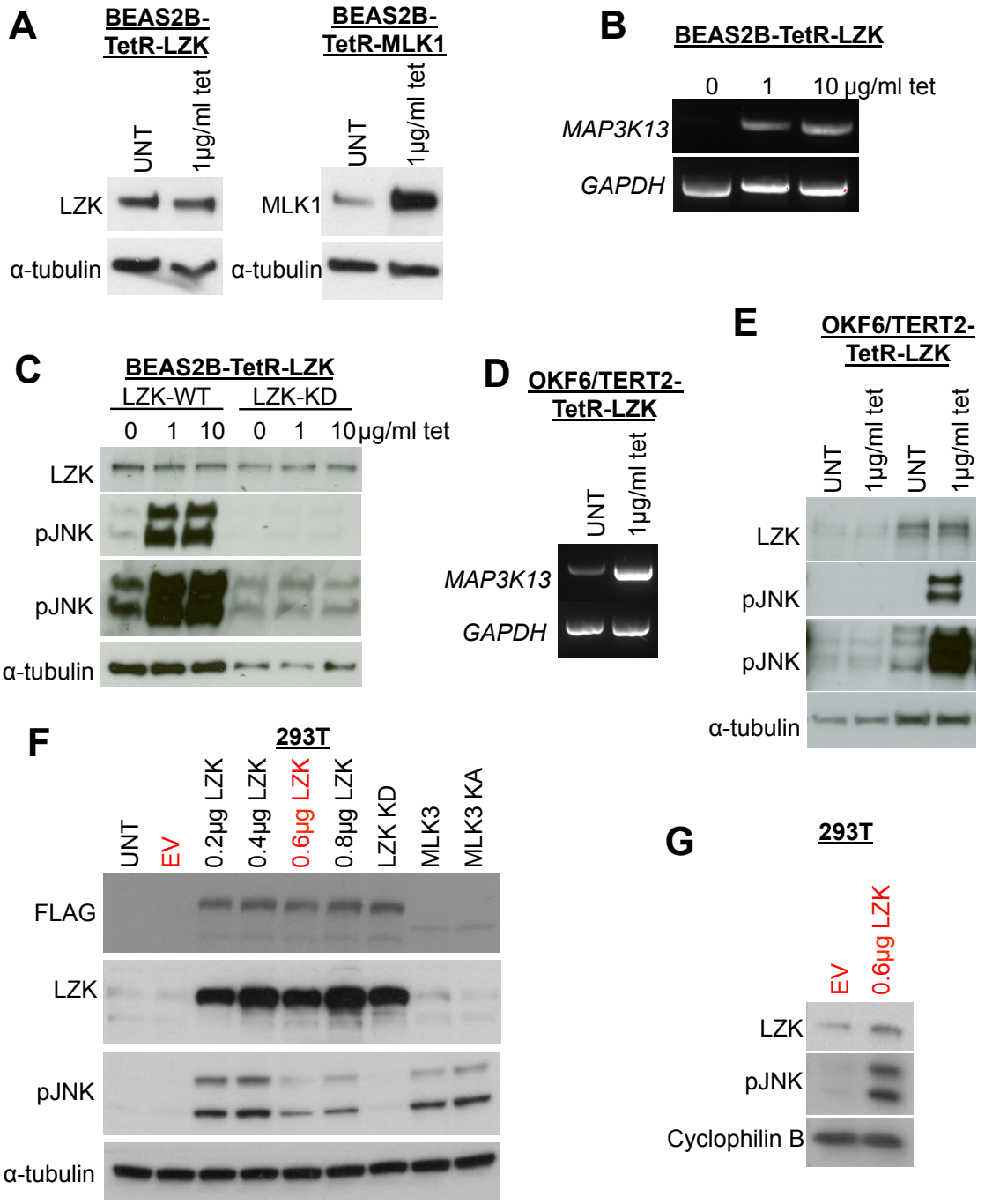

Appendix Figure 2: Antibody issues experienced. A: Concurrent generation of tetracycline-inducible BEAS2B cells for LZK and MLK1 demonstrated that MLK1 expression was effectively induced, but LZK antibody showed no difference in protein levels after induction. **B:** Increased expression of *MAP3K13* mRNA in tetracycline-inducible BEAS2B cells after tetracycline treatment. **C:** Induction of LZK by tetracycline caused JNK activation in a kinase-dependent manner (WT=wild-type LZK, KD=kinase-dead LZK). LZK antibody showed no difference in expression after tetracycline treatment. **D:** Increased expression of *MAP3K13* mRNA in tetracycline-inducible OKF6/TERT2 cells after tetracycline treatment. **E:** Tetracycline treatment activated JNK in LZK-inducible, but not in parental, OKF6/TERT2 cells. LZK antibody showed no difference in expression after tetracycline treatment. **F:** Original blot run early in progress of project, indicating that LZK antibody was detecting overexpressed protein. **G:** Samples from (**F**) re-run recently, showing that later batches of the antibody were not functioning in the same way.

6.4 Appendix IV: Phosphoarrays

Coordinate	Target/Control	Phosphorylation Site
A1, A2	Reference Spot	N/A
A3, A4	p38α	T180/Y182
A5, A6	ERK1/2	T202/Y204, T185/ Y187
A7, A8	JNK 1/2/3	T183/Y185, T221/ Y223
A9, A10	GSK-3α/β	S21/S9
A13, A14	p53	S392
A17, A18	Reference Spot	N/A
B3, B4	EGFR	Y1086
B5, B6	MSK1/2	S376/S360
B7, B8	AMPKα1	T183
B9, B10	AKT 1/2/3	S473
B11, B12	AKT 1/2/3	T308
B13, B14	p53	S46
C1, C2	TOR	S2448
C3, C4	CREB	S133
C5, C6	HSP27	S78/S82
C7, C8	AMPKα2	T172
C9, C10	β-Catenin	N/A
C11, C12	p70 S6 Kinase	T389
C13, C14	p53	S15
C15, C16	c-Jun	S63
D1, D2	Src	Y419
D3, D4	Lyn	Y397
D5, D6	Lck	Y394
D7, D8	STAT2	Y689
D9, D10	STAT5a	Y694
D11, D12	p70 S6 Kinase	T421/S424
D13, D14	RSK1/2/3	S380/S386/S377
D15, D16	eNOS	S1177
E1, E2	Fyn	Y420
E3, E4	Yes	Y426
E5, E6	Fgr	Y412
E7, E8	STAT6	Y641
E9, E10	STAT5b	Y699
E11, E12	STAT3	Y705
E13, E14	p27	T198
E15, E16	PLC-γ1	Y783
F1, F2	Hck	Y411
F3, F4	Chk-2	T68
F5, F6	FAK	Y397
F7, F8	PDGF Rβ	Y751
F9, F10	STAT5a/b	Y694/Y699
F11, F12	STAT3	S727
F13, F14	WNK1	T60
F15, F16	PYK2	Y402
G1, G2	Reference Spot	N/A
G3, G4	PRAS40	T246
G9, G10	PBS (Negative Control)	N/A
G11, G12	HSP60	N/A
G17, G18	PBS (Negative Control)	N/A

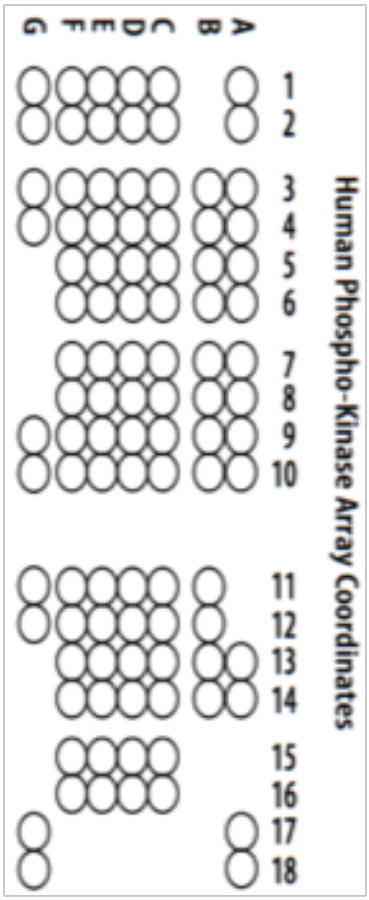

Appendix Table 1: Reference list and coordinates of phospho-antibodies present on phospho-kinase array.

Coordinate	Target/Control	Phosphorylation Site
A1, A2	Reference Spots	N/A
A21, A22	Reference Spots	N/A
B3, B4	AKT1	S473
B5, B6	AKT2	S474
B7, B8	AKT3	S472
B9, B10	AKT pan	S473, S474, S472
B11, B12	CREB	S133
B13, B14	ERK1	T202/Y204
B15, B16	ERK2	T185/Y187
B17, B18	GSK-3α/β	S21/S9
B19, B20	GSK-3β	S9
C3, C4	HSP27	S78/S82
C5, C6	JNK1	T183/Y185
C7, C8	JNK2	T183/Y185
C9, C10	JNK3	T221/Y223
C11, C12	JNK pan	T183/Y185, T221/Y223
C13, C14	MKK3	S218/T222
C15, C16	MKK6	S207/T211
C17, C18	MSK2	S360
D3, D4	p38α	T180/Y182
D5, D6	p38β	T180/Y182
D7, D8	p38δ	T180/Y182
D9, D10	p38γ	T183/Y185
D11, D12	p53	S46
D13, D14	p70 S6 Kinase	T421/S424
D15, D16	RSK1	S380
D17, D18	RSK2	S386
D19, D20	TOR	S2448
E19, E20	PBS	N/A
F1, F2	Reference Spots	N/A

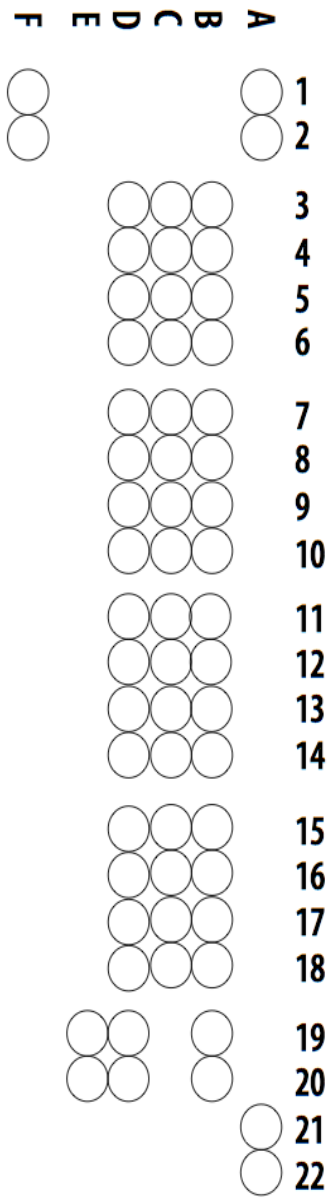

Appendix Table 2: Reference list and coordinates of phospho-antibodies present on MAPK array.